MOJAVE DESERT

Mojave National Preserve
March 18th-21st, 2022
PTYS 590: Planetary Geology Field Studies
Lunar and Planetary Laboratory
University of Arizona

Credit: J. T. Keane

Table of Contents

Acknowledgements

As an undergrad, I'm not entirely sure how I got roped into this.

I am grateful to the LPL faculty, staff, and grad students for not only helping with the assembly of this field guide booklet, but also for welcoming me into the department and nurturing my interest in planetary science over the past three years. Thank you for showing me the wonders of the solar system.

Thank you to Harry for the lovely cover design. The spice must flow.

Thank you to Indujaa for sharing files and directing me to field trip resources.

Thank you to Bert for the help with printing, and for holding everything together.

Thank you to Sondy and Amanda for creating and maintaining resources from past field trips.

I hope everyone has a great time on this field trip. Let's go learn lots of stuff about remote sensing! Remember: don't stop in bat country.

-- Reed

We acknowledge that the Mojave National Preserve is (currently) in what is the traditional, occupied, and unceded territories and ancestral lands of the Timbisha Panamint Shoshone Tribe (o'hya and tu'mbica), the Kawaiisu, the Chemehuevi, the 'Aha Makhav (Mohave), and the Vanyume people.

Respect the land, respect the water, and remember those who were here first.

Stop locations at:
https://www.google.com/maps/d/edit?mid=1DgmMcUI6EQpaF1DzAiE2vVdwUOQplk_V&usp=sharing

Friday 3/18/2022

7 AM Arrive at LPL loading dock with all our gear including breakfast, coffee, ice etc...

8 AM Depart LPL

Drive north on Cherry -> west on Speedway -> enter I10 westbound and drive 124 miles. Take exit 133B to merge onto AZ-101 Loop N. Drive 10 miles and then take exit 11 for US-60/Grand Ave. After 38 miles take a slight right onto US-93. After 58 miles, turn left onto Burro Creek Campground Rd.

12 PM Arrive Burro Creek Campground – Lunch here.

12.45PM Go back to US-93 and go 49 miles north. Transition to I40 west and go 147 miles to Kelbaker Road (stopping for gas in Kingman).

In Kingman, take the exit for US 93 (or W Beagle St.) and head west. Almost immediately, there'll be a 76 gas station on the right. Let's gas up here, check out the exposure of the Peach Springs Tuff in their parking lot, and have **Emileigh** regale us with the full story.

5.30PM Take exit 78 for Kelbaker Rd. Drive north on Kelbaker Road for 14.5 miles. Turn left at Kelso Dunes Road and drive 4-5 miles.

We'll hear from **Harry** about how dunes behave in Radar data and **Claire** about the booms and groans we might hear.

6PM Camp: Kelso Dunes. Hike to the top if there's time… BTW, a full moon rises at 7.35pm…

Elevation 2600'. Sunset 6:55PM AZ time.

Saturday 3/19/2022

8 AM Leave Camp. Sunrise 6.50AM
Backtrack to Kelbaker Road (4-5 miles) via restrooms. Drive north toward Baker for 11 miles.

8.45 AM Stop at a spectrally interesting outcrop of rock just west of the road. **Allison** will tell us what they gleaned from the MASTER data and geologic maps here. **Dingshan** can also talk about the overall geologic history of the Mojave here before we get into the thick of the volcanic fields.
Travel another 12.5 miles north on Kelbaker Road. Take a right turn onto Aiken Mine Road. Head northeast for 2.5 miles. There's a small road to the left that leads about 500m up to a cinder cone.

10AM We're in the Cima Volcanic field, which **Mackenzie** will describe. The summit material of this crater shows a compositional difference in the hyperspectral imagery, **Michael** will expound on why and we can hopefully scramble up the slope to check for ourselves.
Back to Aiken Mine Road and travel another 1.5 miles east. There's a fork in the road and we should bear left. There's a place to park ~400m past the fork, if possible we'll drive a little further (~200m) up this cinder cone. Pay attention to the roughness of the flow here, we'll compare it to a different Cima flow later today.

11.30AM Arrive at a lava tube cave where **Nathan** will talk about such caves on other planets (or perhaps we'll save that talk for the Pisgah cave tomorrow). It's a short cave and easy to explore.

12PM Eat **Lunch** here.
Head southwest on Aiken Mine Road for 5 miles and then north on Kelbaker road for 7.5 miles. Take a left turn onto Old Government Road and travel 11 miles The road is vaguely defined in places, but trends mostly WSW (see overleaf).

2.15PM We're in the middle of Soda Playa, the first of two playas we'll visit. **Zarah** will give us some info on its formation and we'll delve into its radar appearance, which is somewhat unusual. **Kana** can tell us how this fits into the overall Hydrologic history of the area, the Mojave River (no joke!), and lake Manix.
Back along Old Government Road to Kelbaker Road. Turn right and travel 3 miles to Indian Springs trail, take a left turn and travel ~1 mile to the campsite.

4.30PM We're right beside an extremely rough lava flow. **Rishi** will perform the first of a two-parter on roughness and radar. This is also a good place for **Tarunika** to wax lyrical about the flora and fauna of the Mojave too.

5.00PM Camp: Cima Volcanic Field.
Elevation 2600'. Sunset 6:55PM AZ time.

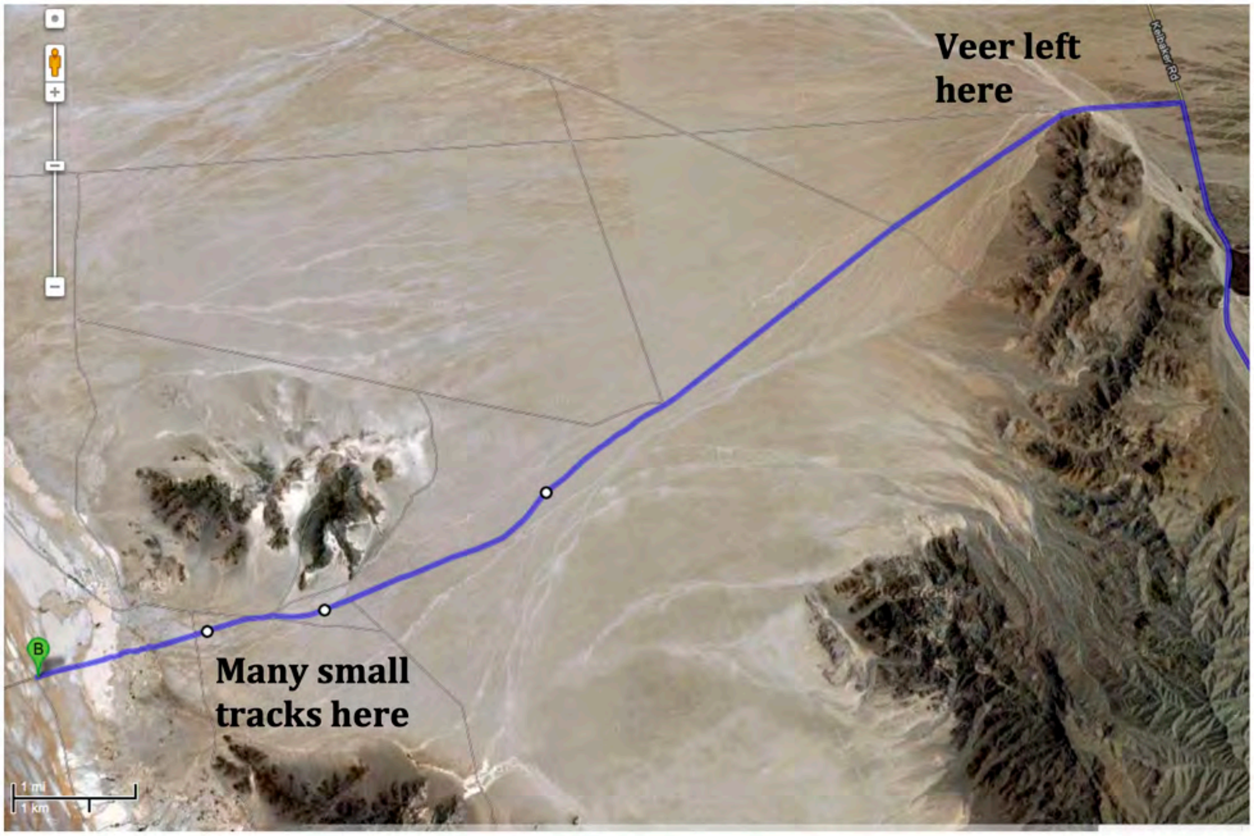

Kelbaker Road to the Soda Lake stop via Old Government Road.

Sunday 3/20/2022

8 AM Leave Camp at Cima. Sunrise 6.50AM.
Backtrack to Kelbaker Road. Drive North to toward Baker for 16 miles. Here's a chance to gas up and hit restrooms.

Head 40 miles west on I15 South until exit 206 for Harvard Road. Travel 4 miles south before turning right onto Riverside road. After 1 mile take a left onto Newberry Road. There's a large agricultural field on the right after about 1.5 miles.

10AM Arrive at the Mojave Agricultural fields where there's an interesting RADAR puzzle for us to solve…
Agriculture in the middle of the desert seems weird, but has been going on a while – **Robert** will fill us in on Human Activities here over the years

10.45AM Leave the fields and continue south on Newberry Road for 4.5 miles, turn left onto National Trails Highway (Rt 66) and travel 3.1 miles. Merge onto I40 east and 9 miles later take exit 33 and continue east, parallel to the freeway, for 4.5 miles. Turn right onto Pisgah Crater Road and travel 2 miles south.

11.15AM Arrive at Pisgah Cone. This part is played somewhat by ear but we should try and drive just southeast of the cone to the start of the lava field. **Lunch** is here either before or after the talks below depending on the time.

We'll walk about 150m south/southeast to a prominent contact in the radar data. **Rishi** can reprise his earlier talk and we'll what the radar data say here and how it corresponds to reality…
There are some lava tubes we'll try and find about 200m east of the base of the cone (they're visible in google maps, see overleaf for location). We should have time to explore the cave and hear from **Nathan** on cave astrobiological research, some of which happened here. This is a long cave and not that easy to explore, but we'll use what time we have to look around.

1PM Leave Pisgah via Pisgah Crater Road and after 2 miles turn right on Route 66 (National Trails Highway). This runs about 40 miles toward Amboy, we'll turn off just before Amboy onto crater road and travel 0.5 miles south.

2.15PM Arrive at the Amboy lava field. We'll walk out onto the flow towards the cone (about a mile, but the trail is smooth) where **Reed** will tell us about the streak and we'll talk about various theories. We'll try to locate some streak edges (difficult up close) and see if we can figure out what's going on.

6PM Camp: Amboy Volcanic Field.
Elevation 800'. Sunset 6:55PM AZ time.

Pisgah
Crater
Road

Monday 3/21/2022

8 AM Break Camp. Sunrise 6.50AM.
Drive west on Rt 66 for 26 miles. Take a right turn onto Crucero road and cross I40 at Ludlow. Continue North for ~7 miles.

9AM **Zarah** may tell us more about Playas and Radar. This one looks quite different in radar data than Soda Lake does – we'll try and figure out why.

9.30am Leave for home. It's ~7 hours driving from Broadwell Playa to LPL.
Stops and lunch along the way means this is probably 8.5 hours minimum.

6 PM Return to LPL. Sunset in Tucson 6:35PM

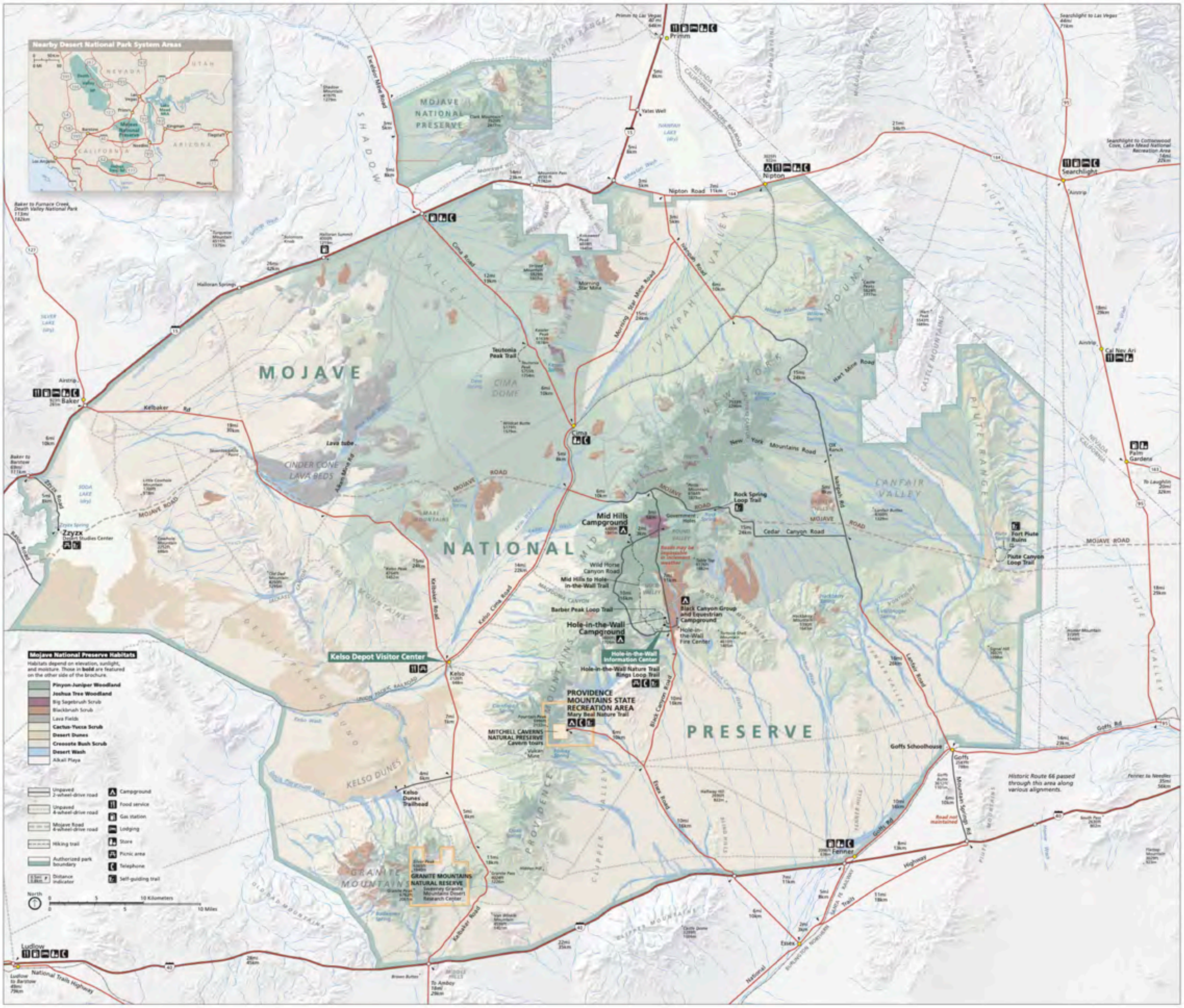

National Park Service map

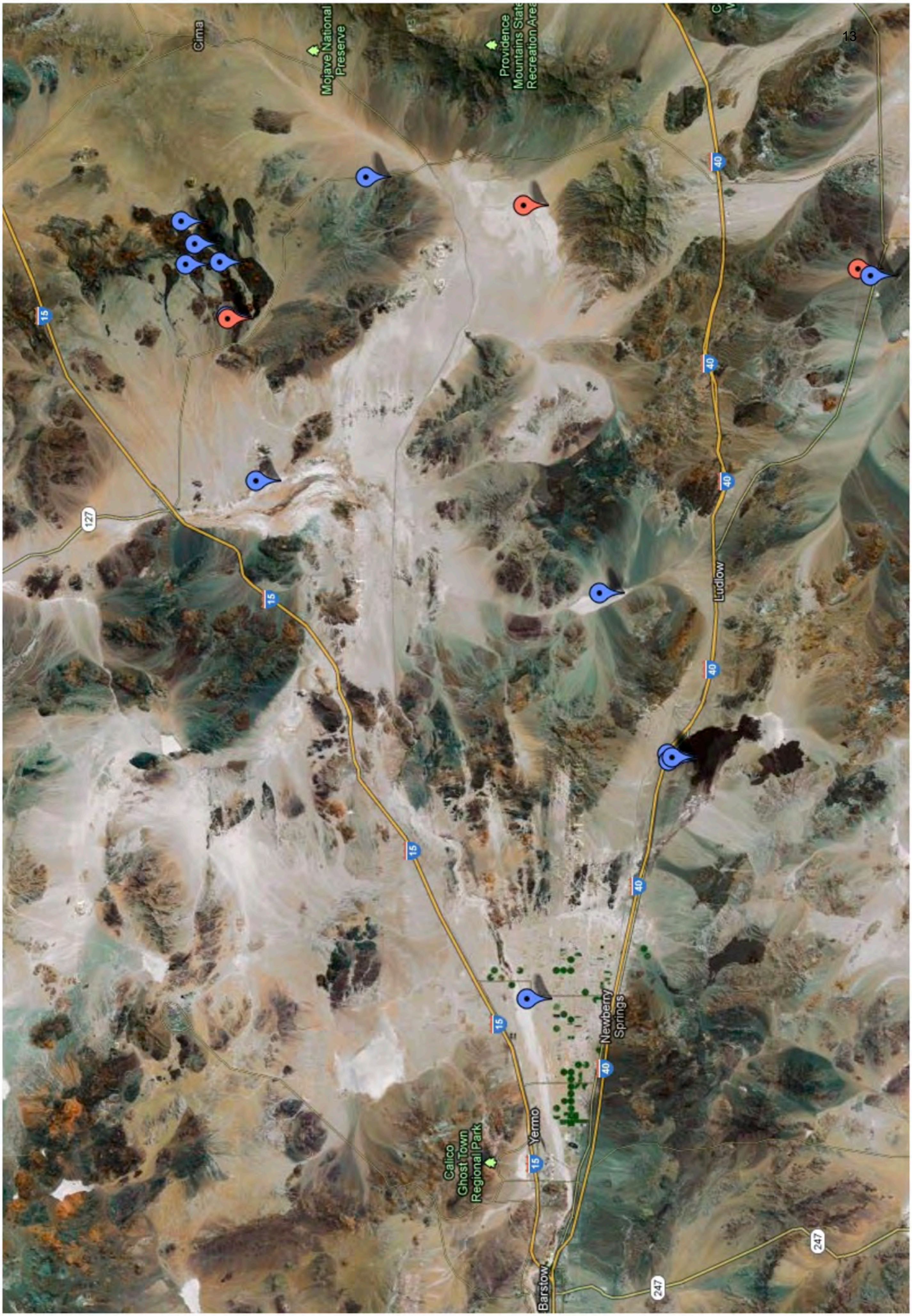
Cima
Mojave National Preserve
Providence Mountains State Recreation Area
15
127
40
Ludlow
Newberry Springs
Yermo
Calico Ghost Town Regional Park
Barstow
247

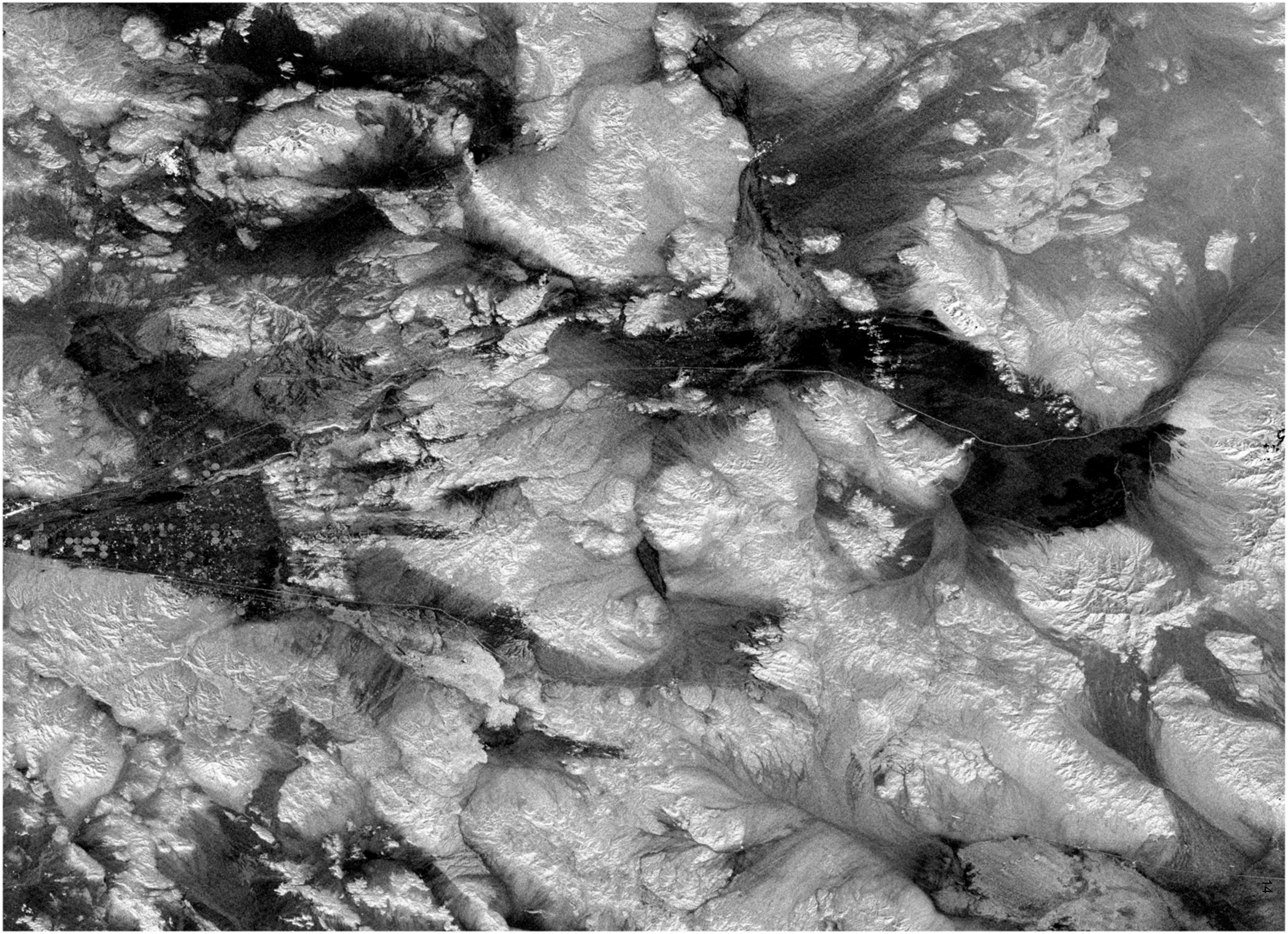

C-band backscatter data from SRTM

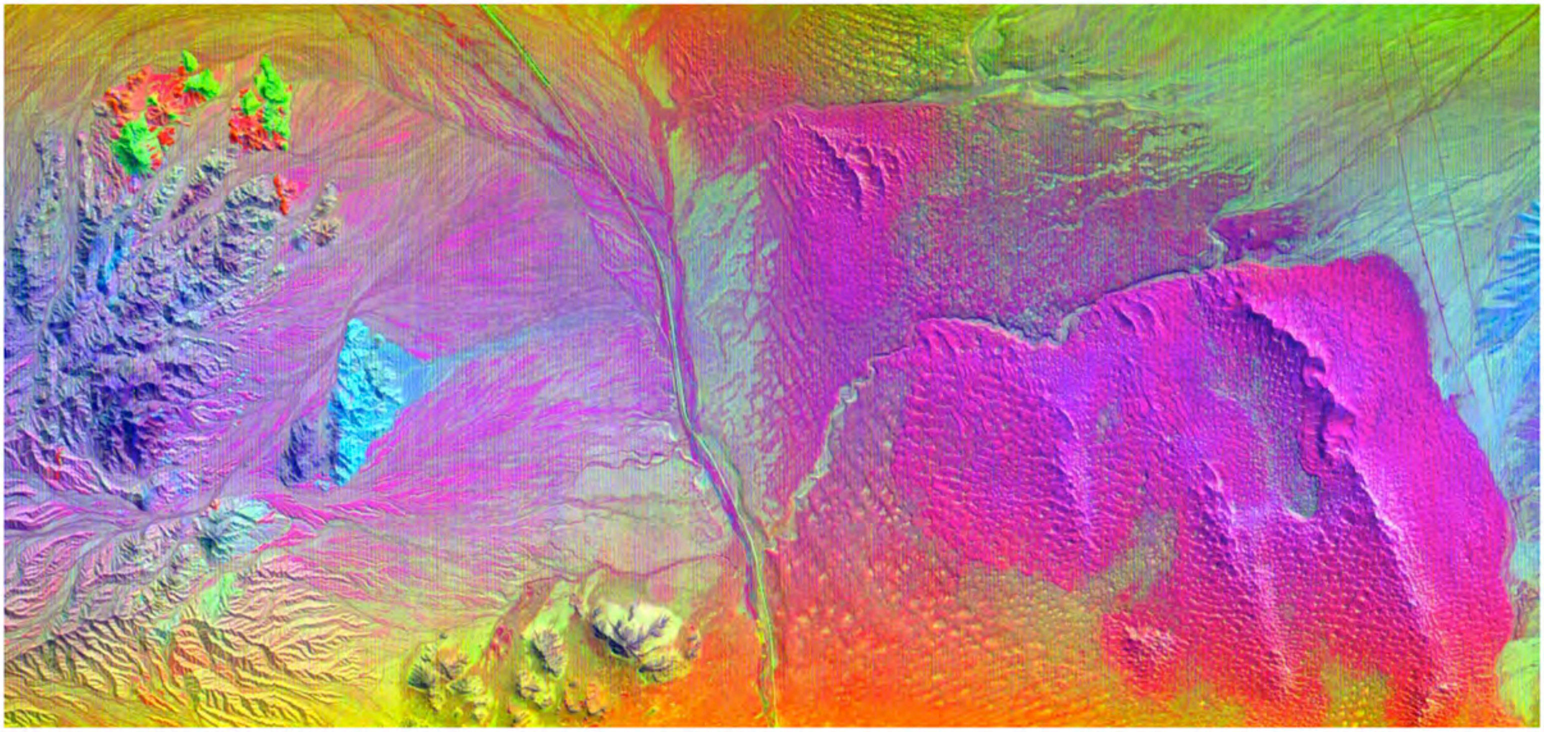

Kelso Dunes
Uniform surface composition IN TIR bands

Kelso Dunes
Old AIRSAR RADAR response

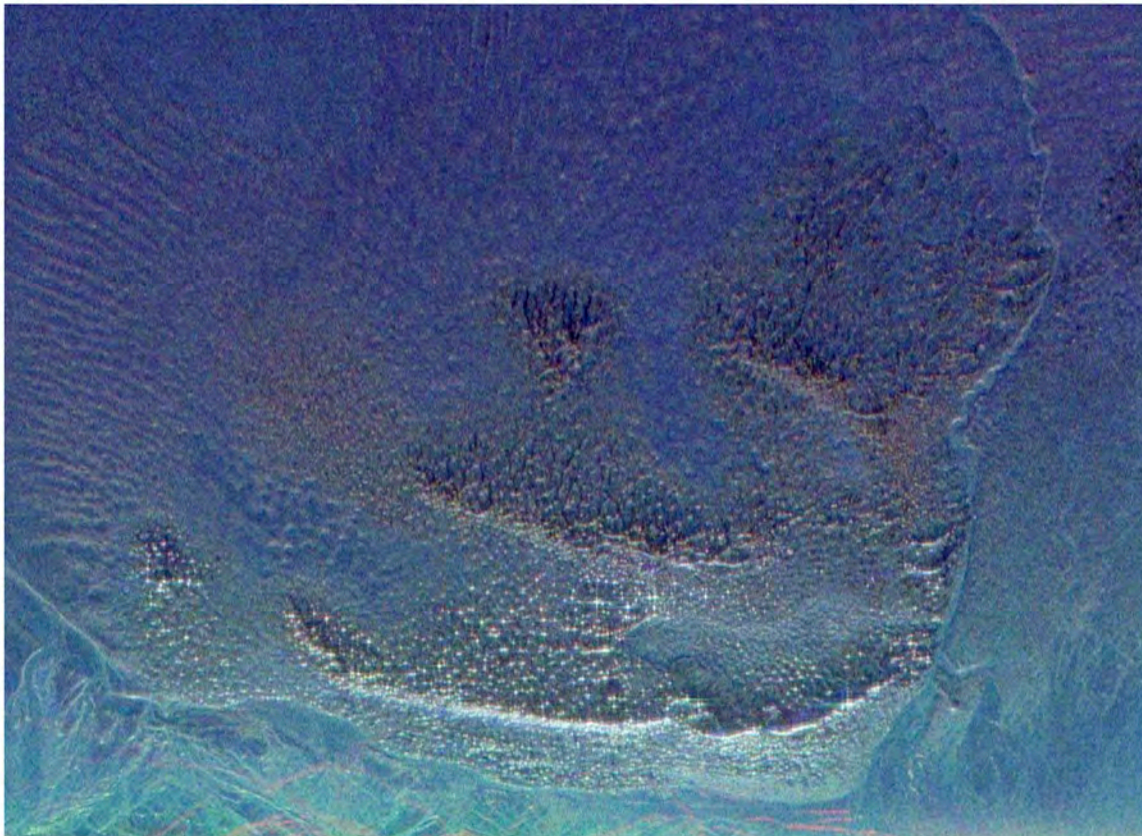

HH

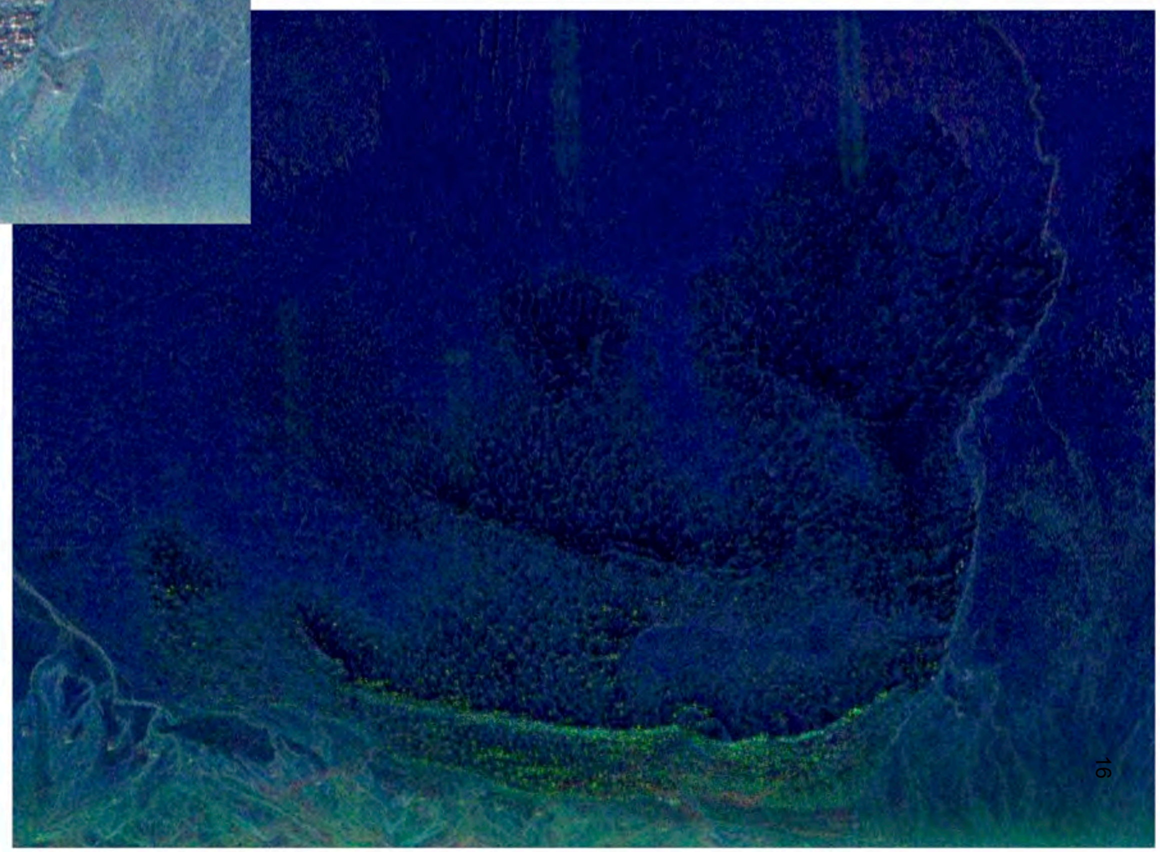

HV

P (80cm)
L (25 cm)
C (5cm)

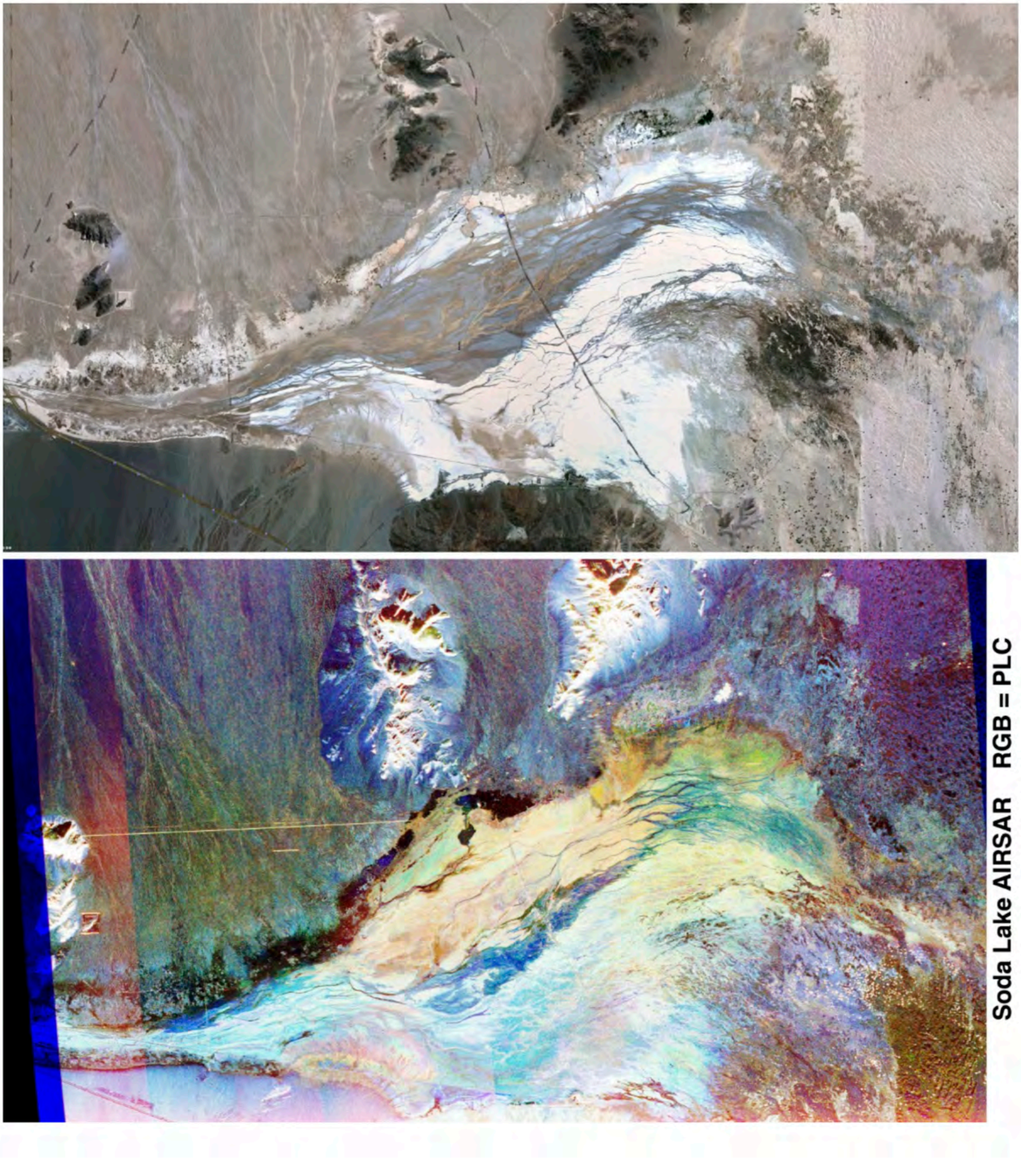

Soda Lake AIRSAR RGB = PLC


Ludlow
Needles Fwy
40
Needles Fwy

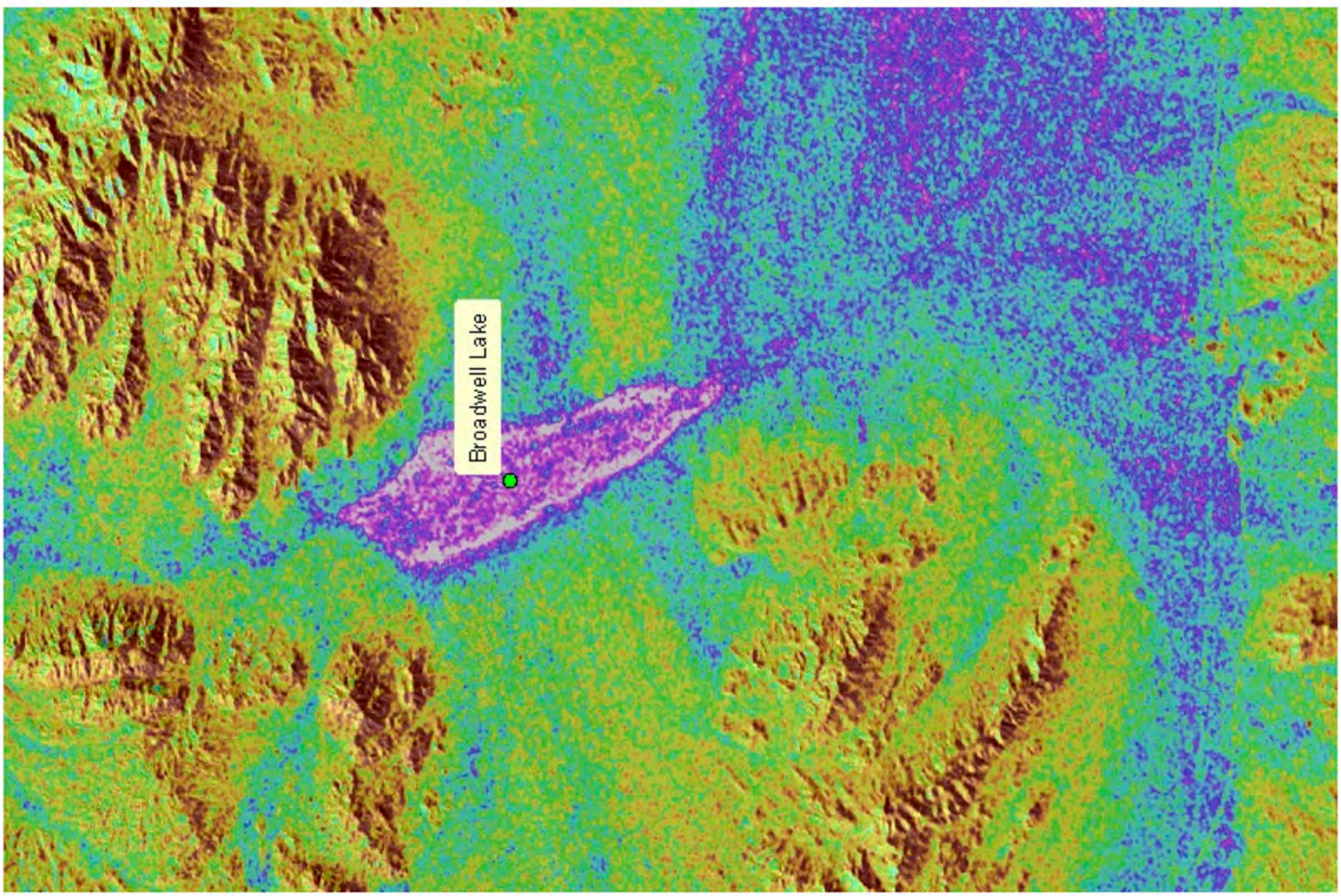
Broadwell Lake

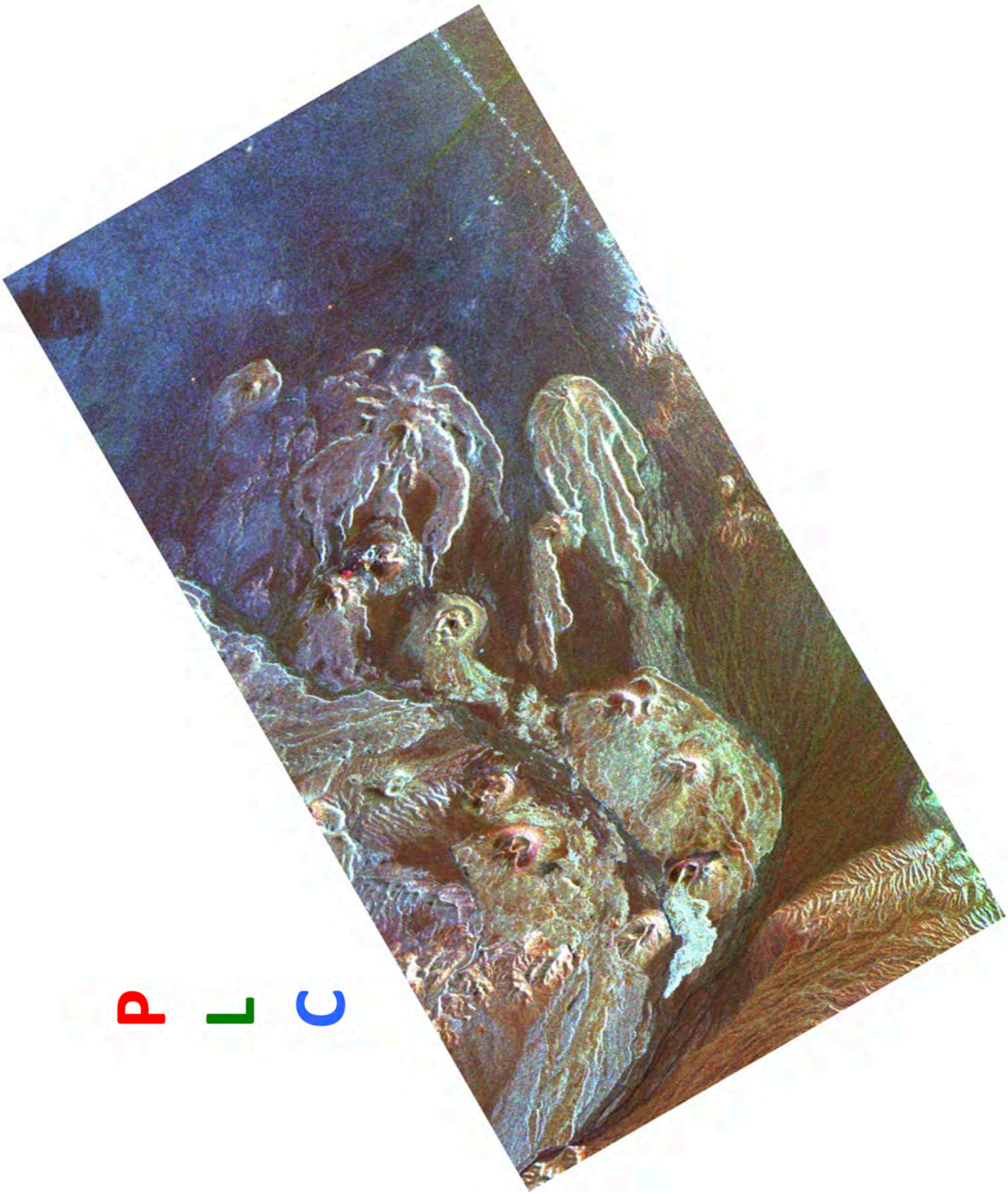
P
L
C

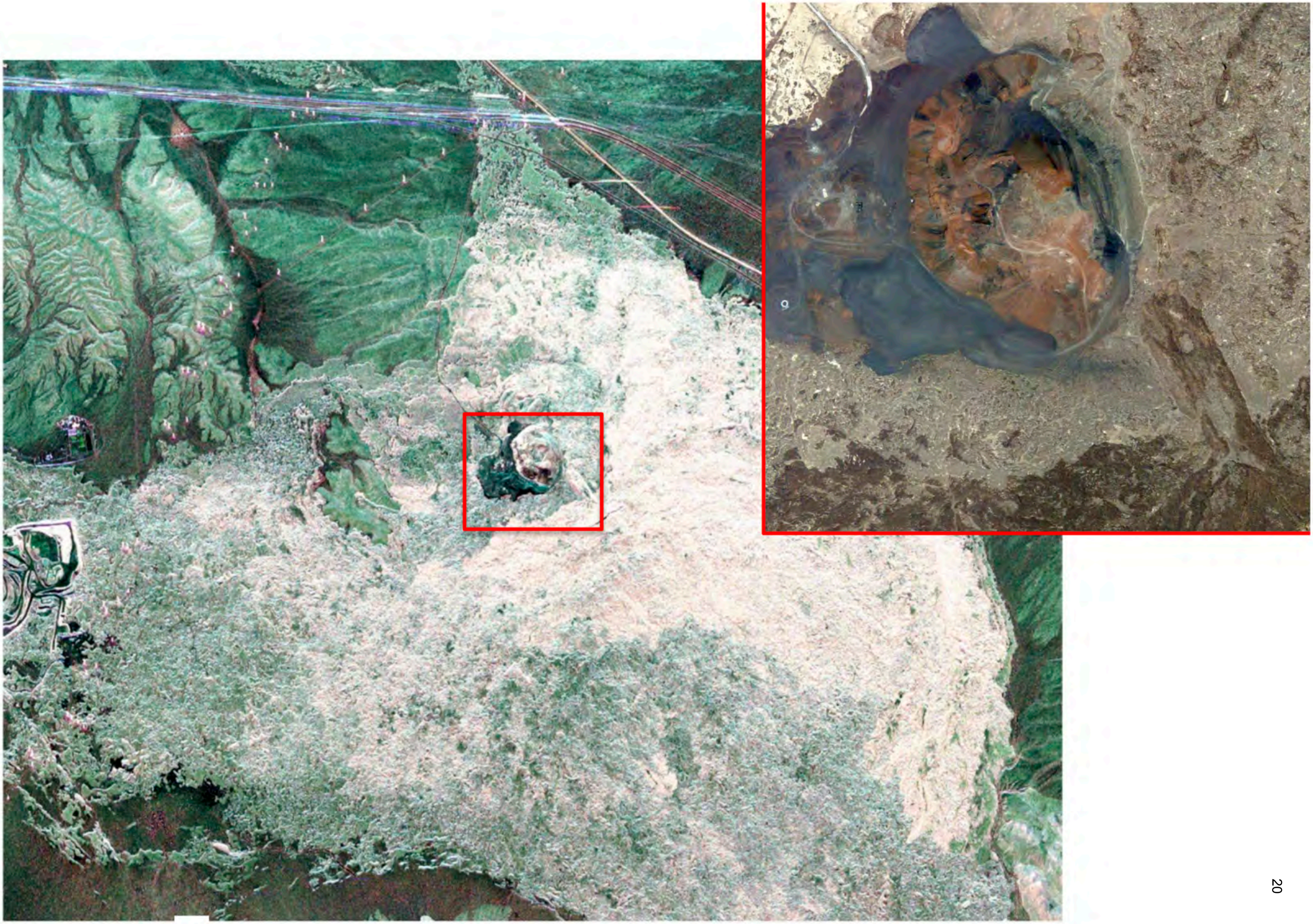

UAVSAR L-band of Pisgah Flow and Cone HV-VV-HH

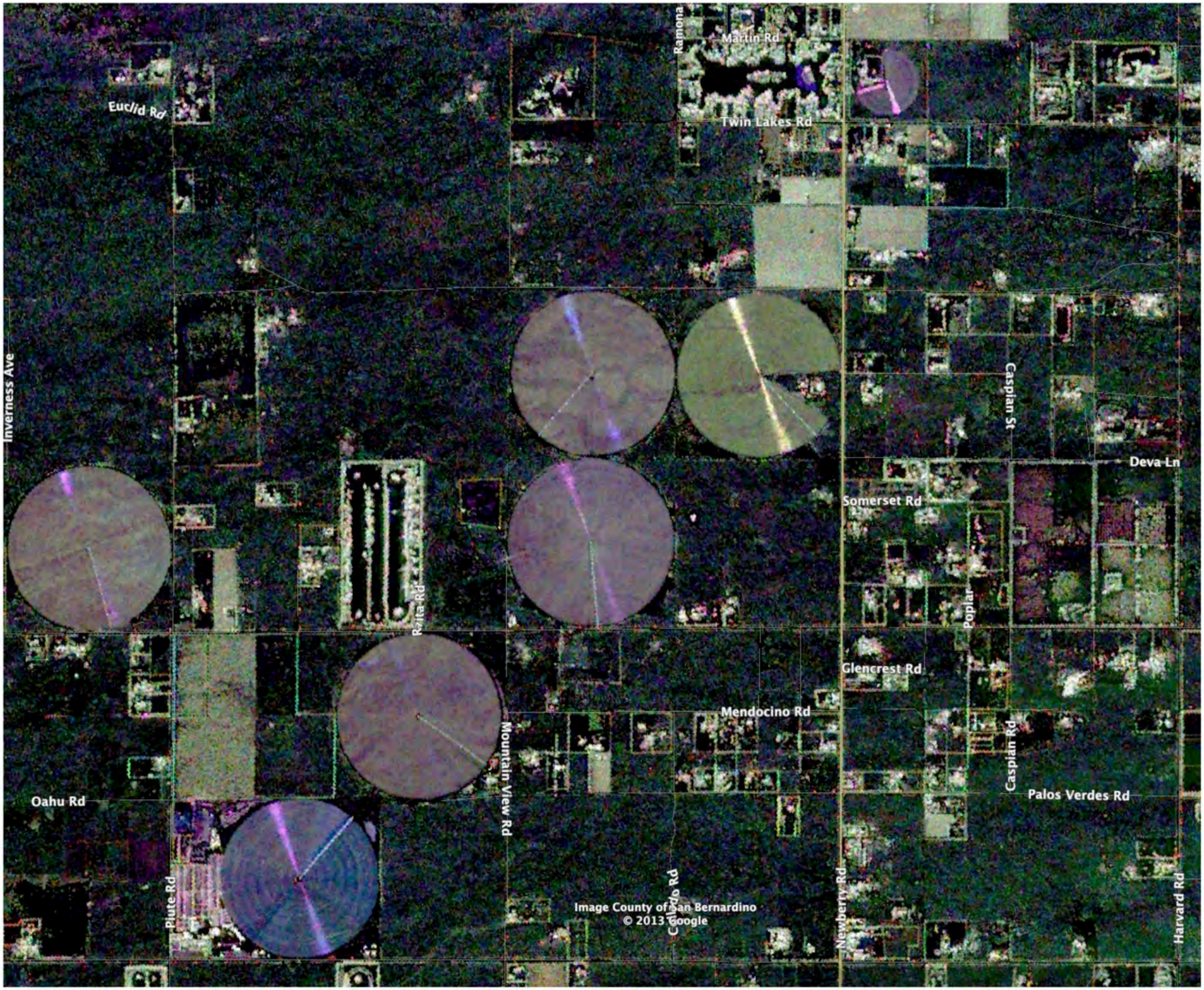

Mojave Agricultural Fields UAVSAR L-band RGB = HH-HV-VV

Kelbaker Road Outcrop

Variable surface composition

Just north of the Kelso Dunes

Kelbaker Road Outcrop

Variable surface composition

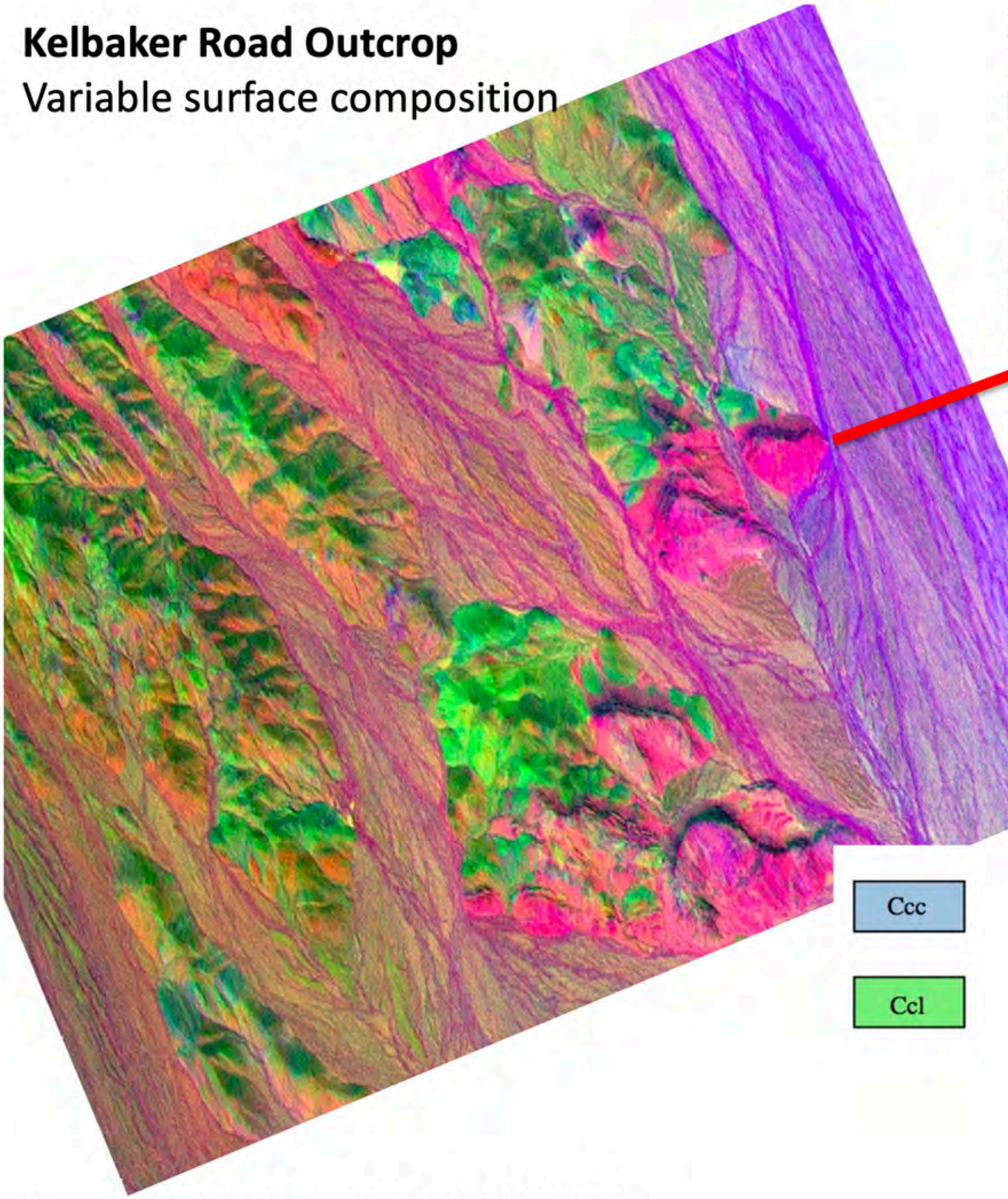

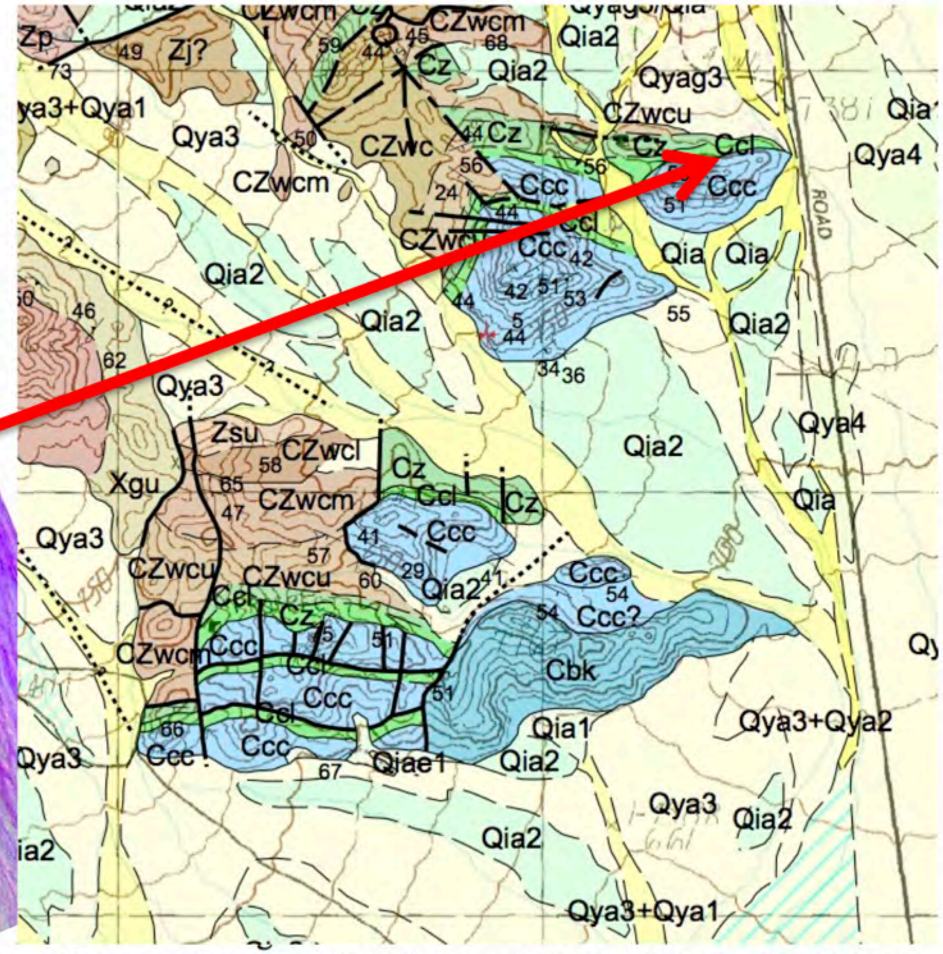

Ccc
Ccl

Carrara Formation (Middle and Early Cambrian) – Divided into:

Chambless Limestone (Early Cambrian) – Light-gray fine-grai
Bedding 1 to 2 meters thick. Heavily fractured with whi
due to faulting

Latham Shale (Early Cambrian) – Dark-green to locally browr
approximately 2 to 3 m below top of unit consists of buf

Bedford (2003)

Decorrelation stretch of MASTER bands 9.1, 2.4, 0.5 microns

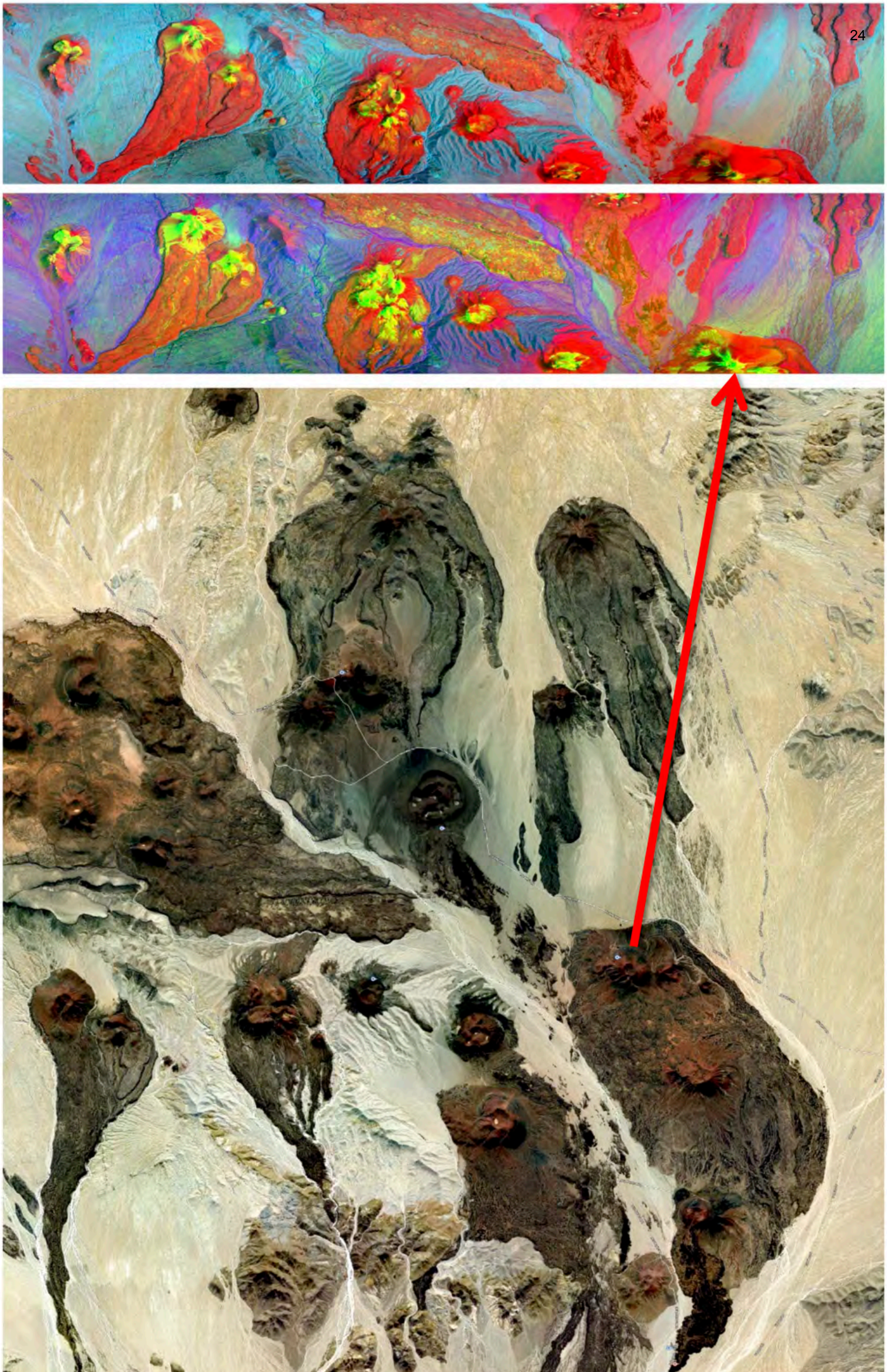

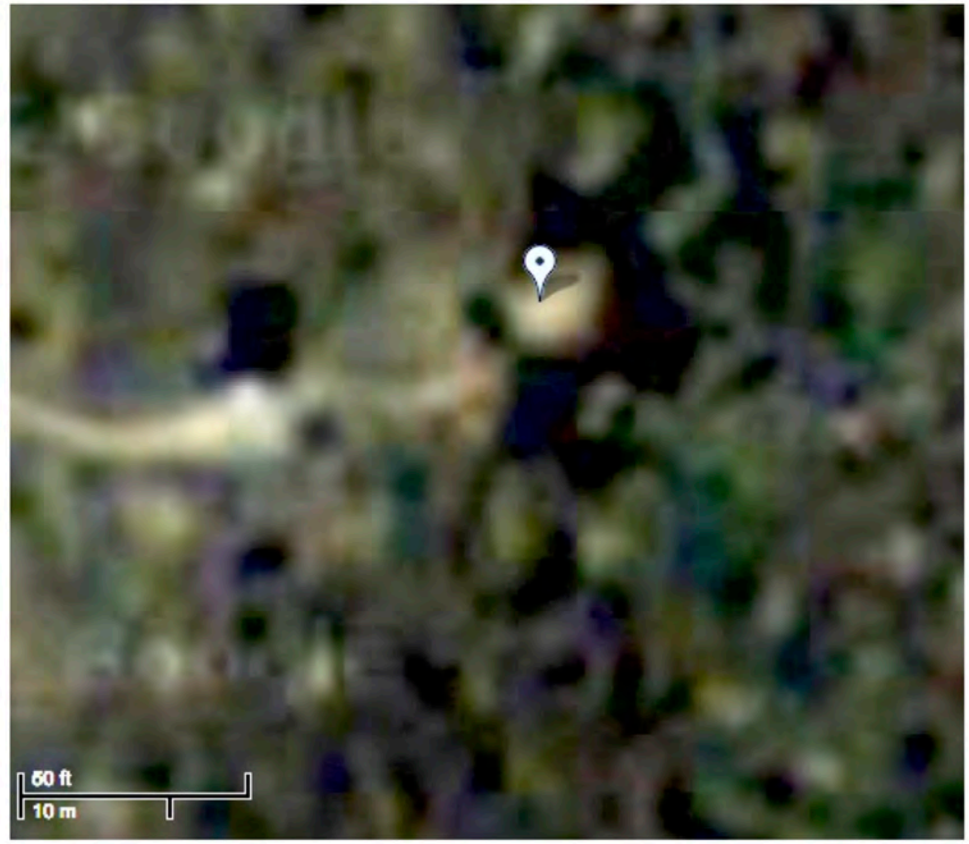

Pisgah

Caves and Pit Craters

Cima

Moon

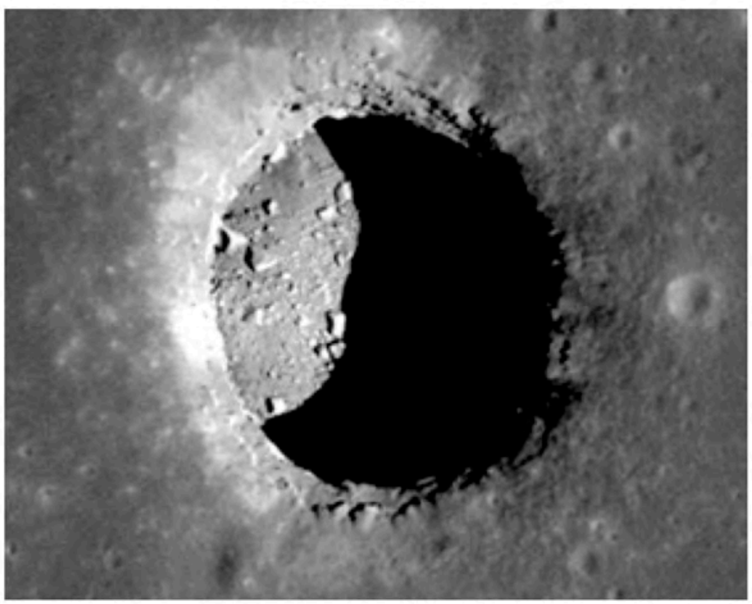

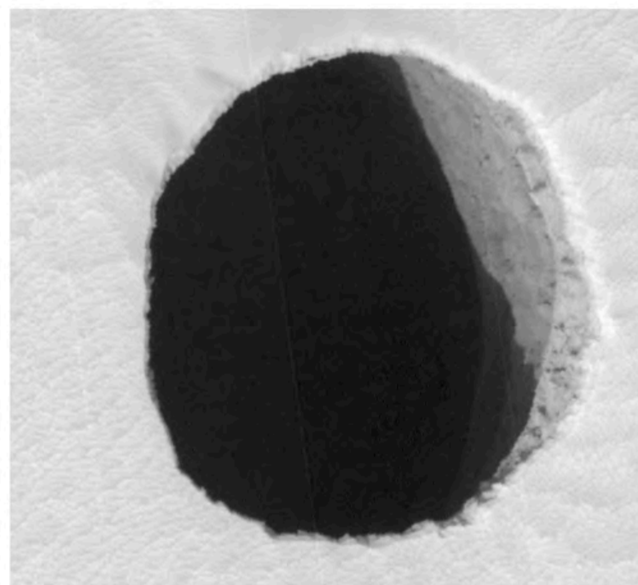

Mars

25

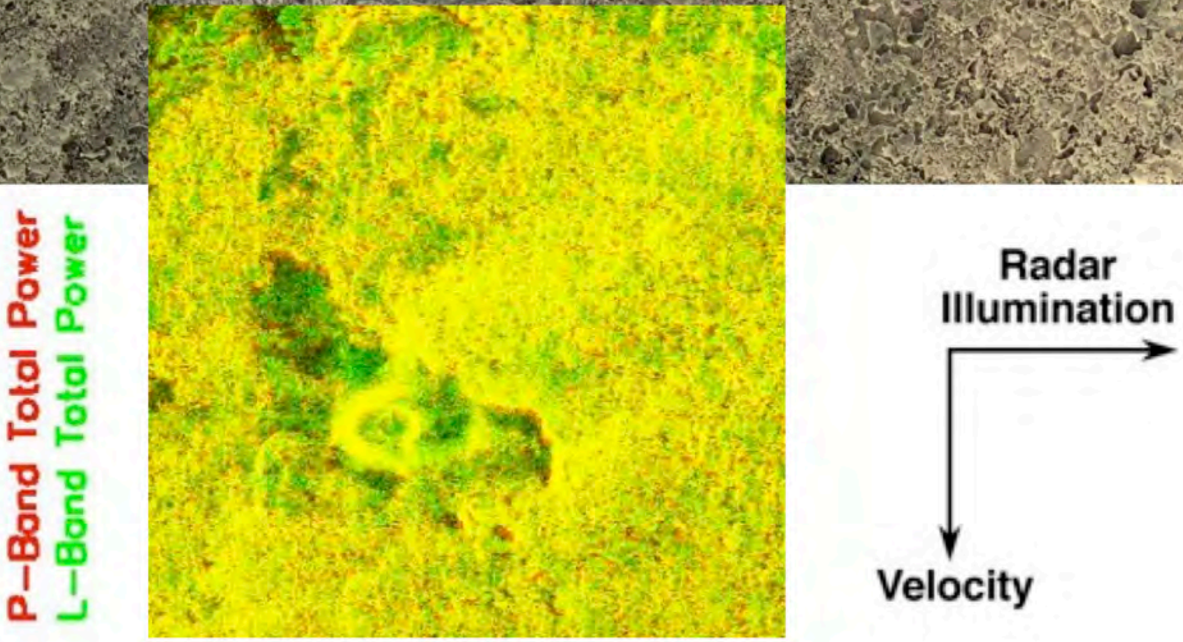
P–Band Total Power
L–Band Total Power
Radar
Illumination
Velocity

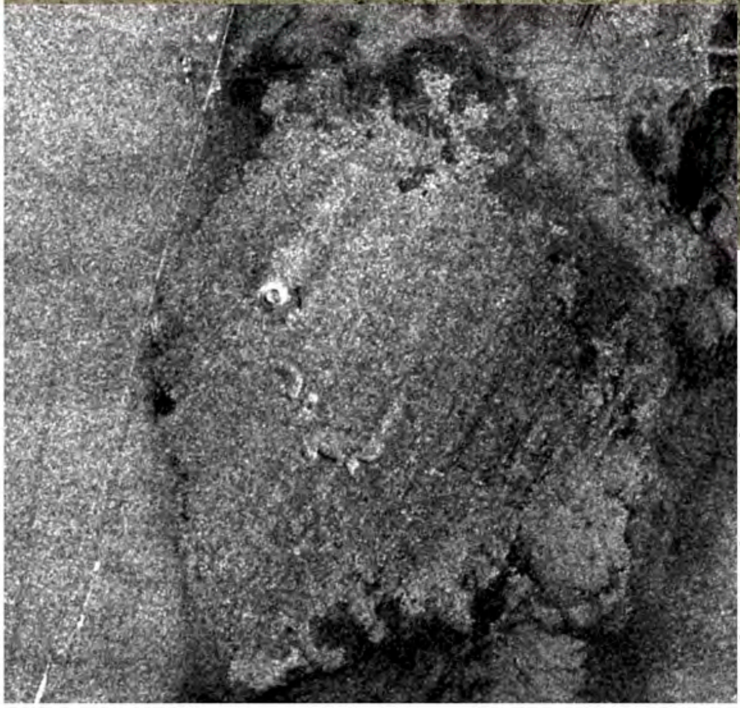

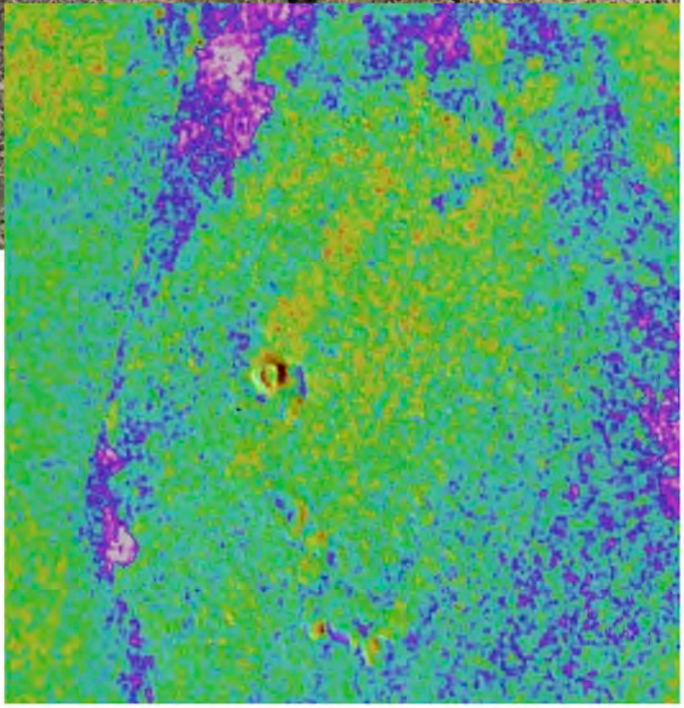

X-band total power
C-band total power

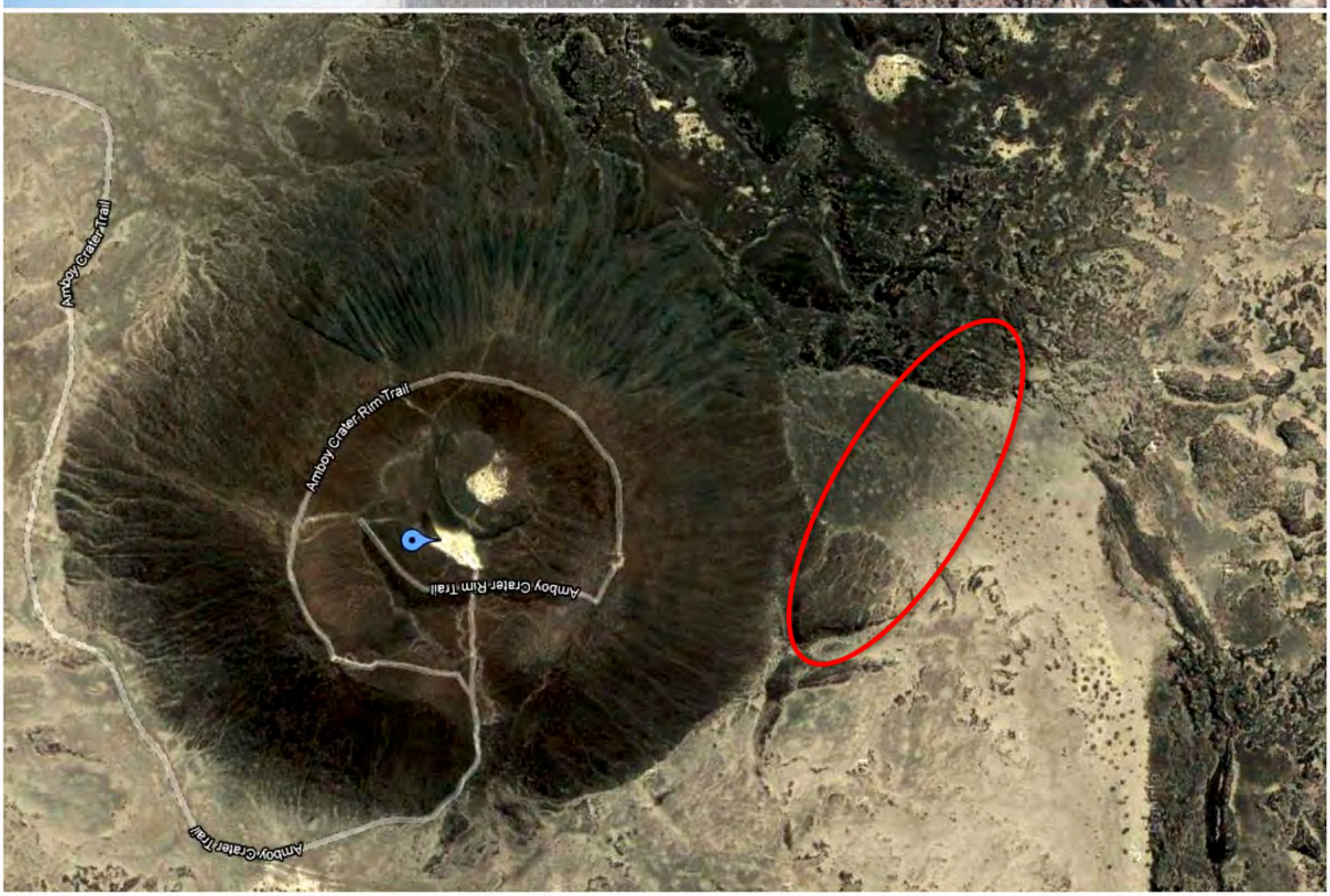
Amboy Crater Trail
Amboy Crater Rim Trail
Amboy Crater Rim Trail
Amboy Crater Trail

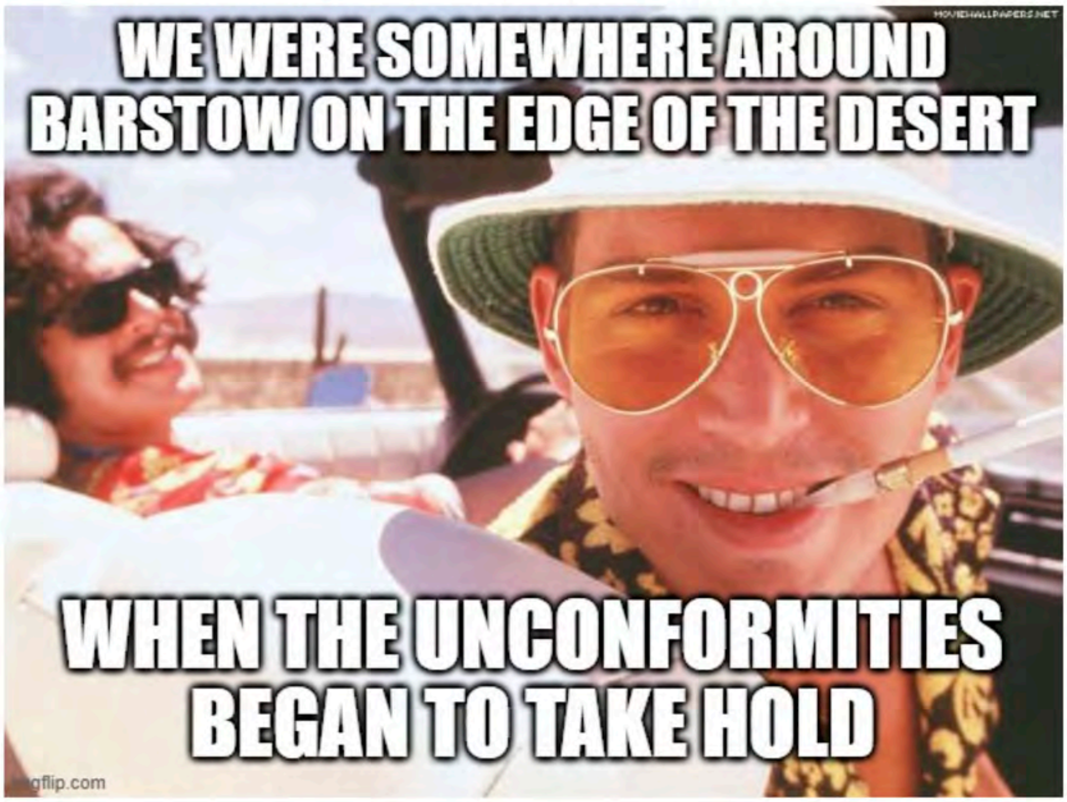
WE WERE SOMEWHERE AROUND BARSTOW ON THE EDGE OF THE DESERT
WHEN THE UNCONFORMITIES BEGAN TO TAKE HOLD
gflip.com

Peach Spring Tuff, Kingman, AZ

Definition of a Tuff: A pyroclastic deposit of > 75% ash (fines) containing pumice clasts sourced from an explosive eruption of a volcanic vent (Schmidt, 1981). In cases where the pyroclastic material is sufficiently hot after eruption when it is emplaced on the surface, it will weld together. The Peach Spring Tuff is an ash flow tuff that was emplaced by pyroclastic density currents and is further classified as an ignimbrite (Young & Brennan, 1974, Roche et al., 2016).

Location and Age of the Peach Spring Tuff

The Peach Spring Tuff (PST), classified as an ash flow tuff (60-80% ash by volume; Roche et al., 2016), is an ~18.8 Ma (Early Miocene) deposit covering ~32,000 km^2 throughout the bordering regions of Nevada, California, and Arizona (Foley et al., 2020). The location of the source caldera was generally known to be where the California, Nevada, and Arizona borders meet based on previous mapping efforts of the PST. The ~10 km diameter Silver Creek Caldera, located near Oatman, AZ, was finally identified as the PST source in 2006 when fragments of its rim were observed during a highway survey in the Black Mountains of Arizona by ADOT and the Arizona Geological Survey (Ferguson et al., 2013; Ferguson, 2016). A summary of the extent of this deposit and the location of its source caldera are shown in Figure 1 below.

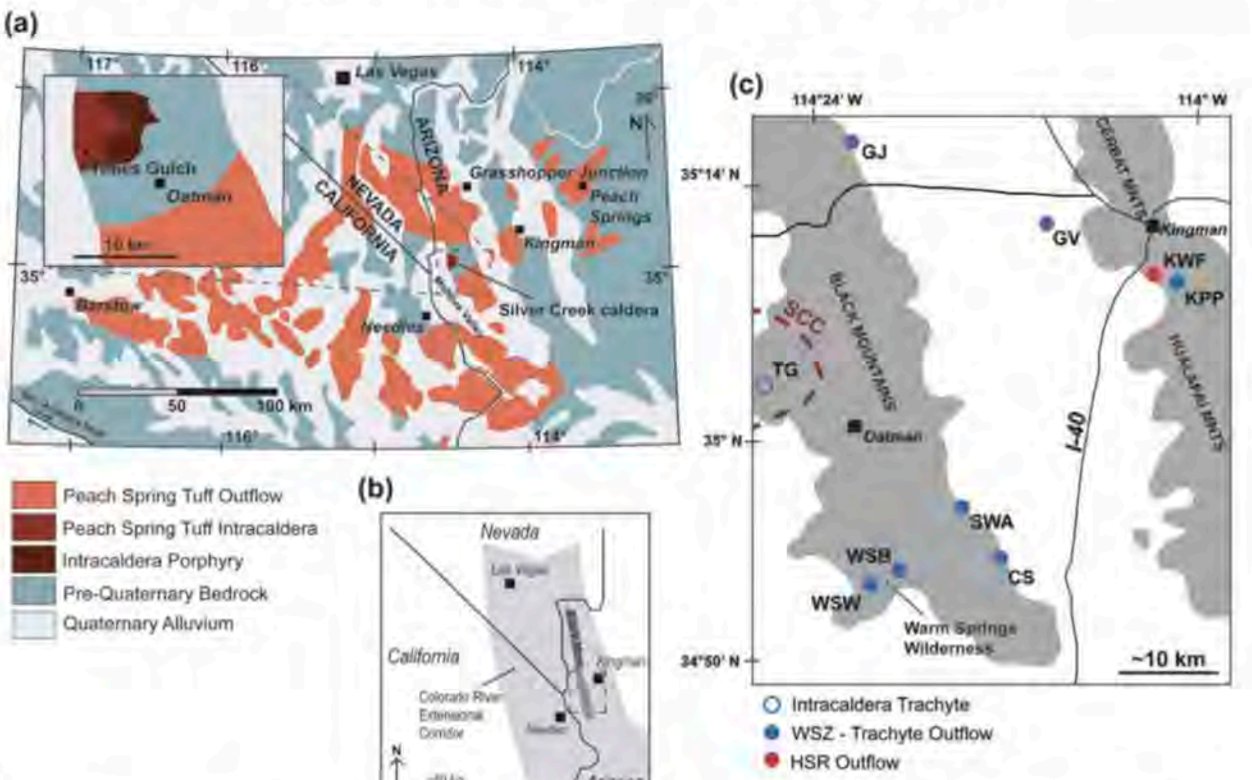

Figure 1. Figure 1 from Foley et al. (2020). Panel (a) is a geologic map summarizing the extent of the Peach Spring Tuff Outflow deposit with other related intracaldera deposits and intrusive porphyry deposits shown in the inset. Panel (b) highlights the location of the Black Mountains and its position in the Colorado River Extensional Corridor. Panel (c) is a summary of the relevant mountain ranges in the region. The Silver Creek Caldera (SCC) is shown with a red dashed line in the Black Mountains west of I-40.

Eruption, Deposit Extent, and Thickness

Figure 2. This is the Warm Springs exposure of the Peach Spring Tuff (PST) in the southern Black Mountains in Mohave County, Arizona. The larger cliff is the 18.8 Ma PST overlying the Cook Canyon Tuff. Image Credit: Charles Ferguson/AZGS.

A dense rock equivalent (DRE) total eruption volume of > 1300 km^3 was emplaced (Ferguson et al., 2013; Roche et al., 2016). This eruption has therefore been classified as a super-eruption by some workers (Pamukcu et al., 2013; Roche et al., 2016). The volume of the tuff itself is ~640 km^3 DRE (Pamukcu et al., 2013). The PST outflow extends ~170 km westward from the caldera after correcting for extension in the region (Foley et al., 2020). PST extends into the Mojave Desert (Glazner et al., 1986). The deposit ranges in thickness from 5-40 m but can be as thick as 220 m at some sites where material accumulated in low-lying topography (Roche et al., 2016). Within the caldera, the deposit thickness approaches ~450 m in thickness (Ferguson et al., 2013). The PST formed a coherent unit when it was originally deposited but erosion and extension post-dating the eruption has since broken up the deposit (Figure 1). The massive extent of the PST is indicative that it was likely sourced from a large magma reservoir at depth (Pamukcu et al., 2013).

Composition and Zones of the PST

The PST outflow is primarily rhyolitic in composition with 68-76% SiO_2 with a 4-20% phenocryst content (Ferguson et al., 2013). The Silver Creek intracaldera ignimbrite is trachytic with 65-68% SiO_2 and ~35% phenocrysts (Ferguson et al., 2013). These differences are indicators of compositional zonation of the ignimbrite, a common feature of large-volume deposits such as this one (Ferguson et al., 2013).

There are five recognized zones of the PST outflow in the Kingman area that are labeled Tp1-5 (Figure 3). Three of the zones are defined by the previously mentioned compositional zonation that is based on phenocryst and pumice content and another two zones are defined primarily by degree of welding (Ferguson & Cook, 2021). The Tp1-Tp2 boundary delineates the lower nonwelded and middle welded zones and the Tp3-Tp4 boundary delineates the middle welded and poorly welded zones. Within the Silver Creek Caldera, the trachytic ignimbrite is densely welded (Ferguson et al., 2013).

Stop on this Field Trip

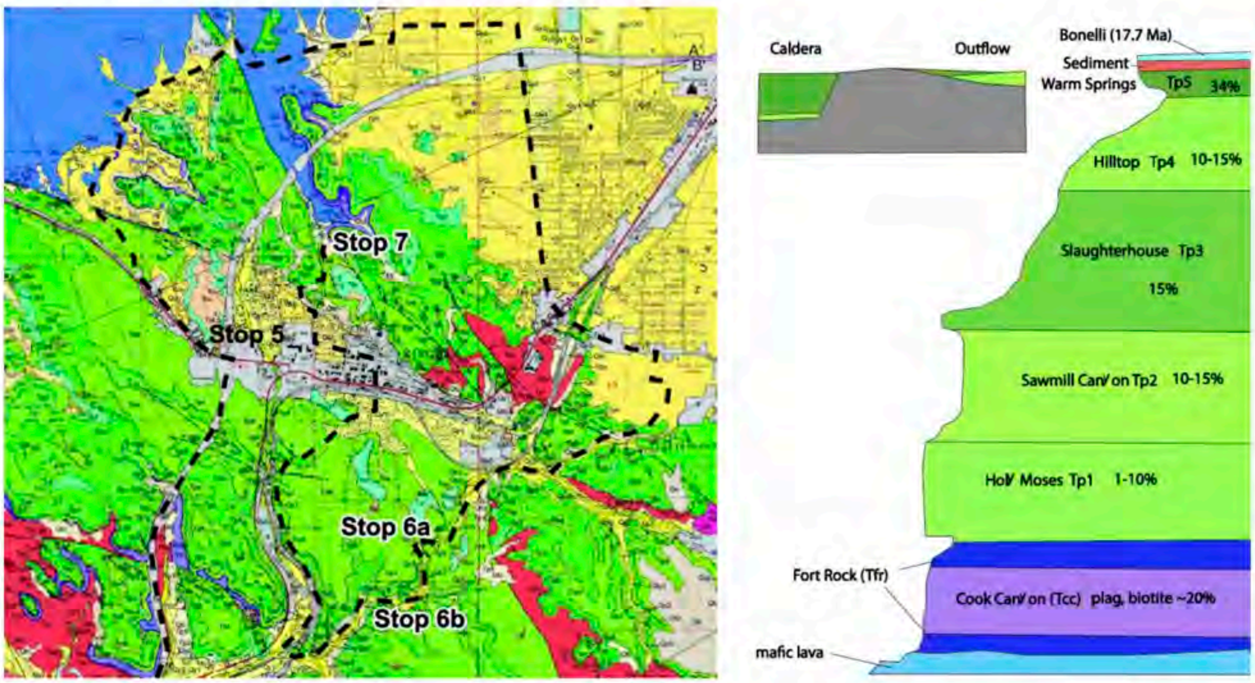

Figure 3. Left: Summary of the geologic units within the Kingman area. Our field trip will stop at Stop 5 on the map. **Right:** Cross-section of the volcanic strata in the Kingman area. Both figures are from field guide by Ferguson (2016). Percentages are estimates of phenocryst content through the column.

The following descriptions in this paragraph are adapted from the field trip guide by Ferguson (2016) on their Stop 5 which provides a view of an interesting road cut into the PST. Tp5 (Warm Springs Zone, trachytic composition and phenocryst-rich) is not shown in the cut but the Tp4 (Hilltop Zone) is covered by 5 m of pumice-rich sandstone and pumice lapilli. This is further covered by the Bonelli House Tuff that is younger than the PST at ~17.7 Ma. This is a rhyolitic ignimbrite that is made up of two flows: one which is < 1 m thick and the upper ~15 m thick flow. There is also a fault contact that is visible here. This fault is the result of strike-slip motion which is motion parallel to the strike resulting from converging crust. This compression created this half flower structure, shown in Figure 4 below, named so because the cross-section of this folded structure looks like that of a flower. The other half is further away by I-40 toward Beale Street.

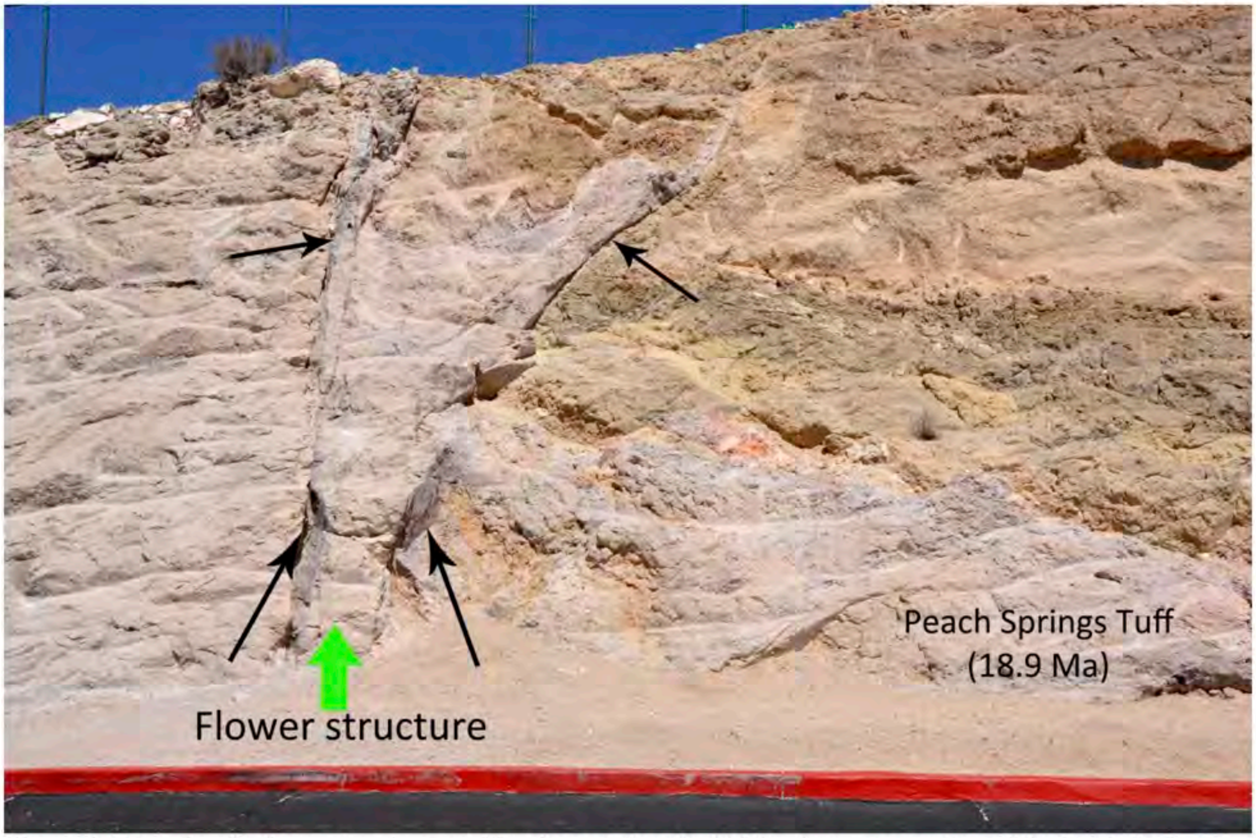

Figure 4. Example of a flower structure resulting from strike-slip faulting in a cross-section of the Peach Spring Tuff Deposit in Kingman, Arizona. Image Credit: Charles Ferguson/AZGS.

Connection to Planetary Science

Pyroclastic deposits are seen on terrestrial bodies such as the Moon, Mars, and Venus. Perhaps more similar to the PST, a highly debated, but large-scale example is the Medusae Fossae Formation (MFF) on Mars. It has been suggested that the MFF is a large pyroclastic deposit, which would make it the largest in the solar system, covering ~10^6 km^2 of the Martian surface (Ojha & Lewis, 2018). Its large size raises questions of how such a large pyroclastic deposit originated – whether it was from a single large eruption, or the result of multiple smaller events over a longer period of time (Ojha & Lewis, 2018).

References

Ferguson, C. A., McIntosh, W. C., & Miller, C. F. (2013). Silver Creek caldera—The tectonically dismembered source of the Peach Spring Tuff. *Geology*, *41*(1), 3–6. https://doi.org/10.1130/G33551.1

Ferguson, C. (2016). The Peach Spring Tuff, its source caldera, and implications for structural geology of the Colorado River Extensional Corridor. *Arizona Geological Society.* 29.

Ferguson, C. A., & Cook, J. P. (2021) Geologic Map of the Kingman 7 ½' Quadrangle, Mohave County, Arizona.

Foley, M. L., Miller, C. F., & Gualda, G. A. R. (2020). Architecture of a Super-sized Magma Chamber and Remobilization of its Basal Cumulate (Peach Spring Tuff, USA). *Journal of Petrology*, *61*(1), egaa020. doi: 10.1093/petrology/egaa020

Glazner, A. F., Nielson, J. E., Howard, K. A., & Miller, D. M. (1986). Correlation of the Peach Springs Tuff, a large-volume Miocene ignimbrite sheet in California and Arizona. *Geology*, *14*(10), 840–843. doi: 10.1130/0091-7613(1986)14<840:COTPST>2.0.CO;2

Ojha, L., & Lewis, K. (2018). The Density of the Medusae Fossae Formation: Implications for its Composition, Origin, and Importance in Martian History. *Journal of Geophysical Research: Planets*, *123*(6), 1368–1379. doi: 10.1029/2018JE005565

Pamukcu, A. S., Carley, T. L., Gualda, G. A. R., Miller, C. F., & Ferguson, C. A. (2013). The Evolution of the Peach Spring Giant Magma Body: Evidence from Accessory Mineral Textures and Compositions, Bulk Pumice and Glass Geochemistry, and Rhyolite-MELTS Modeling. *Journal of Petrology*, *54*(6), 1109–1148. doi: 10.1093/petrology/egt007

Roche, O., Buesch, D. C., & Valentine, G. A. (2016). Slow-moving and far-travelled dense pyroclastic flows during the Peach Spring super-eruption. *Nature Communications*, *7*(1), 10890. doi: 10.1038/ncomms10890

Schmidt, R. (1981). Descriptive nomenclature and classification of pyroclastic deposits and fragments. *Geologische Rundschau*, *70*(2), 794–799. doi: 10.1007/BF01822152

YOUNG, R. A., & BRENNAN, W. J. (1974). Peach Springs Tuff: Its Bearing on Structural Evolution of the Colorado Plateau and Development of Cenozoic Drainage in Mohave County, Arizona. *GSA Bulletin*, *85*(1), 83–90. doi: 10.1130/0016-7606(1974)85<83:PSTIBO>2.0.CO;2

Figure 2: A USGS researcher discovers the source of sand in Kelso Dunes; image from Herbert 1965

Radar and Sand Dunes on Earth and Titan

Harry Tang

Sand dunes at Kelso

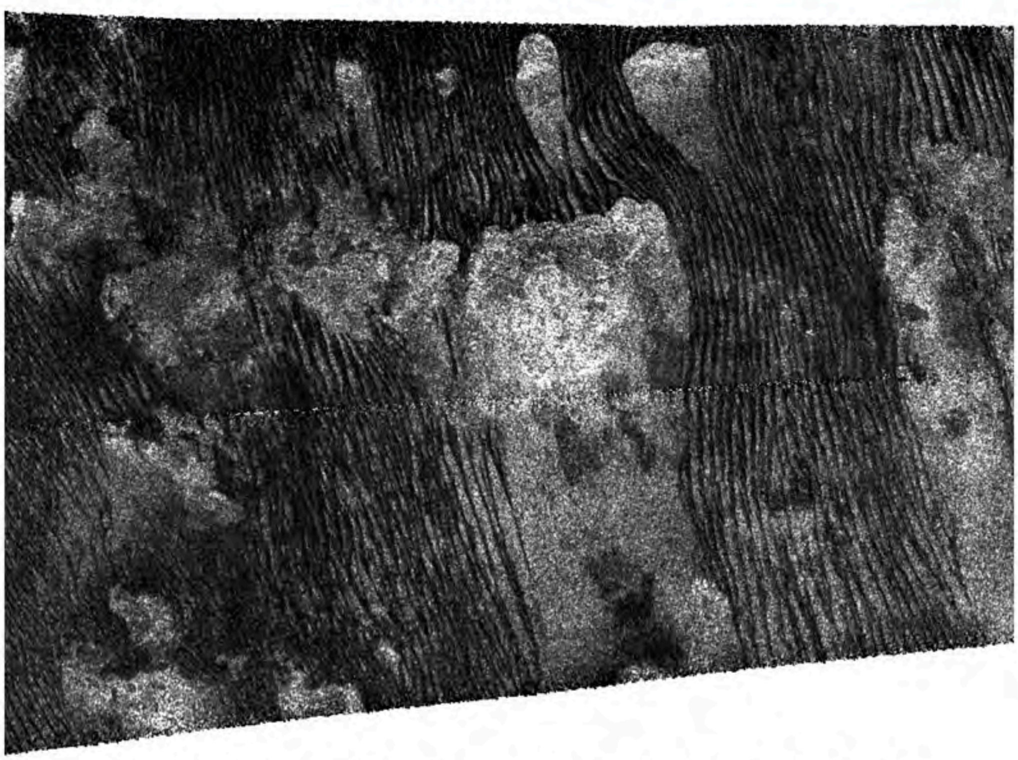

Sand dunes on Titan, Cassini radar (NASA/JPL-Caltech)

Dunes are a product of aeolian processes on a planetary surface, formed from movement of (usually on Earth) sand particles. Sand particles tend to bounce off rocks but stick to sand, allowing them to form hills in very sandy areas. These hills experience different shear forces on the upwind (stoss) and downwind (lee) sides, causing material to be moved from the stoss-slope to the lee-slope.

These materials deposit near the top of the lee-slope, and as they gather, they create steeper slopes, eventually reaching a point where the shear stress becomes zero. This means that the sand particles continue to build up the slope until it approaches the angle of repose, forcing material to move downslope, and the dune to move forward.

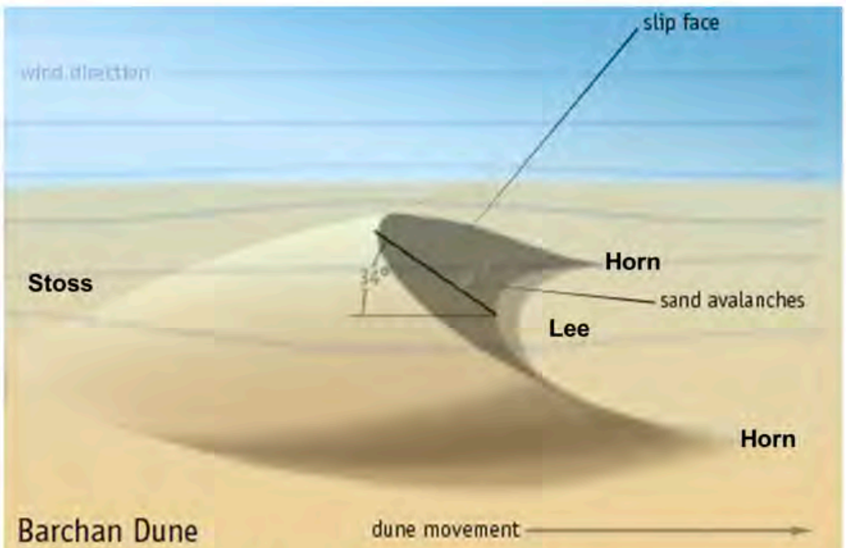

Components of a sand dune

Dunes come in many different forms, which depend on the sand supply and the direction of the wind that forms them. Some of the more prominent ones are listed here.

Barchan Dunes:

Crescent shaped dunes that result from unidirectional winds at a location with a relatively limited amount of sand. Their horns point towards the downwind direction.

Barchan dunes on Mars (NASA HiRISE)

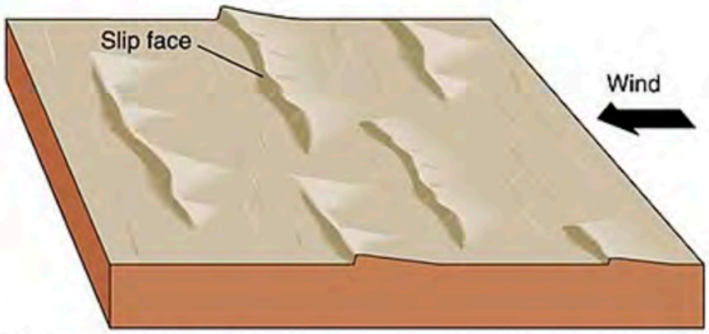

B Transverse dunes

Transverse Dunes:

When there is more abundant sand supply with predominantly unidirectional wind, numerous barchan dunes can form, and merge together to form transverse dunes, where the dunes form lines perpendicular to the wind direction.

Linear/Longitudinal Dunes:

Where there are predominantly bidirectional winds, the dunes will form lines parallel to the average wind direction. Often, context clues from surrounding landforms are useful to differentiate these from the transverse dunes.

Star Dunes:

When the wind direction varies significantly, star dunes can be formed. These pyramidal shaped mounds have slipfaces on three or more “arms” that radiate from the center. These tend to build up instead of moving laterally.

Radar Observations of Sand Dunes:

The brightness of a radar image is the backscattering received by the antenna. This depends on observation angles, surface properties, surface composition, and wavelength of the radar waves. Using the backscatter from a variety of wavelengths and polarizations, we can probe important characteristics of the interested landscape.

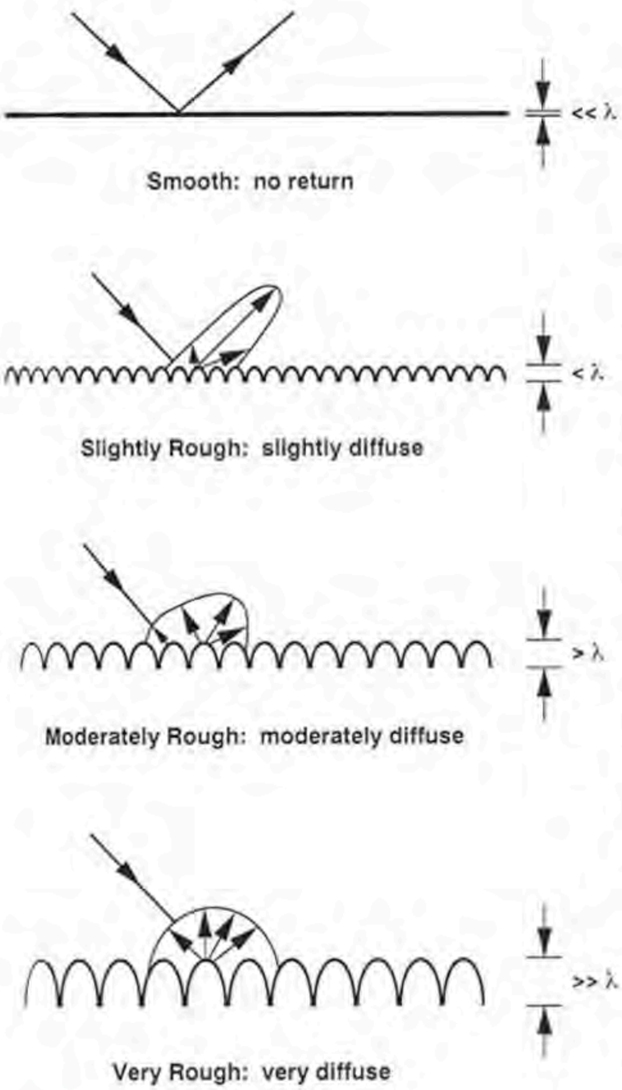

The most prominent features in the Kelso dune radar images are bright spots in the HH images, which appear along and slightly north of the main ridge of the dunes. These strong reflectance are likely due to the shape of the dunes, where star dune formation can form trihedral reflector shapes that produce especially strong radar reflectances.

The difference in backscatter due to wavelength and polarization can reveal information about surface roughness and composition. In general, smooth surfaces are dark. Radar images of the Kelso dunes show strong backscattering in the C-band, especially for the HV polarization. This is likely due to ripples on the dunes, as well as strong volume scattering by vegetation, which can be seen in satellite visual imagery. Curiously, there are also strong L-band HV backscatter near the ridges, which are usually associated with volume scattering by larger foliages.

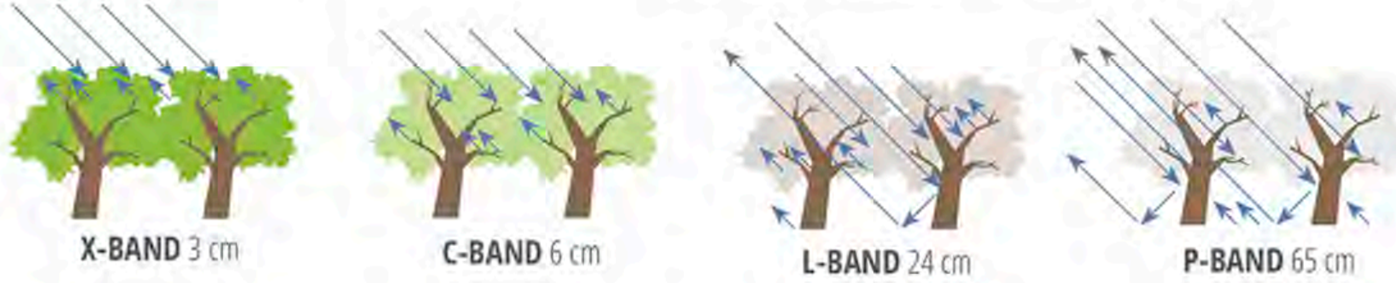

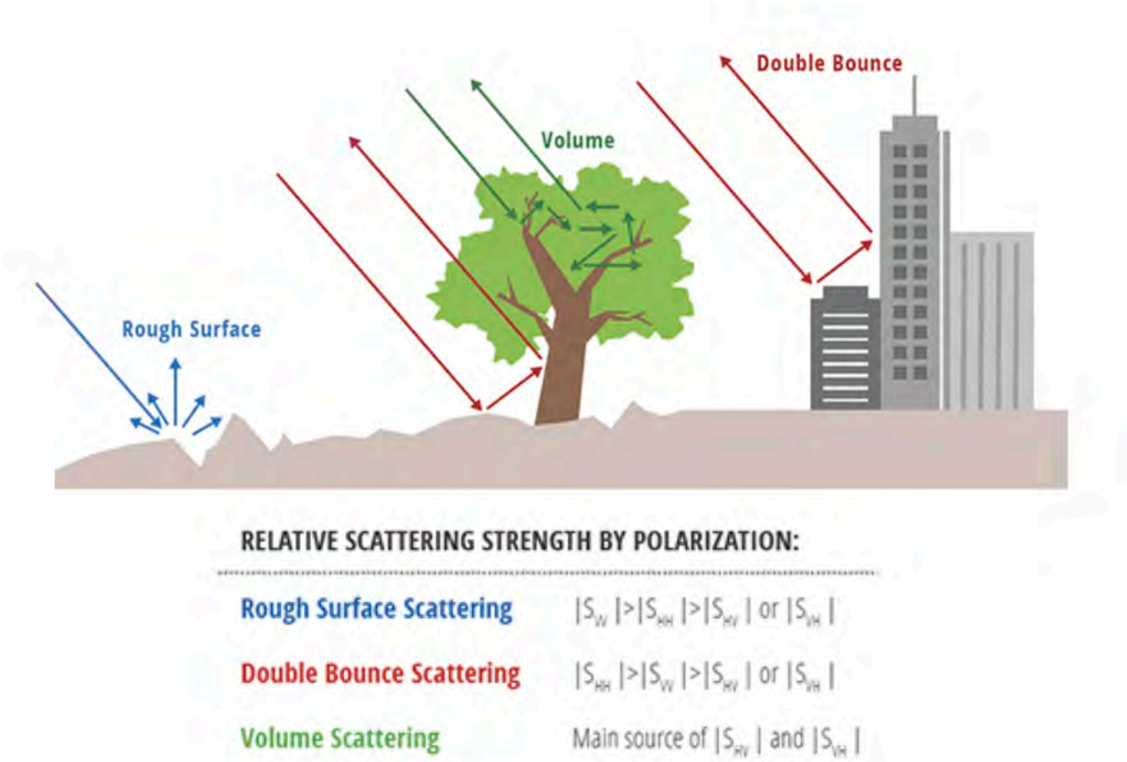

P-band (red color, 80cm) is generally the best for the topography of the Kelso dunes. Dune shapes can be clearly seen.

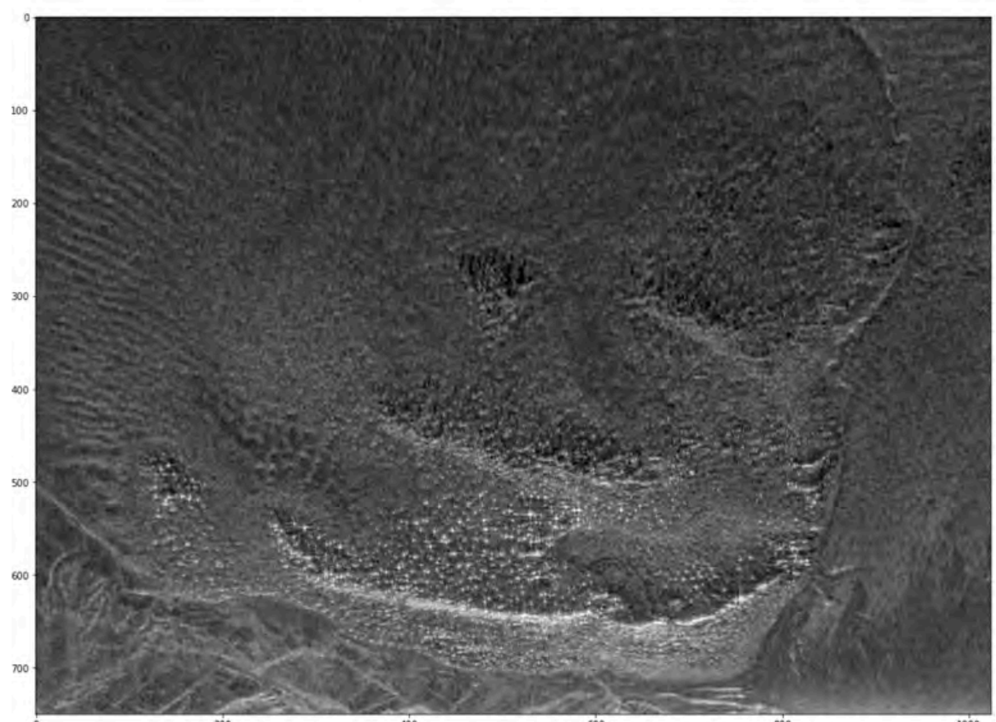

Dunes on Titan:

Large, linear features can be seen in the equatorial regions of Titan in radar data from Cassini, and they were confirmed to be dunes when viewing conditions allowed detections of glints. The dunes are the dark lines, due to their smoothness and composition. The dunes are composed not of quartz sand, but of organic sand, while ice and larger particles make up the lighter interdune areas. The contrast is mainly due to differences in the dielectric constants.

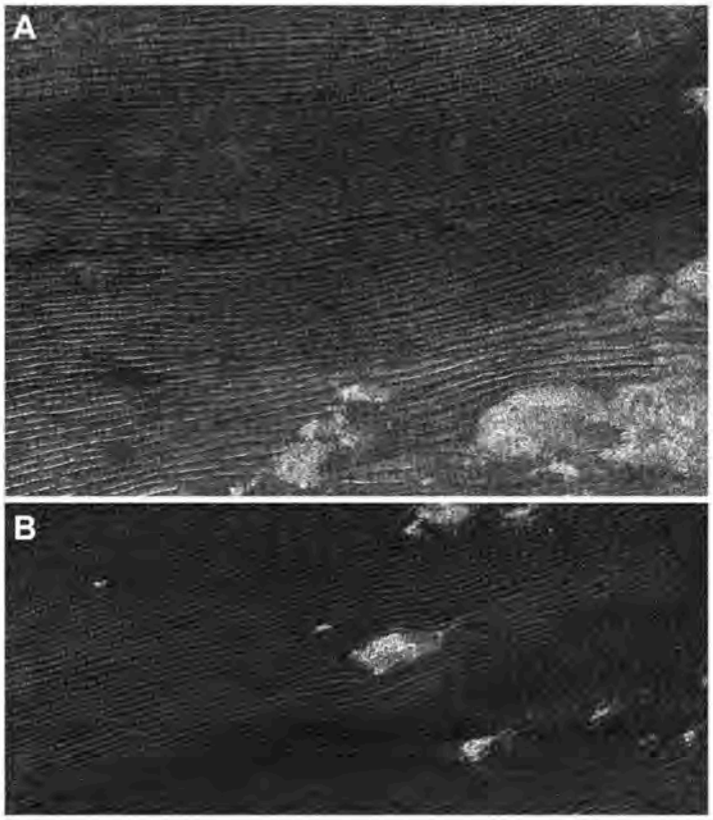

The dunes seen by Cassini radar are ~1km wide, and are only detectable by SAR. It is likely that smaller and different shaped dunes exist on Titan, but are not detectable with Cassini data. The upcoming Dragonfly mission aims to explore the dunes of Titan, and is expected to bring back valuable data.

The origin of the organic sand is highly debated, though will hopefully be resolved by Dragonfly data. However, observations on the sand on surrounding landscapes indicate a west to east particle migration direction. However, this runs counter to global climate models of Titan. This may be resolved by particularly strong winds that occur during equinox storms, which blow in the west-east direction. Since aeolian transport is a function of the cube of the wind speed, this could explain the formation of the Titan dunes.

References:

Course notes, PTYS 554, University of Arizona
Course notes, ASTR 6577, Cornell University
Blumberg, 1998, *REMOTE SENS. ENVIRON. 65*:204-216
https://earthdata.nasa.gov/learn/backgrounders/what-is-sar
Lea Bonnefoy, interviewed on March 10th, 2022
Lorenz et al., 2006, *Science 312*, 724-727

the Fremen cross desert spaces using the sand walk, a dance-like motion with irregular rhythm which emulates the natural sounds of the desert.

Booming Dunes

What are booming dunes?

Booming dunes are those that create a low-frequency, sometimes music-like sound when sheared. The sound has been compared to various instruments including drums, trumpets, and pipe organs, but also to foghorns, thunder, and helicopters, with clearer sounds usually occurring when a smaller amount of sand is moved (Nori et al., 1997). These sounds can be loud, sometimes heard up to 10 km away, and are accompanied by seismic vibrations, which are produced many times more efficiently than the corresponding acoustic vibrations (Nori et al., 1997; Sholtz et al., 1997).

The sounds (Figs 1 and 2) are typically at a frequency between 50 and 300 Hz, though the specific range varies for different dunes and the sound usually lasts for seconds but can last for up to fifteen minutes (Nori et al., 1997). Often, multiple frequencies are emitted, but never more than one harmonic (multiple) of the fundamental (lowest) frequency (Nori et al., 1997). Booming dunes differ from other types of sound-producing dunes (called squeaking dunes), which tend to emit sound more quietly, at a higher frequency (between 500 and 2500 Hz), and for only a fraction of a second (Nori et al., 1997).

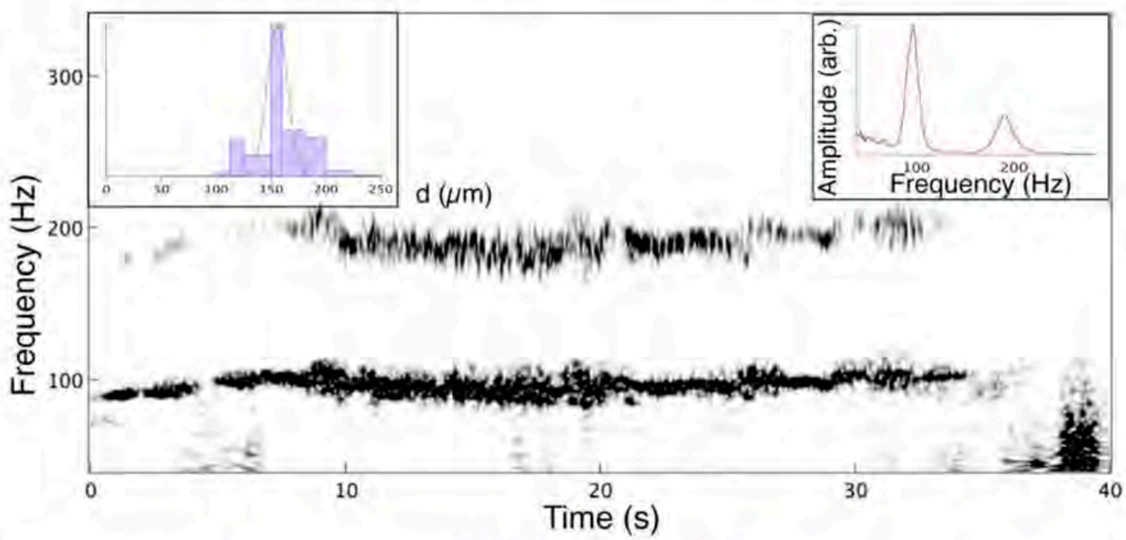

Figure 1: Spectrogram of a sound-producing event at a megabarchan dune near Tarfaya, Morocco. The right inset shows a fundamental frequency of 100 ± 5 Hz and a harmonic at 195 ± 10 Hz. The left inset shows the grain size distribution of the dune, with a peak at 150 μm. From (Dagois-Bohy et al., 2012).

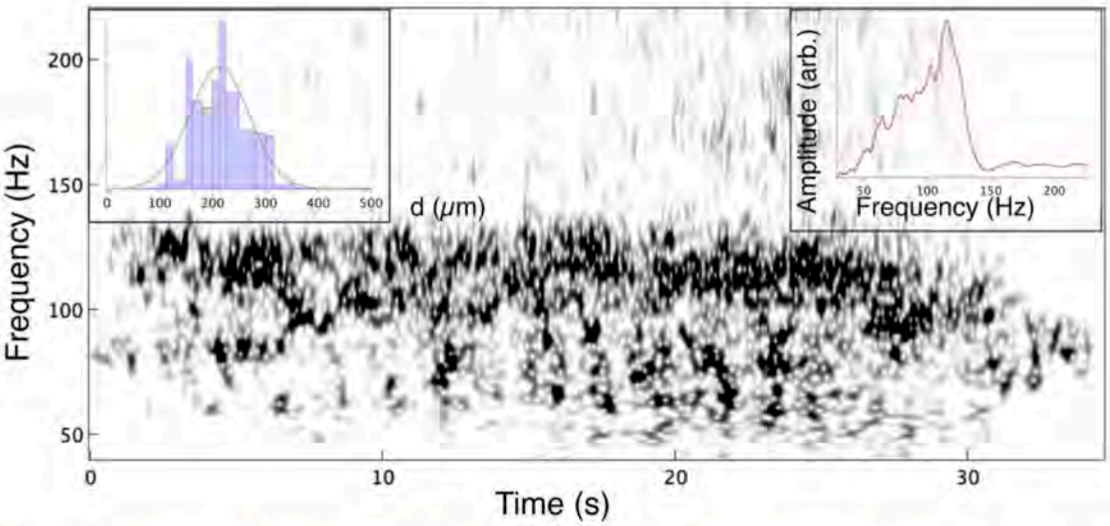

Figure 2: Spectrogram of a sound-producing event at Al-Askhara double-barchan dune, Oman. The right inset shows a broad frequency distribution with a maximum at 120 Hz. The left inset shows the grain size distribution of the dune, also broad. From (Dagois-Bohy et al., 2012)

Booming dunes are usually composed of quartz sand (typical desert sand), but carbonate sand dunes can also boom (Sholtz et al., 1997).

Where are booming dunes found?

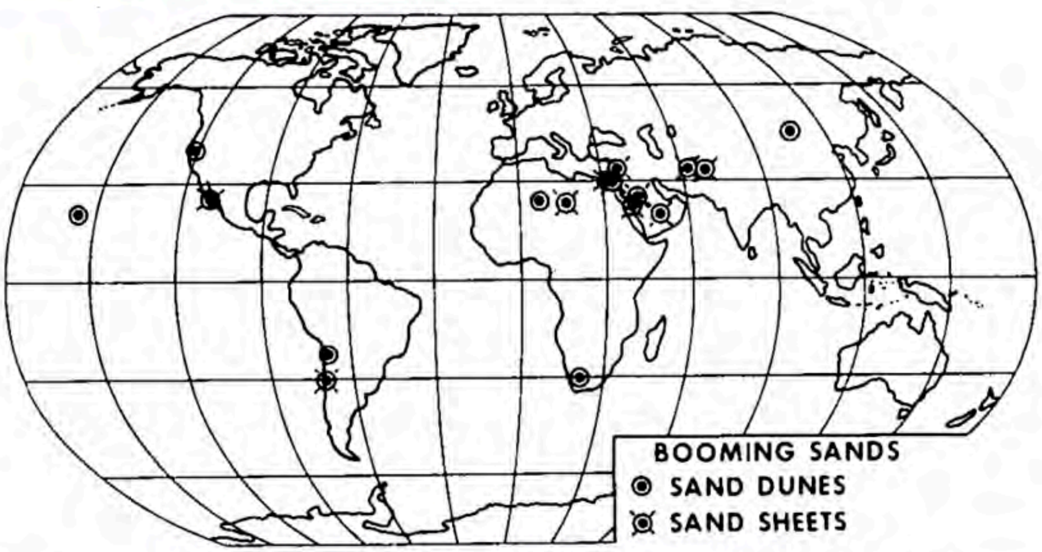

Figure 3: Map of locations of booming sand (both sand dunes and sand sheets). From (Lindsay et al., 1976).

Booming dunes are found in North America (e.g., Kelso Dunes, California and Sand Mountain, Nevada), South America (e.g., El Bramador, Chile), Africa (e.g., Namib Dunes, Namibia), Asia (e.g., Dunhuang, China), and Hawaii (Roaring Sands, Kauai) (Figs 3 and 4) (Nori et al., 1997). There are at least thirty of them, found both in deserts and on beaches, in both cases typically far from the sand source (Nori et al., 1997).

Figure 4: Top: Kelso Dunes, California. Bottom: Namib Dunes, Namibia. Both examples of booming dunes from (Nori et al., 1997).

When do booming dunes boom?

Dunes produce sound when sand is displaced, which occurs naturally when sand avalanches due to wind, but can also be produced by movement of sand by hands or feet, or by moving sand within a container (Nori et al., 1997; Sholtz et al., 1997). Booming occurs only when sand grains are very dry, typically at least a few weeks after the latest rain (Sholtz et al., 1997).

Why do booming dunes boom?

Overview

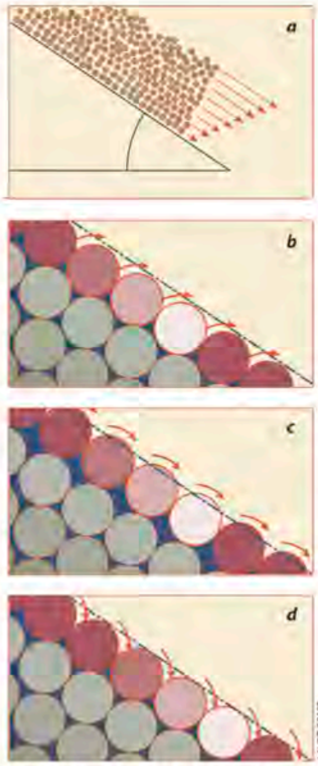

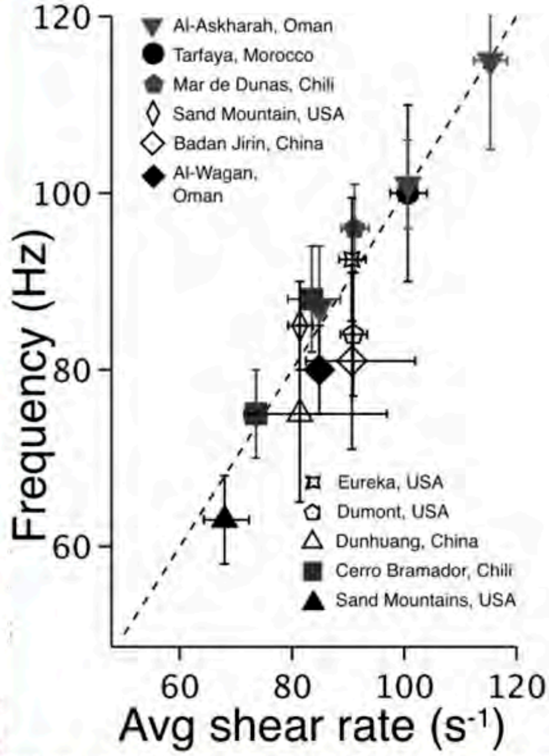

Right: Figure 5: A) As sand is avalanching, upper layers move faster than lower layers. B–D) The grains of the upper layers rise and settle down between the lower grains repeatedly. This may be related to the booming. From (Nori et al., 1997).

Left: Figure 6: Peak frequencies for sound-producing avalanches vs shear rates calculated based on peaks in the grain size distribution. From (Dagois-Bohy et al., 2012).

After reaching the angle of repose (typically around 35° for dry sand), sand begins to avalanche by shearing, with slab-like plates of sand typically breaking off near the leeward crest (Nori et al., 1997). As the sand shears, upper layers of sand move over lower layers (Fig 5). The grains in the upper layers rise over grains in lower layers, fall into the spaces between them, then rise out of them again (Nori et al., 1997). This movement may be related to the booming sound, with the range of frequencies possibly due to multiple modes of vibration in the shearing plates of sand (Nori et al., 1997). The sound frequency increases with the shear rate (Fig 6) (Dagois-Bohy et al., 2012; Sholtz et al., 1997). Often, when the plates of sand in booming dunes reach the gentler slopes near the bottom of the dune, the upper layers collapse into the lower and break up turbulently into free-flowing sand (Nori et al., 1997; Sholtz et al., 1997).

The specific mechanism of sound production is still debated (Dagois-Bohy et al., 2012), with a long history of theories that do not hold up well to observations or fully explain the phenomena. Any appropriate theory must take into account nonlinearity, because the amplitude of vibration experienced by grains in the shear planes is almost as large as the grains themselves (Sholtz et al., 1997). The first comprehensive theory to explain both booming and squeaking sand was developed by Bagnold, suggesting that the acoustic output of the dunes results from nonlinear oscillations in stress along the shear plane in shearing sand due to the movement described above (Nori et al., 1997; Sholtz et al., 1997). Bagnold's theory relates the grain size to the sound frequency, but predictions from this fit squeaking sand better than booming, and don't account for multiple frequencies (Nori et al., 1997; Sholtz et al., 1997).

Contributing Factors

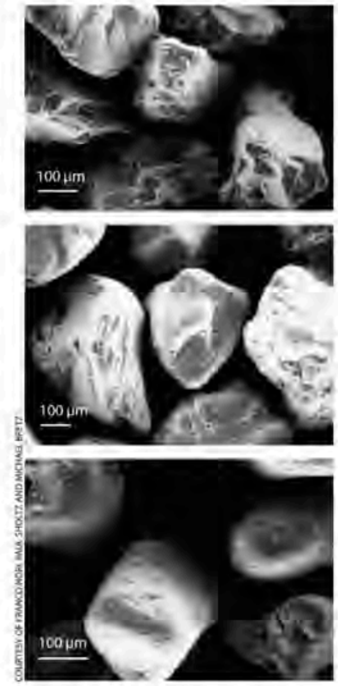

Figure 7: Electron micrographs of sand grains. Top: non-sound-producing beach sand. Middle: squeaking beach sand. Bottom: booming dune sand. From (Nori et al., 1997).

Several factors may contribute to whether sands are booming or not. The most important are the shear resistance and grain smoothness. In addition, a sufficient amount of sand must be moved to cause sound.

- Shear resistance: Sound-producing sand has high shear strength (Sholtz et al., 1997).
- Grain surface smoothness: Sound-producing sand grains tend to have very smooth, polished surfaces (on µm scale; Fig 7), which may lead to amplified vibration at the sand's resonant frequency (Sholtz et al., 1997).
- Grain size: Sound-producing dunes tend to have a narrow particle size distribution (Sholtz et al., 1997). Uniformity in grain size may allow for more efficient shearing, so that smaller size grains don't impede collective movement of larger grains (Nori et al., 1997; Sholtz et al., 1997). However, there are booming dunes without uniform grain size and silent dunes with uniform grain sizes (Nori et al., 1997).
- Grain shape: Sound-producing sand grains tend to be well-rounded, though this seems to be less important for booming sands than squeaking sands (Sholtz et al., 1997).
- Humidity: Booming dunes generally occurs at low humidity. Humidity leads to decreased shear resistance, and increased cohesion between grains, causing clumping (Nori et al., 1997; Sholtz et al., 1997). Both effects can prevent the booming phenomenon. Because of this factor, some have suggested booming dunes might be more common on arid bodies such as Mars (Lindsay et al., 1976).

References

Dagois-Bohy, S., Courrech Du Pont, S., Douady, S., 2012. Singing-sand avalanches without dunes. Geophys. Res. Lett. 39. https://doi.org/10.1029/2012GL052540

Lindsay, J.F., Criswell, D.R., Criswell, T.L., Criswell, B.S., 1976. Sound-producing dune and beach sands. Bull. Geol. Soc. Am. 87, 463–473.

Nori, F., Sholtz, P., Bretz, M., 1997. Booming Sand. Sci. Am. 277, 84–89. https://doi.org/10.1038/scientificamerican0997-84

Sholtz, P., Bretz, M., Nori, F., 1997. Sound-producing sand avalanches. Contemp. Phys. 38, 329–342. https://doi.org/10.1080/001075197182306

When the magma ocean starts to crystallize so you lose all your olivines, pyroxenes and plagioclases and you are left with only the incompatible elements

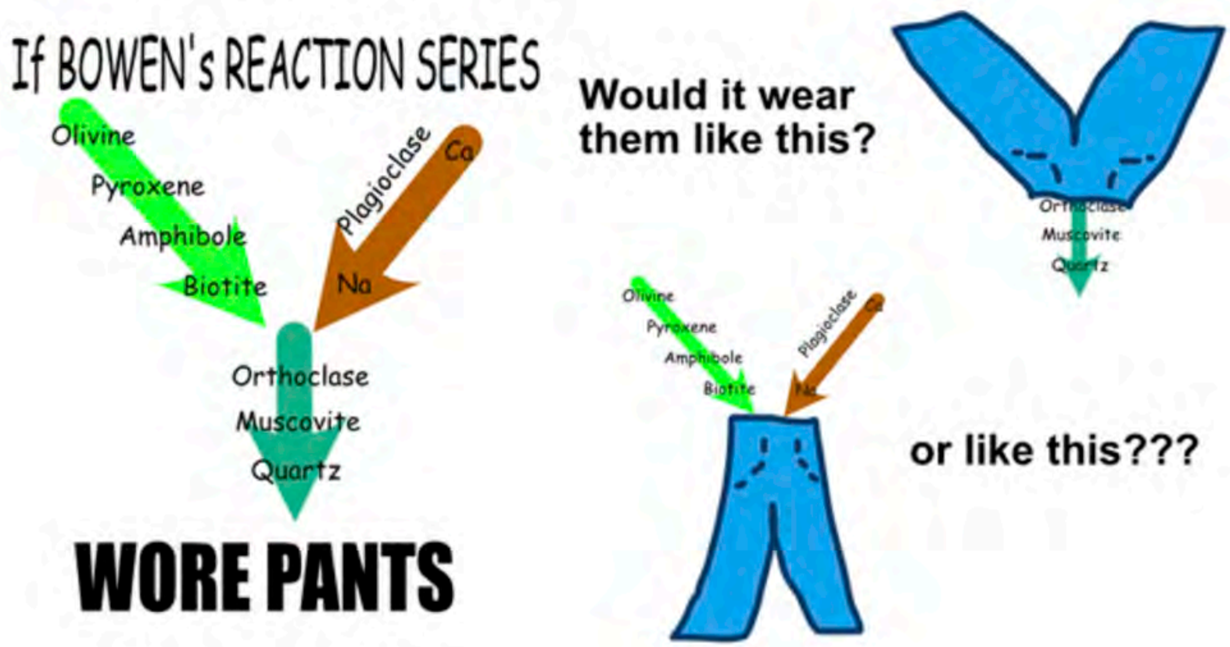

MOJAVE COMPOSITIONS

KELSO DUNES, CIMA VOLCANICS & LIMESTONE IN THE MIDDLE

ALLISON MCGRAW

KELSO DUNES

LARGEST IMMATURE ACTIVE DUNES IN THE SOUTHWEST – QUARTZ POOR!

The Kelso Dune field is one of the largest active fields containing several dune forms derived from multiple wind directions. Located in Southern California within the Mojave desert, they stand impressive as some of the tallest dunes in North America. They are situated within a structural basin (Mojave Sink) of the Basin and Grange physiographic province, dominated by surrounding granitic mountain ranges. Alluvium fans intermediate in age (Pleistocene), light to dark brown, poorly to moderately sorted sand and gravel drape the granitic mountains and supply aeolian sand to the Kelso dunes plus source sediments from the Mojave River sink.

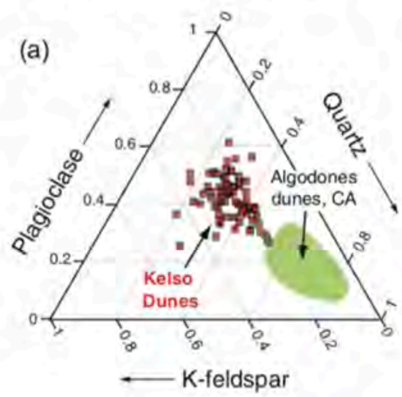

Geochemical analysis reveals a wash of mostly granitic-sourced plagioclase and potassium feldspar (K-feldspar) which translates to a granodiorite (coarse-grained igneous rock). Erosion of this felsic material has also led to arsenic and uranium concentrations downstream on the Mojave River (Muhs et al. 2017). Ramsey et al. (1993) completed sample analysis from the Kelso Dunes showing the presence of magnetite, K-spar, plagioclase and quartz as shown below.

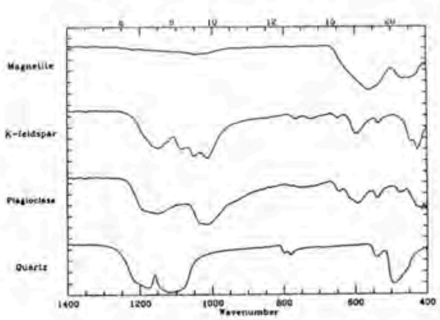

You can see the dunes are a tan light brownish color and on the average are ~33% quartz, 41% plagioclase and 25% K-feldspar (Muhs et al. 1995). The image above shows the Kelso Dune material in red squares. The dunes are considered immature (need to reach ~80-90% quartz-dominated threshold to be mineralogically mature).

The Kelso Dunes are aged at 16,000 years old (Clarke 1994). Portions of the eastern dune field are interbedded with alluvial fan deposits from the Providence Mountains (Clarke 1994, McDonald et al. 2003). Geologic mapping by Sweeny et al. (2015) reveals aeolian and fluvial alternating sequences within the dune material as well as within sand ramps (buildup on flanks of mountains, USGS).

CAMBRIAN LIMESTONE CARBONATE

WHOLE LOTTA LIMESTONE IN THE MIDDLE

The geologic units shown in the figure below (Bedford 2003) depict outcrops to the west of Kelbaker Road and belong to the Carrara Formation which comprises of two main units aged early Cambrian: the Chambless Limestone and the Latham Shale.

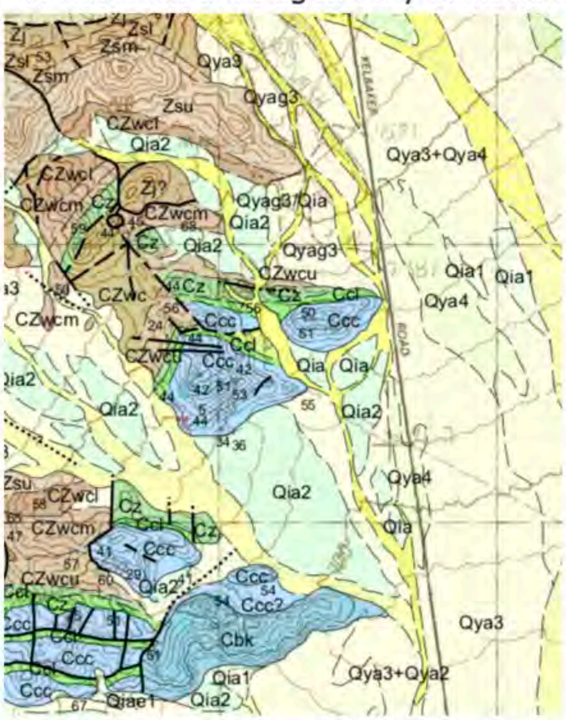

The Chambless Fm. (Ccc) is a light gray fine grained limestone which has 10-13% dark blueish-gray concentric algal nodules. The bedding is 1-2 meters thick and is heavily fractured with white recrystallized calcite.

The Latham shale (Ccl) is dark green to a brownish-reddish shale with sporadic 1-3 centimeter beds of buff fine-grained quartzite. The bedding is 0.7-1.5 meters thick and features shelly fossil creatures.

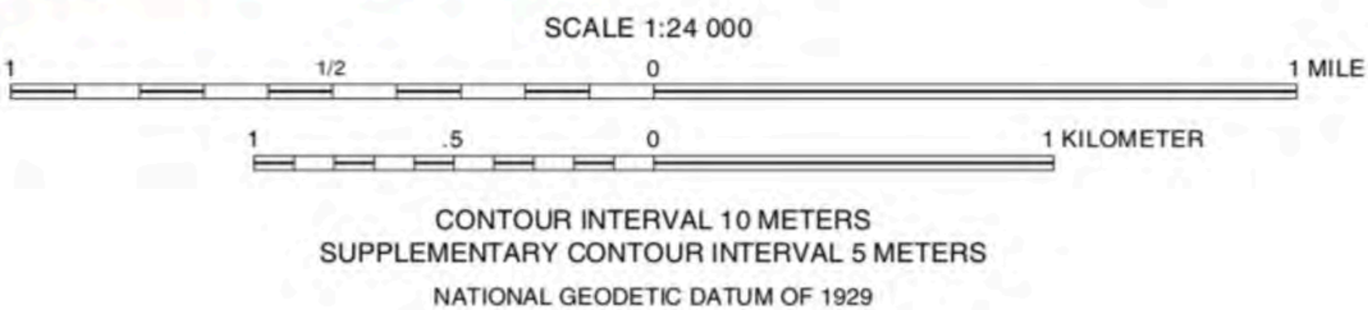

Hyperspectral imaging covers a wide wavelength range and measures continuous spectral bands. Composite image below utilizes 9.1, 2.4 and 0.5 µm and is projected to RGB: red/magenta = quartz-rich, blue/purple = quartz poor, green = carbonates. Left images are a decorrelated stretched to show a bigger range of color variations. Things that affect hyperspectral imaging: surface evolution through aeolian and fluvial processes changing basalt roughness, grain size.

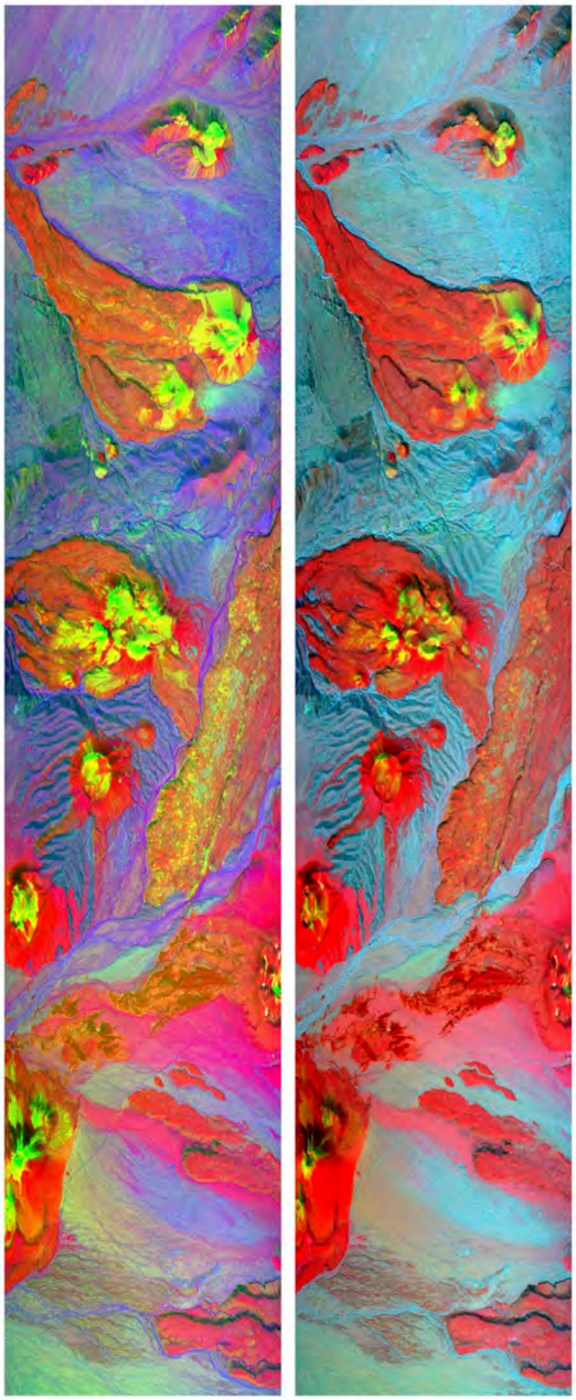

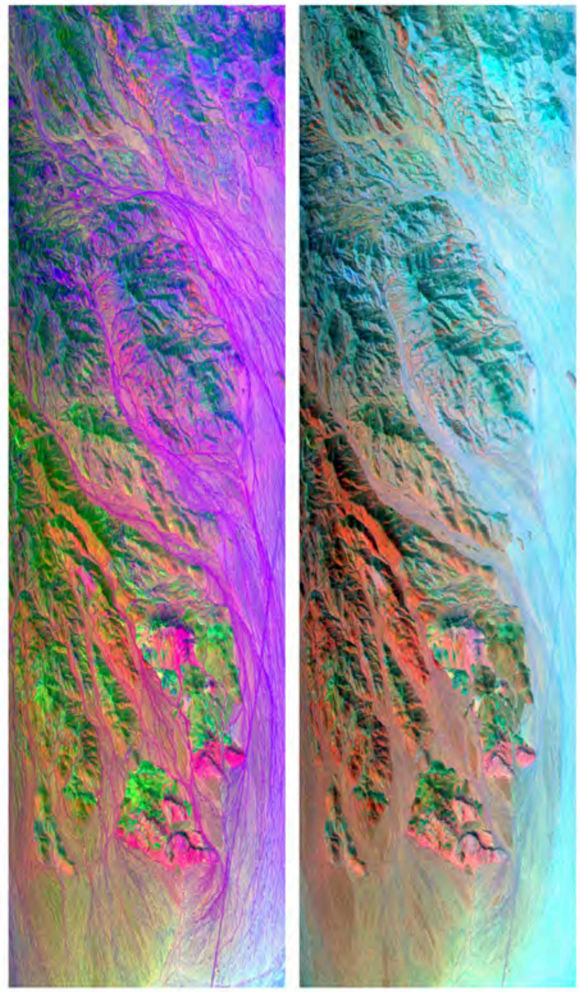

Master three band composite (right 9.1, 2.4 &0.5 microns) and decorrelation stretch (left).

Cima Volcanics and
Kelbaker Road Outcrops

CIMA VOLCANICS

GEOCHEMICAL TECTONIC TRACKING THROUGH 8 MILLION YEARS

The Cima Volcanics are as young as ~15,000 years old up to 7.5 million years (Ma) old (with a notable hiatus 3 to 1 Ma) (Dohrenwend et al. 1984) and contained within 600 square kilometers consisting of ~100-200 meter-scale sized cinder volcanic cones and ~1-9 kilometer in length lava flows.

We drive through a younger section of the volcanic field on this trip off of Kelbaker Road. The volcanic cinder cones within the field are 100-900 meters wide and 100-200 meters in height. Washes cut in and out of outcrop areas that we have been driving over, and many cones still have intact craters (Black Tank cinder scoria cone shown to the right). The taller surrounding mountains (Kelso Mtns., Granite Mtns., Providence Mtns., Old Dad Mtns.) are all mostly granitic bodies Mesozoic-Tertiary in age.

Compositional analysis reveals erupted alkali basalts/trachybasalt with phenocrysts of clinopyroxene, olivine and plagioclase (Wilshire et al. 1991, Farmer et al. 1995). Some lesser prevalent xenoliths of granites, dunites and gabbros are also evident (Kereszturi et al. 2016). Alkali basalt is a fine-grained porphyritic volcanic rock that is characterized by elevated concentrations of potassium and sodium and phenocrysts of olivine, rarely pyroxenes and represents deeper melting sources. The (older grouped) basalt matches that of the Pacific Mid-Ocean Ridge Basalt (MORB), but 3 distinct age groupings are generally identified.

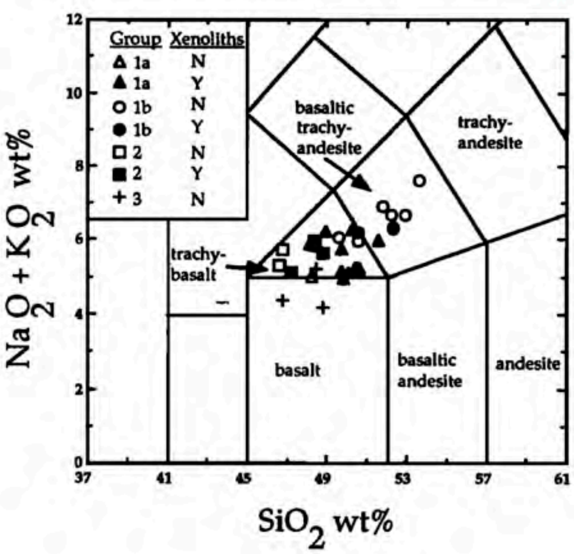

Eruption temperatures at 1110°C with source magma erupted here estimated from the lithosphere or asthenosphere material with little geochemical evidence for crustal composition contamination along the injection motions and path. A large upwelling near the end of the volcanism timeline suggests a change in the local tectonic region from subduction activity to that of the beloved transform boundary of the San Andreas Fault (Farmer et al. 1995). A onset of partial melting and smaller degrees of melting, evidence of fractional crystallization (increase of LREE) and a mantle source change as well as magma ponding within the crust leaving a compositional trail in which you can see this volcanism turning off.

References:

Clarke, M.L., 1994. Infrared stimulated luminescence ages from aeolian sand and alluvial fan deposits from the eastern Mojave Desert, California. Quat. Sci. Rev. (Quat. Geochronol.) 13, 533–538.

Dohrenwend, J.C., L.D. McFadden, B.D. Turrin, S.G. Wells, K-Ar dating of the Cima volcanic field, eastern Mojave Desert, California: late Cenozoic volcanic history and landscape evolution, Geology, 12 (3) (1984), pp. 163-167.

G.L. Farmer, A.F. Glazner, H.G. Wilshire, J.L. Wooden, W.J. Pickthorn, M. Katz, Origin of late Cenozoic basalts at the Cima volcanic field, Mojave Desert, California, J. Geophys. Res. Solid Earth, 100 (B5) (1995), pp. 8399-8415.

Kereszturi, Gábor, and Károly Németh. "Post-eruptive sediment transport and surface processes on unvegetated volcanic hillslopes–a case study of Black Tank scoria cone, Cima Volcanic Field, California." *Geomorphology* 267 (2016): 59-75.

McDonald, E.V., McFadden, L.D., Wells, S.G., 2003. Regional response of alluvial fans to the Pleistocene-Holocene climatic transition, Mojave Desert, California., Geol. Soc. Am., Spec. Pap. 368, 189–205.

Muhs, D.R., Bush, C.A., Cowherd, S.D., Mahan, S., 1995. Geomorphic and geochemical evidence for the source of sand in the Algodones dunes, Colorado Desert, southeastern California. In: Tchakerian, V.P. (Ed.), Desert Aeolian Processes. Chapman and Hall, London, pp. 37–74.

Muhs, D.R., Lancaster, N., Skipp, G.L. (2017) A complex origin for the Kelso Dunes, Mojave National Preserve, California, USA: A case study using a simple geochemical method with global applications, Geomorphology 276 (2017) 222–243.

Ramsey, M.S., Howard, D.A., Christensen, P., R., and Lancaster, N., (1993) Mineralogical variability of the Kelso Dunes, Mojave Desert, California derived from thermal infrared multispectral scanner (TIMS) data.

Wilshire, H.G., A.V. McGuire, J.S. Noller, B.D. Turrin, Petrology of lower crustal and upper mantle xenoliths from the Cima volcanic field, California, J. Petrol., 32 (1) (1991), pp. 169-200.

Cinder Cone By Stan Shebs, CC BY-SA 3.0, https://commons.wikimedia.org/w/index.php?curid=4756537

Bedford 2003, Surficial and Bedrock Geologic Map Database of the Kelso 7.5 Minute Quadrangle, San Bernardino County, California.

Hyperspectral images provided by Professor Byrne.


LONG TIME NO SEA...
imgflip.com

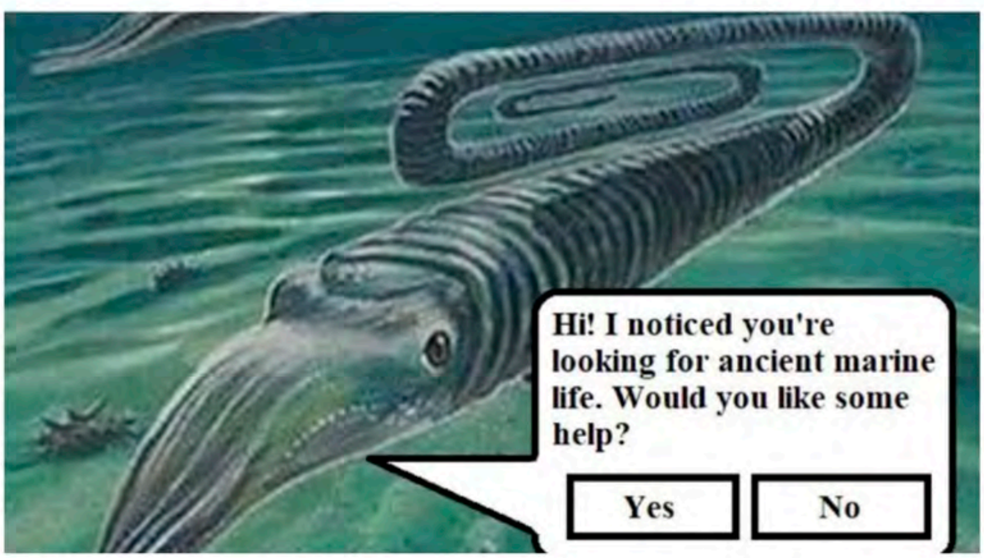
Hi! I noticed you're looking for ancient marine life. Would you like some help?
Yes
No

Geologic History of the Mojave Desert[1]

Dingshan Deng, March 2022

The Mojave Desert is a xeric desert (a very dry desert) in the rain shadow of the Sierra Nevada mountains in the Southwestern United States. Along with Sonoran, Chihuahua and Great Basin deserts, a wide large North American desert is formed. Standing out from its companions, the Mojave Desert is the smallest and driest one, and with even warmer climate.

Figure 1. The North American Deserts [2].

As part of the most ancient geologic evidence on Earth, the oldest rocks exposed in the Mojave Desert is found between 1.7 and 2.5 billion years old, consisting of metamorphic rocks from pre-existing sedimentary, volcanic, and igneous intrusive rocks. Then at about 1.4 billion years ago, magmas intruded those oldest rocks, forming the complex basement of the modern land features. This geologic event is widely extended -- Rocks suggesting with the same evidence are found in the nearby North American desert, extending alongside the Colorado River to the Grand Canyon.

[1] Most of the content summaries from USGS-Mojave National Preserve Website [1].

Starting from about 1.4 billion years ago, the Pangaea supercontinent began to break apart, and a proto-Pacific basin began to develop. The edge of the North America continent gradually sank beneath the ocean surface in a process of passive continental margin, causing a thick sequence of sedimentary rocks accumulating on the continental margin. These deposits formed from sand, mud and limey sediments deposited in shallow marine conditions, like the modern continental shelf around the Gulf of Mexico. This continental margin persisted for nearly 800 million years. It can be seen from the great carbonate-rich (limestone and dolomite) sedimentary rock section preserved in the Mojave region.

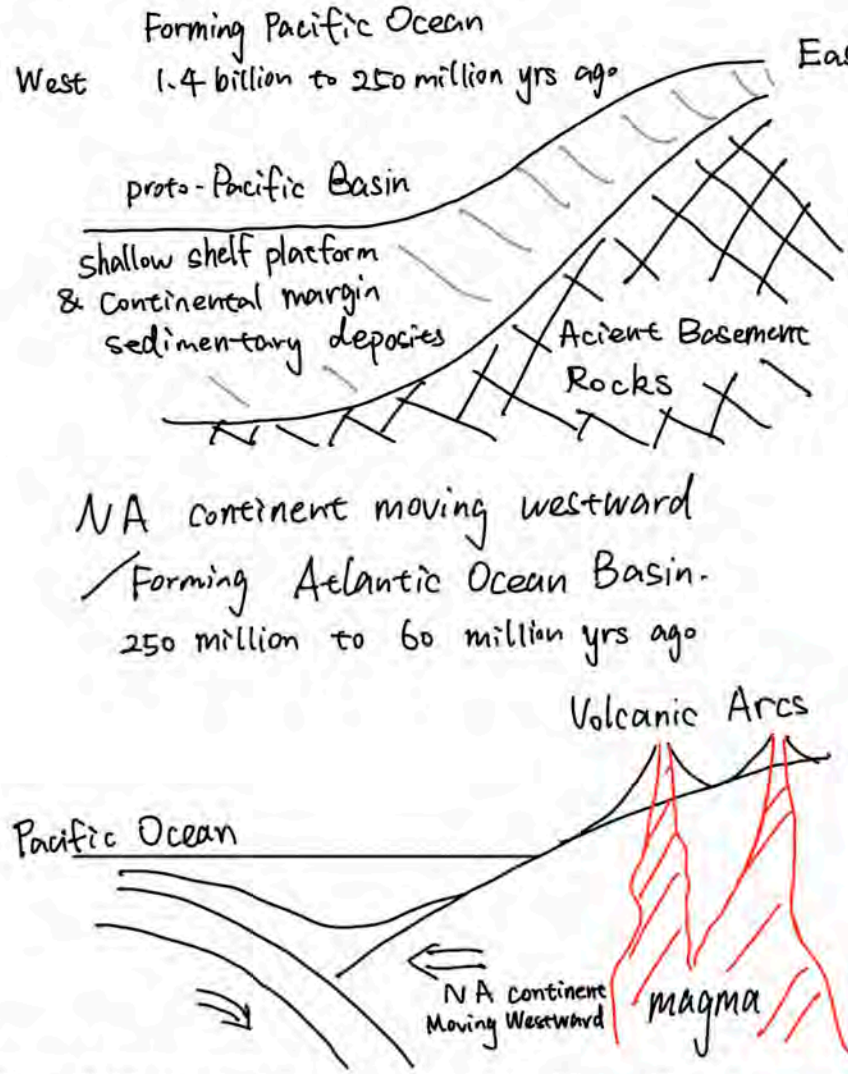

Figure 2. Major tectonic movements at the Mojave Desert region.

Then, at around 250 million years ago, the great ancient Pangaea supercontinent began to rift apart -- The North American continent gradually split away from the Africa and Europe, forming the Atlantic Ocean basin. This westward motion of the North American continent caused the active continental margin, overriding the adjacent oceanic crust beneath the Pacific Ocean. During this process, the subduction of oceanic crustal uplift, and erosion striped away the exposed rocks and sediments. Magma generated by subduction process intruded upwards, resulted in extensive volcanic activities on the surfaces. Deep below the surface, a series of great igneous intrusions gradually became emplaced throughout the region. These igneous rocks form virtually every mountain range in the Mojave Desert. Great granitic intrusions formed between 170 million and 140 million years ago and again at about 100 million years ago.

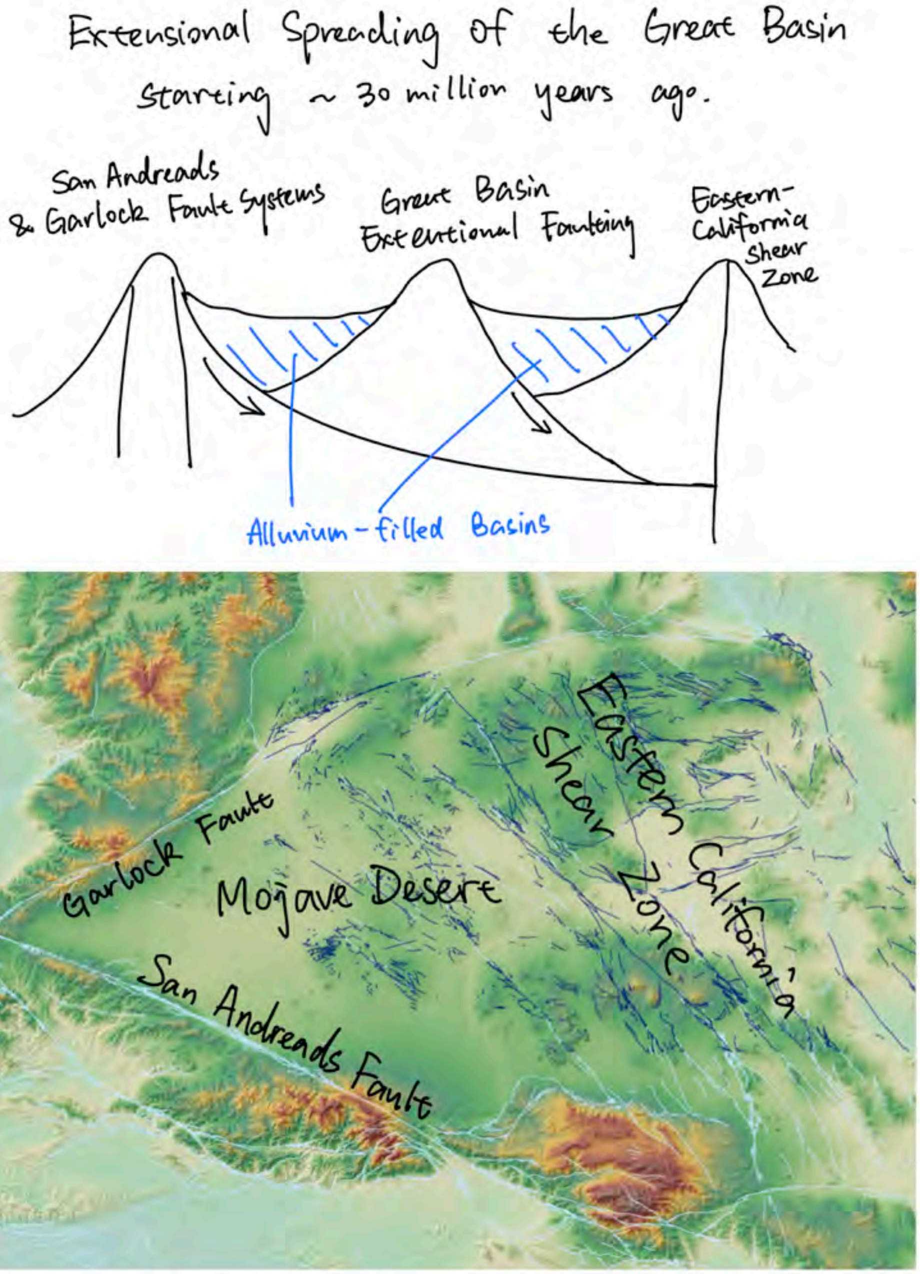

Figure 3. Fault systems at the Mojave Desert [3].

After the extended volcanic activities ended, the erosion dominated, until the new tectonic forces started to modify the landscape at around 30 million years ago. As the Great Basin began to spread apart, a great rift-style fault system developed across the region. The history at this time of the Mojave Desert is similar to the Basin and Range-style structure of Arizona. Two fault systems affected at the desert at around 18 million and 14 million years ago, respectively. However, the faulting today which is still modifying the regional landscape is not the Basin and Range-style faulting. It is mostly associated with the San Andreas Fault, the Garlock Fault, and the Eastern California Shear Zone located at edges of the Mojave Desert. All of these major fault systems display measurable displacements in the range of hundreds of kilometers. More details of the character and movement activity of fault systems in the Mojave Desert are still under investigation to clarify times and amounts of displacement and the role in forming today's topography.

Also starting from around 30 million years ago, large volcanic eruptions occurred fairly frequently in the Great Basin region. Volcanic ash erased the landscape formed before, and many of these ash beds are well preserved in the deposits accumulated in the basins that we are seeing now. The last volcanic eruption in this area occurred only about 8,000 years ago.

Besides the events beneath the ground, most of the features we can see on the land are formed during last million years. Climatic changes are mainly responsible for most of these landscape features.

Reference:

[1]. USGS Western Region Geology and Geophysics Science Center. (2009). *General Geologic History*. https://pubs.usgs.gov/of/2004/1007/geologic.html.

[2]. Whorley, Joshua & Kenagy, G. J.. (2007). *Variation in Reproductive Patterns of Antelope Ground Squirrels, Ammospermophilus leucurus, from Oregon to Baja California. Journal of Mammalogy* - J MAMMAL. 88. 1404-1411. 10.1644/06-MAMM-A-382R.1.

[3]. Geology, Minerals, Energy, and Geophysics Science Center. (2019). *Mojave Desert Faults map.* https://www.usgs.gov/media/images/mojave-desert-faults-map.

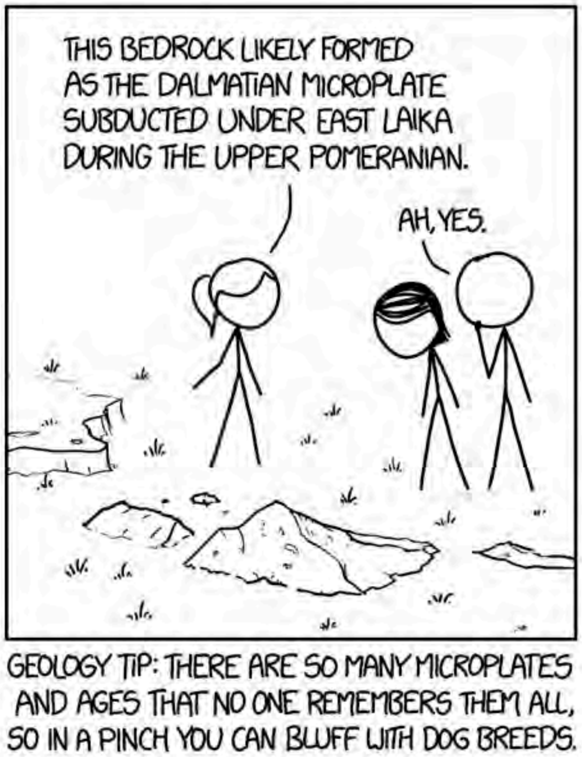
THIS BEDROCK LIKELY FORMED AS THE DALMATIAN MICROPLATE SUBDUCTED UNDER EAST LAIKA DURING THE UPPER POMERANIAN.
AH, YES.
GEOLOGY TIP: THERE ARE SO MANY MICROPLATES AND AGES THAT NO ONE REMEMBERS THEM ALL, SO IN A PINCH YOU CAN BLUFF WITH DOG BREEDS.

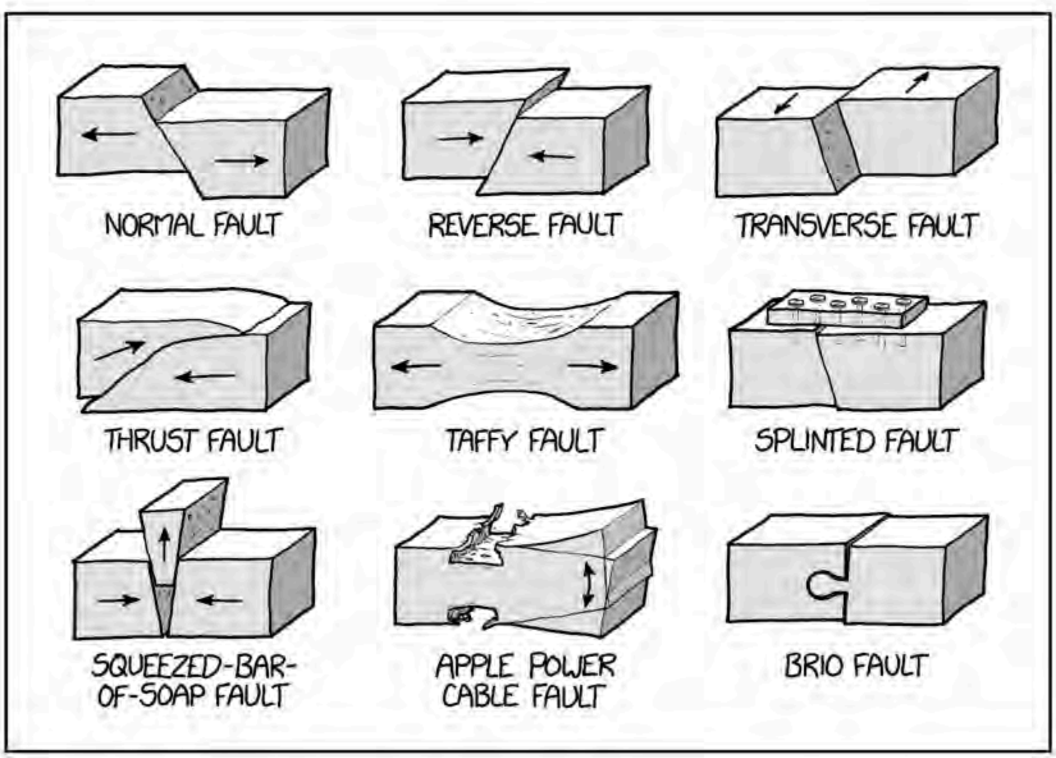
NORMAL FAULT
REVERSE FAULT
TRANSVERSE FAULT
THRUST FAULT
TAFFY FAULT
SPLINTED FAULT
SQUEEZED-BAR-OF-SOAP FAULT
APPLE POWER CABLE FAULT
BRIO FAULT

Cima Volcanic Field Mackenzie Mills

The Cima Volcanic Field is a field of scoria cones in the northeastern part of San Bernardino County, California (overview shown in Figure 1). The scoria cones themselves are Tertiary and Quaternary basaltic volcanoes, with a general north trend (Wilshire et al. 1987). A simplified geologic map of the area, along with the regional setting, is shown in Figure 2 (from Baziotis 2017, adapted from Farmer et al. 1995). Figure 3 also shows a sketch from Dohrenwend, Wells, and Turrin (1986). The field is constructed of several flows of varying ages (0.015-1.09 myr) from K-Ar analyses (Dohrenwend, Wells, and Turrin 1986) and consists of ~30 central cones. Because of the varying ages, the cones have varying levels of degradation from erosion (Wilshire et al. 1987).

Figure 1: An aerial view of the Cima volcanic field from GoogleMaps (credit: GoogleMaps). The cones are shown in the center, along with basaltic flows, the Cima dome is the tawny patch on the right (marked by the red star).

The Cima cones are basaltic in composition and the surrounding surface rock layers are mainly Tertiary sedimentary rocks and intrusive granites (Wilshire et al. 1987). To introduce some lower stratigraphy, the Cima volcanic field is underlain by the early Cambrian Noonday dolomite, the Pahrump series, the Crystal spring formation, and the Goodspring dolomite. There are also Mesozoic sandstones and shales, Cretaceous folding, and then Tertiary erosion (Hewett 1956).

Cones range between 50-155 meters tall, and 400-915 meters wide. These are similar to dimensions measured for scoria cones on the Mauna Kea Volcano in Hawaii. The cones are

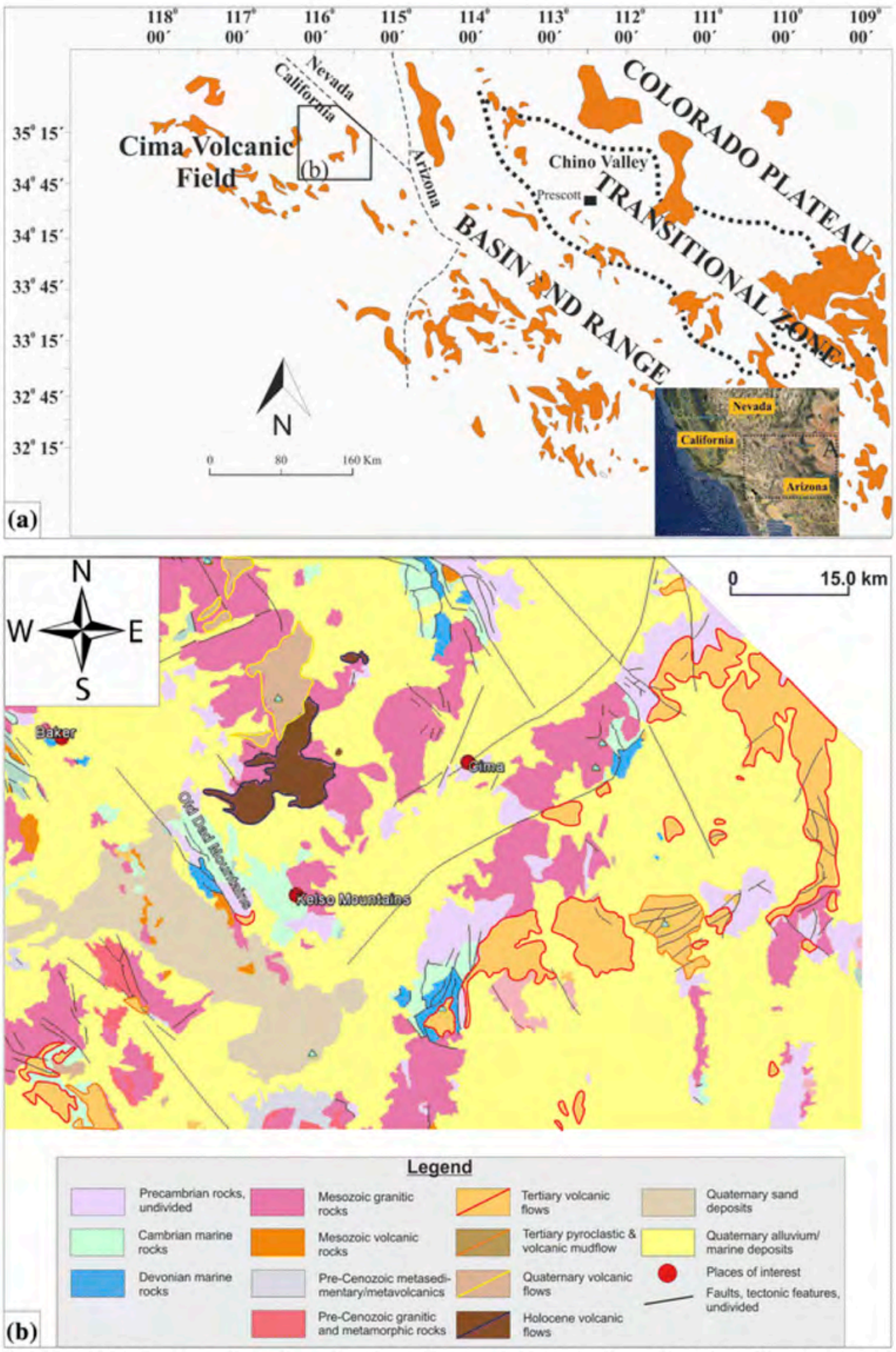

Figure 2: (a) Simplified map showing the locations of Cenozoic volcanics (in orange) in the Mojave Desert region, including Cima Volcanic Field (Map modified after Farmer et al. 1995). Inset gives larger context, with area of map indicated by dashed black box. The black polygon labeled "B" shows the location of the more detailed geologic map shown in part (b). b Generalized geological map of study area (modified from Ludington et al. 2007). Relatively young volcanic units are emphasized; all the xenoliths studied here were found in the Holocene volcanic flows within the Cima Volcanic Field (figure from Baziotis 2017).

composed of cinders, volcanic bombs, agglutinate (welded pyroclastic deposits), and basaltic flows. The cinders are loose but relatively tightly packed. Cinder cones usually form from a single eruption and it is rare for a second eruption to occur from the same vent (Dohrenwend, Wells, and Turrin citing Williams and McBirney, 1979; Wood, 1980a). However, K-Ar dating has shown that multiple Cima cones have erupted discontinuously over hundreds of thousands of years.

Cone composition is primary a trachybasalt, which is an intermediate rock type between basalt and trachyte. A trachyte is a fine-grained volcanic rock type that usually consists of high amounts of alkali feldspar. The basalts resemble Ocean Island Basalts, meaning they resemble the more primitive and less processed basalts that are typically found erupting from ocean island hotspots (i.e. Hawaii). Three different groups of basalts were identified (Farmer et al. 1995). Group 1, ranging from < 1 myr to 3-5 myr, appear to have higher concentrations in rare earth elements, particularly in the 3-5 myr basalts. Groups 2 and 3 are older (5-7.6 myr) and have lower concentrations of rare earth elements, particularly neodymium. The older basalts resemble mid-ocean ridge basalts from the northern hemisphere that have undergone more significant processing. Thus, the Cima field has been suggested to be formed from upwelling asthenosphere in a "slab gap" as the Pacific zone transitions from a subduction to a transform boundary during the late Cenozoic.

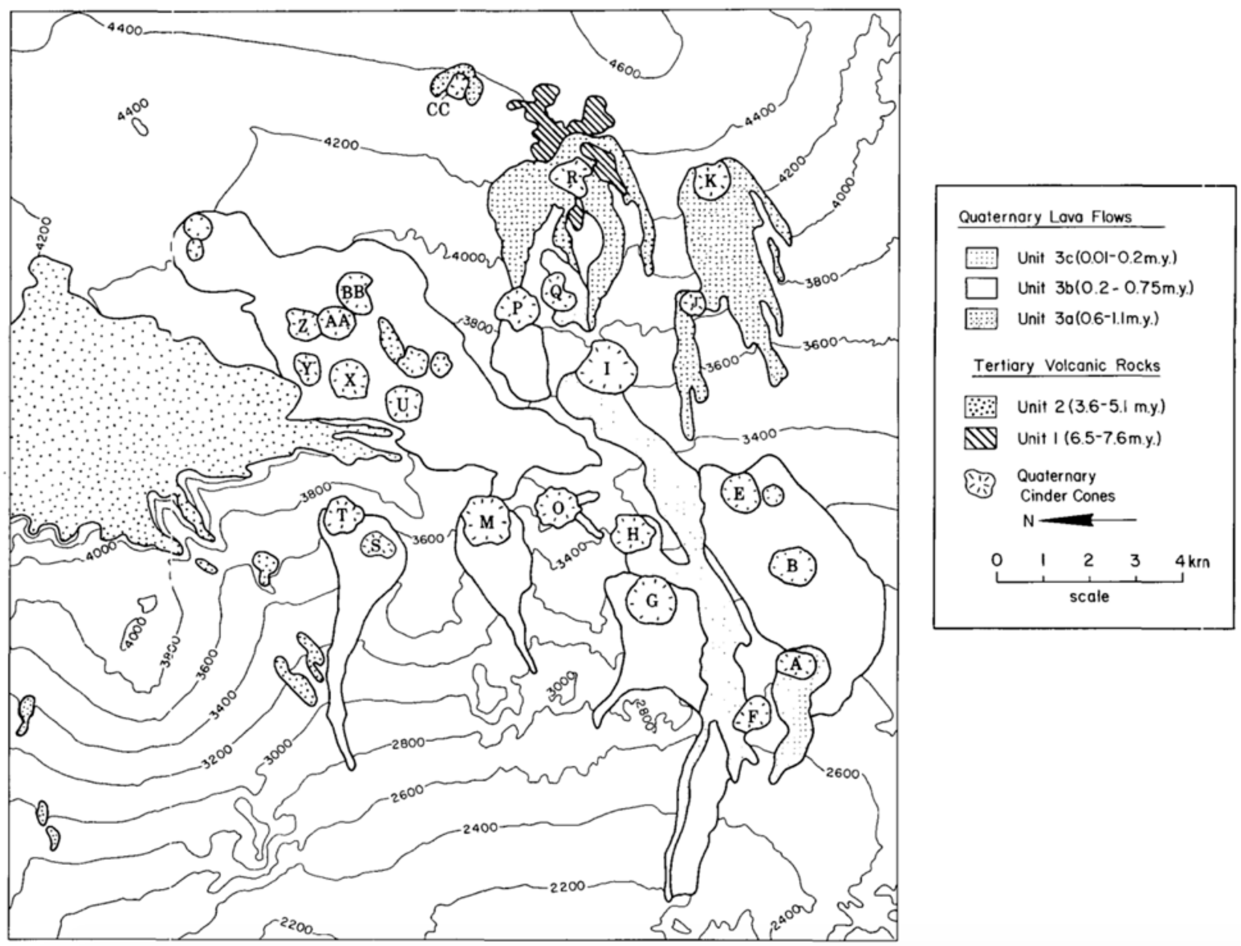

Figure 3: Generalized geologic map of the southern part of the Cima volcanic field showing the locations of cones (from Dohrenwend, Wells, and Turrin, 1986).

References:

- Baziotis I. et al. (2017), Phosphorus zoning as a recorder of crystal growth kinetics: application to second-generation olivine in mantle xenoliths from the Cima Volcanic Field, *Contributions to Mineralogy and Petrology*, 172, 7, 10.1007/s00410-017-1376-7

- Wilshire, H. G., J. G. Frisken, R. C. Jachens, E. V. Prose, C. M. Rumsey, and A. McMahan, Mineral resources of the Cinder Cones Wilderness Study Area, San Bemadino County, Califomia, U.S. Geol. Surv. Bull., 1712-B, 1-13, 1987.

- Farmer, G.L. et al. (1995), Origin of late Cenozoic basalts at the Cima volcanic field, Mojave Desert, California, *Journal of Geophysical Research*, 100, B5, 8399-8415.

- Dohrenwend, J. C., Wells, S. G., and Turrin, B. D. (1986) *Geological Society of America Bulletin*, 97, 421-427.

- Hewett, D.F. (1956), Geology and mineral resources of the Ivanpah Quadrangle, California and Nevada, Issues 275-279.

What people think the mantle is like:

What the mantle is actually like:

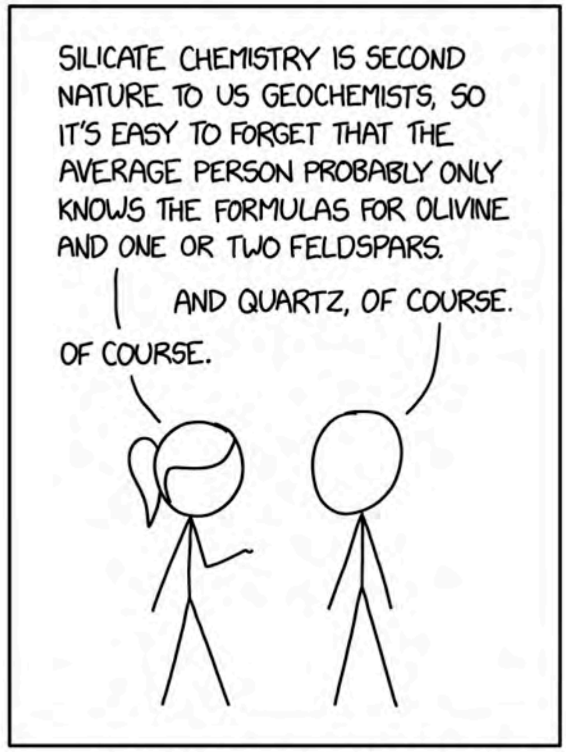

EVEN WHEN THEY'RE TRYING TO COMPENSATE FOR IT, EXPERTS IN ANYTHING WILDLY OVERESTIMATE THE AVERAGE PERSON'S FAMILIARITY WITH THEIR FIELD.

Alteration of Cinder Cones

By: Michael Daniel

Figure 1: Figure 1: Cinder Cone; a cinder cone in Lassen Volcanic National Park that erupted in 1650 CE[1]

Quick Background

- Cinder cones = scoria cones
- Scoria: irregular shaped, many bubble shaped cavaties[1]
    - Cinder: nut- to fist- size scoria pieces[1]
- Cinder cones are mostly basaltic or basaltic andesite, though some are andesetic[1]
- Initially angle of repose ~25-32 degrees
- Often have dark lava flows originating at their base
- Most cones are 100-150m all, rarely larger than 200-300m tall[1]
- Cinder cones often appear in volcanic fields
- Mojave National Preserve cinder cones
    - 32 cinder cones[2]
    - Ages 7.6 million to ~10,000 years old[2]

Alteration of Cinder Cones

Geologic processes on timescale of 100 to 100,000 years[3]

As age increases

1. Cone slope decreases[3]
2. Cone height decreases[3]
3. Cone height to width ratio decreases[3]
4. Crater definition lost

Alteration performed by:

1. Hillslope evolution
    - Rapid hillslope transfer processes on young cinder cones
    - Slower hillslope transfer as cinder cones age
    - Climate
        - Precipitation
        - Soil (grain) size/cinder size
        - Rain splash
        - Land cover
    - Animal impacts
2. Soil production/eroding of scoria
    - Occurs over time, unknown exactly how the rate changes
        - Decaying exponential vs humped model
    - Climate
        - Thermal differentials and weathering
        - Winds
        - Water
            - Freeze-thaw
            - Chemical weathering
    - Plants

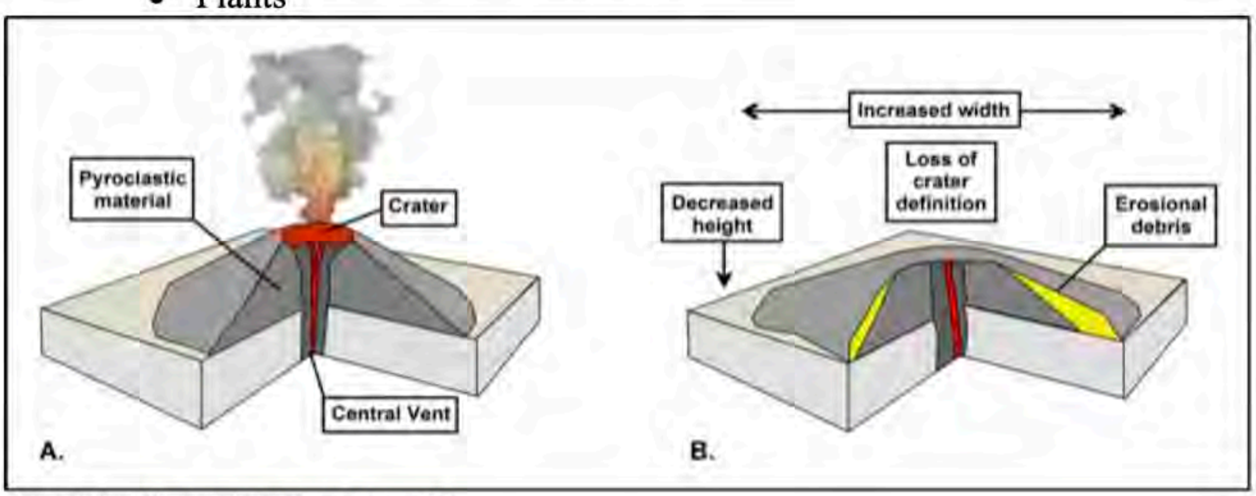

Figure 2: Evolution on cinder cones, a graphic[3]

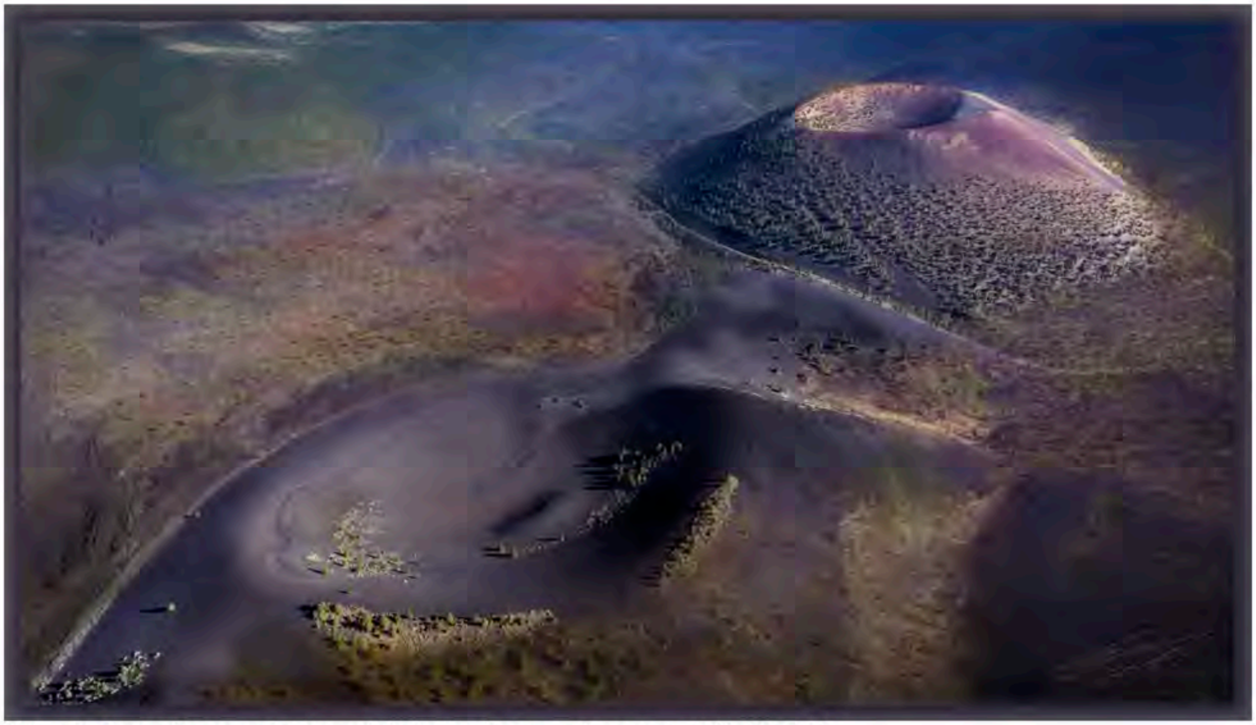

Figure 3:, Sunset Crater and unnamed cinder cone[5], Sunset Crater erupted in 1085 A.D.

Human Caused Alterations

1. Mining for cinders used in construction
2. Some humans want to do rather useless things with them too
   - "In the 1920's, H.S. Colton saved the cone (Sunset Crater) from severe damage by averting the attempt of a Hollywood movie company to blow it up in order to simulate an eruption."[4]
3. Planetary scientists walking on cinder cones -> causing erosion

Conclusion

Over time cinder cones will become shorter, with less defined craters, and gentler slopes

References

(1) https://home.nps.gov/articles/000/cinder-cones.htm
(2) https://www.nps.gov/moja/planyourvisit/upload/cinder_cones_sb_bl_lowres.pdf
(3) https://serc.carleton.edu/vignettes/collection/36642.html
(4) https://www.usgs.gov/volcanoes/san-francisco-volcanic-field/sunset-crater
(5) https://azgs.arizona.edu/photo/sunset-crater-unnamed-cinder-cone-san-francisco-volcanic-field-arizona

Formation and Astrobiology of Lava Tubes

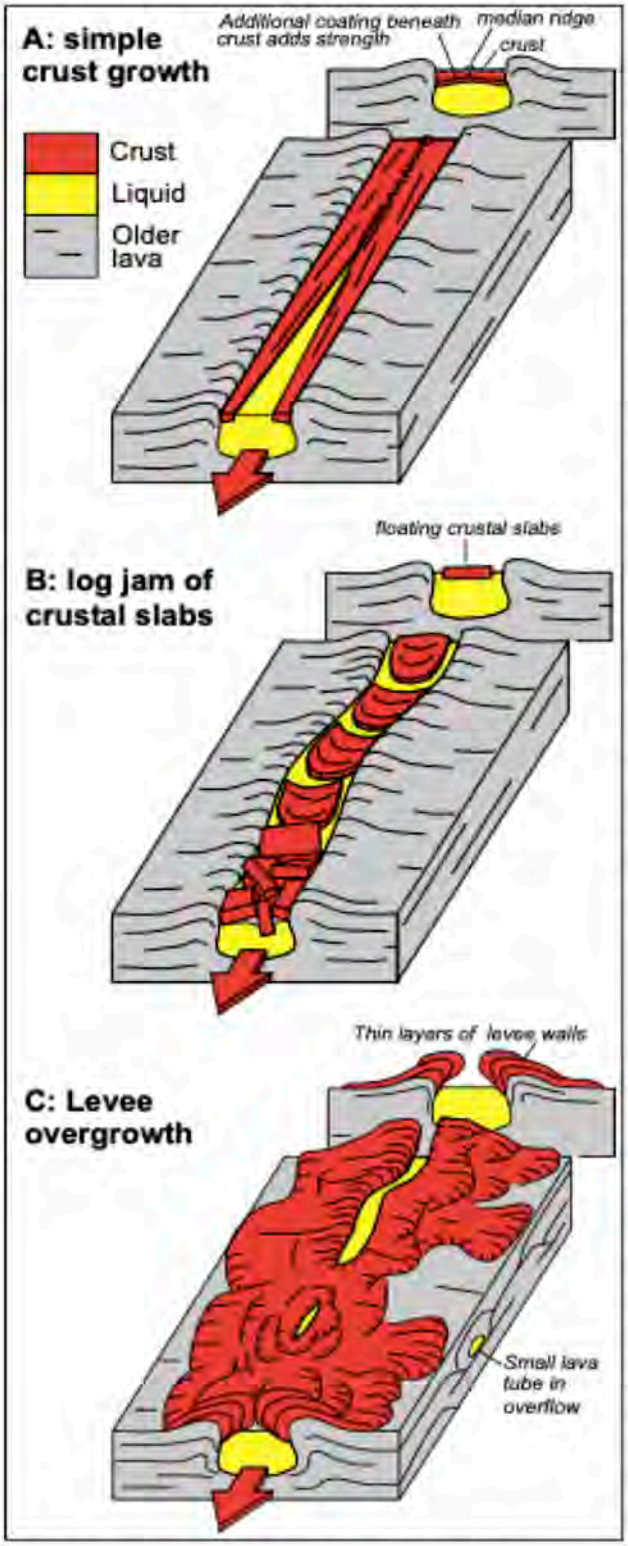

Fig. 1. Overview of different modes of channel roofing leading to tube formation (Grimes 2005).

Lava tubes are common features in volcanic terrains on Earth with many examples of different genetic processes and morphometric characteristics. Lava tubes have also been identified in lunar Maria and on Mars based on gravimetry, radar sounding, and visual observations of skylights.

Formation and Morphological Features:

Observed morphological variability is controlled by formation processes which are affected by effusion rate, topography, and the composition and rheology of the lava. Lava tubes generally form when the outer surface of a lava flow in a channel during an effusive eruption cools more rapidly than the interior, forming a hardened crust. The crust surrounds and insulates the interior flow. The resultant superheated lava flow can thermally erode downward, resulting in a deeper, narrower tube. When the eruption stops or the lava is diverted elsewhere, the remaining liquid lava drains, leaving a vacant conduit. Roofing the lava channel can happen several ways shown in Fig. 1 (Sauro *et al*. 2020):

a. Simple crust growth

b. Log jam of floating slabs

c. Lateral shelf growth

In addition to lava channel-derived tube formation, the inflation of pahoehoe lobes can generate empty conduits (Fig. 2). Pahoehoe is characterized by smooth, slow moving, gently undulating lava and is fed almost entirely internally beneath a partially or completely solidified surface. Consequently, when the surface crust is strong enough, inflationary pressure results in uniform uplift of the sheet. As the flow front advances, lava escapes through a rupture in the skin, developing new lobes. When the supply of lava is cut off, the liquid parts of the lobes may drain out resulting in broad but low roofed chambers. If

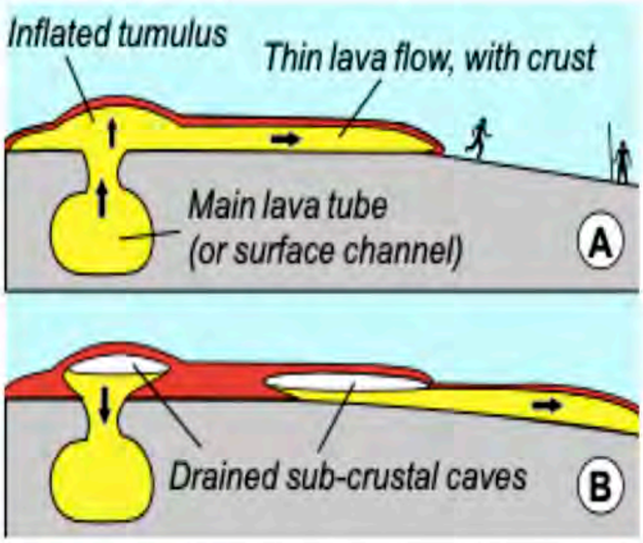

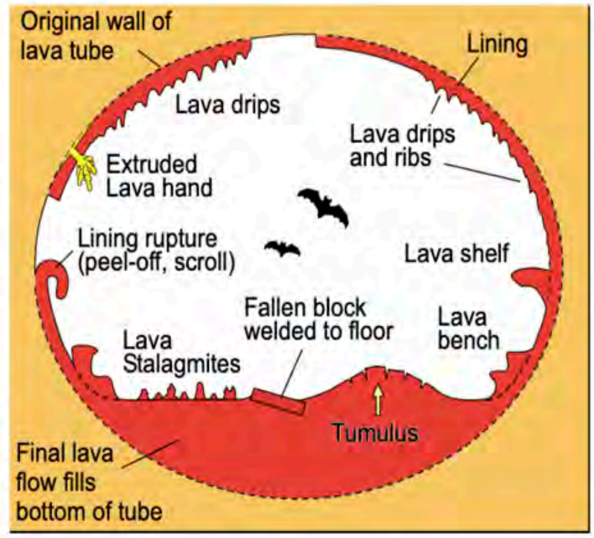

Fig. 2. Pahoehoe inflation followed by lava drainage results in sub-crustal caves that can connect to form a larger lava tube (Grimes 2005).

Fig. 3. As lava drains from the tube, it can leave behind distinctive formations, such as linings on the wall that drip or run down to form other features (Grimes 2005).

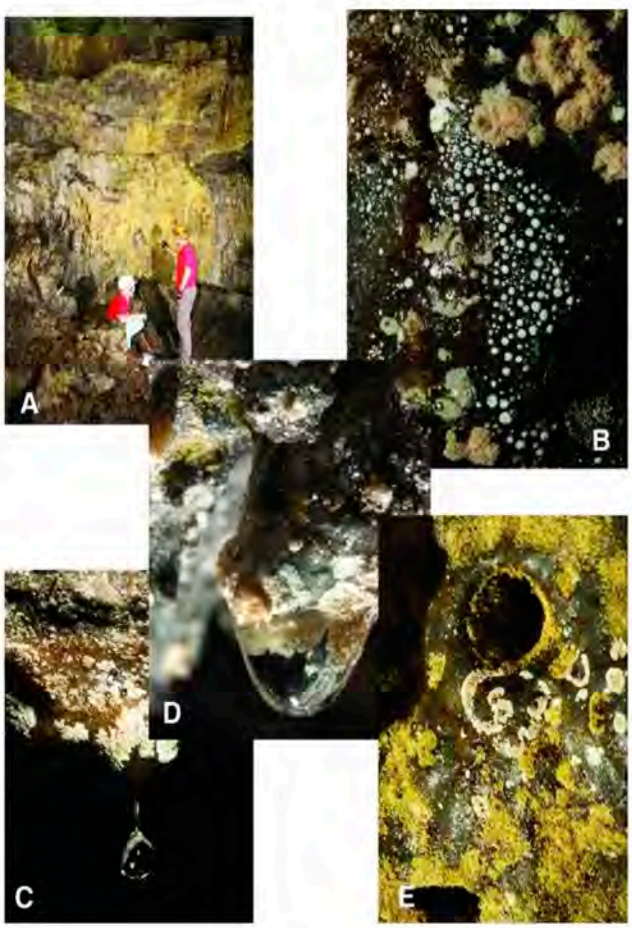

Fig. 4. Microbial mats from Azorean lava caves (an island in the in the Atlantic west of Portugal). Mats range in size from small scattered colonies (B), to covering extensive areas (A, C-E) (adapted from Northup *et al*. 2011).

the eruption continues, these lobes may become concentrated into one large tube, which gets enlarged by thermal erosion. As the lava drains from the tube, they can leave behind a wide range of distinctive features which are shown in Fig. 3. Additionally, during tube development, overpressure can cause collapse. More commonly, when the tube is drained, gravitational effects create similar collapse features including:

1. Complete collapse of the tube leading to pits or channels with vertically steep sides.
2. Skylights

These collapsing events create surficially observable features that are identifiable from orbit, which is useful for studies of Mars and the Moon.

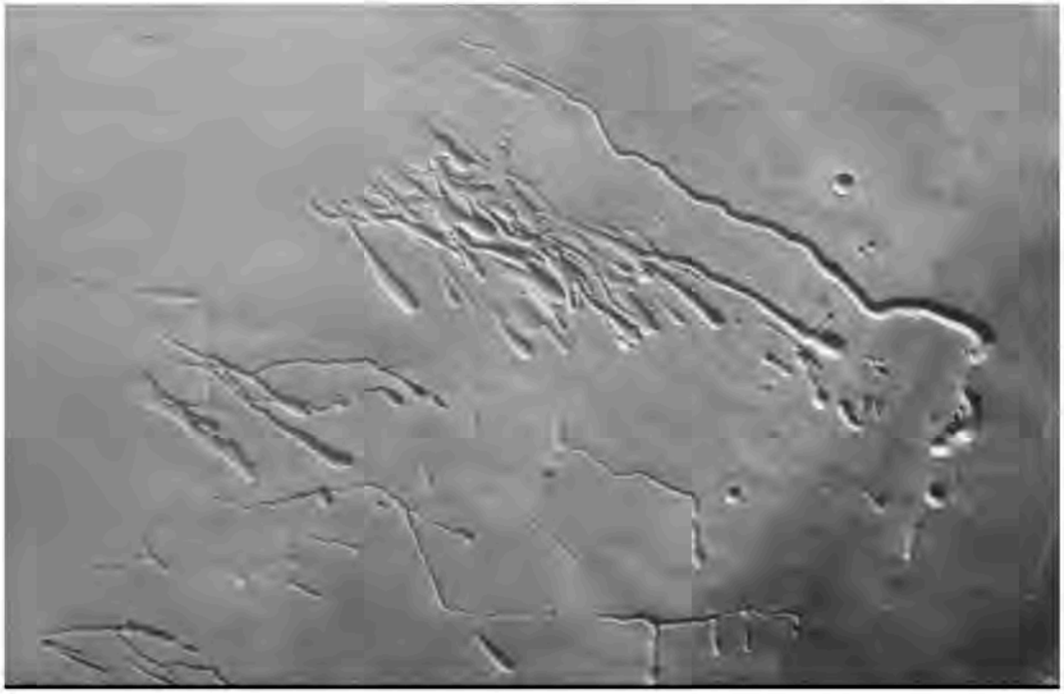

Fig. 5. HRSC (Mars Express) image of the southwest flank of the Pavonis Mons shield volcano in the Tharsis region. Linear channel features have been suggested to be collapsed lava tubes and chains of circular depressions have been suggested to be collapsed pits (adapted from Léveillé and Datta 2010).

Planetary Context: The presence of lava tubes on the Moon and Mars has been proposed since the early 60s (Oberbeck 1969). Many proposed lava tubes appear to be collapsed, leaving semi-linear, channel-like features or a series of collapsed pits. The pits can be differentiated from impact craters by the lack of an elevated crater rim and ejecta deposits. The collapsed channels resulting from lava tubes can often been difficult to differentiate from tectonic features from orbital imagery, but their sinuosity is the main distinguishable characteristic. On Mars, up to 8% of the flanks of Olympus Mons are raised ridges that have been interpreted as uncollapsed lava tubes (Bleacher *et al*. 2006). Tubes on Earth are generally restricted to lava flows that are younger than a few million years due to collapse via weathering processes or sediment/lava infilling. Mars may follow a similar pattern, but they may be stable for longer periods due to the lower weathering rates and lack of abundant planet-wide tectonic activity. The Mars Global Cave Candidate catalogue (Cushing 2015) is a useful resource for identifying lava tubes and other cave counterparts. Similarly, over 300 potential lava tube skylights have been identified in lunar Maria which are of great interest for human exploration and habitation due to the natural protection from micrometeorites, cosmic radiation, and extreme temperature swings.

Astrobiological Context: The hostile surface of Mars is affected by ionizing radiation, low temperatures, low pressures, and a perchlorate-rich environment, which consequently provides few viable niches for life. The subsurface and interiors of rocks provide some protection from these challenges, suggesting that life could have been possible in the past and potentially preserved at detectable levels. Lava tubes could provide the best evidence for past life (chemical, physiological, isotopic, and morphological biosignatures) preserved in cave minerals and protected from surface weathering. For example, microbial activity can leave distinctive secondary minerals, alter the texture of rock surfaces (particularly basaltic glasses) by burrowing inward, or by leaving behind metabolic byproducts (Léveillé and Datta 2010).

On Earth, lava tubes and caves are environmental stable habitats for microbial life including a diverse array of microorganisms, often forming biofilms and thick microbial mats (Fig. 4 and 6). In some deep tubes that a completely closed off from the external atmosphere, entire communities are supported by chemoautotrophic metabolisms. For example, Fe(II) (such as derived from olivine and pyroxene) can serve as an electron source for iron-oxidizing microorganisms and Fe(III) can function as a terminal electron acceptor under anoxic conditions. Other anaerobic metabolisms that have been identified in subsurface environments on Earth have been proposed to be possible on Mars (Table 1). A model habitat by Boston *et al.* 1991 for subsurface life on Mars is shown in Fig. 6 and is applicable to life in lava tubes.

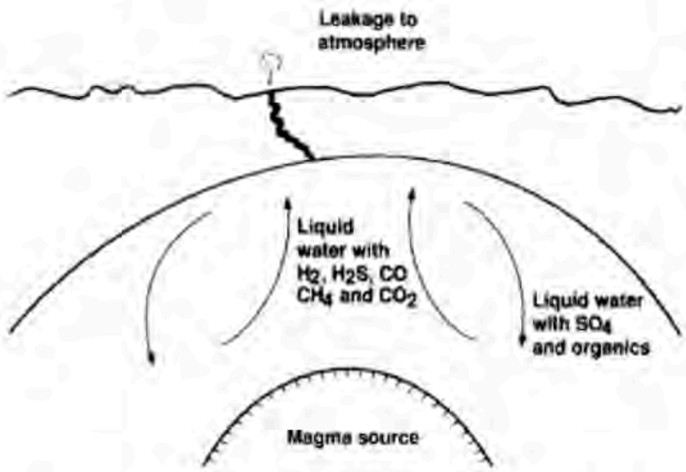

Fig. 6: Water circulating via temperature gradients caused by a geothermal source could carry volcanic gases and other potentially bioavailable nutrients to a microbial habitat while metabolic byproducts are carried downward for recycling.

TABLE 1
Anaerobic Autotrophic Pathways Relevant to Mars

1. Methanogens	$CO_2 + 4H_2 \rightarrow CH_4 + 2H_2O$
	$CO + 3H_2 \rightarrow CH_4 + H_2O$
	$4CO + 2H_2O \rightarrow CH_4 + 3CO_2$
2. Acetogens	$2CO_2 + 4H_2 \rightarrow CH_3COOH + 2H_2O$
3. Sulfate reducers	$H_2SO_4 + 4H_2 \rightarrow H_2S + 4H_2O$
4. Sulfur reducers	$S^\circ + H_2 \rightarrow H_2S$
5. Thionic denitrifing bacteria	$H_2S + NO_3^- \rightarrow SO_4^{2-} + H_2O$
	$S^\circ + NO_3^- \rightarrow SO_4^{2-}$
6. Iron reducers	$2Fe^{3+} + H_2 \rightarrow 2Fe^{2+} + 2H^+$

References

Bleacher, J.E. *et al.* (2006). Comparison of effusive volcanism at Olympus, Arsia, Pavonis, and Ascraeus Montes, Mars from lava flow mapping using Mars Express HRSC data. 37th LPSC. Abstract #1182.

Cushing, G. E. (2015). Mars Global Cave Candidate Catalog PDS4 Archive Bundle. PDS Cartography and Imaging Sciences Node (IMG).

Grimes, K. (2005). "Lava Tube Formation." *Commission on Volcanic Caves* v.1.1.

Léveillé, R. J, & S. Datta. (2010). "Lava Tubes and Basaltic Caves as Astrobiological Targets on Earth and Mars: A Review." *Planetary and Space Science* 58 (4): 592–98.

Northup, D. E. *et al.* (2011). Lava cave microbial communities within mats and secondary mineral deposits: implications for life detection on other planets. *Astrobio*, 11, 601–618.

Sauro, F. *et al.* (2020). "Lava Tubes on Earth, Moon and Mars: A Review on Their Size and Morphology Revealed by Comparative Planetology." *Earth-Science Reviews* 209: 103288.

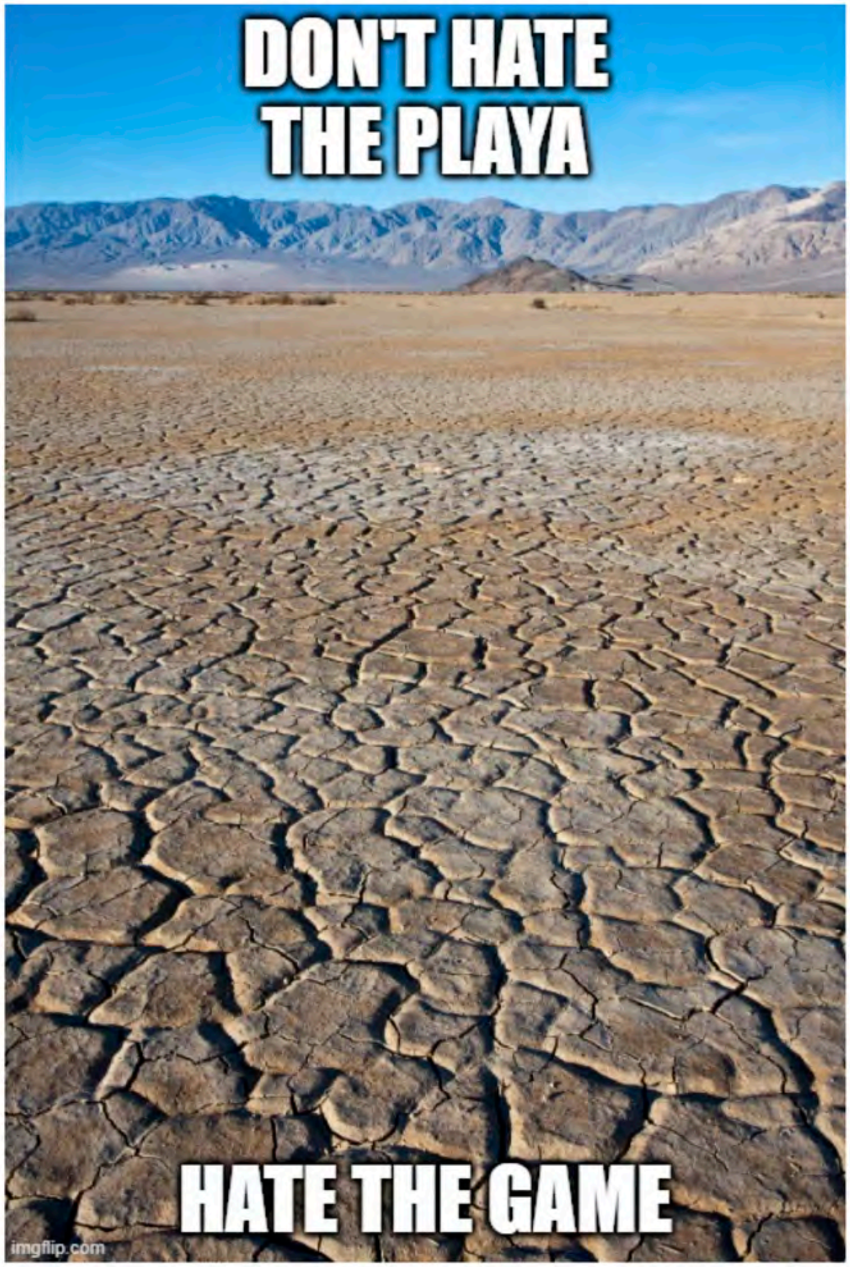
DON'T HATE
THE PLAYA
HATE THE GAME
imgflip.com

Playas on Earth's Mojave Desert and Saturn's MoonTitan

PTYS 594A Spring 2022
Zarah Brown

Soda lake, February 2005 where surface water has ponded in the dry basin following winter rain showers. Photo Credit: David Corby.

Introduction

Monuments to impermanence, playas arise in intermittent and formerlake beds where surface liquid has been to evaporation into the atmosphere or by seeping into the subsurface. Playas typically form in arid climates that experience periodic influxes of water, like interior desert bains and dry, near-coastal regions. Each flooding event has the potential to influence the surrounding drainage channels, playa margins and ecological community. On Earth, many Playas are found in Africa, Australia, Central Asia, Saudi Arabia and in the southwestern United States (including the Mojave Desert)

Liquid Sources/Sinks

The liquids that generate lakes leading to playas are sourced by occasional surface flooding or from upwelling groundwater flow. Those generated by ponded floodwater are more likely to produce a flat, smooth surface. Playas created from groundwater have less sediment influx and foster sometimes rigorous evaporitic or saline crusts. These include carbonates ($CaCO_3$), sulfates ($CaSO_4$) and halides (NaCl). Groundwater flows to the most low lying parts of the playa and moist areas may persist in these regions. Desiccation can occur by the removal of surface liquid by aeolian processes, changing climate and tectonic activity like faulting.

Terrestrial Deposits

As terrestrial lakes dry, they can form two types of playa floors. Pluvial periods result in high water runoff, leading to silty lake bottoms. When desiccated, these produce lacustrine clays. These sediments can shrink and take the form of polygonal terrain. Arid phases of climate result in lake bodies with high mineral content, which dry to form evaporites. These can have a bathtub ring morphology with the least soluble minerals forming the outer ring and subsequently more soluble minerals forming nearer to the center. If the water table rises significantly, areas with thick, salty crusts can re-dissolve, with solution cavities producing a salt karst topography. Playas with thick deposits may be layered with these two deposits. Factors that contribute to the deposit thickness include the duration of accumulation, the depth of the basin, and the supply of material. The fine-grain sediments and salts found in playas evince the composition of the surrounding terrain from which they were eroded. Alkaline deposits in terrestrial playas make it difficult for plants to grow, leaving the terrain relatively free of vegetation.

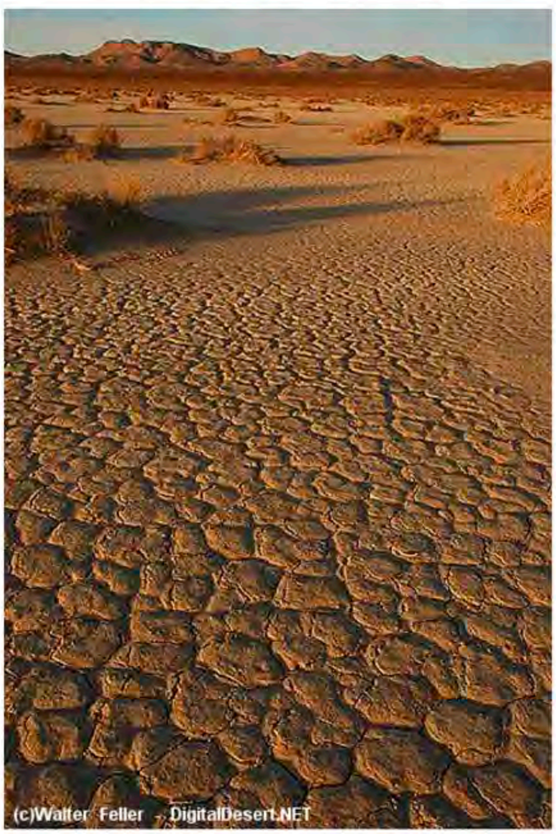

Polygonal terrain, El Mirage Lake, Mojave Desert, southwest of Barstow. Photo Credit: Walter Feller.

Evaporites forming around shallow, ponded water in the Mojave Desert, 2009. Photo Credit: LPL Grad Site

Terrain/Morphology

One of the flattest landforms, on Earth the slope of playa terrain can be less than 20 cm per kilometer. Playas form in low-lying areas, typically where drainage is blocked by faulting, lava flows and the build up of alluvial fans. Nearby mountains can provide a source of water through runoff. The prevalence of fine-grain sediments and salts can lead to the formation of dunes downwind of the playa location.

Playas of the Mojave

The Mojave region prior to the end of the last glacial period approximately 8,000 years ago was far less arid and many of the current playas were lakes and marshes during that time. The Mojave Desert writ large is home to many playas including polygonally-terrained Racetrack Playa and evaporite-rich Devil's Golf Course in nearby Death Valley, the hottest, driest and lowest National Park. The Mojave National Preserve itself has just two large playas: dry Soda Lake and Ivanpah dry Lake. The smaller of the two, Ivanpah Lake is just south of Primm near the Nevada/California border. It recently filled with water in the winter of 2004/2005 following a season of increased rainfall. Repeated pipeline spills from the lanthanide-extracting Mountain Path Mine between 1984 and 1998 contaminated this region with toxic concentrations of uranium, barium, thorium, and radium.

The location of relevant features, including:

Ivanpah Lake
Silver Lake
Soda Lake
Soda Mountains
Cowhole Mountains
Kelso Dunes
Zzyzx Mineral Springs
Mojave River

Credit: Google Maps

Soda Lake

At approximately 60 square miles, Soda Lake is the larger of the two dry lake beds in the Mojave National Preserve and also is home to its lowest point at 284 meters (932 feet) above sea level. It lies between the Soda Mountains to the northwest and the Cowhole Mountains to the east. It is fed by ephemeral streams including the Mojave river, which provide the clay, silt and sand that make up the floor of the playa. These deposits are picked up by aeolian processes, producing periodic hazy conditions in the late summer and fall. Sand from Soda Lake is the primary source of material for Kelso Dunes, located ~30 km to the southeast. Silver Lake is located to the north of Soda Lake across I-15 and is 10 feet lower in elevation. Today these two dry lake beds are connected by a human-modified channel, however, during the Last Glacial Maximum floodwaters conjoined them. Springs near the western side of Soda Lake near Zzyzx also periodically feed into Soda Lake when the groundwater table is sufficiently high. At the north end of Soda Lake, the water table is lower. Without the capillary action of salty groundwater accumulating these minerals at the surface, this end of the lake does not form the salt crusts that are prevalent in the south and southwest portions of the playa. The alkali salts in this region of Soda Lake are composed mostly of sodium carbonate and sodium bicarbonate.

Soda Lake, with bright salt deposits near the southern end and overlapped with interweaving channels.The dark Mojave river proceeds from the southwest. Credit: Google Maps.

Playas on Titan

Saturn's moon, Titan, is the only other body in the solar system known to have a hydrological system. The average surface temperature of Titan is 91 K, and surface minerals are made predominantly of water ice and the hydrological system is comprised mainly of liquid methane and ethane. Like many icy moons in the solar system, Titan's is thought to have a thick shell of water ice overlying a subsurface ocean and rocky core. Extensive mapping of Titan's surface

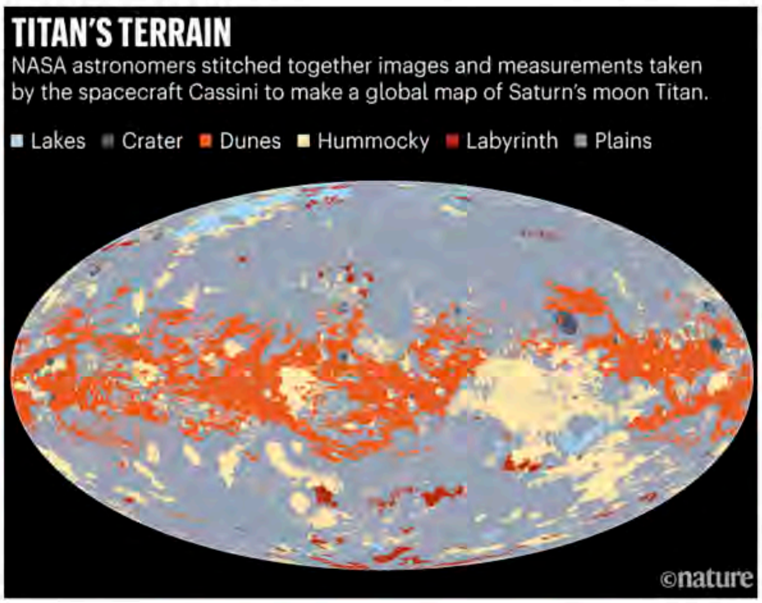

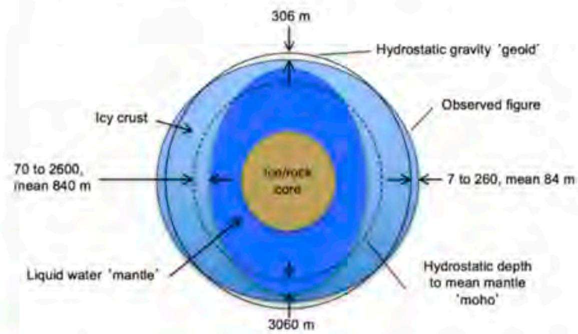

Left: Global geologic map of Titan based on radar and visible-light images. Blue indicates lakes and seas. Purple indicates dunes. Credits: NASA/JPL-Caltech/ASU, Nature

Right: A model of Titan's interior based on Cassini observations of gravity and topology, assuming isostatic compensation. The shallow polar geoid allows mobile liquids to lie closer to the surface (Lopes et al. 2019).

was made possible by the 13-year Cassini mission to the Saturn system, with its RADAR instrument piercing the thick cloud layer to measure topography and the Visual and Infrared Mapping instrument (VIMS) observing surface brightness through spectral windows. Most of the seas and lakes this mission observed are located at Titan's polar regions, particularly the north. Measurements of the surface indicate that Titan's polar flattening is greater than expected for a hydrostatic body, meaning that topographic lows near the poles are exaggerated and that the distance to any subsurface ocean is minimized there. This, along with the possibility of increased polar heat dissipation from tidal interactions with Saturn, could explain the prevalence of lakes near the poles. Despite this overall trend, lakes have been observed globally in the tropics and middle latitudes.

Barnes et al. (2011) mapped dry lake beds in the north-polar sea, Ligeia Mare previously identified by Hayes et al. (2008). Using VIMS observations they categorize depressions as dark (likely containing surface liquid), bright (likely dry) or granular (likely transitional). They found that RADAR-empty-lake morphologies were positively correlated with 5-micron-bright spectral units, concluding that these must be sedimentary or evaporitic deposits. Ngami Lacuna, Racetrack Lacuna, and Melrhir Lacuna are examples. Unlike water, methane and ethane are nonpolar and sedimentation and chemistry with these solvents is much different than that on

Earth. Possible candidates are complex hydrocarbons like those found in Titan's atmospheric haze and dunes, or more volatile species like CO_2. These authors note that the spectral characteristics of these polar lake beds is similar to the lakes in the regional basins of Tui and Hotei Regios, located in Titan's tropics. These 5-micron-bright depressions may indicate the presence of dry lake beds in the low latitudes.

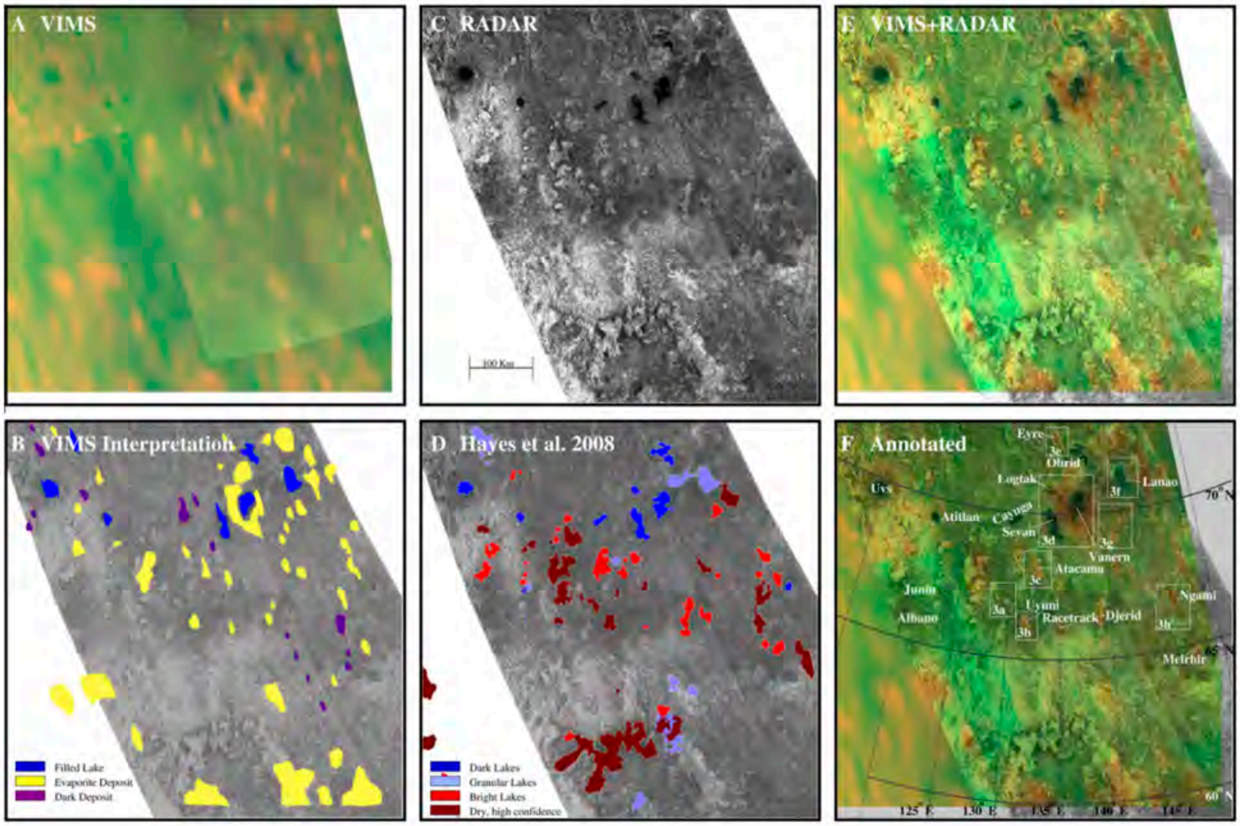

Region south of Ligeia Mare on Titan. a) VIMS data color-mapped with red = 5 microns, green = 2 microns, blue = 1.3 microns. b) Interpretation of a. c) Synthetic Aperture Radar (SAR) data, brightness measures the radar scatterinig cross-section parameter. d) Hayes (2008) interpretation of this region. e) Combined VIMS-RADAR view. f) Annotated version of e.

References

- Baker, Victor R.. "playa". Encyclopedia Britannica, 27 Jan. 2020, https://www.britannica.com/science/playa.
- Barnes, Jason W. et al., Icarus 216 (2011) 136-140 https://doi.org/10.1016/j.icarus.2011.08.022.
- Cone, Marla. "Desert Lands Contaminated by Toxic Spills" Los Angeles Times, April 4, 1997, https://www.latimes.com/archives/la-xpm-1997-04-24-mn-51903-story.html.
- Lopes, R.M.C. et al., Space Sci Rev (2019) 215:33 https://doi.org/10.1007/s11214-019-0598-6.
- USGS. "Playas" USGS Western Region Geology and Geophysics Science Center, December 18, 2009, https://pubs.usgs.gov/of/2004/1007/playas.html.

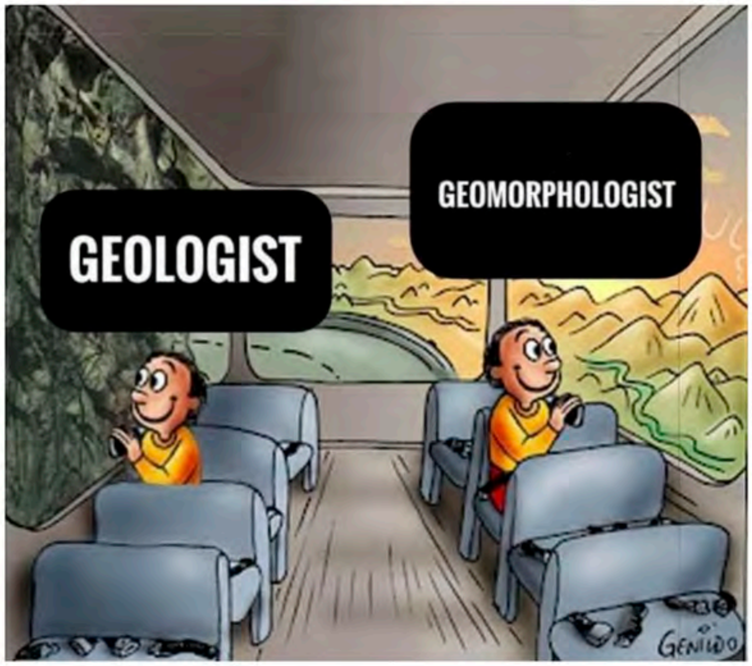
GEOLOGIST
GEOMORPHOLOGIST


OOPS! YOU ADDED TOO MUCH:
BUTTER
SUGAR
FLOUR
BAKING SODA
EGG
HYDRO-THERMAL WEATHERING

Current and Historical Climate and Hydrology of Mojave Desert

Kana Ishimaru

Climate of Mojave Desert

In late Pleistocene (ca. 129–11 ka.), temperature was 3 – 8 °C lower and precipitation was 60 – 300% greater than today, which created large lakes. The high precipitations resulted from southward displacement of the jetstream, and strongly zonal flow, bringing high winter precipitation especially of snow to the Sierra Nevada feeding Lake Lahontan, and to the Transverse Ranges in southern California feeding Lake Mojave. Over the mountain ranges within the Great Basin and the Mojave areas precipitation totals were also high, as evidenced by the presence of lakes in smaller enclosed basins. Lake Mojave sustained high levels during and after the glacial maximum (ca. 18.5–11.5 ka.). After the glacial maximum, high precipitation may have been enhanced by increased energy in the global circulation, resulting in more moisture in the atmosphere and greater penetration into continental interiors.

During the Holocene (ca. 11 ka. to present) and at present the existence of ephemeral lakes in the Mojave Desert, and river floods elsewhere in the southwest, have been particularly associated with meridional airflow and monsoonal conditions, allowing the penetration of tropical air into the desert Southwest. Anomalous atmospheric pressure patterns over the eastern Pacific and high sea surface temperatures, especially under El Nino conditions, enhance this effect, bringing heavy precipitation into the southwest, particularly to the source areas of the Mojave River in southern California.

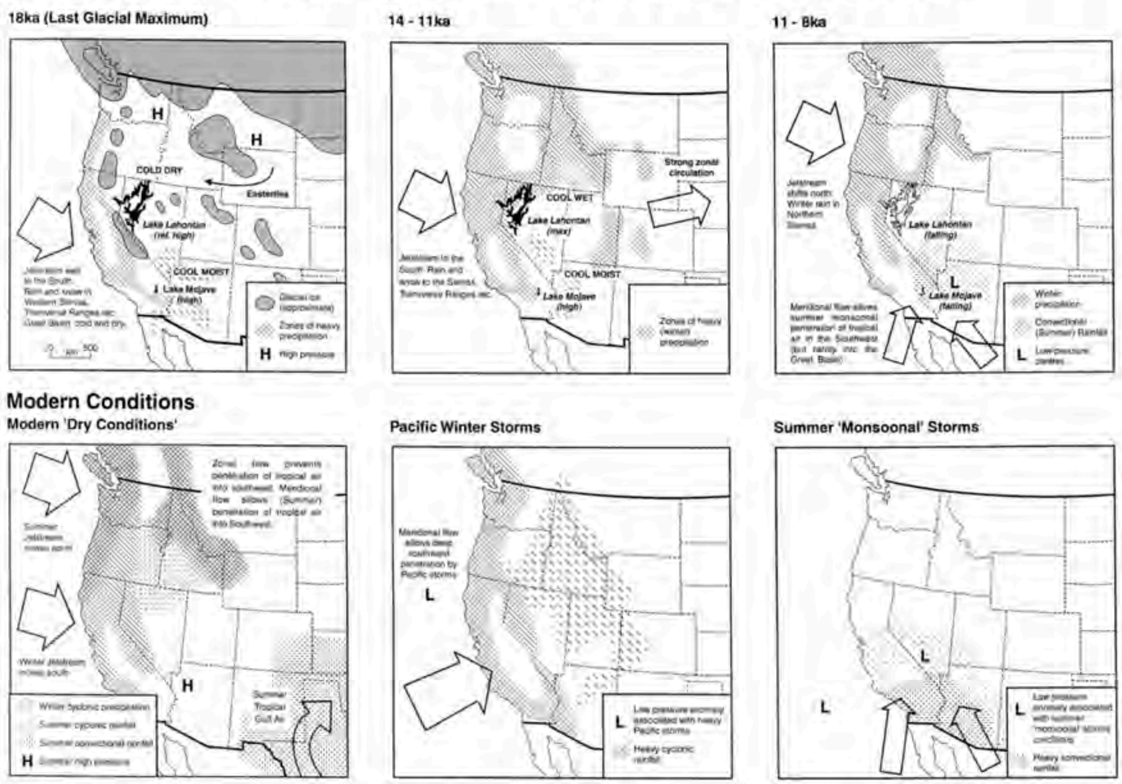

Figure 1. Climate history of Mojave Desert. The lakes were produced by high precipitation over the lake-source areas (enhanced by cool conditions and low evaporation rates over the lake basins themselves), conditions favored by a southerly track of Pacific storms. Geomorphic activity on the fans results primarily from 'monsoonal' conditions involving the penetration of moist tropical air into the Southwest.

Hydrology of Mojave Desert

The Mojave River and Morongo groundwater basins are in the southwestern part of the Mojave Desert in southern California, approximately 130 km north and 65 km northeast, respectively, of Los Angeles (Figure 2). The Mojave River and Morongo groundwater basins together encompass about 6,200 km^2. The climate of these basins is typical of the Mojave Desert region of southern California. Most areas of the basin floor receive 100 to 150 mm of precipitation per year, although annual precipitation can be greater than 1000 mm in the southern and eastern San Bernardino and the San Gabriel Mountains. Recharge to the groundwater system from direct infiltration of precipitation is minimal.

Figure 2. Location of the Mojave River and Morongo groundwater basins.

Surface water in these basins is minimal and normally is limited to ephemeral flow during winter and spring storms and discharge from perennial springs in some areas of the Morongo groundwater basin. The major source of surface water is the Mojave River; however, its flow is unpredictable and not a dependable source for water supply because most of the river's 160-km channel usually is dry. The lack of significant surface-water resources has resulted in the use of groundwater as the primary source for private, agricultural, and municipal supply. Because of increasing urbanization, demands on local water supplies have created overdraft conditions in some areas of the desert basins. Significantly lowered water levels have the potential to induce or renew land subsidence in the Mojave River and Morongo groundwater basins. Land subsidence can result in the disruption of surface drainage, reduction of aquifer-system storage capacity, formation of earth fissures, and damage to wells, buildings, roads, and utility infrastructure.

Mojave River Groundwater Basin

The Mojave River groundwater basin is approximately 3,600 km^2 and extends from the San Bernardino and the San Gabriel Mountains in the south to north of Harper and Coyote Lakes (dry). The groundwater basin is bordered on the west by Antelope Valley and shares its southeastern boundary with the Morongo groundwater basin. For water-management purposes, the Mojave River groundwater basin was divided into five subareas, partially based on the Mojave River drainage basin boundary: Baja, Centro, Alto, Este, Oeste.

The primary source of groundwater recharge in the Mojave River groundwater basin is intermittent streamflow in the Mojave River, which usually occurs during January through March, and from sporadic releases of imported water from the California State Water Project (SWP). The basin has received SWP water at the Rock Springs recharge site (near well 4N/3W-29E5) southeast of Hesperia since 1994, and has also received SWP water at the Hodge recharge site (near well 9N/3W-23D2) since 1999, at the Lenwood recharge site (near well 9N/3W-1R7) since 1999, at the Yermo/Daggett recharge site (near well 9N/1E-20B3) since 2003, and at the Newberry Springs recharge site (near well 9N/3E-22R7) since March 2006.

Morongo Groundwater Basin

The Morongo groundwater basin is about 2,600 km^2 and is surrounded by the Ord and Granite Mountains to the north, the Bullion Mountains to the east, the San Bernardino Mountains to the southwest, and the Little San Bernardino Mountains to the south. The Morongo groundwater basin is separated into 17 subbasins: Lucerne, Fry, Johnson, Upper Johnson, Means, Pipes, Reche, Emerson, Giant Rock, Copper Mountain, Surprise Spring, Deadman, Mesquite, Mainside, Warren, Joshua Tree, and Twentynine Palms. The Morongo groundwater basin is recharged by infiltration from flow in ephemeral stream channels and, since 1995, from SWP water recharged to ponds at three Hi-Desert recharge sites (near wells 1N/5E-36M5 and 1N/5E-34Q1) in the Warren subbasin.

Geohydrology

The boundaries of the Mojave River and the Morongo groundwater basins generally are defined by the contact between the water-bearing unconsolidated deposits and the surrounding and underlying non-water-bearing consolidated igneous and metamorphic rocks. The groundwater system in the Mojave River Basin consists of two interconnected unconfined aquifers (a body of permeable rock which can contain or transmit groundwater) —a floodplain aquifer and an underlying and surrounding regional aquifer, which are part of the Basin and Range aquifers in southern California (Figure 3). The most productive aquifer is the floodplain aquifer, which is composed of permeable young river deposits of Holocene age and older river deposits of Pleistocene age. This aquifer is as much as 60 m thick and yields most of the groundwater pumped from the Mojave River Basin. The most widespread aquifer in the area is the regional aquifer; it is composed of unconsolidated older alluvium and fan deposits of Pleistocene to Tertiary age. In some places, the regional aquifer also consists of partly consolidated to consolidated sedimentary deposits of Tertiary age. The regional aquifer is as much as 300 m thick. Other geologic units, such as bedrock and lake deposits, commonly contain groundwater, but they are not considered reliable sources of ground water in the study area.

The Mojave River and Morongo groundwater basins are separated by the Helendale Fault, which acts as a barrier to groundwater flow near Lucerne Valley. The regional aquifer in the Morongo groundwater basin consists of continental deposits of Quaternary and Tertiary age that extend to as much as 3,000 m deep. Perched groundwater has been identified in four areas of the Mojave River and Morongo groundwater basins. Perched groundwater is unconfined ground water separated from an underlying body of groundwater by an unsaturated zone. The approximate areas of perched groundwater in the Mojave River groundwater basin are near El Mirage Lake (dry) and northeast of the city of Adelanto, and in the Morongo groundwater basin are Lucerne Valley and Mesquite Lake (dry).

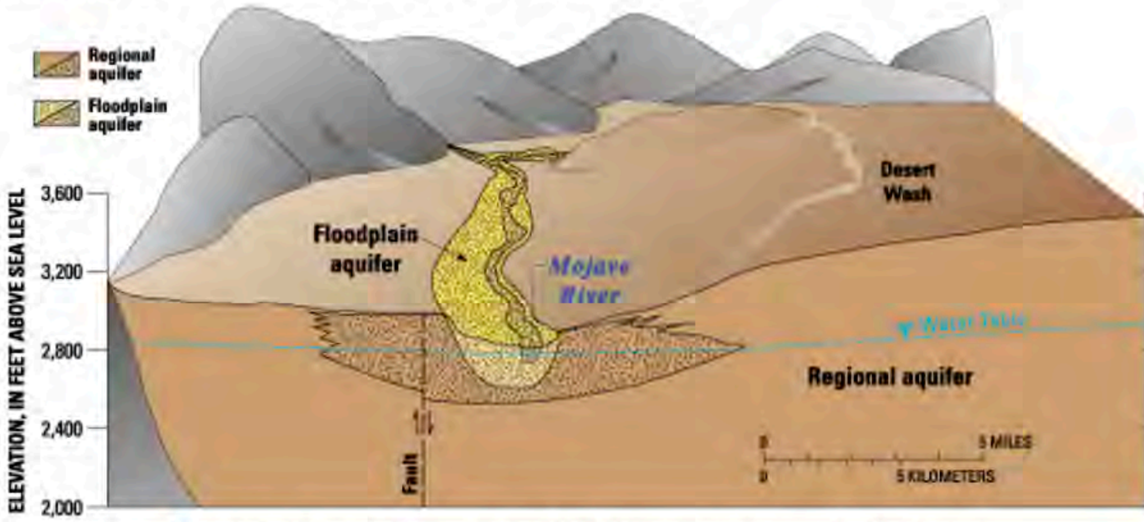

Figure 3. The aquifer system in the Mojave river groundwater basin.

Resources

Harvey et al., (1999) Response of alluvial fan systems to the late Pleistocene to Holocene climatic transition: contrasts between the margins of pluvial Lakes Lahontan and Mojave, Nevada and California, USA. *Catena* 36, 255 – 281.

USGS Mojave Groundwater Resources. Water-Level, Water-Quality and Land-Subsidence Studies in the Mojave River and Morongo Groundwater Basins.

USGS Water Supply in the Mojave River Ground-Water Basin, 1931-99, and the Benefits of Artifical Recharge

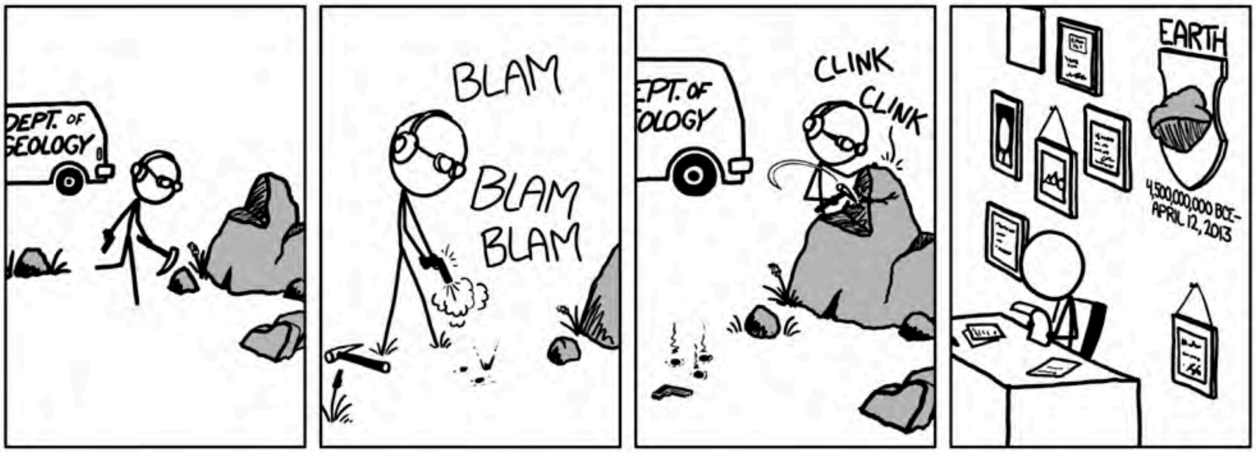
DEPT. OF GEOLOGY
BLAM
BLAM
BLAM
CLINK
CLINK
EARTH
4,500,000,000 BCE–
APRIL 12, 2013


Olivine at Earth's surface:
This is unbearable.
@tectonic_city
Olivine in the mantle:
THIS IS FINE.

Radar and Roughness

Rishi Chandra

Radar and SAR: how do they do it?

Radar is a handy remote sensing technique useful for understanding several properties of planetary surfaces, but it is quite different from optical, ultraviolent, or infrared wavelength observations. Radar stands for RAdio Detection And Ranging, and is an active remote sensing technique where an instrument emits a radio wave which reflects off of a surface and returns to a receiver. The receiver measures the intensity, polarization state, and timing of the returned signal, using which properties of the reflector can be determined [1].

Synthetic Aperture Radar, or SAR, is a technique by which high resolution two-dimensional Radar images can be constructed without the need of an overwhelmingly large aperture, as is the case for ground-based radio telescopes like Arecibo or FAST [2]. While cameras and telescopes sensitive to optical, IR, and UV radiation have a compact physical aperture that light passes through to create a 2D image, radio waves need inordinately sized optics to do the same. Instead, an orbiting satellite or moving aircraft collects multiple overlapping Radar observations of the surface as it travels along an extremely well known path. These observations and knowledge of the flight path are processed together to produce high resolution Radar images, where the travel path of the Radar receiver acts as a kilometers-long *synthetic* aperture that can resolve features on the surface as small as tens or ones of meters, depending on the wavelength used. For our purposes, the term Radar implies the use of SAR.

Spaceborne Imaging Radar-C/X-band Synthetic Aperture Radar (SIR-C/X-SAR) in the payload bay of space shuttle Endeavour. Because it uses SAR, it can quite easily be placed in orbit. 1994. Image credit: NASA/JPL

Radar reflectance can be a quite complicated function of many variables, on Earth including roughness, surface moisture, vegetation, electromagnetic material properties, and more. All of these properties' effects on reflectance also strongly depend on the wavelength under consideration. We'll only concern ourselves with roughness today.

Various wavelengths of Radar used for SAR, from earthdata.nasa.gov

Band	Frequency	Wavelength	Typical Application
Ka	27–40 GHz	1.1–0.8 cm	Rarely used for SAR (airport surveillance)
K	18–27 GHz	1.7–1.1 cm	rarely used (H2O absorption)
Ku	12–18 GHz	2.4–1.7 cm	rarely used for SAR (satellite altimetry)
X	8–12 GHz	3.8–2.4 cm	High resolution SAR (urban monitoring,; ice and snow, little penetration into vegetation cover; fast coherence decay in vegetated areas)
C	4–8 GHz	7.5–3.8 cm	SAR Workhorse (global mapping; change detection; monitoring of areas with low to moderate penetration; higher coherence); ice, ocean maritime navigation
S	2–4 GHz	15–7.5 cm	Little but increasing use for SAR-based Earth observation; agriculture monitoring (NISAR will carry an S-band channel; expends C-band applications to higher vegetation density)
L	1–2 GHz	30–15 cm	Medium resolution SAR (geophysical monitoring; biomass and vegetation mapping; high penetration, InSAR)
P	0.3–1 GHz	100–30 cm	Biomass. First p-band spaceborne SAR will be launched ~2020; vegetation mapping and assessment. Experimental SAR.

Interpreting roughness from Radar

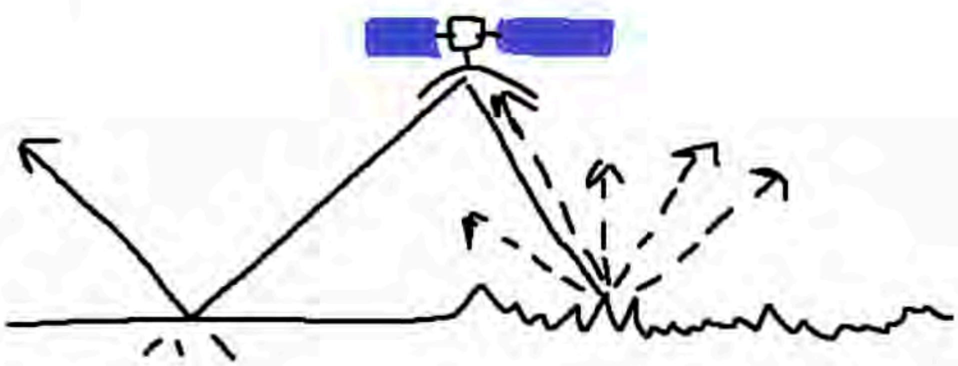

In the above MS Paint drawing, we see a diagram that intuitively illustrates why rough surfaces appear brighter in Radar reflectance images. Surfaces that are smooth cause incident radio waves to undergo specular reflection, where a quite small fraction of the radio wave energy reflects back (backscatters) to the receiver, and the region appears dark in our Radar backscatter image. Contrastingly, on rough terrain, a greater proportion of the radio wave energy backscatters and returns to the receiver, and this region will appear brighter in our Radar backscatter image.

In the absence of vegetation (as is the case on most planets), greater Radar backscatter generally corresponds to greater surface roughness. We can interpret sharp spatial discontinuities in Radar backscatter coinciding with boundaries between geologic units as indicating that one geologic unit is much rougher than the other. This effect is pronounced where young lava flows superimpose old, smooth terrain, and can be used to quickly see the extent of the lava flow even if in optical wavelengths the flow is difficult to distinguish from the surrounding terrain. Weathering processes can either smoothen or roughen a surface, so this method alone isn't enough to tell which geologic unit is older and which is younger. Additionally, the backscatter intensity at a given observational wavelength corresponds to the roughness at a particular significantly smaller spatial length scale. For example, C band reflectance with a wavelength of ~5cm corresponds to roughness at the millimeter scale.

The reader can go to the field guide insert and inspect the figures titled *C-band backscatter data from SRTM* (Shuttle Radar Topography Model) and *UAVSAR L-band of Pisgah Flow and Cone*. In both of these, bright regions correspond to rougher terrains, and dark patches correspond to very smooth terrains.

National Defense Applications (I got severely carried away writing this)

One salient terrestrial application of SAR that a peace-loving graduate student may not consider is the observation of mass movements of military equipment on week-to-week timescales. Sentinel-1 is one satellite whose data has been used by Western intelligence to observe westward Russian troop and equipment movements immediately prior to the 2022 invasion of Ukraine [3]. Below are images of Yelnya, a Russian town near Belarus, determined by open-source intelligence to be a staging ground for heavy Russian military equipment [4]. The per-pixel resolution of the SAR images is roughly 10m, so the bright pink pixels don't represent individual vehicles so much as the "roughness" effected by the presence of trucks and tanks. SAR images captured at regular time intervals can be compared to one another to identify mobilizations of large military equipment, and these images can be captured at any time of day in any weather conditions. While camouflage may successfully hide equipment in optical imagery, it is far more difficult to hide heavy military equipment from SAR.

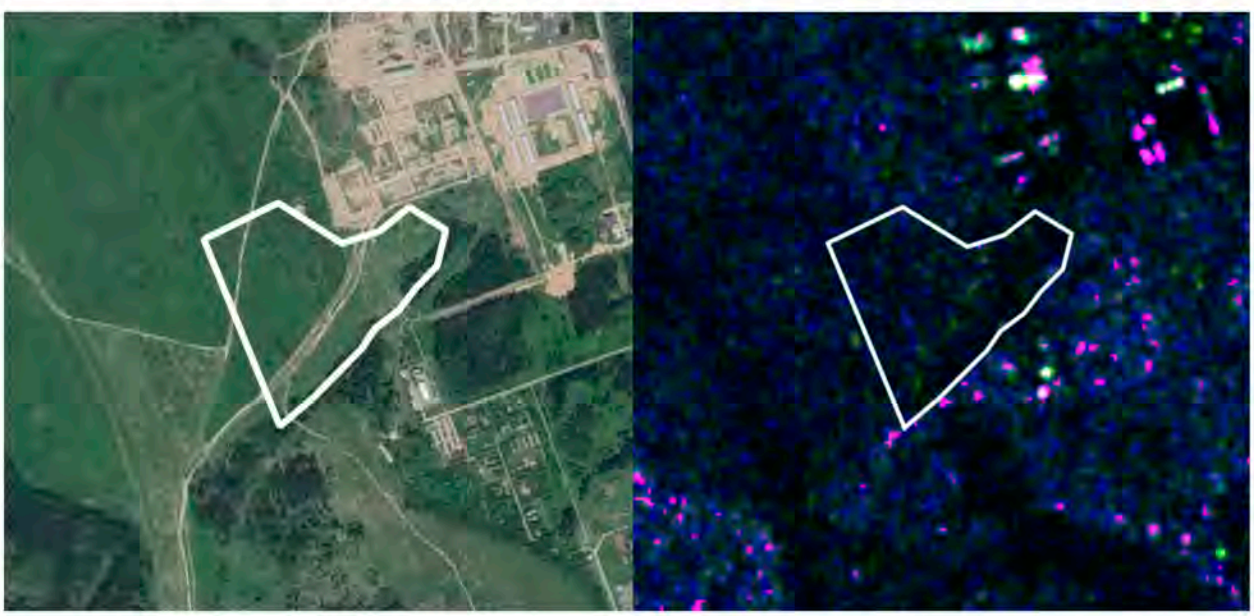

Yelnya, Russia, in early 2021. MAXAR optical imagery on the left and Sentinel-1 SAR imagery on the right.

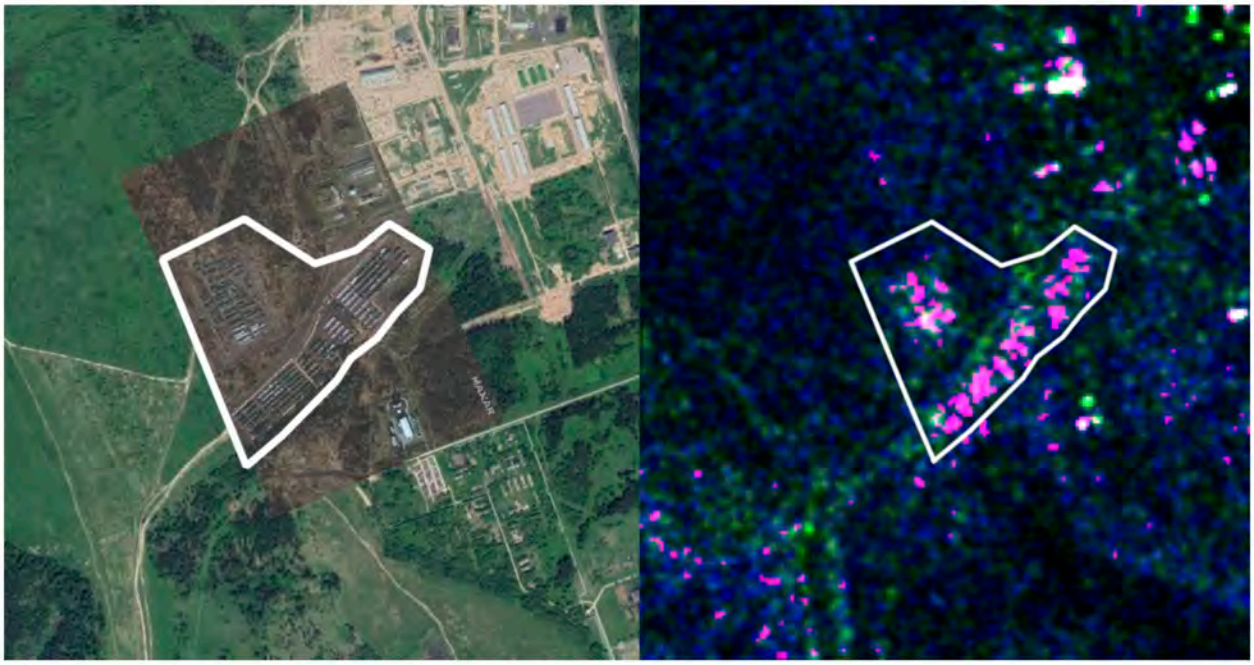

Yelnya, Russia in November 2021, displaying an accumulation of military equipment

Works Cited

[1] Selley R. C. et al. (2005) *Encyclopedia of Geology*.

[2](N.d.) "What is Synthetic Aperture Radar? | Earthdata," can be found under https://earthdata.nasa.gov/learn/backgrounders/what-is-sar/.

[3](N.d.) "Sentinel-1 - Missions - Sentinel Online - Sentinel Online," can be found under https://sentinel.esa.int/web/sentinel/missions/sentinel-1.

[4](N.d.) A LOT of intense people on Twitter who seem to know a lot about what's going on in Ukraine


The Western US during the basin and range extension


LIVE
BREAKING NEWS
LOCAL ROCK IN GREAT MOOD TODAY
19:41
EROSION IS NOT MUCH HAPPENING & WE BOUT TO GET IGNEOUS

Mojave Desert Flora and Fauna

-Tarunika Ramprasad

Flora

The Mojave desert is the host to approximately 200 endemic plant species, that are instrumental in defining its geophysical boundaries. This is one of the largest clustering of endemic species anywhere in the world. In general, the plants of the Mojave desert are distinct to the various geographic features, forming various flora communities. Another important characteristic of the flora of the Mojave desert is that they are relatively recent in origin, evolving as the result of climate trends and water availability over the part 10,000 years. For example, plants that currently occupy the desert mountains were previously widespread in the lowlands when there were abundant freshwater lakes. Similarly heat-tolerant species migrated to higher elevations with increasing temperatures. Below we discuss the distribution of flora in the various geographic regions of the Mojave desert.

- ***Ash Meadows***: This part of the Mojave desert receives approximately 3 inches of rainfall per year and presents a breathtaking bloom of over 330 species of flowers and shrubs. Of particular interest are Ash Meadows milkvetch and Ash Meadows sunray, which are threatened species that being flowering early in spring. The screwbean mesquite is the most common tree in this region. The seeds of the plants in this region are capable of surviving decades of heat and drought spells, often sprout quickly under favorable conditions.

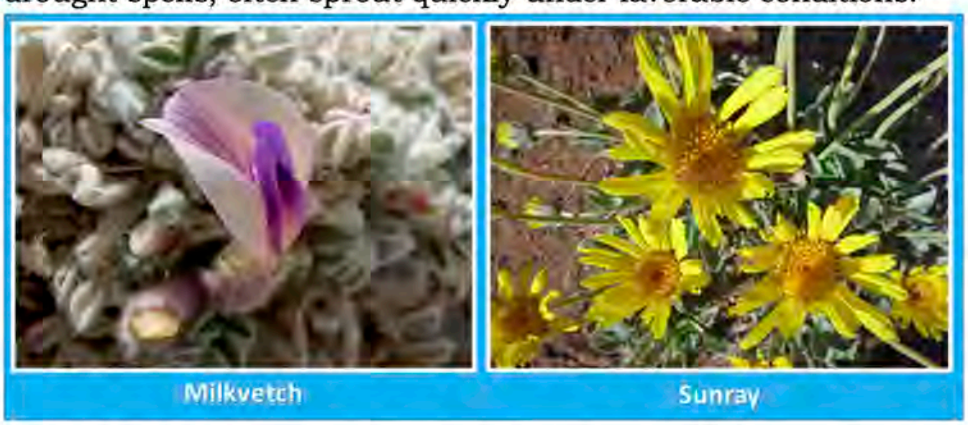

- ***Death Valley***: The vegetation in this region of the Mojave desert varies according to elevation. At the lower elevation, the landscape is dominated by creosote bush, desert holly and mesquite. As the elevation increases, the first to appear are shadscale, blackbush, Joshua tree and pinyon-juniper; followed by sub-alpine limber pine and bristlecone pine woodlands. The saltpan region of the Death valley is devoid of vegetation. On the years that the valley receives plenty of rainfall, it also plays host to a variety of desert wildflowers.
- ***Hover Dam***: This region of the Mojave desert hosts various species that are adapted to surviving with varying levels of water availability. The plants most

common in this area are barrel cactus, beavertail cactus, cholla cactus, creosote bush, desert mallow, desert marigold, Indian paint-brush, prickly pear cactus, sacred datura and rock nettle.

- ***Mojave Preserve***: The vegetation in this region is primarily composed of plants attributed to the Mojave desert, but also contains flora species from Great Basin, Sonoran desert and California Chaparral zone.
- ***Valley of Fire***: This part of the Mojave desert is dominated by creosote bush, burro bush, brittle bush, beavertail cactus and cholla cactus. During the spring, the valley is filled with blooms of these plants as well as wildflowers, predominantly the desert mallow.
- ***Vasquez Rocks***: The vegetation in this part of the Mojave desert is sparse, composed of various succulent desert plants, yucca, scattered scrub oak and California juniper.

List of various types of flora:

- ***Cactus***: Foxtail, Teddybear, Silver cholla, Pencil cholla, Cottontop, Hedgehog, Mojave mound, California barrel, Beavertail pricklypear and Grizzlybear pricklypear.
- ***Shrubs***: Creosote bush, Mojave yucca, Chaparral yucca, Desert holly, Manzanite, California buckwheat, Mormon tea, Rabbitbrush, Yerba mansa, Yerba santa and Arrowweed.
- ***Trees***: Joshua tree, Pinyon pine, Mesquite, California juniper, California fan palm oases, Cottonwood and Desert willow
- ***Wildflowers (selected)***: Blue dicks, Brown-eyed primrose, California fagonia, California poppy, Canterbury bells, Catura, Desert calico, Desert Star, Fiddleneck, Golden gilia, Lacy phacelia, Mojave aster, Mojave poppy, Red maids, Thistle sage, White rhatany and Yerba mansa.

Indian use of native plants:

- ***Honey Mesquite***: Mesquite beans have high nutritional value and are eaten either fresh or dried. When dried, they are pounded into a meal and formed into small cakes that are then sun dried. Wood from these trees is the primary source of firewood, as well as the base for weapons, homes and roofs.
- ***Pinyon Pine***: The cones are harvested while still green and roasted to release the nuts, that are then used as a food source.
- ***Oak***: The acorns are used as bait in animal traps and to make toys for children. In the past, acorns were important trade items.
- ***Creosote Bush***: Tea made from the leaves of this shrub is considered a cure-all medicine.
- ***Chia***: Seeds from this plant are used as an eye cleanser.
- ***Ephendra***: Tea made from this plant is used as a health tonic.
- ***Mistletoe***: The berries are ground into flour and used to treat wounds.

Creosote Bush

Desert Holly

Cattle Saltbush

White Burrobush

Brittlebush

Joshua Tree

Fauna

Unlike the flora, the fauna of the Mojave desert are less endemic and often extend into the neighboring Sonoran and Great Basin deserts. However, there are endemic fauna such as the Kelso Dunes shieldback katydid, Kelso Dunes Jerusalem cricket, Mojave ground squirrel and Amargosa vole. While not strictly endemic, the Mojave fringe-toes lizard is almost exclusively present only in the Mojave desert. One of the most interesting fauns of the region is the desert tortoise, that is well adapted to surviving arid climates by remaining inactive for majority of the year and having slow growth and reproductive rates.

The Mojave National Preserve is home to 50 species of mammals, 36 species of reptiles, 3 species of amphibians, 3 species of fish, over 200 species of birds and numerous species of insects and arachnids. Of the amphibians, the red-spotted toad is the only naturally occurring inhabitant of the Mojave National Preserve. Of the fish, the Mohave tui chub is the only native fish to the Mohave river basin, the other two were introduced into the reservoirs.

List of various types of fauna:

- ***Amphibians***: Red-spotted toad, Pacific treefrog and California treefrog
- ***Birds (selected)***: Ravens, Cactus wren, Roadrunner, Golden eagle, Red-tailed hawk, Turkey vulture, Vaux's swift, Broad-tailed hummingbird, Mourning dove, Prairie falcon, Horned lark, Sage sparrow and Pinyon jay.
- ***Fish***: Mohave tui chub, Arroyo chub and Gila orcutti
- ***Insects and Arachnids (selected)***: Scorpion, Ticks, Mites, Harvestmen, Black widow spider, Brown recluse spider, Tarantula, Pronuba moth, Dragonfly and Cicadas.
- ***Mammals (selected)***: Coyote, Hoary bat, Bighorn sheep, Black-tailed jackrabbit, North American porcupine, Kit fox, Bobcat, Rock squirrel, Desert woodrat and Panamint chipmunk.
- ***Reptiles (selected)***: Chuckwalla, Gila monster, Desert iguana, Gopher snake, Coachwhip, Common kingsnake, Mojave rattlesnake and Desert tortoise.

Relevant Terms:

- ***Endemism*** is the state of a plant or animal species being found in one defined geographic location.
- ***Species*** (in biology) is the classification comprising related organisms that share common characteristics and are capable of interbreeding.

Gopher Tortoise

Desert Cottontail

Cactus Wren

Costa's Hummingbird

Great Basin Collared Lizard

Desert Bighorn Sheep

Black-tailed Jackrabbit

Greater Roadrunner

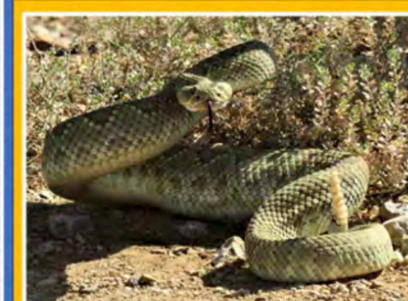

Mojave Green

The Native People of the Mojave

The land upon which we travel is the ancestral territory of the Chemehuevi, Hopi, Navajo, and Mojave peoples. These peoples' origins, histories, and mythologies stem from this region which provided their grounds for agriculture, hunting, peopling, and war. These four nations are now recognized members of the Colorado River Indian Reservation [1]

The region of the Mojave Desert has been populated by these groups for an estimated 2000 years, but certain petroglyphs suggest the earliest human presence to be 15000 years ago [2].

Chemehuevi Indians

"Those who play with fish"

Considered a desert tribe, these people lived in relative harmony amongst the neighboring Mojave peoples. Distinctions can be made in their cultural artifacts from differences in the materials used for the crafting of bows and pottery [3].

The Chemehuevi were primarily hunter/gatherers. Some farming was possible along the banks of the Mojave river which is mainly subterranean and flows north from the San Bernardino mountains and flows out into the Soda Lake [4].

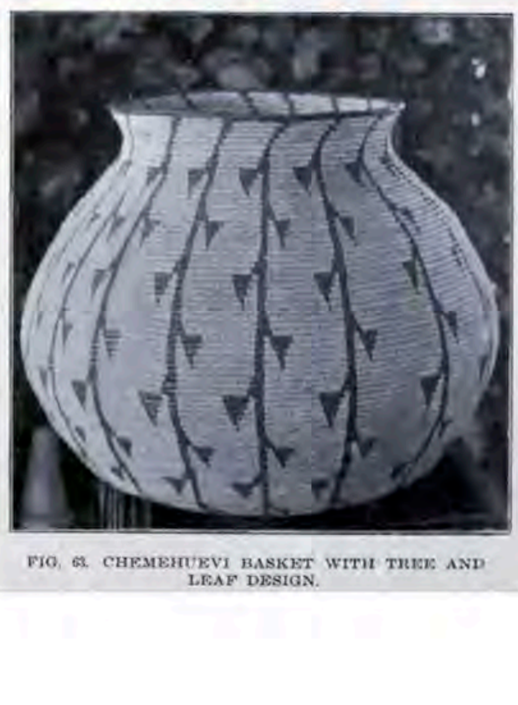

FIG. 63. CHEMEHUEVI BASKET WITH TREE AND LEAF DESIGN.

Mojave Indians
Pipa Aha Macav or "The People Who Live Along the River"

In the beginning there was chaos. The Great Spirit Matavilya brought people into this world, but, before they could be taught, he was killed by his sister Frog Women. The Great Spirit had a little brother, Matsamho, who wished to finish what was started. Driving a willow stick into the ground, Matsamho drew the waters that have become the Colorado River. He brought the mountains, animals, sun, and moon. He gave his people fingers and toes; teaching them how to count, cook, and craft. Matsamho gave his people the river and so they were "The People Who Live Along the River". [5, 6]

The Mojave peoples lived within a patrilinear clan system originally consisting of 22 clans. Dreams and visions held great cultural power and were viewed as the source of knowledge. Tribe members who frequently dreamt where considered gifted and were given a special test. The art of tattoo was also of particular importance. Tribe members who died without tattoos were said to have their spirits trapped in a rat hole. [6]

The Colorado River was the center of their existence. They used the regular annual overflow to irrigate their crops which were planted along the banks. The primary economic activity was always agriculture with Mesquite trees holding historical importance as a highly versatile crop. The tribal uses of the Mesquite tree ranged from food source to construction resources, weapons, shampoo, and even charcoal for tattoos [7].

European Contact

The first people to encounter the people of Mojave were early American explorers in search of fortunes. These early encounters were reportedly peaceful with white descriptions of the Mojave to be 'friendly'. Famously, the mountain man Jedediah Smith came through the Mojave with a party of fur trappers in 1826. What started off amicably soon fell into bloodshed however as the Mojave began to observe the brutality with which the trappers completed their work. Years of conflict would ensue between the peoples and the western travelling trappers. The conflict reached its peak when 26 Mojave were killed by the Canadian Hudson Bay Co.

Jedediah Strong Smith - George Mathis, ca. 1970

In the 1850s the United States Army moved in. After a scandal regarding two white girls who were raised by a Mojave tribe, Fort Mojave was established. This land became the home of the Colorado Indian Reservation in 1865 and the Fort was repurposed as a boarding school which practiced indoctrination and assimilationist methods. The last legs of the original tribal structure of the Mojaves buckled when the Great Chief Hobelia (a ten-year-old) had his name anglicized to Pete Lambert. [6]

The boarding school closed in the 1930's. The Native American's who live on Colorado Indian Reservation now attend public schools in Needles CA. They continue to practice agriculture but have also economically diversified with casinos, golfing, and boating enabling tourism of the region [8].

References:

1. https://www.crit-nsn.gov/crit_contents/about/
2. http://mojavedesert.net/overview/h01.html
3. http://mojavedesert.net/chemehuevi-indians/chemehuevi.html
4. https://digital-desert.com/mojave-river/
5. https://www.nps.gov/moja/learn/historyculture/mojave-tribe.htm
6. http://mojavedesert.net/mojave-indians/
7. https://www.sandiego.edu/kumeyaay-garden/plants/mesquite.php
8. https://www.fortmojaveindiantribe.com/about-us/

The Amboy Streak

Reed Spurling

Landsat

Maxar

The Amboy crater streak—and similar nearby dark streaks on the Amboy lava field—align with the local wind direction. **This suggests that these streaks were formed by aeolian processes.**

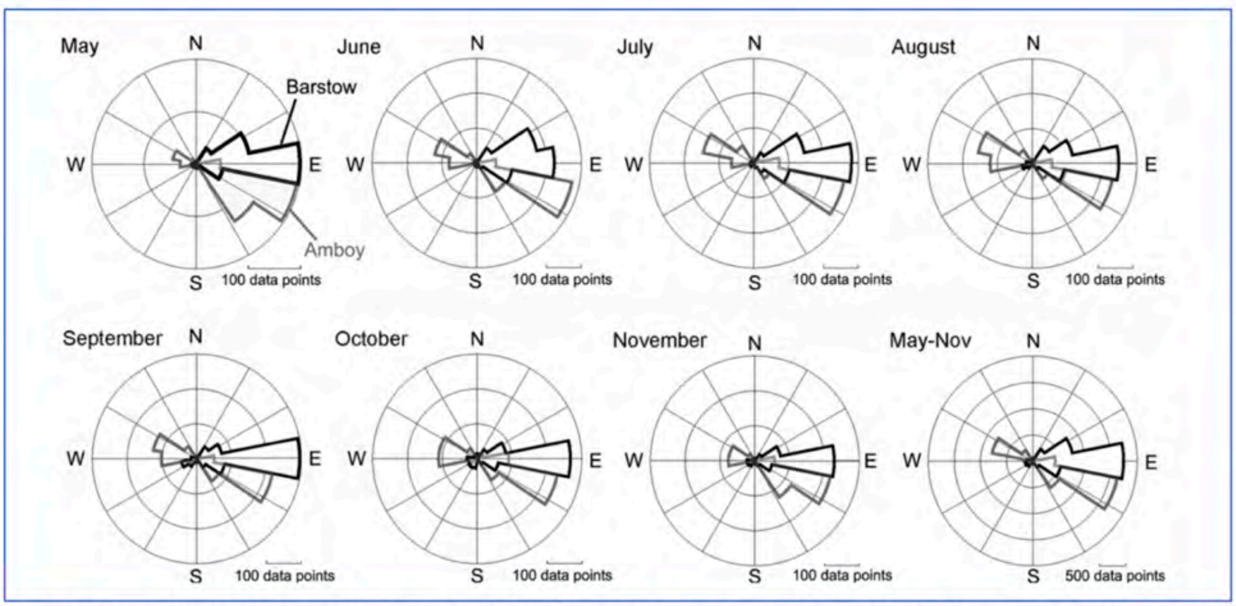

Figure from Kienenberger & Greeley (2012): Locally measured wind directions in Barstow and Amboy. Note the prevailing east-southeast direction of the winds flowing over the Amboy lava field.

If we did not have local wind measurements at this site, we would we still be able to test the hypothesis that these streaks are aeolian in origin by using remote sensing and modeling.

Remote sensing evidence for the streaks' origins

1) Topography

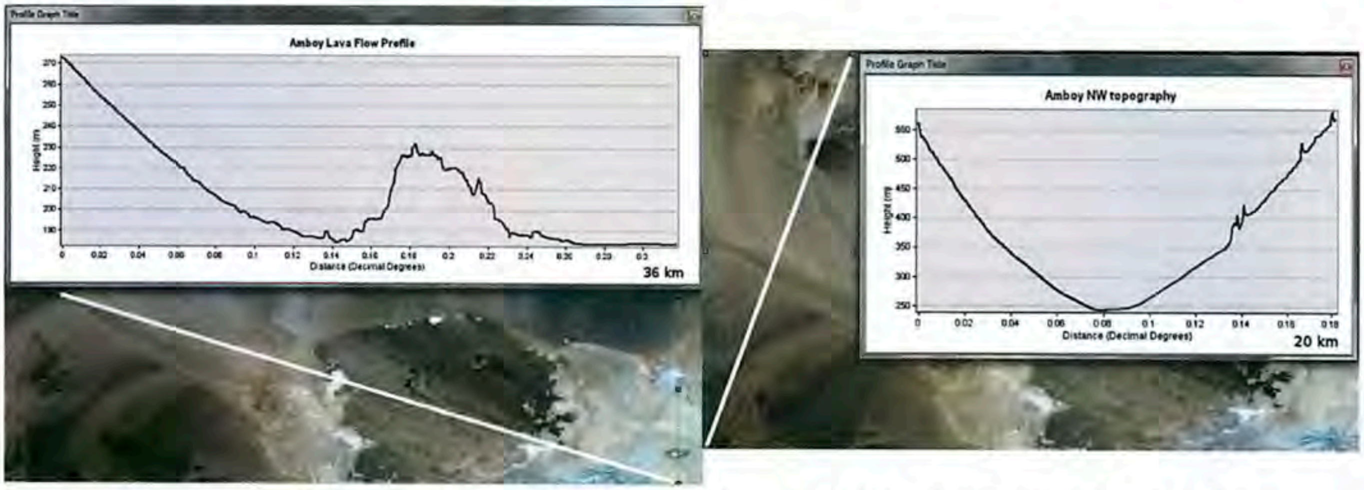

Figure shamelessly (maybe a bit shamefully) copied from a 2013 field guide section by Melissa Dykhuis, Cecilia Leung, and Gabriel Muro: Topography of the Amboy lava field and surroundings, with elevation profiles displayed from left to right. Note the long slope of the valley down towards the lava field. Surface winds in this area could plausibly be affected by the topography, perhaps being funneled down the valley towards Amboy crater.

2) Surface composition

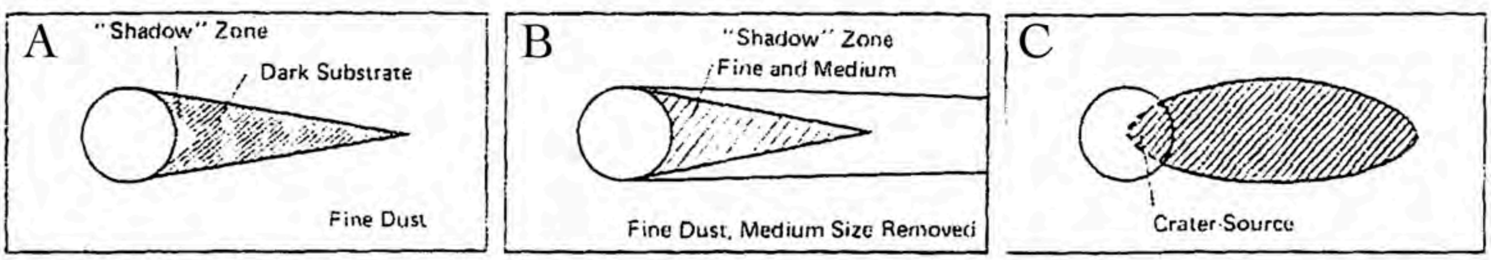

Figure adapted from Greeley & Iverson (1987): Possible formation methods for aeolian dark streaks. In (A), the surface could be initially covered in bright, fine dust, which is then removed by turbulent air flow or other types of wind directly behind the crater. Alternatively, (A) could represent a scenario in which a dark underlying surface is covered by windblown bright, fine dust, except where blocked by the tall crater. (B) represents a scenario in which medium-size grains of darker material are removed by wind everywhere except the lee of the crater. (C) represents a scenario where the crater itself is the source of dark material being blown downwind.

By using remote sensing to compare the thermal emissivities of the crater, the dark streak, and the surrounding lighter material, we can begin to determine if a specific aeolian formation scenario is more likely than other aeolian or non-aeolian formation scenarios. Let's look at that emissivity data:

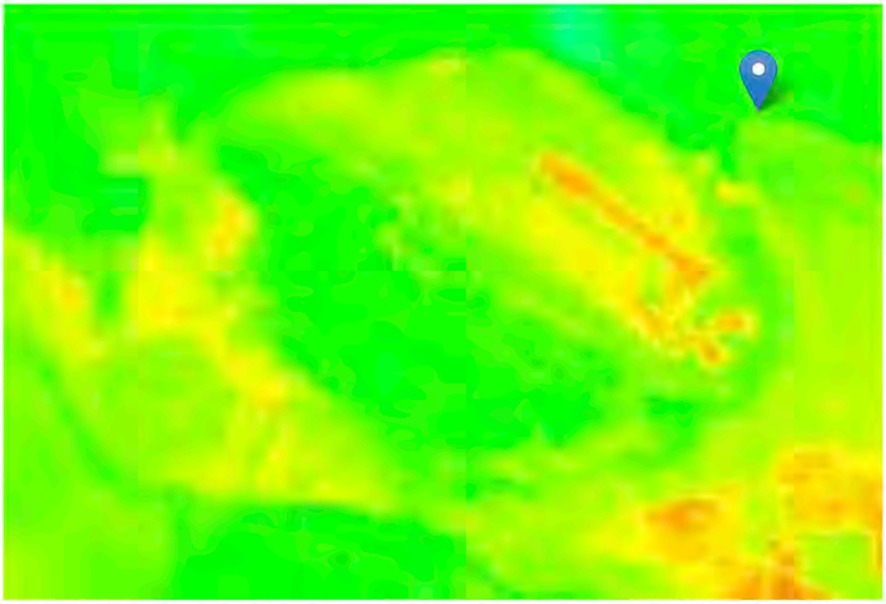

Thermal emissivity (8.3–11.3 µm) of the Amboy lava field, with the town of Amboy indicated by the blue marker. We clearly see the main streak from the Amboy crater in this view. Some smaller streaks may be visible as well. **It is significant that the thermal emissivity signature of the streak ends right at the edge of the lava flow field.** Image from the ASTER Global Emissivity Database, 100 meter/pixel resolution, accessed via the partially broken website earthexplorer.usgs.gov

3) Synthetic Aperture Radar

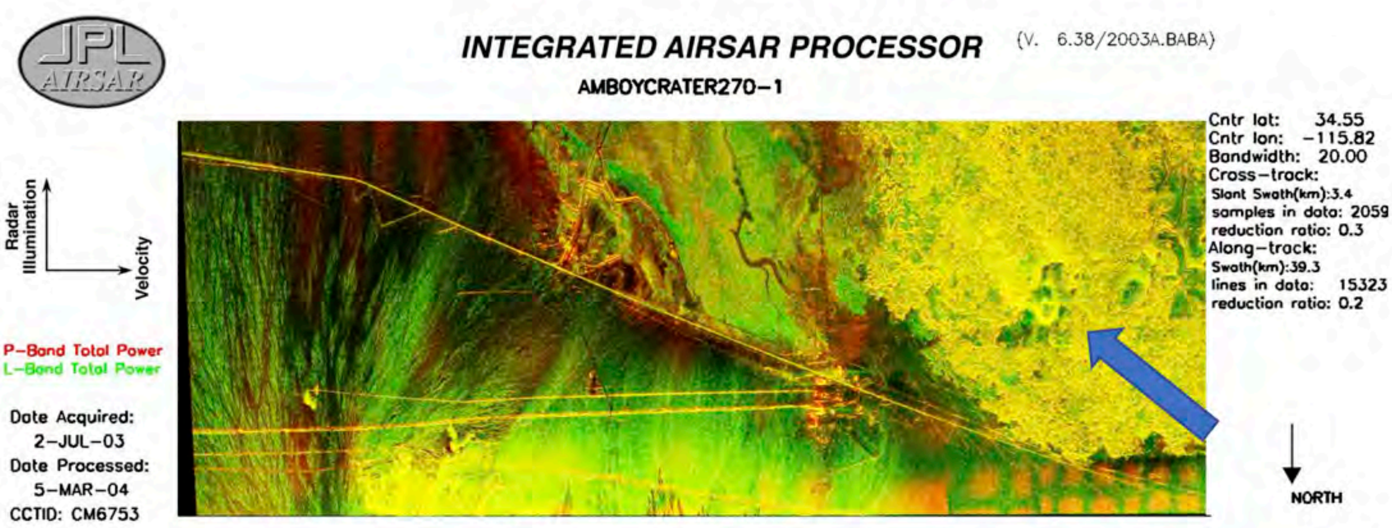

I don't know much about SAR, so I will leave this figure to the RADAR people for interpretation. Note that the Amboy crater and its streak are distinct from the surrounding surface in their L/R band power radio. Yet more evidence that the crater and its streak are composed of similar material with similar surface properties. What implications does this have for the various streak formation hypotheses?

4) A Martian analogue

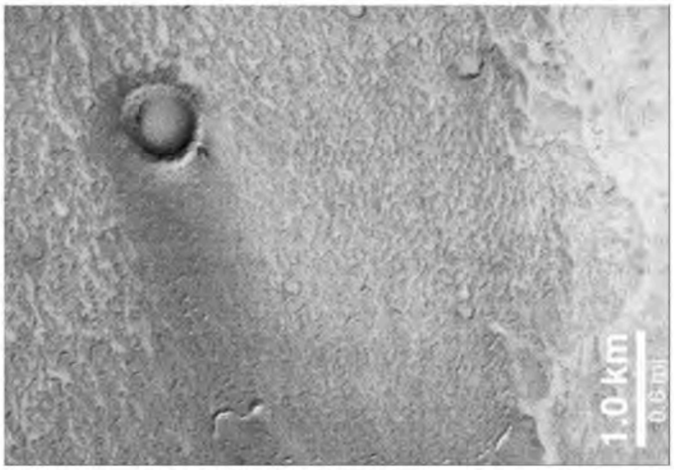

MOC image AB1-10905, showing an impact crater (with a raised rim) in Daedalia Planum.

Model-based insights into the streaks' origins

1) Wind tunnel tests

Fig. 6.17. (*a*) Iowa State University wind tunnel simulation of a crater wake dark streak. The deflation streak is dark because the wind tunnel floor is black and the particles are white. Crater rim height is 3 cm and its diameter is 30 cm. The material on the floor is sugar, with an average diameter of 393 μm. Terminal speed-threshold friction speed ratio is 10.1. (From Iversen *et al.*, 1973.)

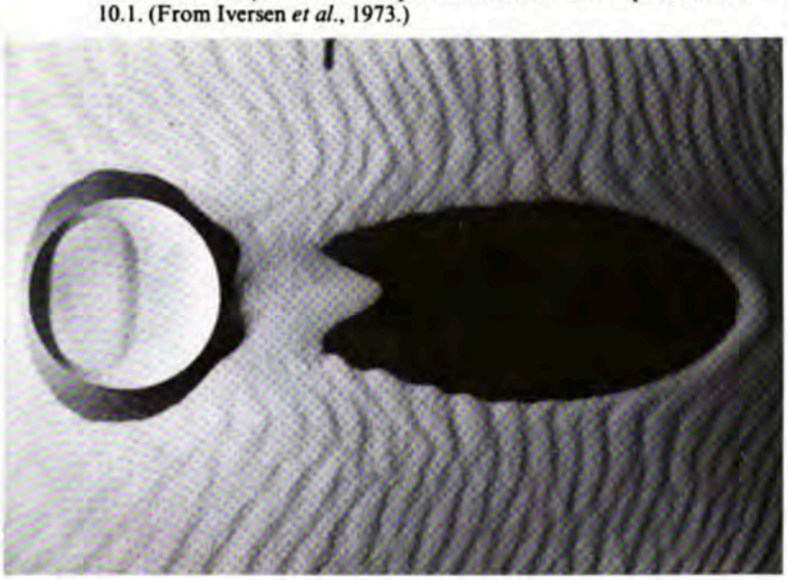

Figure and caption from Greeley & Iverson (1987). The shape of the particle-less streak in the lee of the crater differs depending on the particle size, but a streak or divot was formed at most particle sizes tested by the authors. Other tests used glass particles instead of sugar.

2) Atmospheric Modeling

A cautionary tale: Cohen-Zada et al. (2017) used atmospheric modeling to predict the prevailing wind direction over the Amboy lava field and obtained significantly different results than were produced by in-situ observations. Cohen-Zada et al. suggested that this is because the valley where the Amboy lava field is situated, between the Bristol and Bullion mountains, channels the regional-scale westerly winds towards the east-southeast on a local scale. The point being: Don't trust atmospheric models too much at local scales unless they are backed up by in-situ observations. This has implications for studies of similar wind-blown streaks on Mars.

References

Byrnes, J., Finnegan, D., Anderson, S., & Ramsey, M. (2006). Analysis of Amboy Crater, Mojave Desert, California, as an Analog for Small Martian Volcanoes. Presented at the Lunar and Planetary Science XXXVII, League City, Texas. Retrieved from https://www.lpi.usra.edu/meetings/lpsc2006/pdf/1205.pdf

Cohen-Zada, A. L., Maman, S., & Blumberg, D. G. (2017). Earth aeolian wind streaks: Comparison to wind data from model and stations. *Journal of Geophysical Research: Planets*, *122*(5), 1119–1137. https://doi.org/10.1002/2016JE005242

Greeley, R., & Iversen, J. D. (1987). *Wind as a Geological Process: On Earth, Mars, Venus and Titan*. CUP Archive.

https://www.jpl.nasa.gov. (n.d.). Wind Streaks of Daedalia, Mars, and Amboy, California. Retrieved March 15, 2022, from https://www.jpl.nasa.gov/images/pia02363-wind-streaks-of-daedalia-mars-and-amboy-california

Kienenberger, R. L., & Greeley, R. (2012). Field analog studies of the distribution of windblown sediments at Amboy Crater, California, with application to Mars. *Planetary and Space Science*, *68*(1), 25–33. https://doi.org/10.1016/j.pss.2011.03.003

Parker, R. B. & California. (1963). *Recent volcanism at Amboy crater, San Bernardino County, California*. Retrieved from https://catalog.hathitrust.org/Record/101731437

Common Rock Forming Minerals

Dark-Colored minerals

Hardness	Cleavage	Physical Properties	Name
Hardness >5	Excellent or good	Dark gray, Blue-gray or black. May be iridescent. Cleavage in 2 planes at nearly right angles. Striations. Hardness-6	**Plagioclase Feldspar**
		Brown, gray, green or red. Cleavage in 2 planes at nearly right angles. Exsolution Lamellae. Hardness-6	**Potassium Feldspar**
		Opaque black. 2 cleavage planes at 60° and 120°. Hardness- 5.5	**Hornblende (Amphibole)**
	Poor or absent	Opaque red, gray, hexagonal prisms with striated flat ends. Hardness- 9	**Corrundum**
		Gray, brown or purple. Greasy luster. Massive or hexagonal prisms and pyramids. Transparent or translucent. Hardness- 7	**Quartz Black or brown- Smoky , Purple- Amethyst**
		Opaque red or brown. Waxy luster. Hardness- 7. Conchoidal Fracture	**Jasper**
		Opaque black. Waxy luster. Hardness- 7	**Flint**
		Transparent- translucent dark red to black. Hardness- 7	**Garnet**
Hardness < 5	Excellent or good	Colorless, purple, green, yellow, blue. Octahedral cleavage. Hardness- 4	**Flourite**
		Green. Splits along 1 excellent cleavage plane. Hardness- 2-3	**Chlorite**
		Black to dark brown. Splits along 1 excellent cleavage plane. Hardness- 2.5-3	**Biotite mica**
	Poor or absent	Opaque green, yellow or gray. Silky or greasy luster. Hardness- 2-5	**Serpentine**
		Opaque white, gray or green. Can be scratched with fingernail. Soapy feel. Hardness- 1	**Talc**
		Opaque earthy red to light brown. Hardness- 1.5-6	**Hematite**

Light-colored minerals

Hardness	Cleavage	Physical Properties	Name
Hardness >5	Excellent or good	White or gray, Cleavage in 2 planes at nearly right angles, Striations. Hardness-6	**Plagioclase Feldspar**
		Orange, brown, white, gray, green or pink. Cleavage in 2 planes at nearly right angles. Exsolution Lamellae. Hardness-6	**Potassium Feldspar**
		Pale brown, white or gray. Long slender prisms. Cleavage in 1 plane. Hardness- 6-7	**Sillimanite**
	Poor or absent	Opaque red, gray, white hexagonal prisms with striated flat ends. Hardness- 9	**Corrundum**
		Colorless, white, gray or other colors. Greasy luster. Massive or hexagonal prisms and pyramids. Transparent or translucent. Hardness- 7	**Quartz White-Milky, Yellow-Citrine, Pink- Rose**
		Opaque gray or white. Waxy luster. Hardness- 7. Conchoidal Fracture	**Chert**
		Colorless, white, yellow, light brown. Translucent opaque. Laminated or massive. Cryptocrystalline. Hardness- 7	**Chalcedony**
		Pale olive green. Conchoidal fracture. Transparent or translucent. Hardness- 7	**Olivine**
Hardness < 5	Excellent or good	Colorless, white, yellow, blue, green. Excellent cleavage in 3 planes. Breaks into rhombohedrons. Effervesces in HCl. Hardness- 3	**Calcite**
		Colorless, white, yellow, blue, green. Excellent cleavage in 3 planes. Breaks into rhombohedrons. Effervesces in HCl only if powdered. Hardness- 3.5-4	**Dolomite**
		White with tints of brown. Short tabular crystals or roses. Very heavy. Hardness- 3-3.5	**Barite**
		Colorless, white or gray. Massive or tabular crystals, blades or needles. Can be scratched by fingernail. Hardness- 2	**Gypsum**
		Colorless, white. Cubic crystals. Salty taste. Hardness- 2.5	**Halite**
		Colorless, purple, green, yellow, blue. Octahedral cleavage. Hardness- 4	**Flourite**
		Colorless, yellow, brown. Splits along 1 excellent cleavage plane. Hardness- 2-2.5	**Muscovite mica**
	Poor or absent	Yellow crystals or earthy masses. Hardness 1.5-2.5	**Sulfur**
		Opaque green, yellow or gray. Silky or greasy luster. Hardness- 2-5	**Sepentine**
		Opaque white, gray or green. Can be scratched with fingernail. Soapy feel. Hardness- 1	**Talc**
		Opaque earthy white to light brown. Hardness- 1-2	**Kaolinite**

Metallic

	Streak	Physical Properties	Name
Hardness > 5	Dark Gray	Brass yellow	**Pyrite**
		Dark gray-black, attracted to magnet	**Magnetite**
	Brown	Silvery black to black tarnishes gray	**Chromite**
Harness < 5	Red-Red/Brown	Silvery gray, black, or brick red	**Hematite**
	Dark Gray	Brass yellow, tarnishes dark brown or purple	**Chalcopyrite**
		Iridescent blue, purple or copper red, tarnishes dark purple	**Bornite**
		Silvery gray, tarnishes dull gray Cleavage good to excellent	**Galena**
		Dark gray to black, can be scratched with fingernail	**Graphite**

Sedimentary Rocks

McBride, 1963 & Dott, 1964 Classification Scheme for Clastic Sedimentary Rocks

Scheme based on the normalized percentages of the visible grains: quartz and chert(Q), feldspar (F), and lithic rock fragments (R) – as well as the percent composed of matrix (mud & silt)

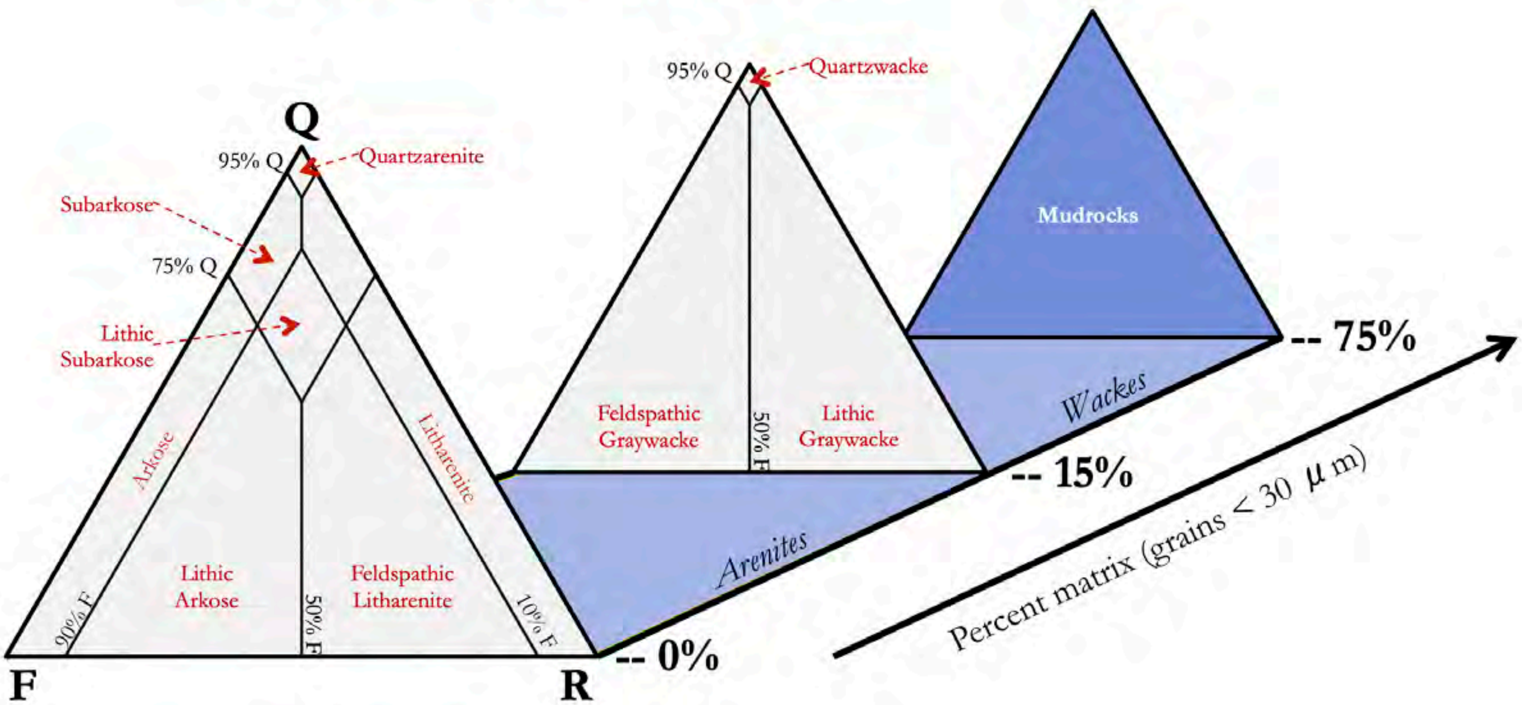

Tectonic Setting for Clastic Sedimentary Rocks

Scheme based on the normalized percentages of the visible grains: quartz and chert(Q), feldspar (F), and lithic rock fragments (R) – as well as the percent composed of matrix (mud & silt). Regions based upon field data.

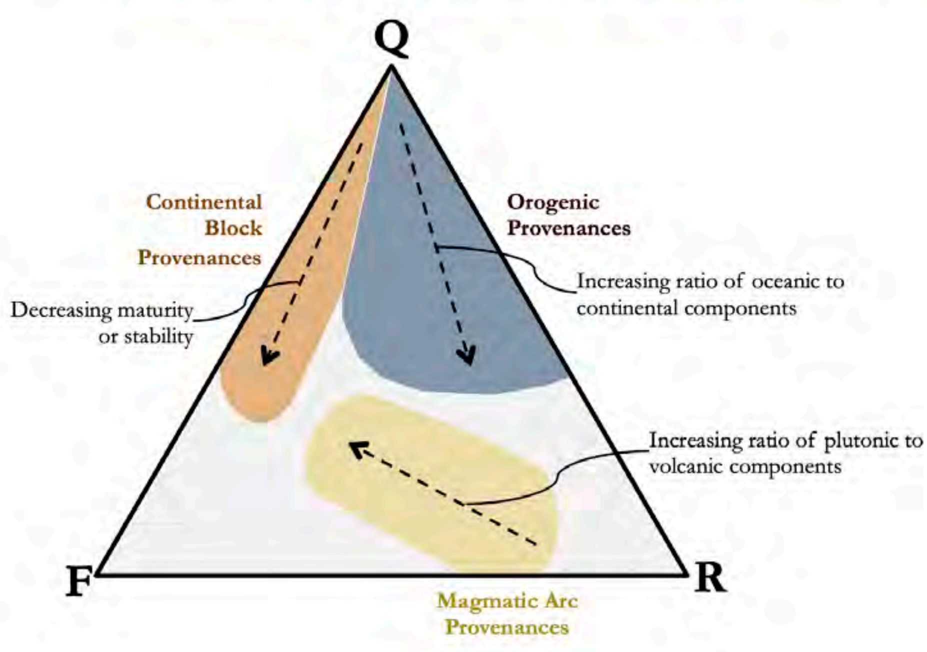

Sedimentary Rocks

	Mudrocks (containing > 50% mud)			Rocks with <50%mud
	Silt dominant (> 2/3 of rock)	Clay and Silt	Clay dominant (> 2/3 of rock)	Sand-sized or larger grains dominant
Non-laminated	Siltstone	Mudstone	Claystone	Conglomerates, Breccias, Sandstones, etc.
Laminated	Laminated Siltstone	Mudshale	Clayshale	

Classification Scheme for Mudrocks

Scheme based on clay/silt content, and whether the rock is laminated (layered) or not.

Classification Scheme for Sub-Conglomerates and Sub-Breccias

Scheme based on percent of a rock composed of: gravel or pebbles (size >2 mm), sand (2 mm > size > 1/16 mm), and mud (size < 1/16 mm).

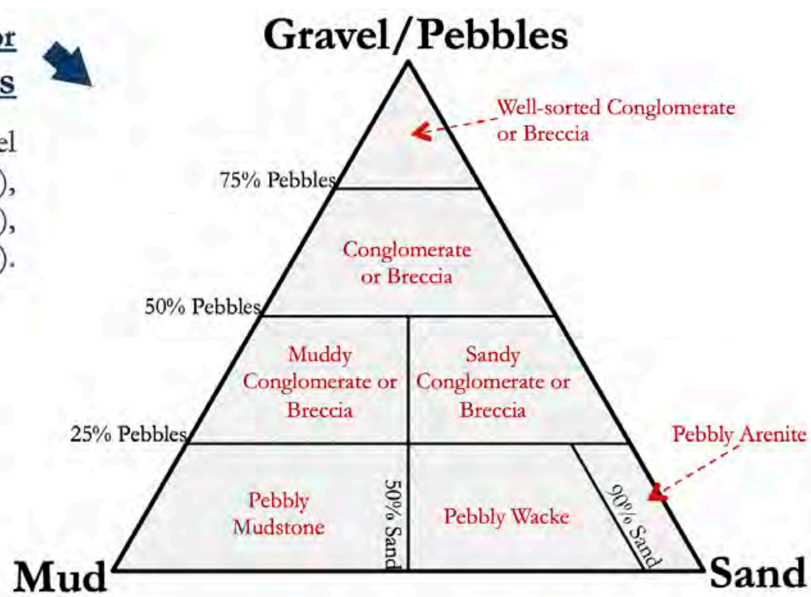

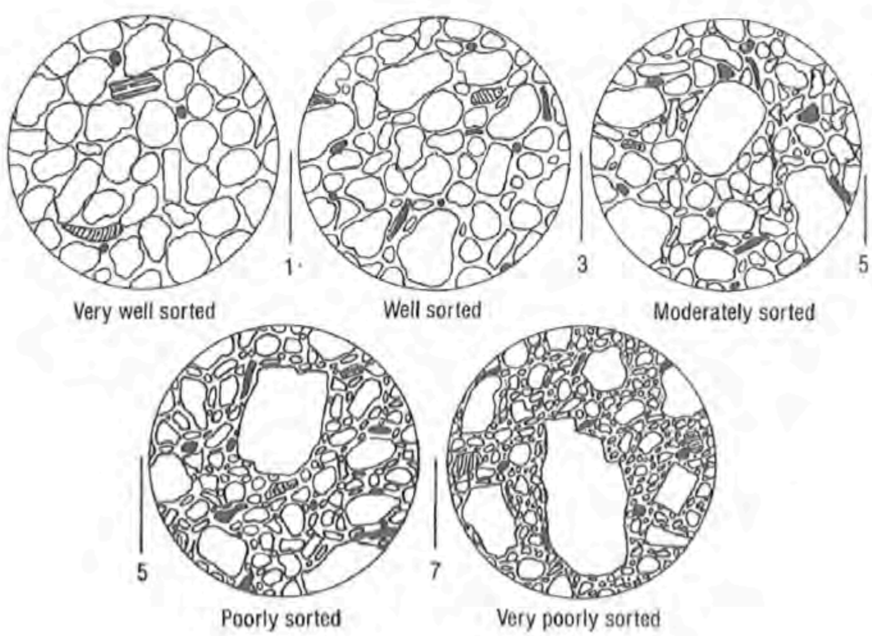

Estimating Sorting

Example hand-lens view of detritus. From Compton, 1985

Degrees of Rounding

Example hand-lens view of detritus of varying degrees of roundedness. The top row are equidimensional (spherical) grains, while the lower row are elongated grains. From Compton, 1985 and Davis & Reynolds, 1996, respectively.

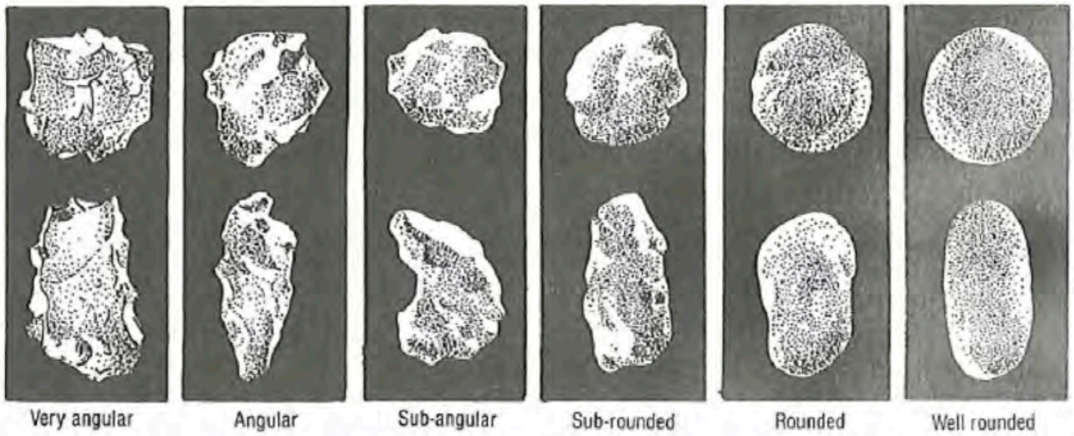

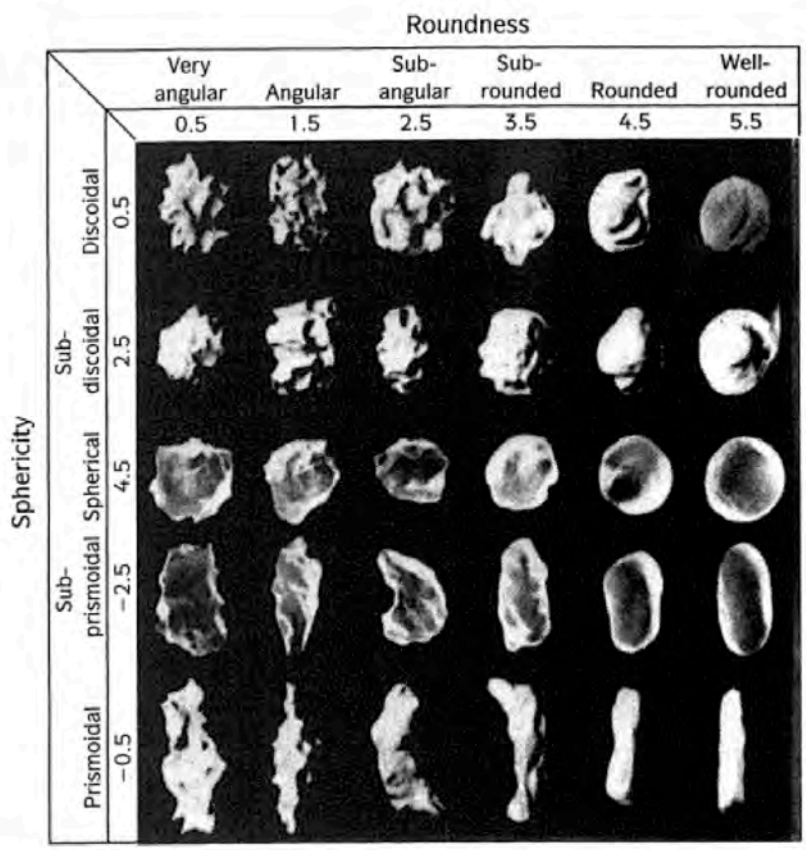

Sedimentary Rocks

Percentage Diagrams for Estimating Composition by Volume

Example hand-lens view of rocks with varying composition. To find weight percents, simply multiply each volume percent by the specific gravity of that mineral, and re-normalize. Compton, 1985

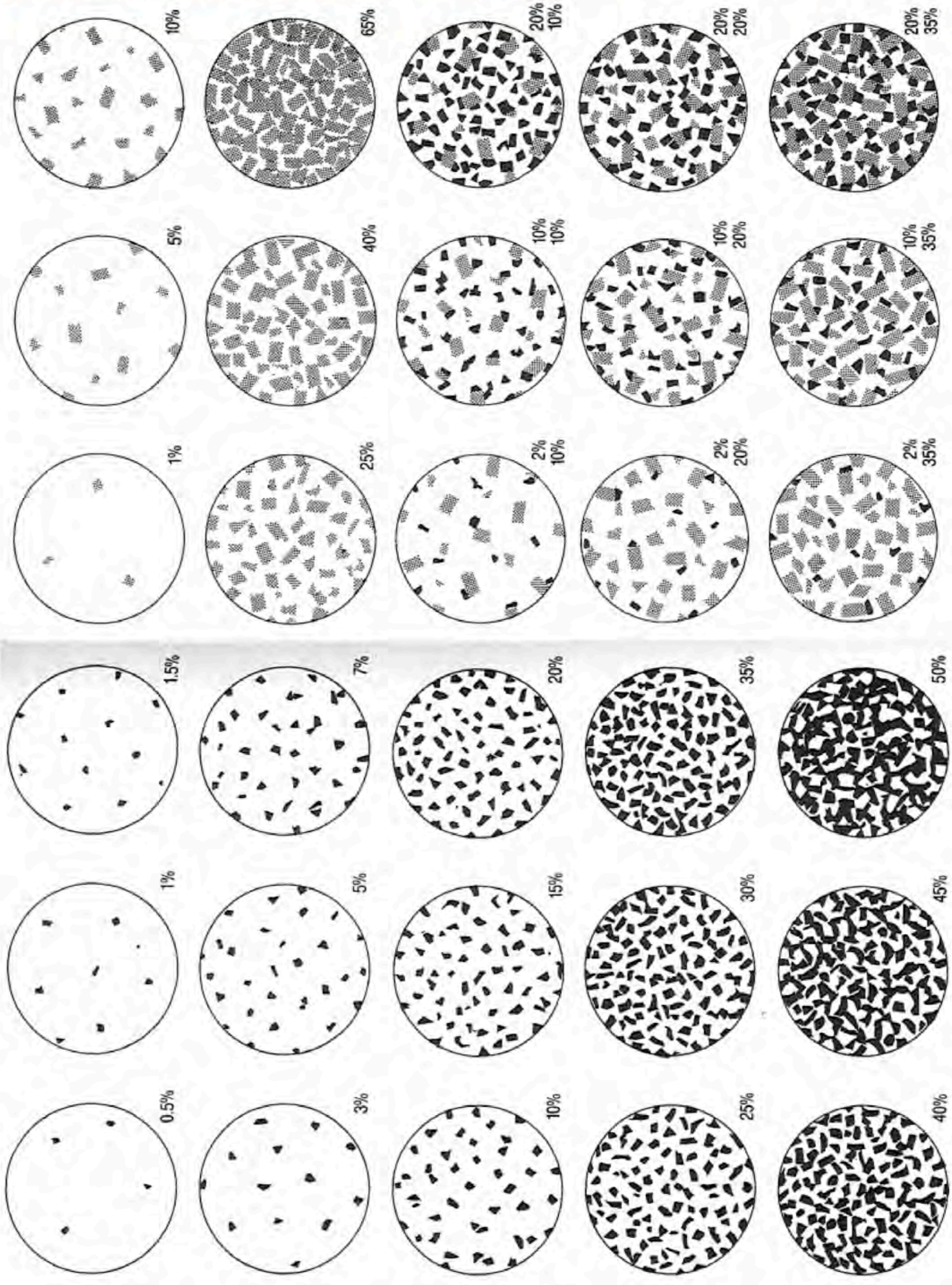

Sedimentary Rocks

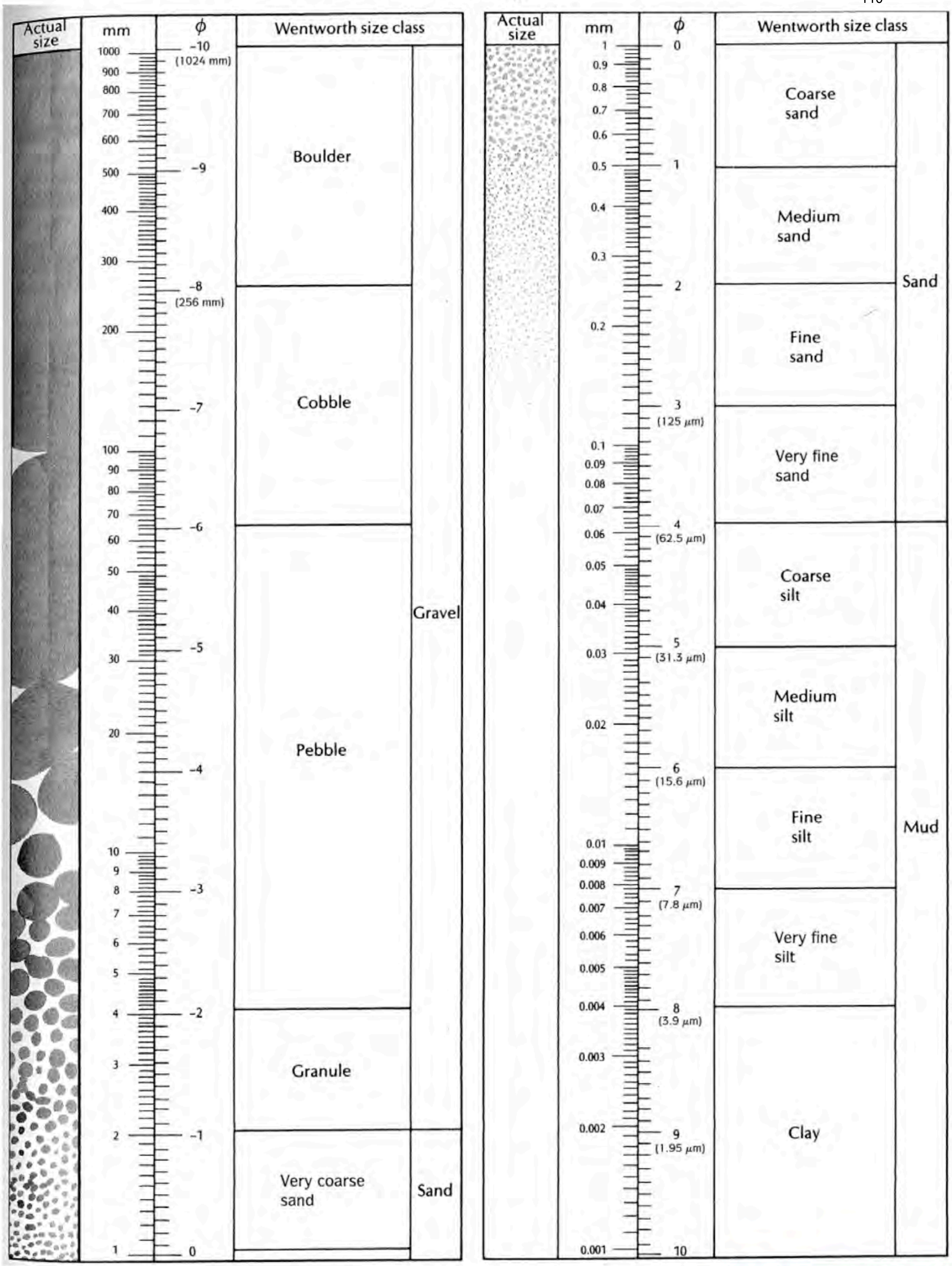

From Prothero and Schwab, 2004

Sedimentary Rocks: Carbonates

Folk Classification Scheme for Carbonate Rocks

Folk's classification scheme is based upon the composition (and type of allochems) within a limestone. Figures from Prothero and Schwab, 2004

Principle Allochems in Limestone	Limestone Type			
	Cemented by Sparite		Cemented by Micritic Matrix	
Skeletal Grains (Bioclasts)	Biosparite		Biomicrite	
Ooids	Oosparite	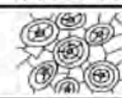	Oomicrite	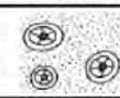
Peloids	Pelsparite	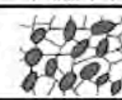	Pelmicrite	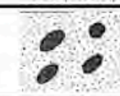
Intraclasts	Intrasparite		Intramicrite	
Limestone formed in place	Biolithite	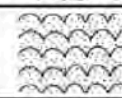	Terrestrial Limestone	

Dunham Classification Scheme for Carbonate Rocks

Dunham's classification scheme is based upon depositional textures within a limestone.

Allochthonous Limestone (original components not organically bound during deposition)						Autochthonous Limestone (original components organically bound during deposition; reef rocks)		
Of the allochems, less than 10% are larger than 2 mm				Of the allochems, greater than 10% are larger than 2 mm				
Contains carbonate mud			No mud	Matrix supported	Grain supported	Organisms acted as baffles	Organisms are encrusting and binding	Organisms building a rigid framework
Grain supported		Grain supported						
Less than 10% grains	More than 10% grains							
Mudstone	Wackestone	Packstone	Grainstone	Floatstone	Rudstone	Bafflestone	Bindstone	Framestone

Igneous Rocks

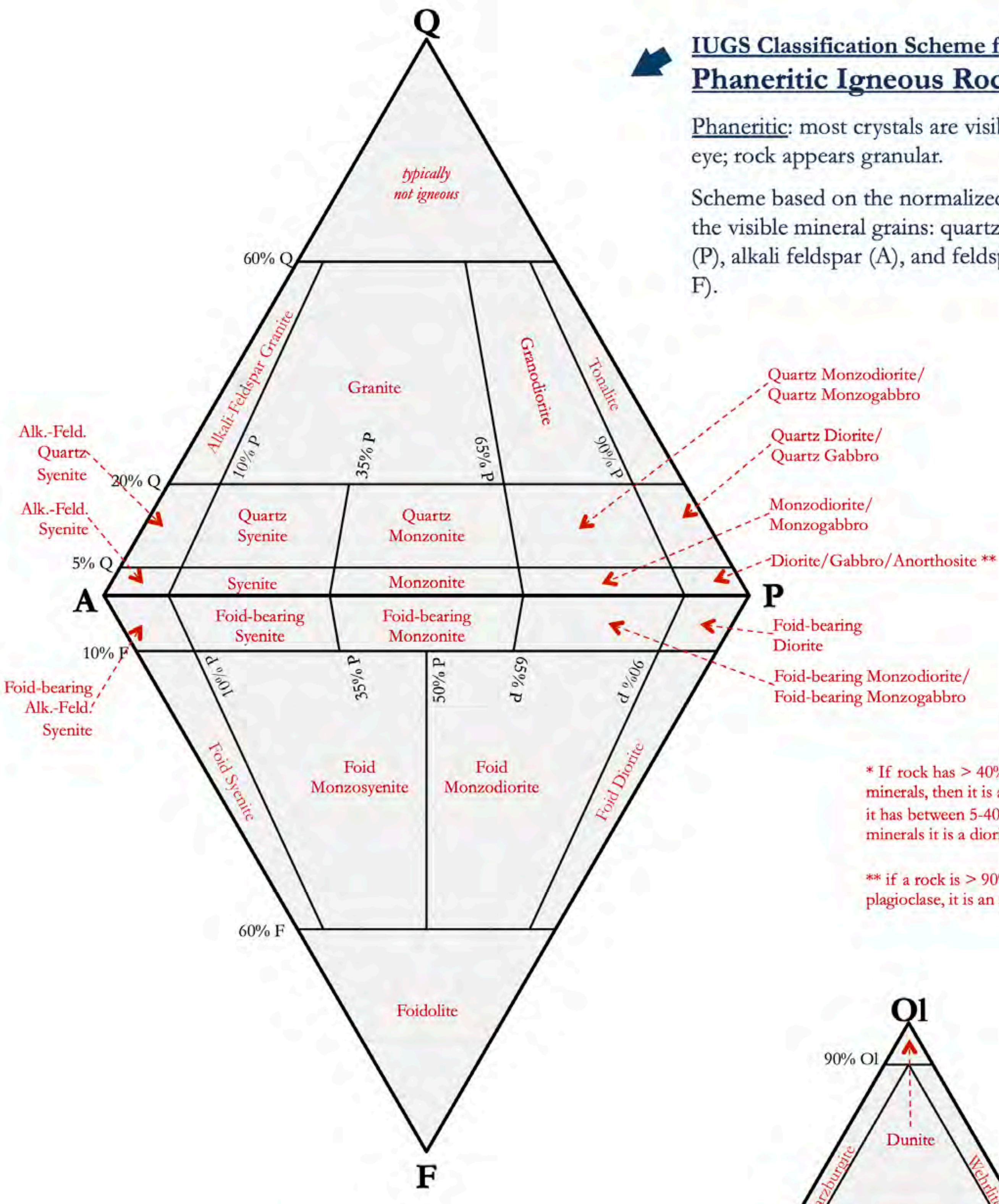

IUGS Classification Scheme for Phaneritic Igneous Rocks

Phaneritic: most crystals are visible to the naked eye; rock appears granular.

Scheme based on the normalized percentages of the visible mineral grains: quartz (Q), plagioclase (P), alkali feldspar (A), and feldspathoids (foids, F).

* If rock has > 40% mafic minerals, then it is a gabbo. If it has between 5-40% mafic minerals it is a diorite.

** if a rock is > 90% plagioclase, it is an anorthosite

IUGS Classification Scheme for Phaneritic Ultramafic Igneous Rocks (1)

Ultramafic: more than 90% of the total minerals are mafic.

Scheme based on the normalized percentages of the visible minerals: olivine (Ol), orthopyroxene (Opx), and clinopyroxene (Cpx).

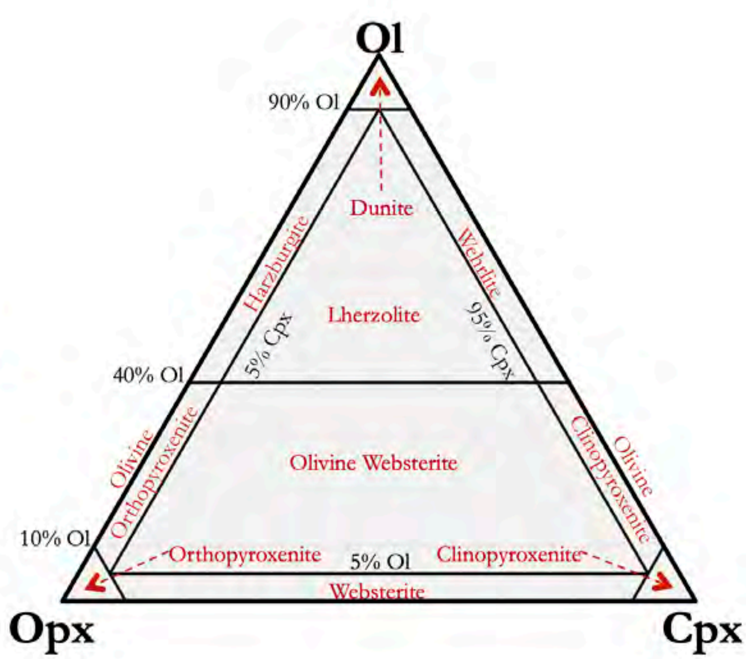

Igneous Rocks

IUGS Classification Scheme for Aphanitic Igneous Rocks

Aphanitic: the majority of crystals are not visible to the naked eye.

Aphanetic rocks are hard to classify due to the lack of visible minerals. However, you may still be able identify them based on phenocryst content, if phenocrysts are present. Scheme based on the normalized percentages of the visible phenocrysts: quartz (Q), plagioclase (P), alkali feldspar (A), and feldspathoids (foids, F).

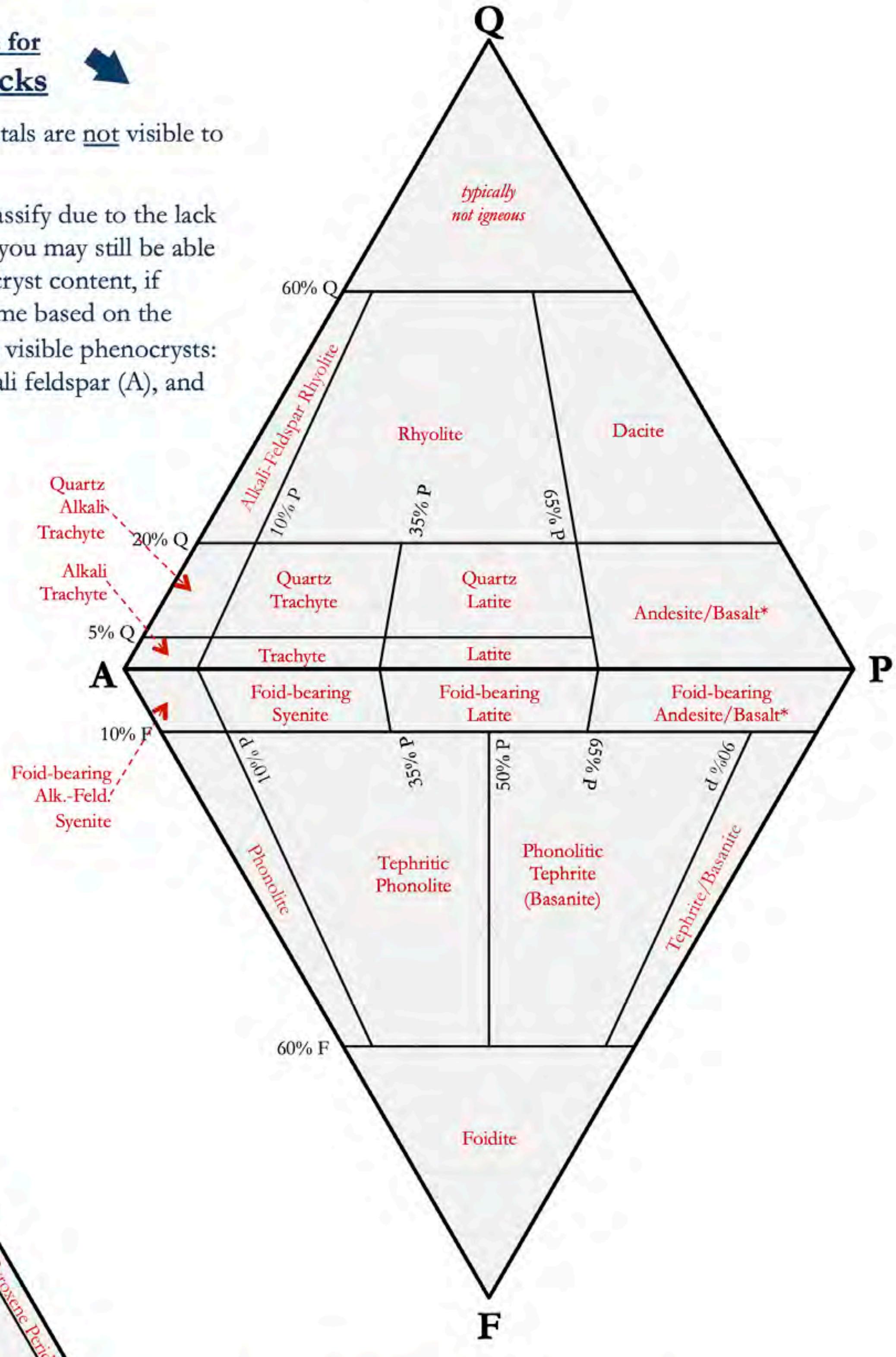

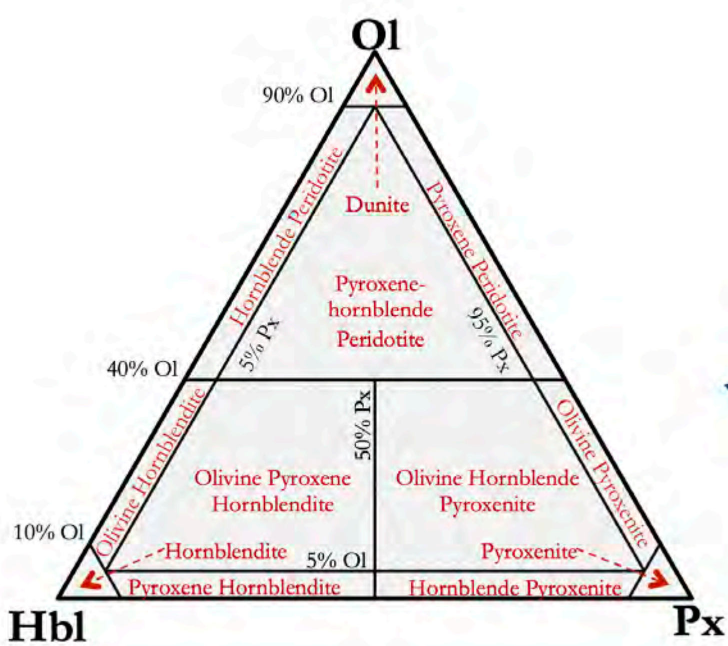

IUGS Classification Scheme for Phaneritic Ultramafic Igneous Rocks (2)

Ultramafic: more than 90% of the total minerals are mafic.

Scheme based on the normalized percentages of the visible minerals: olivine (Ol), hornblende (Hbl), and pyroxene (Px).

Igneous Rocks

Classification Scheme for
Pyroclastic Igneous Rocks

Pyroclastic rocks are formed via the accumulation of fragments of volcanic rock scattered by volcanic explosions. They are frequently classified based upon the size distribution of clasts.

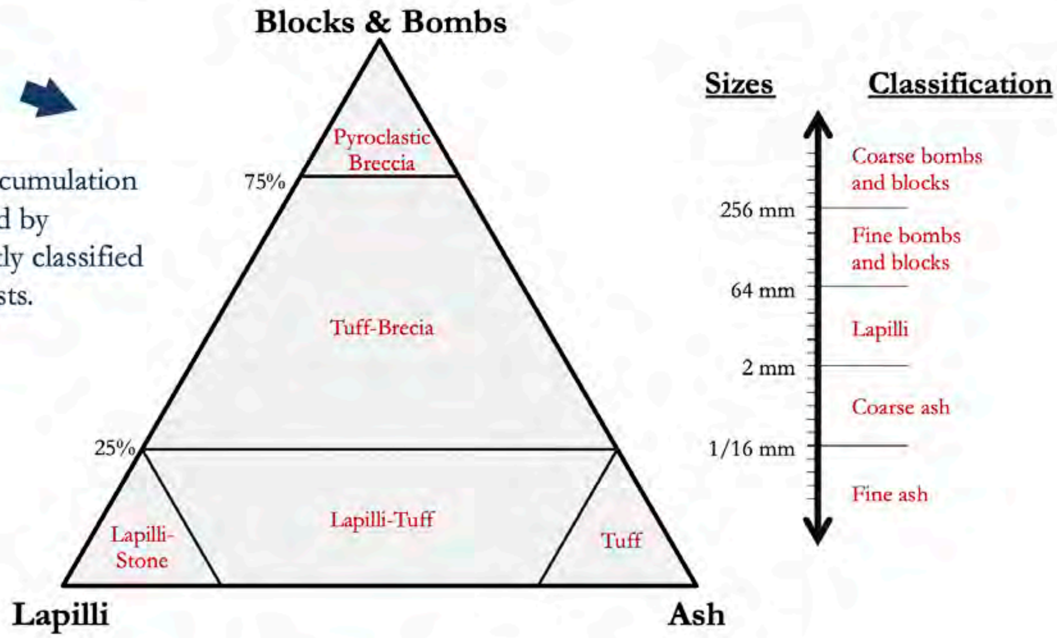

Types of Tephra (Pyroclasts)

In each row, the viscosity of the lava increases to the right. From Compton, 1985.

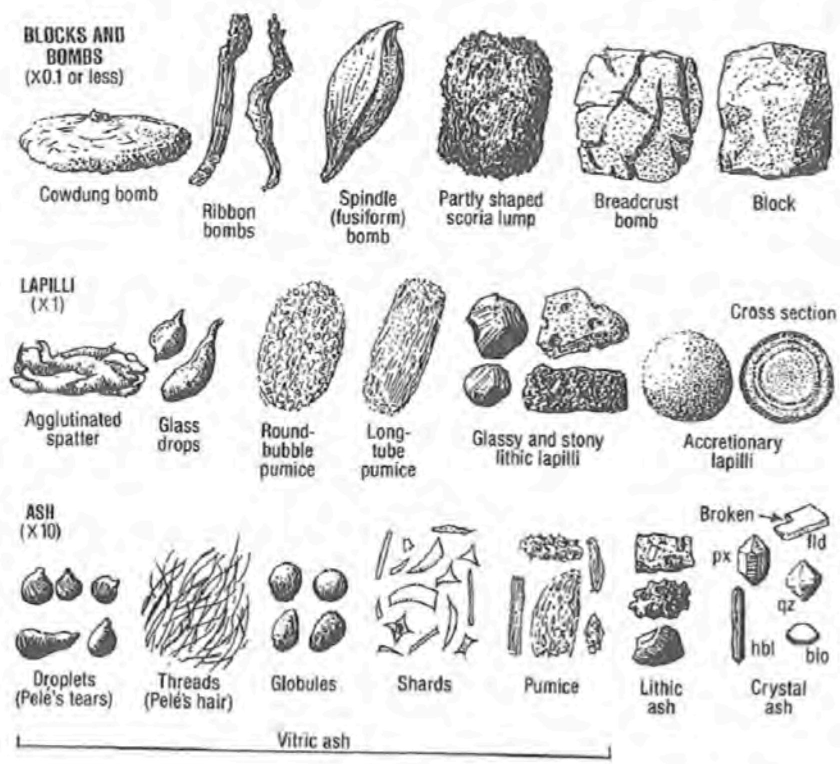

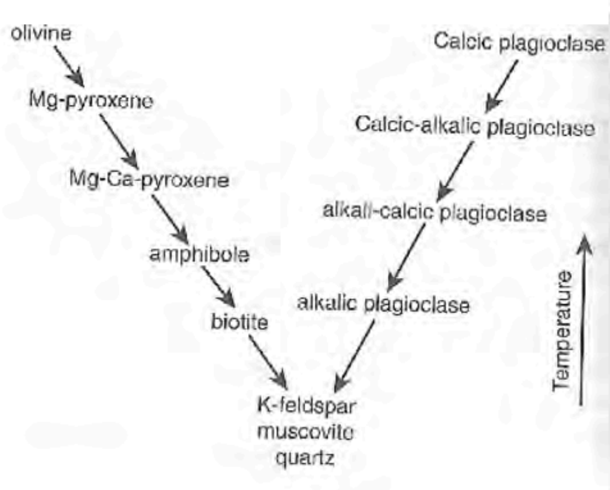

Bowen's Reaction Series

From Winter, 2010.

Metamorphic Rocks

Classification Scheme for Metamorphic Rocks

Based upon texture and mineralogical composition.

Structure & Texture		Characteristic Properties	Characteristic Mineralogy	Rock Name
Foliate (layered)	Increasing grain size, and degree of metamorphism ↓	Dull luster; very flat fracture surface; grains are too small to readily see; more dense than shale	No visible minerals	Slate
		Silky sheen; Crenulated (wavy) fracture structure; A few grains visible, but most are not	Development of mica and/or hornblende possible	Phyllite
		Sub-parallel orientations of individual mineral grains; wavy-sheet like fracture; often contains porphyroblasts; thinly foliated	Abundant feldspar; Quartz and mica are common; hornblende possible	Schist
		Sub-parallel, alternating bands or layers of light and dark material; coarsely foliated; blocky fracture	Abundant feldspars; Quartz, mica, and hornblende are common	Gneiss
Foliate (layered)		Interlocking crystals; effervesces in dilute HCl; softer than glass	Calcite	Marble
		Nearly equigranular grains; fracture across grains (not around them); sub-vitreous appearance; smooth feel compared to sandstone	Quartz	Quartzite

Mineralogy for Metamorphic Rock Facies

Facies	Definitive Mineral Assemblages in Mafic Rocks
Zeolite	zeolites: especially laumontite, wairakite, analcime (in place of other Ca-Al silicates such as prehnite, pumpellyite and epidote)
Prehnite-Pumpellyite	prehnite + pumpellyite (+ chlorite + albite)
Greenschist	chlorite + albite +epidote (or zoisite) + actinolite ± quartz
Amphibolite	hornblende + plagioclase (oligoclase, andesine) ± garnet
Granulite	orthopyroxene + clinopyroxene + plagioclase ± garnet
Blueschist	glaucophane + lawsonite or epidote/zoisite (± albite ± chlorite ± garnet)
Eclogite	pyralspite garnet + omphacitic pyroxene (± kyanite ± quartz), no plagioclase
Contact Facies	mineral assemblages in mafic rocks of the facies of contact metamorphism do not differ substantially from those of the corresponding regional facies at higher pressure

Metamorphic Rocks

Metamorphic Rock Facies, P vs. T diagram

From Winter, 2010

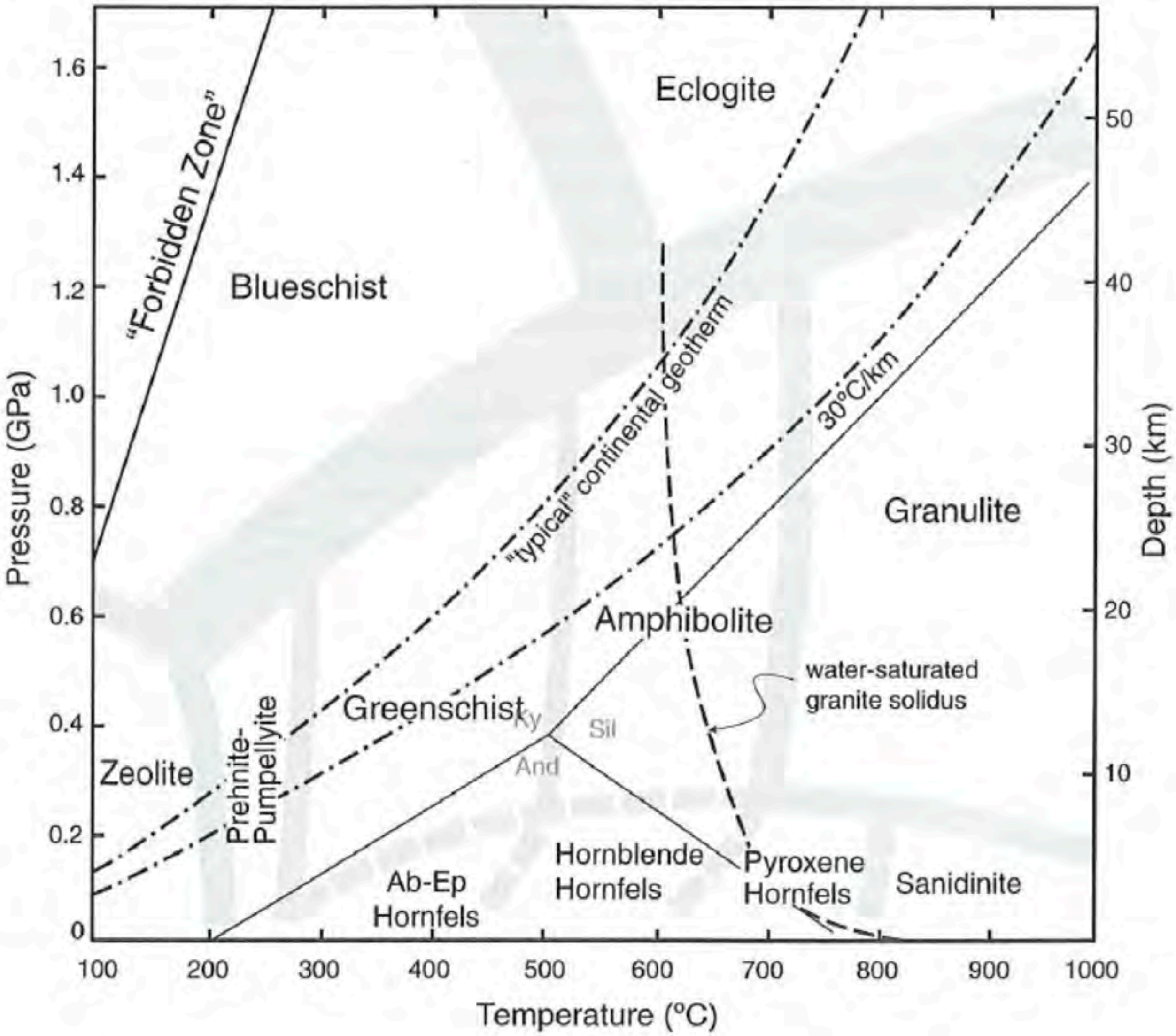

Schematic of Island Arc, and the origins of Metamorphic Facies

A schematic cross section of an island arc. Light gray lines are isotherms. From Winter, 2010

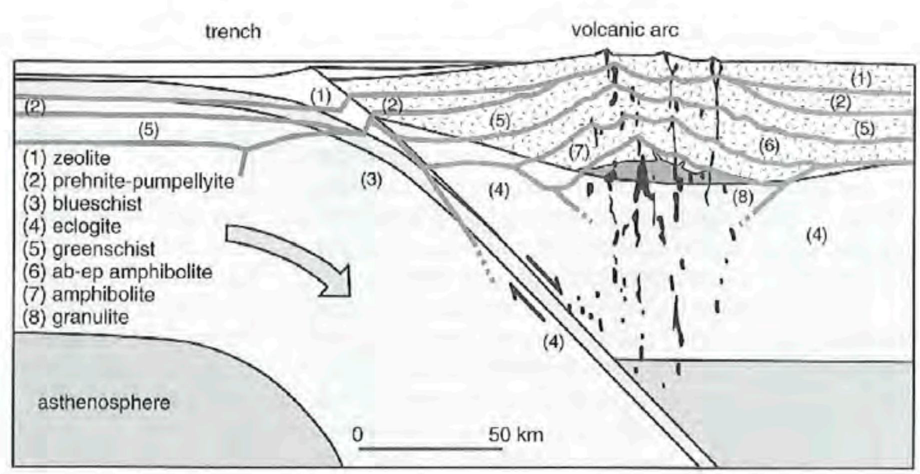

Structural Geology: Normal Faults

Normal Faults

In normal faults, the footwall goes up with respect to the hanging wall. Normal faults are indicative of extension. Figures from Davis & Reynolds, 1996.

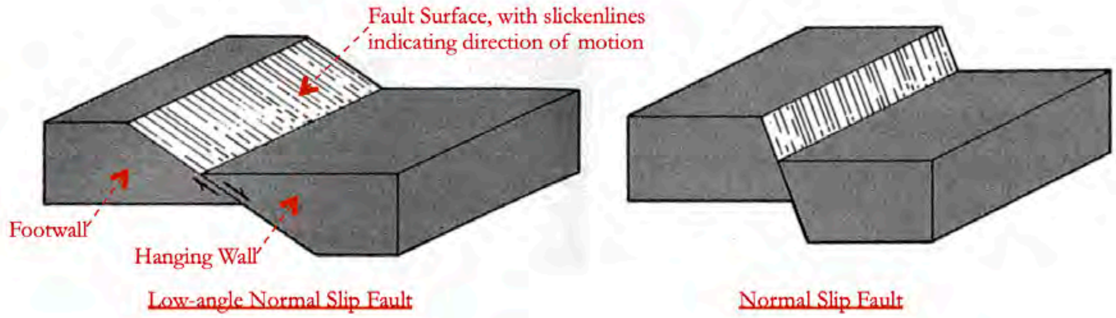

Effects of Brittle or Ductile Shear in Normal Faults

The block diagrams below illustrate the effects of changing the nature of deformation, between brittle deformation (which results in clear fault planes, fractures and fault rocks), ductile deformation (which causes deformation over a larger shear zone). Often, strata of different rheologies will behave differently, as is shown in the figure at right. The dashed layer was weak and deformed ductilely, while the middle grey layer was rigid and formed boudins. Figures from Davis & Reynolds, 1996.

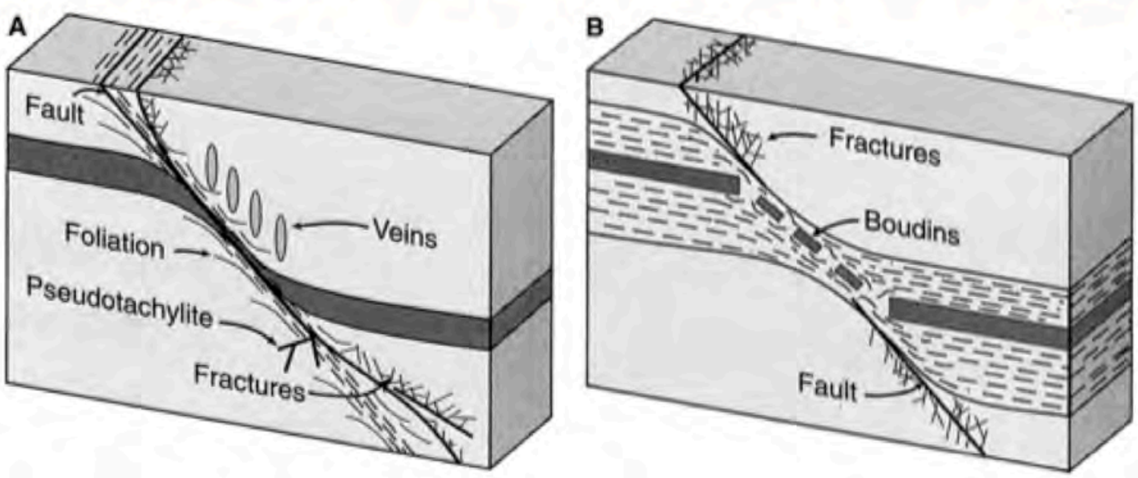

Inversion Tectonics

If the regional stresses change, previously inactive faults can reactivate, and change their sense of motion. In the figure at left, layer-A was formed prior to the formation of a normal fault. Layer-B and layer-C were deposited after the formation, and shut down of the fault. In the figure at the right, the fault has reactivated, though as a reverse fault. The resulting stratigraphic sequence is a combination of effects one would expect from both normal and reverse faults. Figures from Davis & Reynolds, 1996.

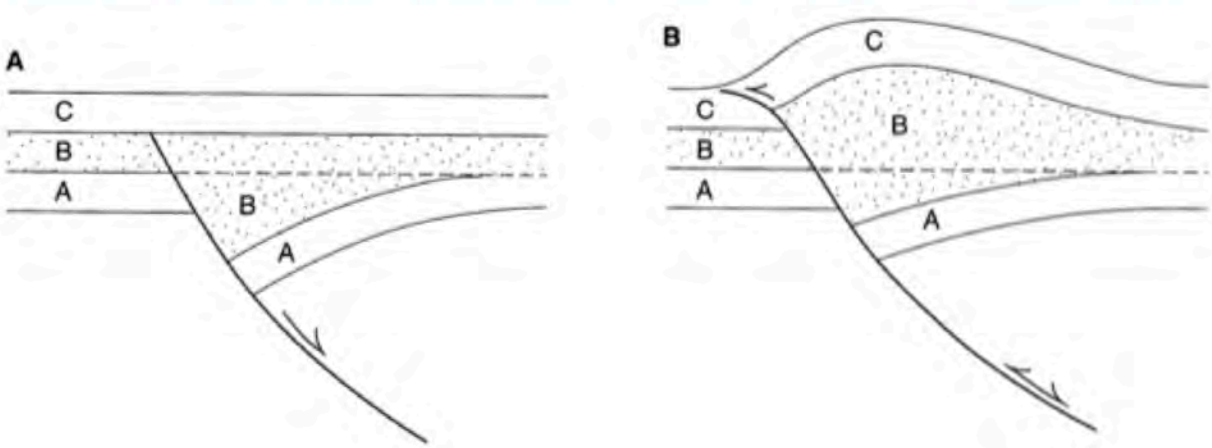

Structural Geology: Normal Faults

Normal Faults Geometries

Various normal fault geometries are possible. They all allow for lithospheric extension. (A) Domino style faulting. (B) Listric normal faulting with reverse drag. (C) Imbricate listric normal faulting. Note that listric faulting can cause extreme rotation of faulted blocks. (D) Listric normal faulting bounding a family of planar normal faults. Figures from Davis & Reynolds, 1996.

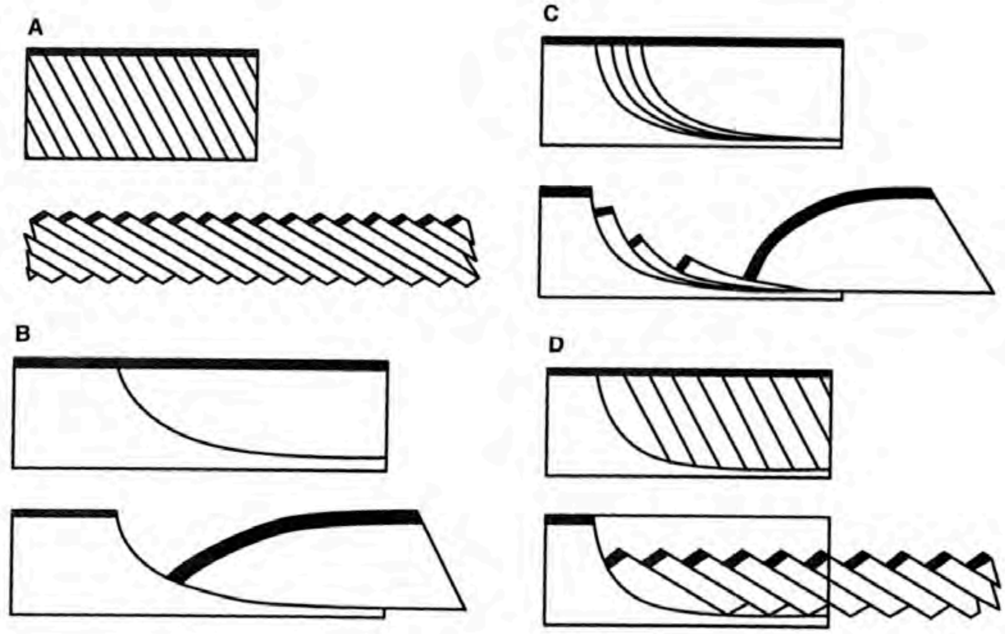

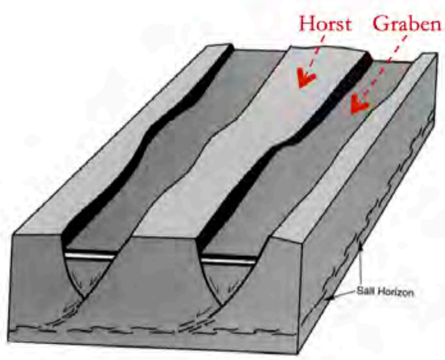

Horsts & Grabens

Classical formation describing fault-bounded uplifted (horsts) and down-dropped blocks (grabens). Figures from Davis & Reynolds, 1996.

Drag Folds, Reverse Drag, and Step Faulting

Faulting does not always produce clean displacement along the fault surface. Fault blocks are frequently folded or fractured, and the nature of these deformations are non-trivial. Figures from Davis & Reynolds, 1996.

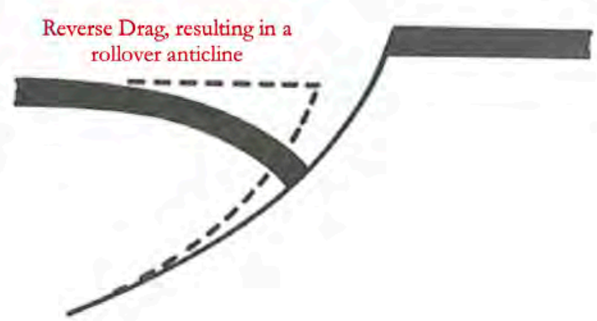

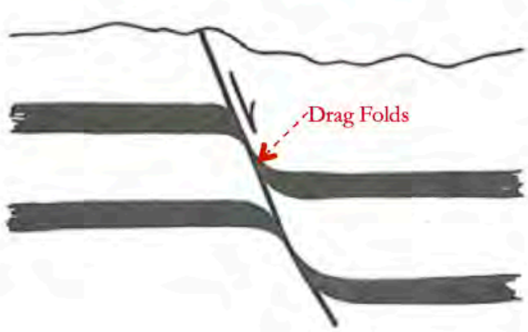

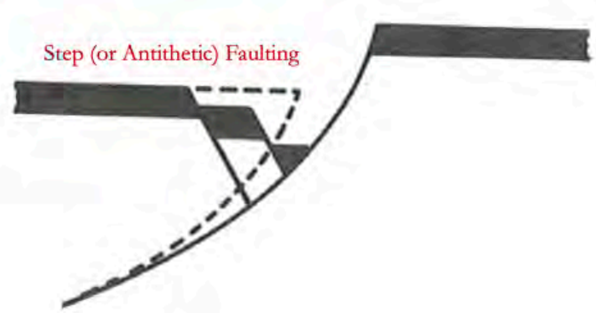

Structural Geology: Reverse & Thrust Faults

Reverse Faults

In reverse faults, the footwall goes down with respect to the hanging wall. Normal faults are indicative of compression. Thrust faults are reverse faults with fault dips <45 degrees. Figures from Davis & Reynolds, 1996.

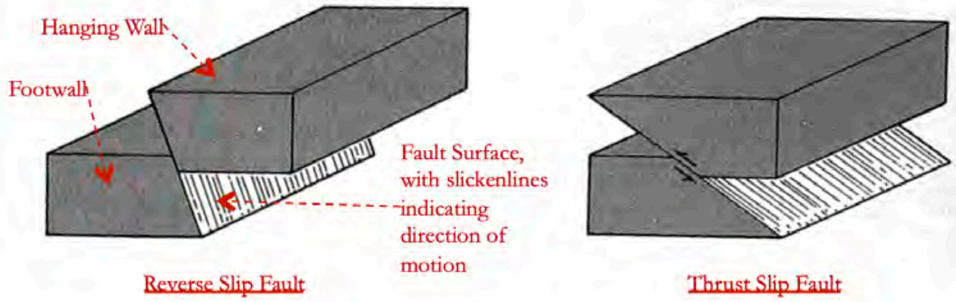

"Ramp-Flat" Geometry of Typical Thrust Fault Systems

In a regional thrust, faulted blocks are "thrust" on top of younger strata. The exact geometry of these thrust systems can vary significantly. Figures from Davis & Reynolds, 1996.

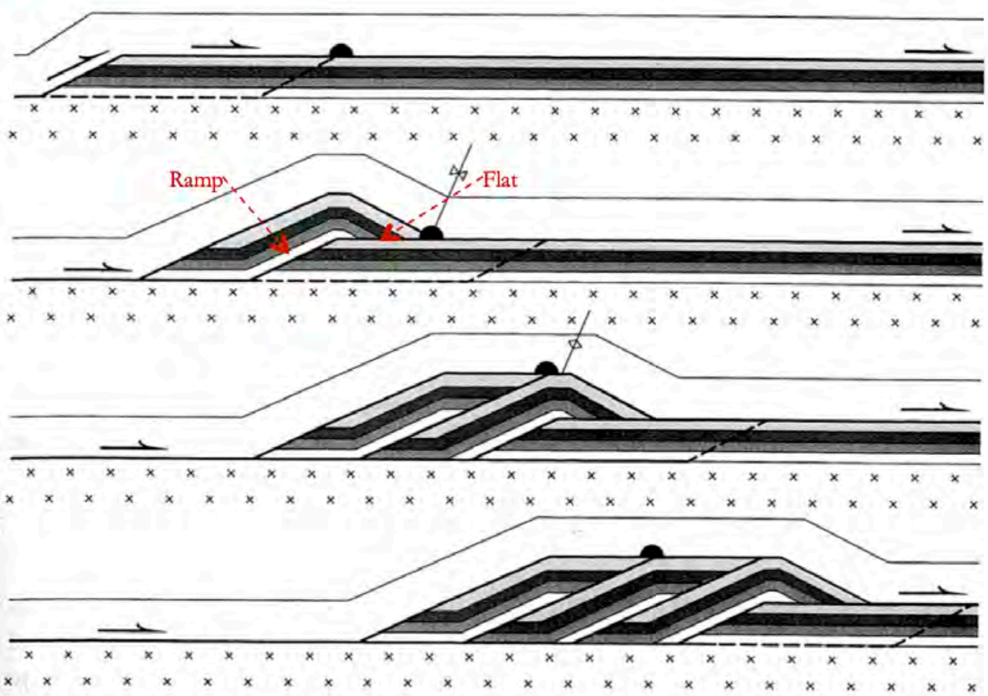

Klippe & Windows

Thrust faults move large blocks of non-indigenous rock (referred to as "allochthonous" rock) over emplaced rock (referred to as "autochthonous" rock). If the overlying allochthonous rock is eroded, it can create windows into the lower underlying autochthonous rock. Erosion can also create islands of isolated allochthonous rock, called klippe. Figures from Davis & Reynolds, 1996.

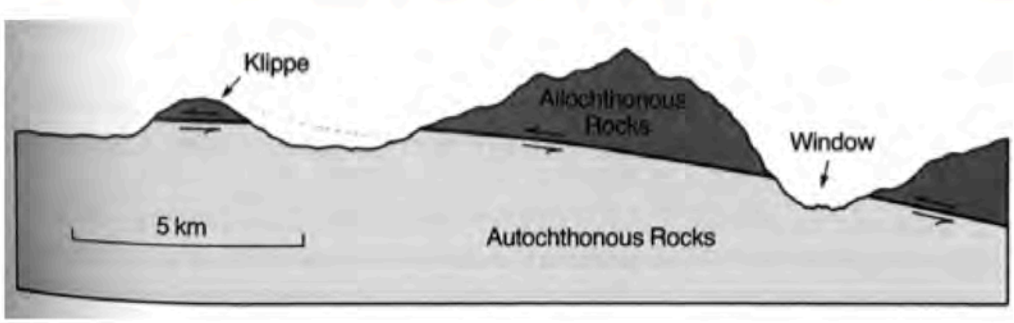

Structural Geology: Reverse & Thrust Faults

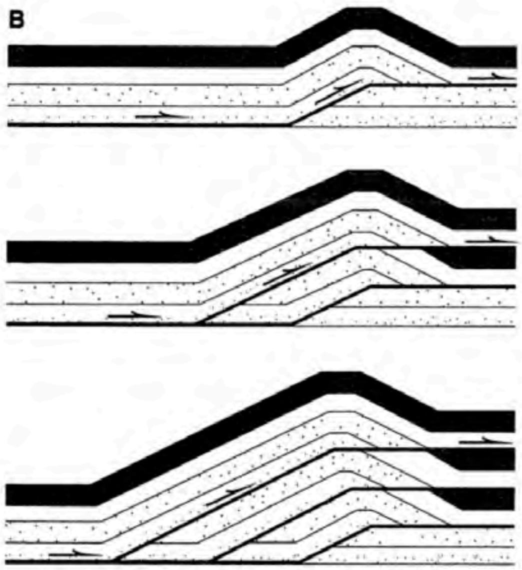

Out-of-Sequence Thrust Fault System

Unlike "in-sequence" thrust fault systems (as shown on the previous page, the "roof" of the thrust block in an out-of-sequence system becomes the "flat" for subsequent fault blocks. Figures from Davis & Reynolds, 1996.

Imbricate Fans vs. Duplexes

Two thrust fault geometries: imbricate fans (top) and duplexes (bottom). Figures from Davis & Reynolds, 1996.

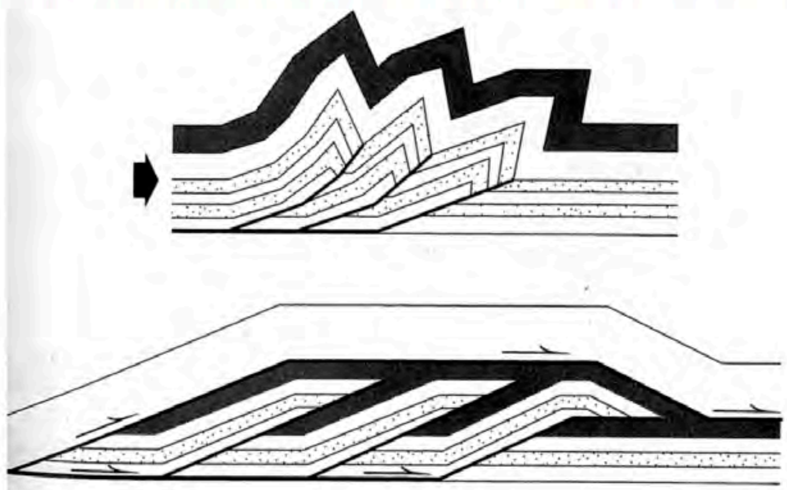

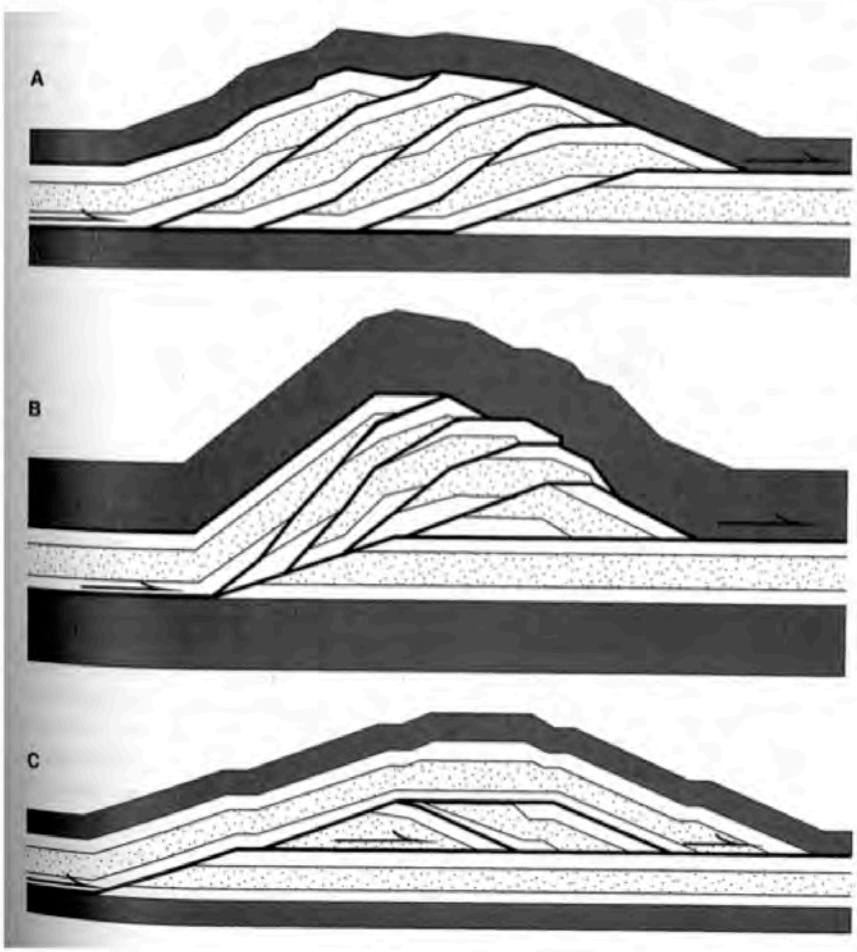

Forms of Duplexes

The exact form of a duplex or imbricate fan depends on the spacing of ramps and the amount of slip. (A) A normal duplex develops when slice length exceeds the fault slip. (B) An antiformal duplex develops when slice length and fault slip are effectively equal. (C) A forward-dipping duplex develops when the fault slip is greater than the slice length. Figures from Davis & Reynolds, 1996.

Structural Geology: Strike-Slip or Transform Faults

Strike-Slip Faults

In reverse faults, the footwall goes down with respect to the hanging wall. Normal faults are indicative of compression. Thrust faults are reverse faults with fault dips <45 degrees. Figures from Davis & Reynolds, 1996.

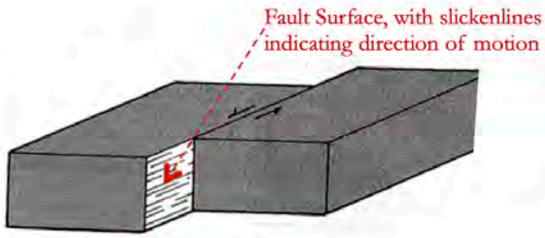

Left Lateral (Sinistral) Strike-Slip Fault

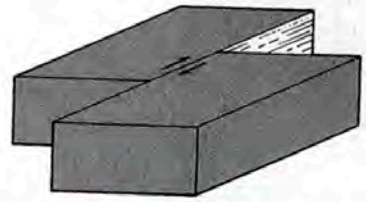

Right Lateral (Dexteral) Strike-Slip Fault

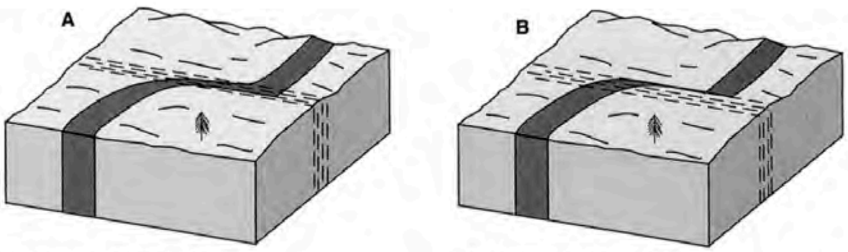

Continuous Shear Zone

Discontinuous Shear Zone

Ductile Shear Zones

Shear in a strike-slip fault is not always located in a single plane. Sometimes, shear takes place over an extended region. Figures from Davis & Reynolds, 1996.

Brittle Shear Zones

Figures from Davis & Reynolds, 1996.

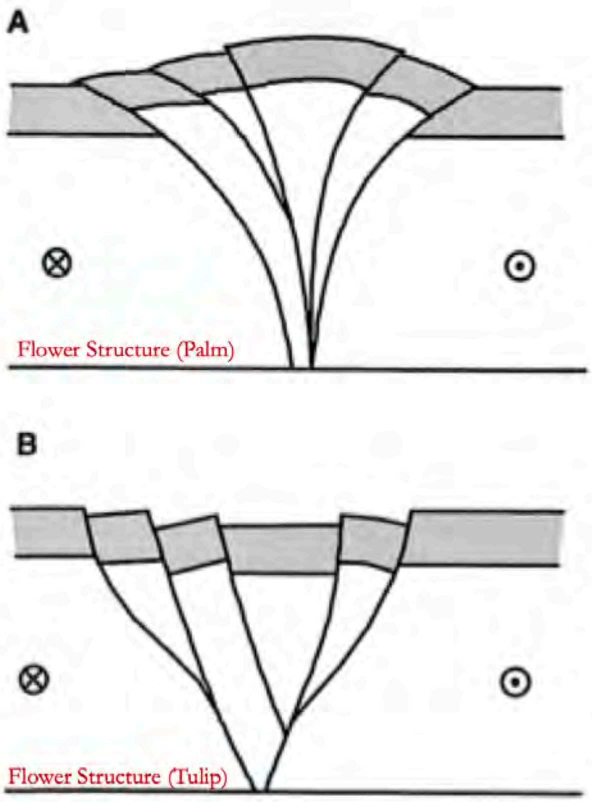

Flower Structure (Palm)

Flower Structure (Tulip)

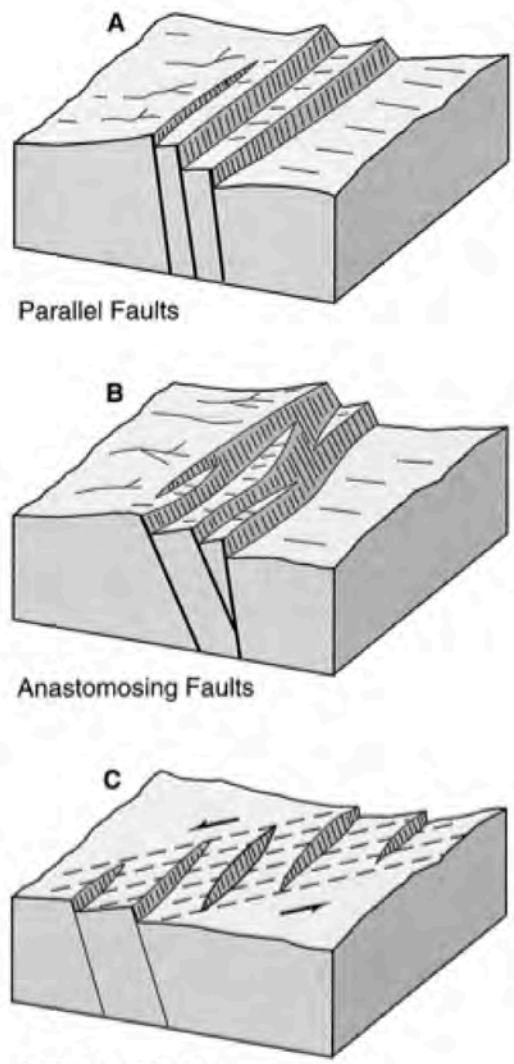

Parallel Faults

Anastomosing Faults

En Echelon Faults

Structural Geology: Strike-Slip or Transform Faults

Bends in Strike-Slip Faults

Strike-slip faults along irregularly curved faults creates localized regions of extension and compression. Figures from Davis & Reynolds, 1996.

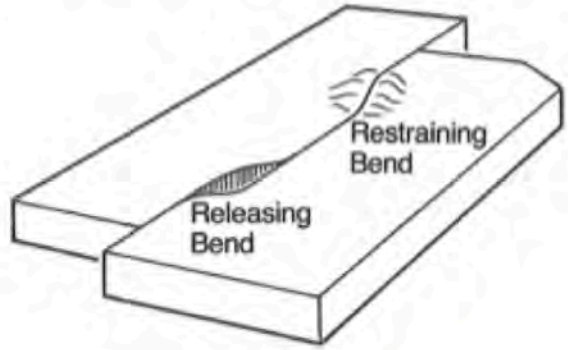

Strike-Slip Duplexes

(A) Extensional duplexes can form at releasing bends. (B) Compressional duplexes can form at restraining bends. Figures from Davis & Reynolds, 1996.

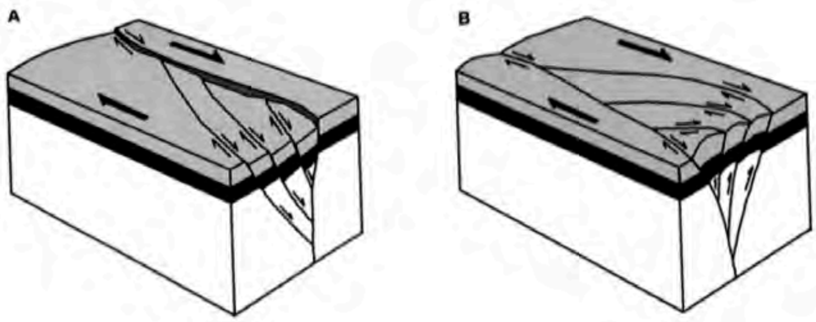

Slip Indicators in Strike-Slip Systems

In strike-slip systems, the maximum (S_1) and minimum compressional stresses (S_3) are at an angle with respect to the sense of shear. This can lead to the formation of both large scale folds and faults, or small scale fractures or veins, which are indicative to the sense of motion. Figures from Davis & Reynolds, 1996.

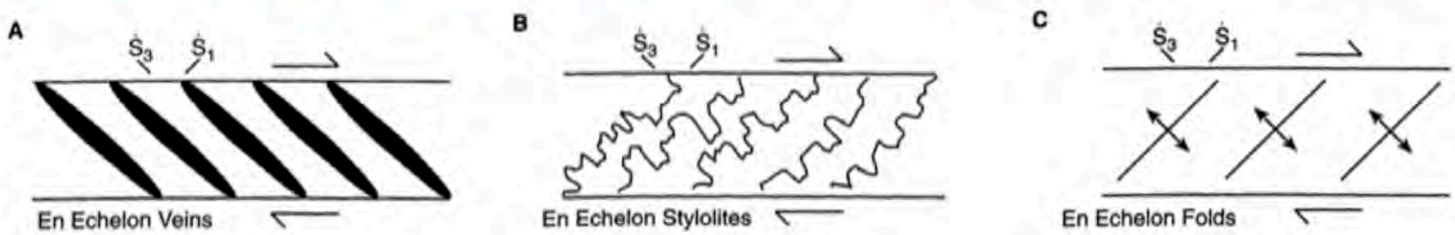

Even more Geometric Arrangements of Strike-Slip Faults

Figures from Davis & Reynolds, 1996.

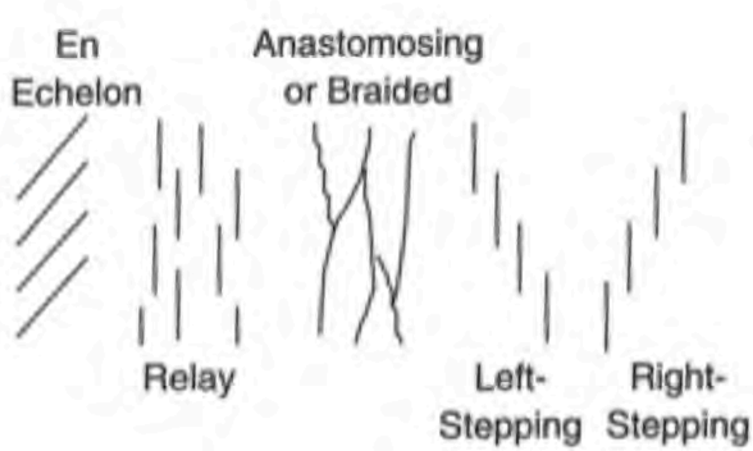

Structural Geology: Strike-Slip or Transform Faults

Riedel Shears

When under compression, rocks tend to form fail with faults forming 30° from the primary compressional stress. In a strike-slip fault, the primary compressional stress (σ_1) is 45° away from the plane of strike-slip shearing. The combination of these two facts results in fractures at interesting angles with respect to the motion of shear. These are called Riedel shears. The figure below shows a left-handed strike-slip zone. Figures from Davis & Reynolds, 1996.

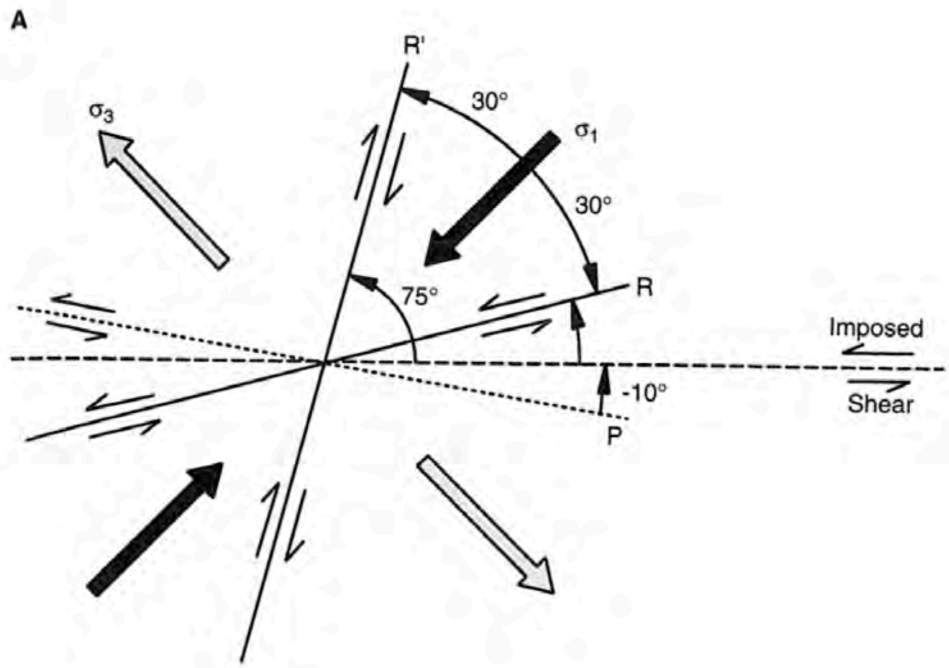

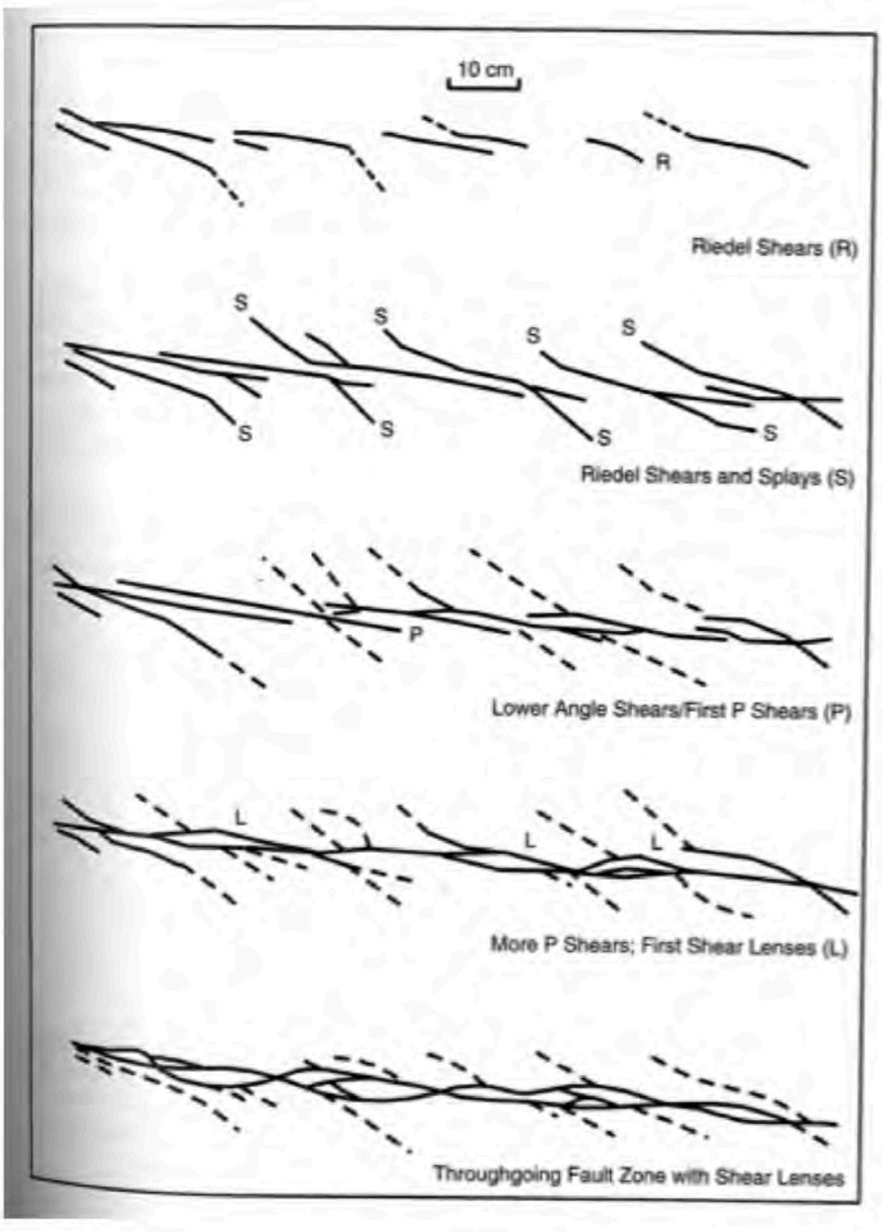

The figure at left illustrate the formation sequence of Riedel shears and other splays and shears in a right-handed strike-slip zone. Figures from Davis & Reynolds, 1996.

Structural Geology: Folds

Anticlines & Antiforms, and Synclines & Synforms

Antiforms are concave-down folds, while Synforms are concave-up folds. Anticlines are antiforms were we know that the younger strata lie on top of older strata. Similarly, Synclines are antiforms where younger strata lie on top of older strata. Figures from Davis & Reynolds, 1996.

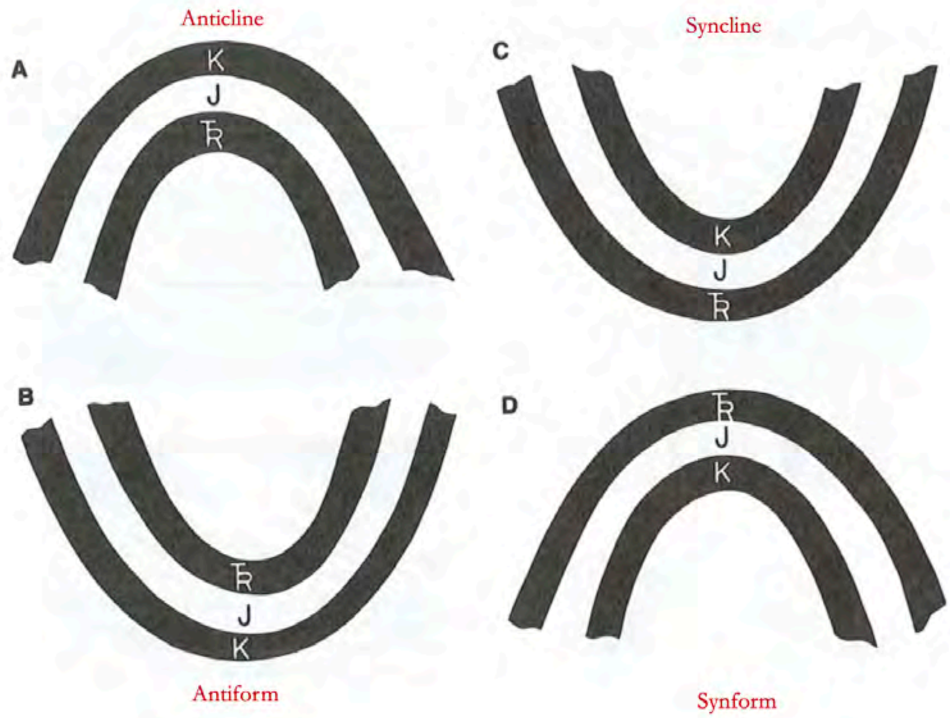

Plunging Folds

Folds (defined by hinge lines and axial surfaces) are not necessarily perpendicular to the Earth's surface. They can be dipping into or out of the surface. This can create interesting patterns of exposed surface rock, or even topography. Figures from Jones, 2001.

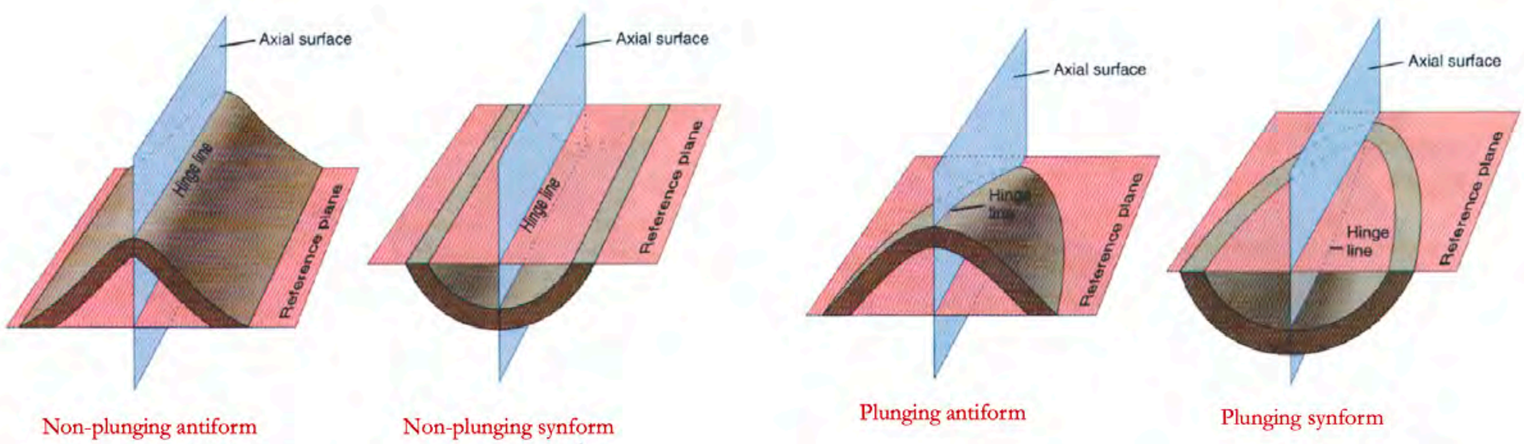

Fold Shapes

Folds can come in a variety of shapes. Davis & Reynolds, 1996.

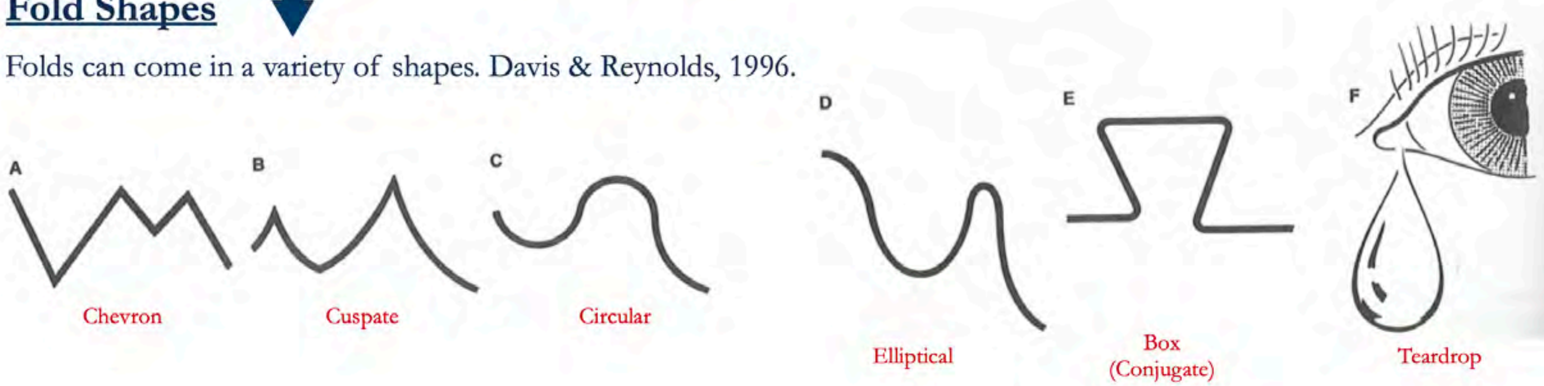

Structural Geology: Folds

Fold Tightness

Fold tightness is based upon the size of the inter-limb angle. Figures from Davis & Reynolds, 1996.

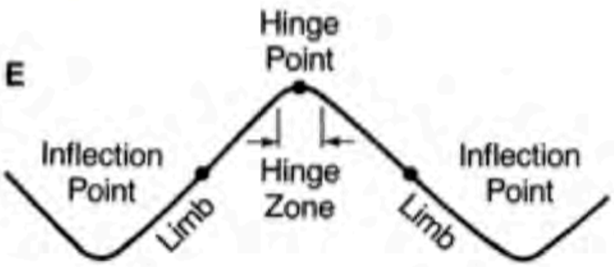

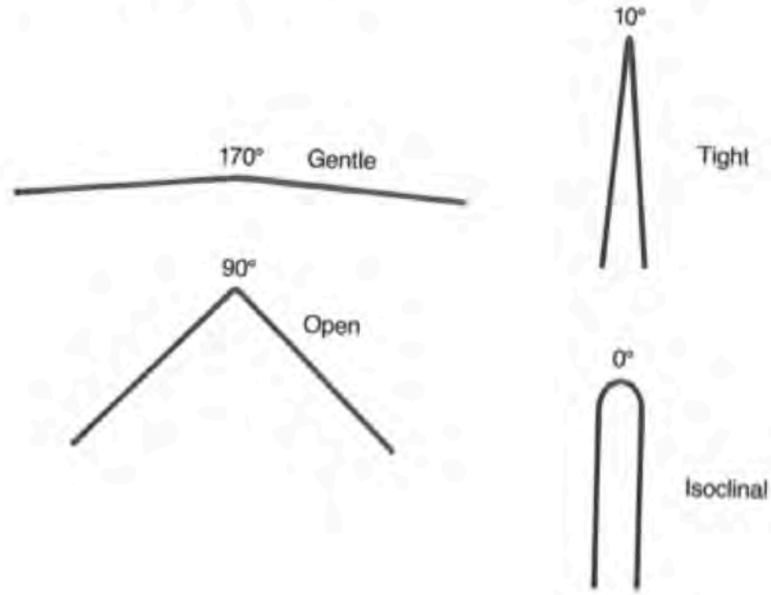

Minor Structures in Folds

When folding layers of strata, layer-parallel stretching occurs in the outer arc of a folded layer, while layer-parallel shortening occurs in the inner arc. Figures from Davis & Reynolds, 1996.

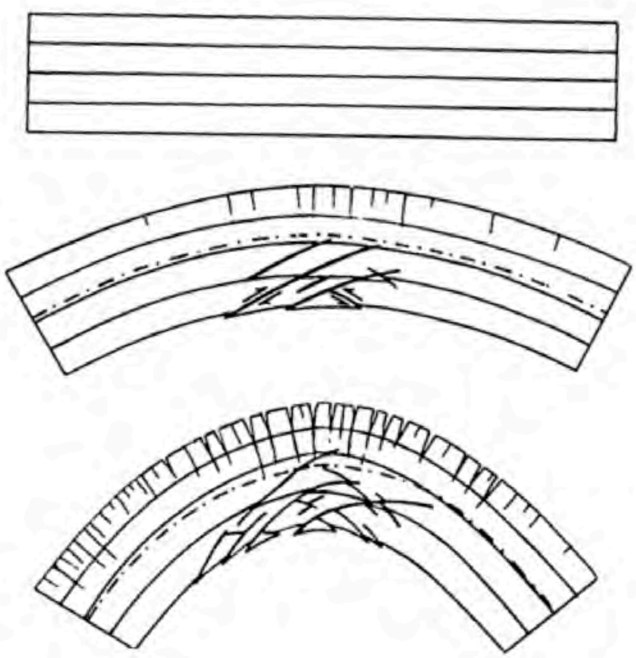

Boudins

Layer-parallel stretching can pinch off layers of strata, depending on the ductility contrast between layers. This can result in pinch-and-swell structures or boudins (where the pinching completely pinches off portions of a given strata). Figures from Davis & Reynolds, 1996.

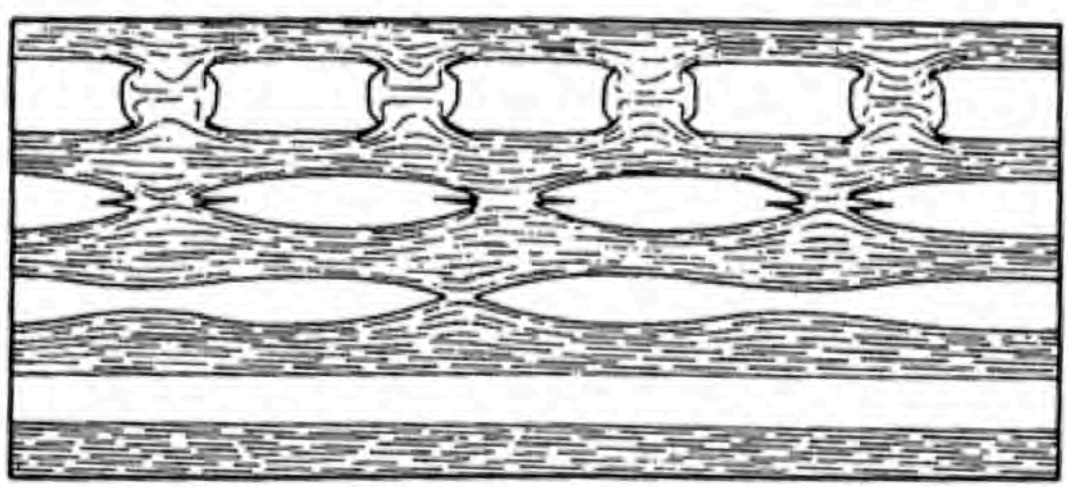

Geologic Map Symbols

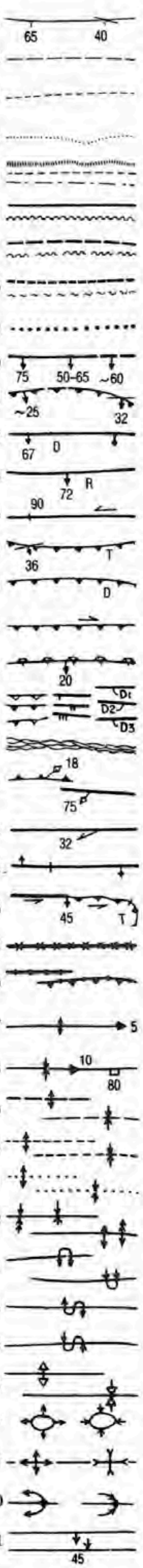

1. Contact, showing dip where trace is horizontal, and strike and dip where trace is inclined
2. Contact, located approximately (give limits)
3. Contact, located very approximately, or conjectural
4. Contact, concealed beneath mapped units
5. Contact, gradational (optional symbols)
6. Fault, nonspecific, well located (optional symbols)
7. Fault, nonspecific, located approximately
8. Fault, nonspecific, assumed (existence uncertain)
9. Fault, concealed beneath mapped units
10. Fault, high-angle, showing dip (left) and approximate dips
11. Fault, low-angle, showing approximate dip and strike and dip
12. Fault, high-angle normal (D or ball and bar on downthrown side)
13. Fault, reverse (R on upthrown side)
14. Fault, high-angle strike-slip (example is left lateral)
15. Fault, thrust (T on overthrust side)
16. Fault, low-angle normal or detachment (D on downthrown side)
17. Fault, low-angle strike-slip (example is right lateral)
18. Fault, low-angle, overturned (teeth in direction of dip)
19. Optional sets of symbols for different age-groups of faults
20. Fault zone or shear zone, width to scale (dip and other accessory symbols may be added)
21. Faults with arrows showing plunge of rolls, grooves or slickensides
22. Fault showing bearing and plunge of net slip
23. Point of inflection (bar) on a high-angle fault
24. Points of inflection on a strike-slip fault passing into a thrust
25. Fault intruded by a dike
26. Faults associated with veins
27. Anticline, showing trace and plunge of hinge or crest line (specify)
28. Syncline (as above), showing dip of axial surface or trough surface
29. Folds (as above), located approximately
30. Folds, conjectural
31. Folds beneath mapped units
32. Asymmetric folds with steeper limbs dipping north (optional symbols)
33. Anticline (top) and syncline, overturned
34. Antiformal (inverted) syncline
35. Synformal (inverted) anticline
36. Antiform (top) and synform (stratigraphic sequence unknown)
37. Separate dome (left) and basin
38. Culmination (left) and depression
40. Vertically plunging anticline and syncline
41. Monocline, south-facing, showing traces of axial surfaces

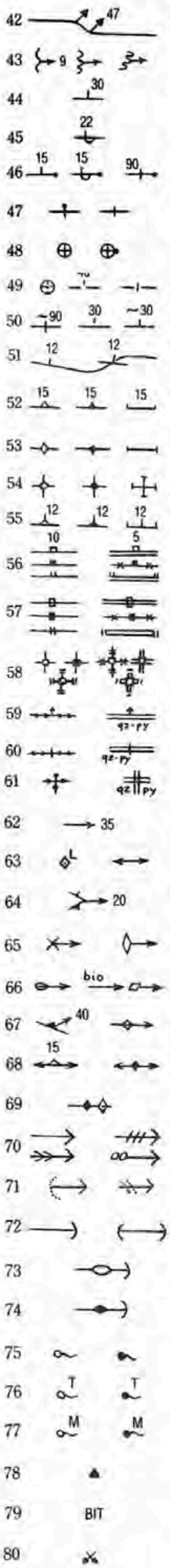

42. Steeply plunging monocline or flexure, showing trace in horizontal section and plunge of hinges
43. Plunge of hinge lines of small folds, showing shapes in horizontal section
44. Strike and dip of beds or bedding
45. Strike and dip of overturned beds
46. Strike and dip of beds where stratigraphic tops are known from primary features
47. Strike and dip of vertical beds or bedding (dot is on side known to be stratigraphically the top)
48. Horizontal beds or bedding (as above)
49. Approximate (typically estimated) strike and dip of beds
50. Strike of beds exact but dip approximate
51. Trace of single bed, showing dip where trace is horizontal and where it is inclined
52. Strike and dip of foliation (optional symbols)
53. Strike of vertical foliation
54. Horizontal foliation
55. Strike and dip of bedding and parallel foliation
56. Strike and dip of joints (left) and dikes (optional symbols)
57. Vertical joints (left) and dikes
58. Horizontal joints (left) and dikes
59. Strike and dip of veins (optional symbols)
60. Vertical veins
61. Horizontal veins
62. Bearing (trend) and plunge of lineation
63. Vertical and horizontal lineations
64. Bearing and plunge of cleavage-bedding intersection
65. Bearing and plunge of cleavage-cleavage intersections
66. Bearings of pebble, mineral, etc. lineations
67. Bearing of lineations in plane of foliation
68. Horizontal lineation in plane of foliation
69. Vertical lineation in plane of vertical foliation
70. Bearing of current from primary features; from upper left: general; from cross-bedding; from flute casts; from imbrication
71. Bearing of wind direction from dune forms (left) and cross-bedding
72. Bearing of ice flow from striations (left) and orientation of striations
73. Bearing of ice flow from drumlins
74. Bearing of ice flow from crag and tail forms
75. Spring
76. Thermal spring
77. Mineral spring
78. Asphaltic deposit
79. Bituminous deposit
80. Sand, gravel, clay, or placer pit

From Compton, 1985

Geologic Map Symbols

81	Mine, quarry, or open pit
82	Shafts: vertical, inclined, and abandoned
83	Adit, open (left) and inaccessible
84	Trench (left) and prospect
85	Water wells: flowing, nonflowing, and dry
86	Oil well (left) and gas well
87	Well drilled for oil or gas, dry
88	Wells with shows of oil (left) and gas
89	Oil or gas well, abandoned (left) and shut in
90	Drilling well or well location
91	Glory hole, open pit, or quarry, to scale
92	Dump or fill, to scale

Fossil and Structural Symbols for Stratigraphic Columns

Algae
Algal mats
Ammonites
Belemnites
Brachiopods
Bryozoans
Corals, solitary
Corals, colonial
Crinoids
Echinoderms
Echinoids
Fish bones
Fish scales

Tree trunk fallen
Trilobites
Vertebrates
Wood
Beds distinct
Beds obscure
Unbedded
Graded beds
Planar cross-bedding
Trough cross-bedding
Ripple structures
Cut and fill
Load casts

Foraminifers, general
Foraminifers, large
Fossils
Fossils abundant
Fossils sparse
Gastropods
Graptolites
Leaves
Ostracodes
Pelecypods
Root molds
Spicules
Stromatolites
Tree trunk in place

Scour casts
Convolution
Slumped beds
Paleosol
Mud cracks
Salt molds
Burrows
Pellets
Oolites
Pisolites
Intraclasts
Stylolite
Concretion
Calcitic concretion

From Compton, 1985

Lithologic Patterns for Stratigraphic Columns & Cross Sections


1. Breccia

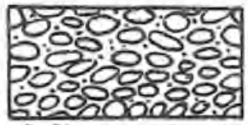
2. Clast-supported conglomerate

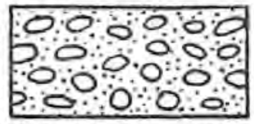
3. Matrix-supported conglomerate

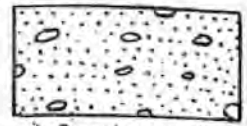
4. Conglomeratic sandstone

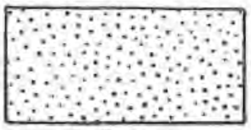
5. Coarse sandstone

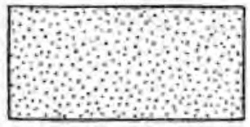
6. Fine sandstone

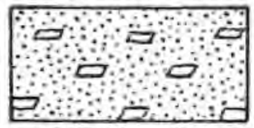
7. Feldspathic sandstone

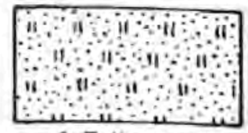
8. Tuffaceous sandstone

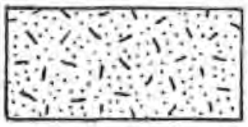
9. Graywacke

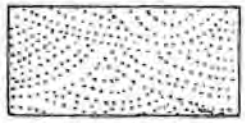
10. Cross-bedded sandstone

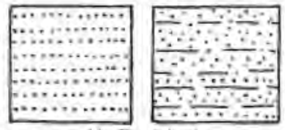
11. Bedded sandstone

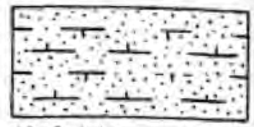
12. Calcite-cemented sandstone

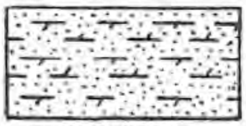
13. Dolomite-cemented sandstone

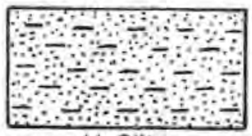
14. Silty sandstone


15. Siltstone

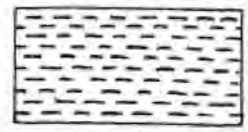
16. Mudstone


17. Shale


18. Coal bed with carbonaceous shale

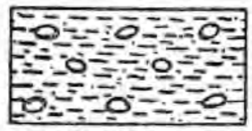
19. Pebbly mudstone

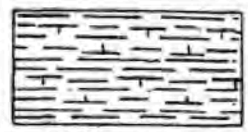
20. Calcareous shale

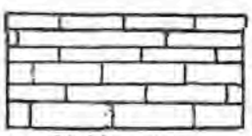
21. Limestone


22. Cross-bedded limestone


23. Dolomite (dolostone)

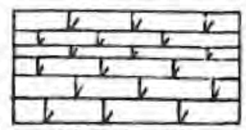
24. Dolomitic limestone


25. Calcitic dolomite

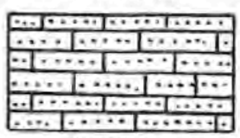
26. Sandy limestone

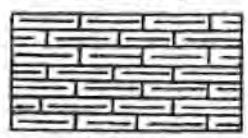
27. Clayey limestone

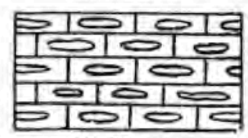
28. Cherty limestone

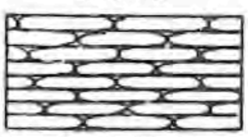
29. Bedded chert

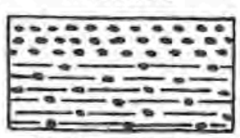
30. Phosphorite, phosphatic shale

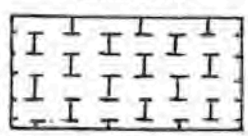
31. Chalk

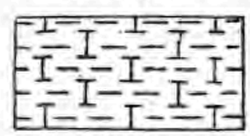
32. Marl

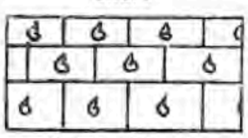
33. Fossiliferous limestone

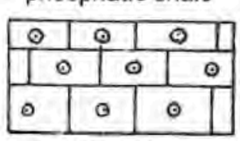
34. Oolitic limestone

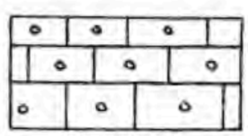
35. Pelletal limestone

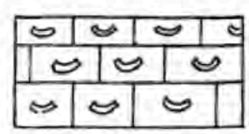
36. Intraclastic limestone


37. Crystalline limestone

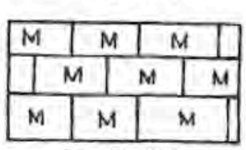
38. Micritic limestone

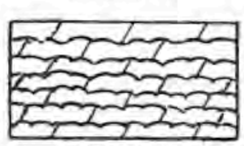
39. Algal dolomite


40. Limestone conglomerate

From Compton, 1985

Lithologic Patterns for Stratigraphic Columns & Cross Sections

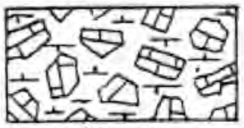
41. Limestone breccia


42. Algal dolomite breccia

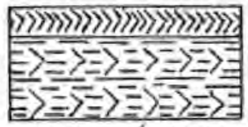
43. Gypsum bed, gypsiferous shale

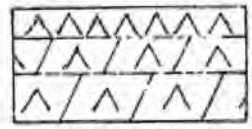
44. Anhydrite, anhydritic dolomite


45. Rock salt, salty mudstone

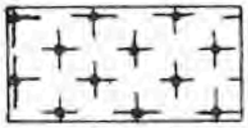
46. Peridotite

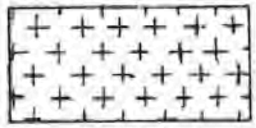
47. Gabbro

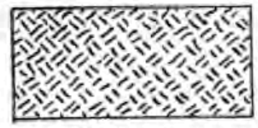
48. Mafic plutonic rock

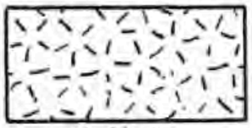
49. Coarse granitic rock

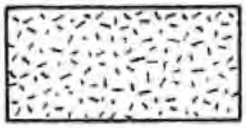
50. Fine granitic rock

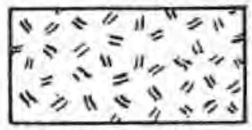
51. Porphyritic plutonic rock

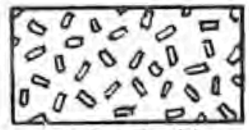
52. Porphyritic plutonic rock


53. Mafic lava


54. Silicic lava

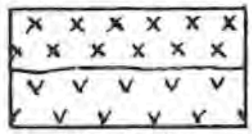
55. Intrusive volcanic rocks

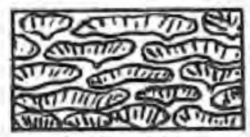
56. Pillow lava

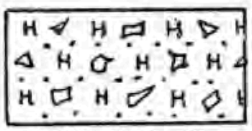
57. Hyaloclastite

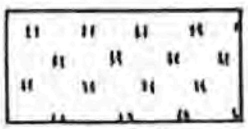
58. Tuff

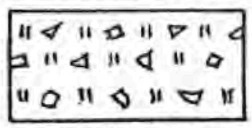
59. Tuff-breccia

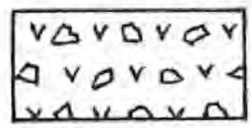
60. Volcanic breccia

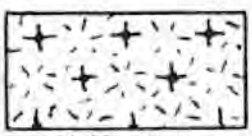
61. Massive serpentinite


62. Foliated serpentinite

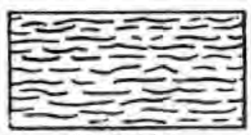
63. Schist

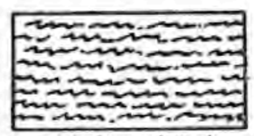
64. Crenulated schist


65. Folded schist

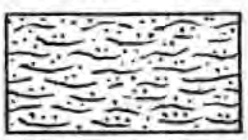
66. Semischistose sandstone


67. Semischistose limestone

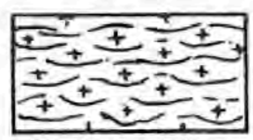
68. Semischistose gabbro


69. Greenstone

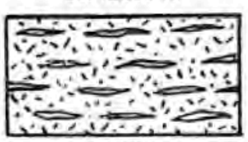
70. Silicic gneiss

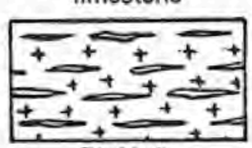
71. Mafic gneiss

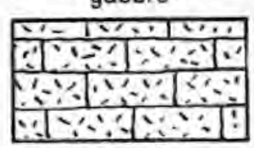
72. Marble

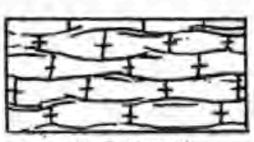
73. Foliated marble

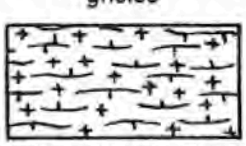
74. Foliated calc-silicate rock

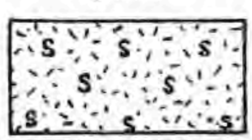
75. Massive skarn

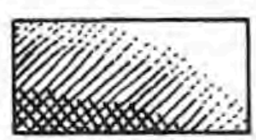
76. Alteration zones

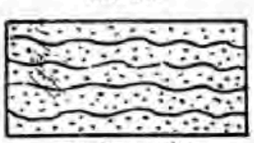
77. Quartzite

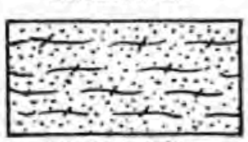
78. Quartzite

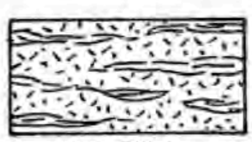
79. Silicic migmatite

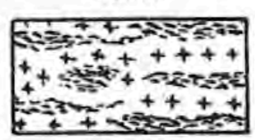
80. Mafic migmatite

From Compton, 1985

Geologic Timescale

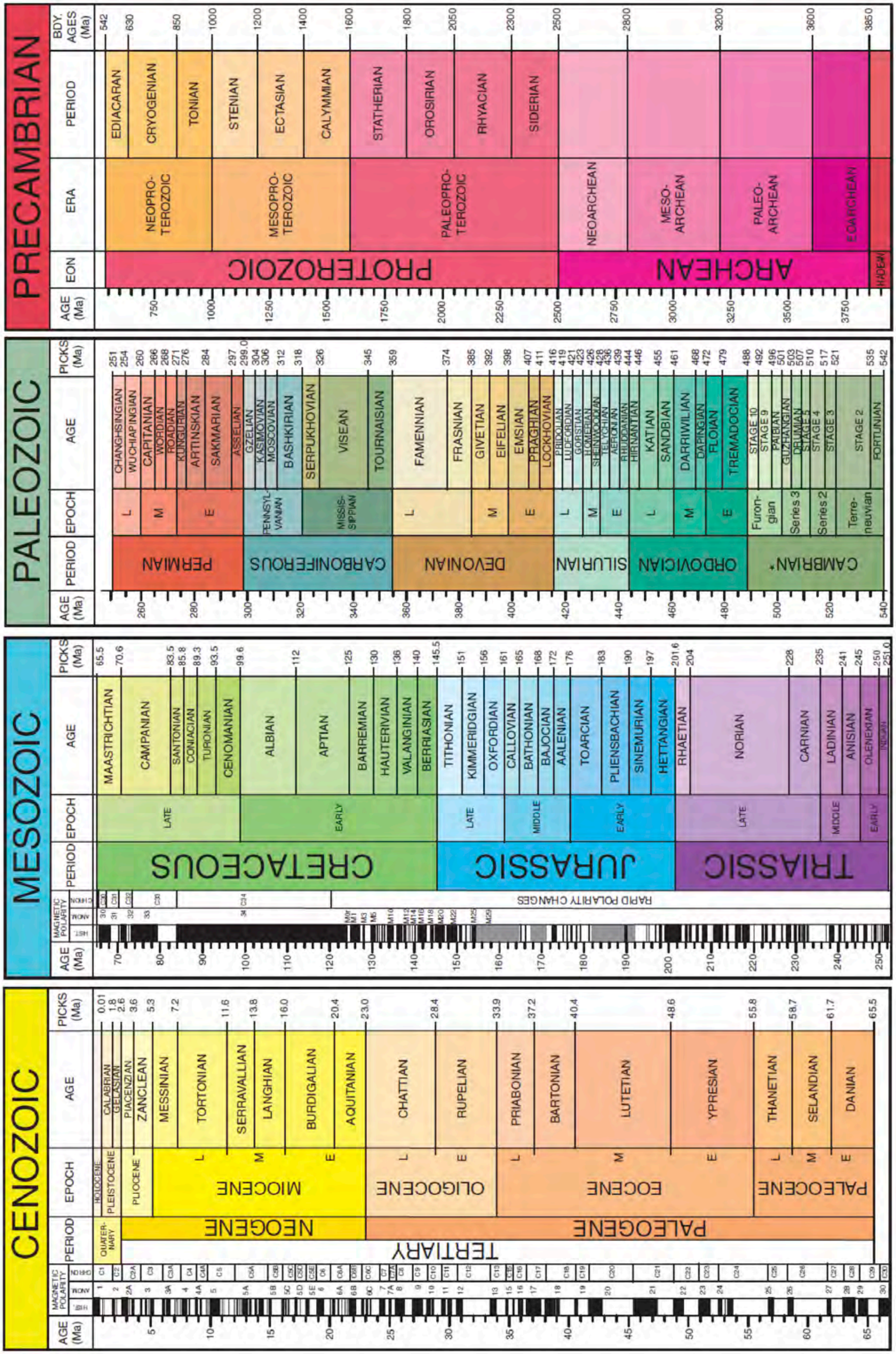

2009 version, from the Geologic Society of A

Aa: A blocky and fragmented form of lava occurring in flows with fissured and angular surfaces.
Alkali metal: A strongly basic metal like potassium or sodium.
Alluvial fan: A low, cone shaped deposit of terrestrial sediment formed where a stream undergoes an abrupt reduction of slope.
Alluvium: Unconsolidated terrestrial sediment composed of sorted or unsorted sand, gravel, and clay that has been deposited by water.
Angle of repose: The steepest slope angle in which particular sediment will lie without cascading down.
Aquifer: A permeable formation that stores and transmits groundwater in sufficient quantity to supply wells.
Arroyo: A steep-sided and flat-bottomed gully in an arid region that is occupied by a stream only intermittently, after rains.
Artesian well: A well that reaches an aquifer containing water under pressure. Thus water in the well rises above the surrounding water table.
Barchan: A crescent-shaped sand dune moving across a clean surface with its convex face upwind and its concave slip face downwind.
Basalt: A fine-grained, dark, mafic igneous rock composed largely of plagioclase feldspar and pyroxene.
Basement: The oldest rocks recognized in a given area, a complex of metamorphic and igneous rocks that underlies all the sedimentary formations.
Basic rock: Any igneous rock containing mafic minerals rich in iron and magnesium, but containing no quartz and little sodium rich plagioclase feldspar.
Basin: In tectonics, a circular, syncline-like depression of strata. In sedimentology, the site of accumulation of a large thickness of sediments.
Batholith: A great irregular mass of coarse-grained igneous rock which has either intruded the country rock or been derived from it through metamorphism.
Bathymetry: The study and mapping of sea-floor topography.
Bedding: A characteristic of sedimentary rocks in which parallel planar surfaces separating different grain sizes or compositions indicate successive depositional surfaces that existed at the time of sedimentation.
Bolson: In arid regions, a basin filled with alluvium and intermittent playa lakes and having no outlet.
Butte: A steep sided and flat topped hill formed by erosion of flat laying strata where remnants of a resistant layer protect the softer rocks underneath.
Caldera: A large, circular depression in a volcanic terrain, typically originating in collapse, explosion, or erosion.
Carbonate rock: A rock composed of carbonate minerals, especially limestone and dolomite.
Cataclastic rock: A breccia of powdered rock formed by crushing and shearing during tectonic movements.
Chemical weathering: The total set of all chemical reactions that act on rock exposed to water and atmosphere and so change it minerals to stable forms.
Chert: A sedimetary form of amorphous or extremely fine-grained silica, partially hydrous, found in concretions and beds.
Cinder cone: A steep, conical hill built up about a volcanic vent and composed of coarse pyroclasts expelled from the vent by escaping gases.
Clastic rock: A sedimentary rock formed from mineral particles (clasts) that were mechanically transported.
Clay: Any of a number of hydrous aluminosilicate minerals formed by weathering and hydration of other silicates.
Composite cone: The volcanic cone of a stratovolcano, composed of both cinders and lava flows.
Deflation: The removal of clay and dust from dry soil by strong winds.
Delta: A body of sediment deposited in an ocean or lake at the mouth of a stream.
Deposition: A general term for the accumulation of sediments by either physical or chemical sedimentation.
Deposition remnant magnetization: Magnetization created in sedimentary rocks by rotation of magnetic crystals into line with the ambient field during settling.
Desert pavement: A deposit produced by continued deflation, which removes the fine grains of a soil and leaves a surface covered with closely packed cobbles.
Detrital sediment: Sediment deposited by a physical process.
Diagenesis: The physical and chemical changes undergone by a sediment during lithification and compaction, excluding erosion and metamorphism.
Diatreme: A volcanic vent filled with breccia by the explosive escape of gases.
Dip: The angle by which a stratum or other planar feature deviates from the horizontal. The angle is measured in a plane perpendicular to the strike.
Drainage basin: A region of land surrounded by divides and crossed by streams that eventually converge to one river or lake.
Drift (glacial): A collective term for all the rock, sand, and clay that is transported and deposited by a glacier either as till or as outwash.
Dune: An elongated mound of sand formed by wind or water.
Eolian: Pertaining to or deposited by wind.
Epicenter: The point on the Earth's surface directly above the focus or hypocenter of an earthquake.
Erosion: The set of all processes by which soil and rock are loosened and moved downhill or downwind.
Evaporite: A chemical sedimentary rock consisting of minerals precipitated by evaporating waters, especially salt and gypsum.
Exfoliation: A physical weathering process in which sheets of rock are fractured and detached from an outcrop.
Fault: A planar or gently curved fracture in the Earth's crust across which there has been relative displacement.
Fault plane: The plane that best approximates the fracture surface of a fault.
Felsic: An adjective used to describe a light-colored igneous rock poor in iron and magnesium content, abundant in feldspars and quartz.
Fissure: An extensive crack, break, or fracture in the rocks.
Flood basalt: A plateau basalt extending many kilometers in flat, layered flows originating in fissure eruptions.
Flow cleavage: In a metamorphic rock, the parallel arrangement of all planar or linear crystals as a result of rock flowage during metamorphism.
Fluid inclusion: A small body of fluid that is entrapped in a crystal and has the same composition as the fluid from which the crystal formed.
Focus (earthquake): The point at which the rupture occurs; synonymous with hypocenter.
Fold: A planar feature, such as a bedding plane, that has been strongly warped, presumably by deformation.
Foliation: Any planar set of minerals or banding of mineral concentrations including cleavage, found in a metamorphic rock.
Forset bed: One of the inclined beds found in crossbedding; also an inclined bed deposited on the outer front of a delta.
Friction breccia: A breccia formed in a fault zone or volcanic pipe by the relative motion of two rock bodies.
Fumarole: A small vent in the ground from which volcanic gases and heated groundwater emerge, but not lava.
Geochronology: The science of absolute dating and relative dating of geologic formations and events, primarily through the measurement of daughter elements produced by radioactive decay in minerals.
Geomorphology: The science of surface landforms and their interpretation on the basis of geology and climate.
Geosyncline: A major downwarp in the Earth's crust, usually more than 1000 kilometers in length, in which sediments accumulate to thicknesses of many kilometers. The sediments may eventually be deformed and metamorphosed during a mountain-building episode.
Geotherm: A curving surface within Earth along which the temperature is constant.
Geyser: A hot spring that throws hot water and steam into the air. The heat is thought to result from the contact of groundwater with magma bodies.
Glacial rebound: Epeirogenic uplift of crust that takes place after the retreat of a continental glacier in response to earlier subsidence under the weight of ice.
Glacial striations: Scratches left on bedrock and boulders by overriding ice, and showing the direction of motion.
Glacial valley: A valley occupied or formerly occupied by a glacier, typically with a U-shaped profile.
Glacier: A mass of ice and surficial snow that persists throughout the year and flows downhill under its own weight, of sizes 100 m–10,000 km.
Glass: A rock formed when magma is too rapidly cooled (quenched) to allow crystal growth.
Graben: A downthrown block between two normal faults of parallel strike but converging dips; hence a tensional feature. See also horst.
Graded bedding: A bed in which the coarsest particles are concentrated at the bottom and grade gradually upward into fine silt.
Granite: A coarse-grained, intrusive igneous rock composed of quartz, orthoclase feldspar, sodic plagioclase feldspar, and micas.
Gravity anomaly: The value of gravity left after subtracting the reference value based on latitude, and possibly the free-air and Bouguer corrections. Gravity survey: The measurement of gravity at regularly spaced grid points with repetitions to control instrument drift.
Groundwater: The mass of water in the ground below the phreatic zone occupying the total pore space in the rock.
Horst: An elongate, elevated block of crust forming a ridge or plateau, typically bounded by parallel, outward-dipping normal faults.
Hydration: A chemical reaction, usually in weathering, which adds water or OH to a mineral structure.
Hydraulic conductivity: A measure of the permeability of a rock or soil: the volume of flow through a unit surface in unit time with unit hydraulic pressure difference as the driving force.

Hydrologic cycle: The cyclical movement of water from the ocean to the atmosphere, through rain to the surface, through runoff and groundwater to streams, and back to the sea.
Hydrology: The science of that part of the hydrologic cycle between rain and return to the sea; the study of water on and within the land.
Hydrothermal activity: Any process involving high-temperature groundwaters, especially the alteration and emplacement of minerals and the formation of hot springs and geysers.
Hydrothermal vein: A cluster of minerals precipitated by hydrothermal activity in a rock cavity.
Igneous rock: A rock formed by congealing rapidly or slowly from a molten state.
Inclination: The angle between a line in the Earth's magnetic field and the horizontal plane; also a synonym for dip.
Infiltration: The movement of groundwater or hydrothermal water into rock or soil through joints and pores.
Intrusion: An igneous rock body that has forced its way in a molten state into surrounding country rock.
Intrusive rock: Igneous rock that is interpreted as a former intrusion from its cross-cutting contacts, chilled margins, or other field relations.
Isograd: A line or curved surface connecting rocks that have undergone an equivalent degree of metamorphism.
Isostasy: The mechanism whereby areas of the crust rise or subside until the mass of their topography is buoyantly supported or compensated by the thickness of crust below, which "floats" on the denser mantle. The theory that continents and mountains are supported by low-density crustal "roots."
Isotope: One of several forms of one element, all having the same number of protons in the nucleus but differing in number of neutrons and atomic weight.
Joint: A large and relatively planar fracture in a rock across which there is no relative displacement of the two sides.
Laccolith: A sill-like igneous intrusion that forces apart two strata and forms a round, lens-shaped body many times wider than it is thick.
Lahar: A mudflow of unconsolidated volcanic ash, dust, breccia, and boulders mixed with rain or the water of a lake displaced by a lava flow.
Laminar flow: A flow regime in which particle paths are straight or gently curved and parallel.
Lapilli: A fragment of volcanic rock formed when magma is ejected into the air by expanding gases.
Lava: Magma or molten rock that has reached the surface.
Lava tube: A sinuous, hollow tunnel formed when the outside of a lava flow cools and solidifies and the molten material passing through it is drained away.
Leaching: The removal of elements from a soil by dissolution in water moving downward in the ground.
Left-lateral fault: A strike-slip fault on which the displacement of the far block is to the left when viewed from either side.
Levee: A low ridge along a stream bank, formed by deposits left when floodwater decelerates on leaving the channel.
Limb (fold): The relatively planar part of a fold or of two adjacent folds (for example, the steeply dipping part of a stratum between an anticline and syncline).
Limestone: A sedimentary rock composed principally of calcium carbonate ($CaCO_2$), usually as the mineral calcite.
Lithification: The processes that convert a sediment into a sedimentary rock.
Lithology: The systematic description of rocks, in terms of mineral composition and texture.
Lithosphere: The outer, rigid shell of the Earth, situated above the asthenosphere and containing the crust, continents, and plates.
Lode: An unusually large vein or set of veins containing ore minerals.
Longitudinal dune: A long dune parallel to the direction of the prevailing wind.
Lopolith: A large laccolith that is bowl-shaped and depressed in the center, possibly by subsidence of an emptied magma chamber beneath the intrusion. Maar volcano: A volcanic crater without a cone, believed to have been formed by an explosive eruption of trapped gases.
Mafic mineral: A dark-colored mineral rich in iron and magnesium, especially a pyroxene, amphibole, or olivine.
Magma: Molten rock material that forms igneous rocks upon cooling. Magma that reaches the surface is referred to as lava.
Magma chamber: A magma-filled cavity within the lithosphere.
Magnetic anomaly: The value of the local magnetic field remaining after the subtraction of the dipole portion of the Earth's field.
Magnetic north pole: (1) The point where the Earth's surface intersects the axis of the dipole that best approximates the Earth's field. (2) The point where the Earth's magnetic field dips vertically downward.
Magnetic stratigraphy: The study and correlation of polarity epochs and events in the history of the Earth's magnetic field as contained in magnetic rocks.
Magnetometer: An instrument for measuring either one orthogonal component or the entire intensity of the Earth's magnetic field at various points.
Mantle: The main bulk of the Earth, between the crust and core, ranging from depths of about 40–3,480 km It is composed of dense mafic silicates and divided into concentric layers by phase changes that are caused by the increase in pressure with depth.
Mass spectrometer: An instrument for separating ions of different mass but equal charge (mainly isotopes in geology) and measuring their relative quantities.
Mechanical weathering: The set of all physical processes by which an outcrop is broken up into small particles.
Mesophere: The lower mantle.
Metamorphism: The changes of mineralogy and texture imposed on a rock by pressure and temperature in the Earth's interior.
Meteorite: A stony or metallic object from inter-planetary space that penetrates the atmosphere to impact on the surface.
Micrometeorite: A meteorite less than 1 millimeter in diameter.
Microseism: A weak vibration of the ground that can be detected by seismographs and which is caused by waves, wind, or human activity.
Mineral: A naturally occurring element or non-organic compound with a precise chemical formula and a regular internal lattice structure.
Mohorovic discontinuity ("Moho"): Boundary between crust and mantle, marked by a rapid increase in seismic wave velocity to >8 km/s (depth 5-45 km).
Mohs scale of hardness: An empirical, ascending scale of mineral hardness.
Monocline: The S-shaped fold connecting two horizontal parts of the same stratum at different elevations. Its central limb is usually not overturned.
Moraine: A glacial deposit of till left at the margin of an ice sheet.
Normal fault: A dip-slip fault in which the block above the fault has moved downward relative to the block below.
Oblique-slip fault: A fault that combines some strike slip motion with some dip-slip motion.
Ore: A natural deposit in which a valuable metallic element occurs in high enough concentration to make mining economically feasible.
Orogenic belt: A linear region, often a former geo-syncline, that has been subjected to folding, and other deformation in a mountain-building episode.
Orogeny: The tectonic process in which large areas are folded, thrust-faulted, metamorphosed, and subjected to plutonism. The cycle ends with uplift and the formation of mountains.
Outgassing: The release of juvenile gases to the atmosphere and oceans by volcanism.
Oxidation: A chemical reaction in which electrons are lost from an atom and its charge becomes more positive.
Pahoehoe: A basaltic lava flow with a glassy, smooth, and undulating, or ropy, surface.
Paleoclimate: The average state or typical conditions of climate during some past geologic period.
Paleomagnetism: The science of the reconstruction of the Earth's ancient magnetic field and the positions of the continents from the evidence of remnant magnetization in ancient rocks.
Paleowind: A prevailing wind direction in an area, inferred from dune structure or the distribution of volcanic ash for one particular time in geologic history.
Pangaea: A great proto-continent from which all present continents have broken off by the mechanism of sea-floor spreading and continental drift.
Pediment: A planar, sloping rock surface forming a ramp up to the front of a mountain range in an arid region. It may be covered locally by thin alluvium.
Preferred orientation: Any deviation from randomness in the distribution of the crystallographic or grain shape axes of minerals of a rock produced by deformation and non-uniform stress during crystallization in metamorphic rocks or by depositional currents in sediments.
P-wave: The primary/fastest wave traveling away from a seismic event through the solid rock, consisting of a train of compressions/dilations of the material.
Pyroclastic rock: A rock formed by the accumulation of fragments of volcanic rock scattered by volcanic explosions.
Radiative transfer: One mechanism for the movement of heat, in which it takes the form of long-wavelength infrared radiation.
Recrystallization: The growth of new mineral grains in a rock at the expense of old grains, which supply the material.
Recumbent fold: An overturned fold with both limbs nearly horizontal.
Regolith: Any solid material lying on top of bedrock. Includes soil, alluvium, and rock fragments weathered from the bedrock.
Relief: The maximum regional difference in elevation.

Remote sensing: The study of Earth surface conditions and materials from airplanes and satellites by means of photography, spectroscopy, or radar.
Rhyolite: The fine-grained volcanic or extrusive equivalent of granite, light brown to gray and compact
Ridge (mid-ocean): A major linear elevated landform of the ocean floor, from 200–20,000 km in extent It is not a single ridge, but resembles a mountain range and may have a central rift valley.
Rift valley: A fault trough formed in a divergence zone or other area of tension.
Right-lateral fault: A strike-slip fault on which the displacement of the far block is to the right when viewed from either side.
Ripple: A very small dune of sand or silt whose long dimension is formed at right angles to the current
Saltation: The movement of sand or fine sediment by short jumps above the ground or stream bed under the influence of a current too weak to keep it permanently suspended.
Sandblasting: A physical weathering process in which rock is eroded by the impact of sand grains carried by the wind, frequently leading to ventifact formation of pebbles and cobbles.
Sandstone: A detrital sedimentary rock composed of grains from 1/16–2 mm in diameter, dominated in most sandstones by quartz, feldspar, and rock fragments, bound together by a cement of silica, carbonate, or other minerals or a matrix of clay minerals.
Sea-floor spreading: The mechanism by which new sea floor crust is created at ridges in divergence zones and adjacent plates are moved apart to make room. This process may continue at 0.5–10 cm/year through many geologic periods.
Secular variation: Slow changes in orientation of the Earth's magnetic field that appear to be long lasting and internal in origin.
Sedimentary rock: A rock formed by the accumulation and cementation of mineral grains transported by wind, water, or ice to the site of deposition or chemically precipitated at the depositional site.
Sedimentary structure: Any structure of a sedimentary or weakly metamorphosed rock that was formed at the time of deposition.
Sedimentation: The process of deposition of mineral grains or precipitates in beds or other accumulations.
Seismic reflection: Mode of seismic prospecting in which a seismic profile is examined for waves that reflected from near-horizontal strata below the surface.
Seismic refraction: Mode of seismic prospecting in which the seismic profile is examined for waves that have been refracted upward from seismic discontinuities below the profile. Greater depths may be reached than through seismic reflection.
Seismic surface wave: A seismic wave that follows the earth's surface only, with a speed less than that of S-waves.
Stratification: A structure of sedimentary rocks, which have recognizable parallel beds of considerable lateral extent
Stratigraphic sequence: A set of beds deposited that reflects the geologic history of a region.
Stratigraphy: The science of the description, correlation, and classification of strata in sedimentary rocks.
Stratovolcano: A volcanic cone consisting of both lava and pyroclastic rocks, often conical.
Stress: A quantity describing the forces acting on each part of a body in units of force per unit area.
Striation: See Glacial striation.
Strike: The angle between true North and the horizontal tine contained in any planar feature (inclined bed, dike, fault plane, etc.).
Strike-slip fault: A fault whose relative displacement is purely horizontal.
Subduction zone: A dipping planar zone descending away from a trench and defined by high seismicity, interpreted as the shear zone between a sinkingoceanic plate and an overriding plate.
Sublimation: A phase change from the solid to the gaseous state, without passing through the liquid state.
Subsidence: A gentle epeirogenic movement where a broad area of the crust sinks without appreciable deformation.
Syncline: A large fold whose limbs are higher than its center; a fold with the youngest strata in the center.
Tectonics: The study of the movements and deformation of the crust on a large scale. including epeirogeny. metamorphism, folding, faulting, plate tectonics.
Thermal conductivity: A measure of a rock's capacity for heat conduction.
Thermal expansion: The property of increasing in volume as a result of an increase in internal temperature.
Thermoremnent magnetization: Permanent magnetization acquired by igneous rocks in the Earth's magnetic field as they cool through the Curie point Thrust fault A dip-slip fault in which the upper block above the fault plane moves up and over the lower block, so that older strata are placed over younger.
Tilt: An unconsolidated sediment containing all sizes of fragments from clay to boulders deposited by glacial action, usually unbedded.
Topography: The shape of the Earth's surface, above and below sea level; the set of landforms in a region; the distribution of elevations.
Topset bed: A horizontal sedimentary bed formed at the top of a delta and overlying the foreset beds.
Trace element: An element that appears in minerals in a concentration of less than 1% (often <0.001%).
Transform fault: A strike-slip fault connecting the ends of an offset in a mid-ocean ridge. Some pairs of plates slide past each other along transform faults.
Transverse dune: A dune that has its axis transverse to the prevailing winds or to a current
Trench: A long and narrow deep trough in the sea floor; interpreted as marking the line along which a plate bends down into a subduction zone.
Tuff: A consolidated rock composed of pyroclastic fragments and fine ash. If particles are melted slightly together from their own heat, it is a "welded tuff".
Turbulent flow: A high-velocity flow in which streamlines are neither parallel nor straight but curled into small tight eddies (compare Laminar flow).
Ultramafic rock: An igneous rock consisting dominantly of mafic minerals, containing less than 10% feldspar.
Unconformity: A surface that separates two strata
Unconsolidated material: Nonlithified sediment that has no mineral cement or matrix binding its grains.
Uplift: A broad and gentle epeirogenic increase in the elevation of a region without a eustatic change of sea level.
Vadose zone: The region in the ground between the surface and the water table in which pores are not filled with water. Also called the unsaturated zone.
Valley glacier: A glacier that is smaller than a continental glacier or an icecap, and which flows mainly along well-defined valleys, many with tributaries.
Vein: A deposit of foreign minerals within a rock fracture or joint
Ventifact: A rock that exhibits the effects of sandblasting or "snowblasting" on its surfaces. which become flat with sharp edges in between.
Vesicle: A cavity in an igneous rock that was formerly occupied by a bubble of escaping gas.
Viscosity: A measure of resistance to flow in a liquid.
Volcanic ash: A volcanic sediment of rock fragments, usually glass, less than 4 mm in diameter, formed when escaping gases force out a fine spray of magma.
Volcanic bomb: A pyroclastic rock fragment that shows the effects of cooling in flight in its streamlined or "breadcrust" surface.
Volcanic breccia: A pyroclastic rock in which all fragments are more than 2 mm in diameter.
Volcanic cone: The deposit of lava and pyroclastic materials that has settled close to the volcano's central vent
Volcanic dome: A rounded accumulation around a volcanic vent of congealed lava too viscous to flow away quickly; hence usually rhyolite lava.
Volcanic ejecta blanket: A collective term for all the pyroclastic rocks deposited around a volcano, especially by a volcanic explosion.
Volcano: Any opening through the crust that has allowed magma to reach the surface, including the deposits immediately surrounding this vent
Warping: In tectonics, refers to the gentle, regional bending of the crust, which occurs in epeirogenic movements.
Water table: A curved surface below the ground at which the vadose zone ends and the phreatic zone begins; the level to which a well would fill with water.
Weathering: The set of all processes that decay and break up bedrock, by a combination of physically fracturing or chemical decomposition.
Xenolith: A piece of country rock found engulfed in an intrusion.

SUPER TIC TAC TOE

Like the normal version, but more. The board is made up of 9 sub-games within the larger supergame. Player one begins by placing an X inside one of the sub-games. The square chosen within that sub-game determines the next sub-game for player two to make their move, and so on. For example, if player one chooses the middle square in the upper-right sub-game, player two must place their move within the middle sub-game. If you win a sub-game, you win that space in the uber-game. Connect three squares in a row in the super game to win. This game can be broken. There might not be a winner. Maybe you'll have fun. You'll probably get mad at your opponent.

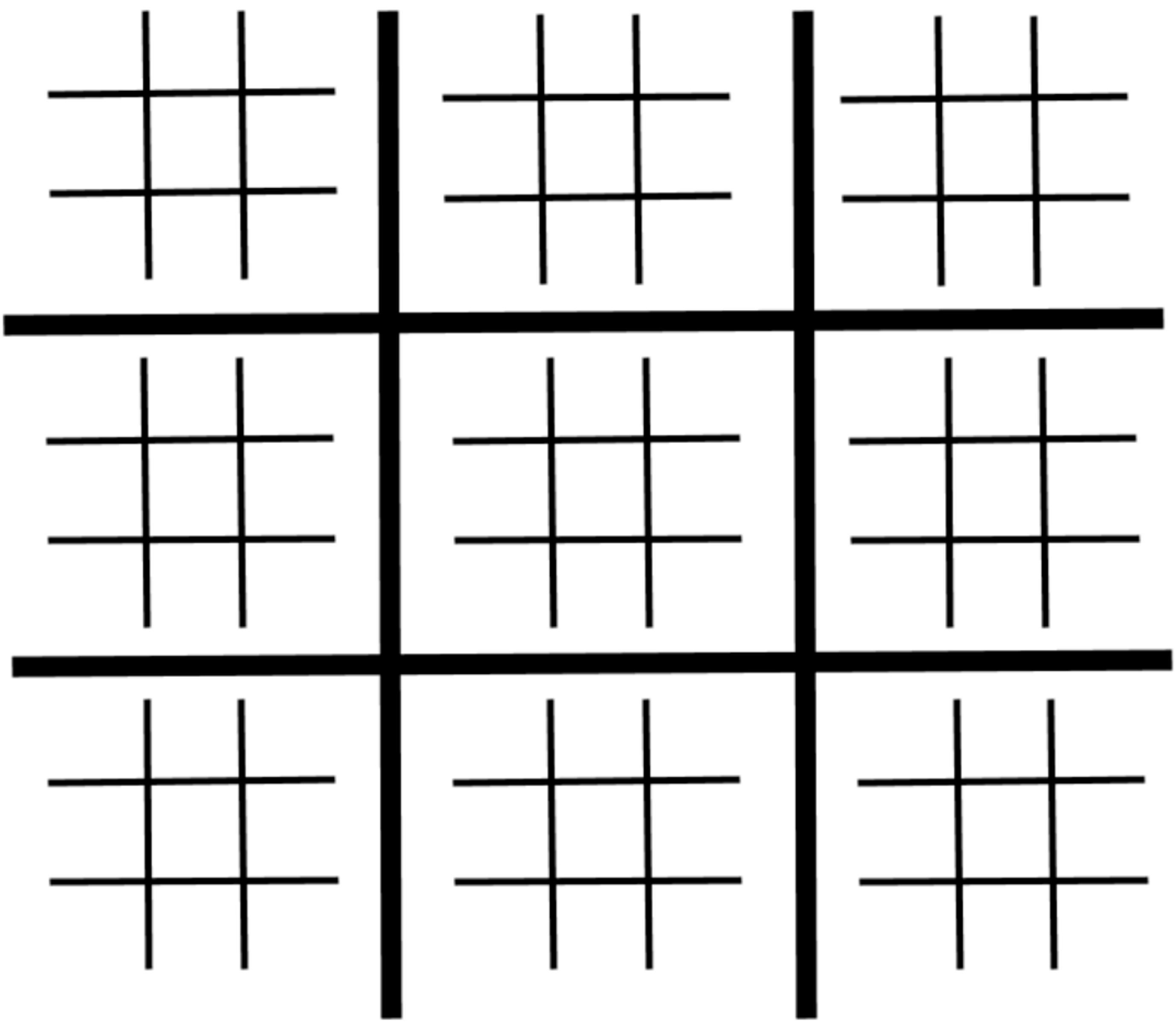

1

		5			7			
						9		2
7		1	2		9	6		
9	5			8		3		
	2			3	6			
		7			5		1	
			6				5	9
5	3			9				
			1	5		2	6	

2

		2		8				
	1				3	4	9	
		9		7				5
6	4					3		
					4	8		9
		5		2	7			4
	9						1	
			8	9	2			
		7	1	4			2	

3

			6	5				
7				4		9	5	2
3		5	1					4
		3					4	5
2		7					9	
4			5	2	6		7	
	7				8	5		
		4				7	2	
	9				5		6	

4

	4		3					9
		7	6		5			
		2	4			5		1
1		3						2
8					4			
2					6	9	8	
	3	1	7					
	9			2				5
	2					1	9	4

5

					1		8	2
			5	6		1		7
6	3			7	2			
			7			9	1	
		3	4		6	7		
		2					4	
	1				3		7	
	2	5		1				
		6		5		3		

6

			4			8		2
3		7			5			
		2				9		
9		3				1		
		1			7	4	9	8
			6		1			7
	3		8	6		2	4	
	4		3	5				
2	9						3	

7

	3		2		4	5		8
		4	6		7			2
		5			3			4
	2	1					4	
	5		9	3	2			
	6					3		
5			4	7				
6			3	1		7	5	
7							1	6

8

2	5			7				
			5	9		1	3	
				2	3		6	7
							9	6
8	1	4						
			7		5			
4		2	1			6		
		8			6	3	1	
		1		3		8		9

9

		8	2				1	5
2			3	6				
9	5	6					2	
								4
7		5		3	2			
			6	5	7		8	
	6	1				4		
			1	4	3	5		
	2					8	7	

10

1			7	8	4			
8	2					9	3	
	6				2			
			3	2				7
		5		9			8	2
6	1							
					8	5	9	
9		6		5				
7						8	2	3

11

	5	9		8				
						2		7
		7	6	1				
	1	6	5	9			8	
			7					1
	9	8				6	2	
8					9		4	
2							1	8
9	6				5			2

12

					5	4		6
	6	2			9	1		
9				8	4			
	9					6		5
3		8		2				
		5			8	2	1	
8			7	6			2	
							4	7
1		7	4					

Battleship

Another fun activity from:

www.funorama.com

Defensive Grid

A										
B										
C										
D										
E										
F										
G										
H										
I										
J										
	1	2	3	4	5	6	7	8	9	10

Put the following ships on your defensive grid by placing the appropriate letters -- horizontally, vertically or diagonally.

1 - Aircraft Carrier

A	A	A	A	A

1 - Battleship

B	B	B	B

1 - Cruiser

C	C	C

2 - Destroyers

D	D

D	D

Offensive Grid

A										
B										
C										
D										
E										
F										
G										
H										
I										
J										
	1	2	3	4	5	6	7	8	9	10

Instructions (2 Players Required):

Both players place their ships on the defensive grid according to the chart above. Whoever goes first calls out a position (i.e. G-6). The other player says either “Hit” or “Miss” depending upon whether one of his ships is in the position called out. The person calling out should mark a hit or a miss on the “offensive grid” to keep track of the shots. The other person should mark the shot on the “defensive grid”. If the shot is a “Hit”, the player goes again--otherwise the other player takes a turn. Once the opposing player has scored a hit on all of the spaces for a particular ship, you must call out “Hit...you sunk my Cruiser“ (or whatever type of ship it was). Once a player has sunk all the opponents ships, he is declared the winner.

Help Shane Byrne Escape from Zombies!

start

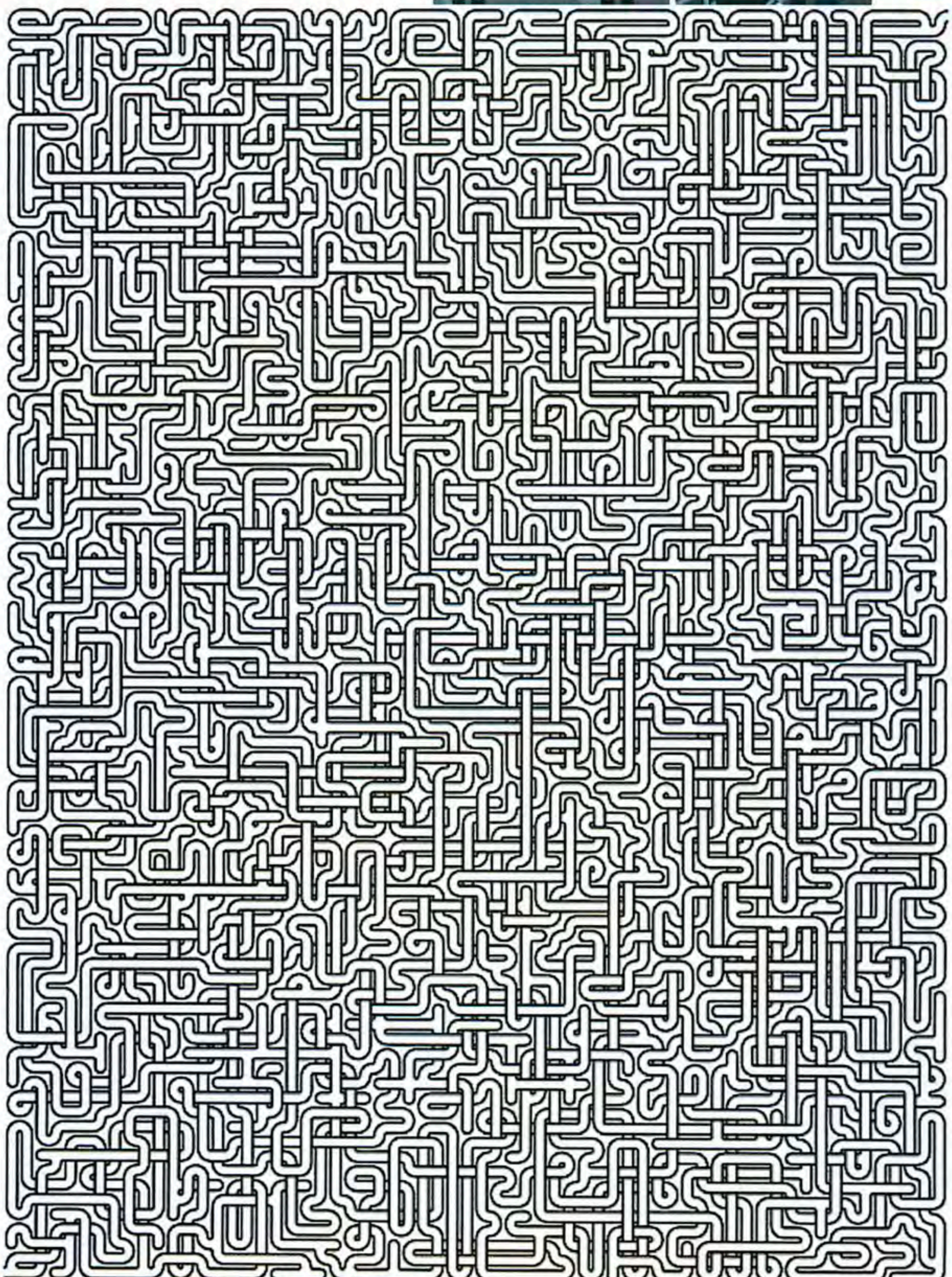

finish

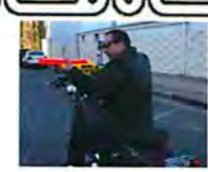

Rescued by Tom Zega!

When the field trip went wrong... Mad Lib

Adjective ______________________
Place ______________________
Any person on the field trip ______________________
Noun ______________________
Time ______________________
Type of vehicle ______________________
Place ______________________
Person on the field trip #1 ______________________
Noun ______________________
Adjective ______________________
Person on the field trip #1 ______________________
Medical issue or disease ______________________
Body part ______________________
Different person on field trip #2 ______________________
Noun ______________________
Place ______________________
Person on the field trip #1 ______________________
Same medical issue ______________________
Noun - Plural ______________________
Person on the field trip #1 ______________________
Place ______________________
food ______________________
Any person on the field trip ______________________
number ______________________
Verb - Present ends in ING ______________________
Different person ______________________
Noun ______________________
Same noun ______________________
Same noun ______________________
Verb - Base Form ______________________
Person on field trip #2 ______________________
Person on field trip #2 ______________________
Body part ______________________
Adverb ______________________
Person on field trip #2 ______________________
Same noun ______________________
Same noun ______________________
weapon ______________________
Any person on the field trip ______________________
Meat food ______________________
Asian food ______________________
Generic food ______________________
Any person on the field trip ______________________
Type/brand of alcohol ______________________
Any person on the field trip ______________________
Song ______________________
Animal plural ______________________
Any person on the field trip ______________________
Any person on the field trip ______________________

When the field trip went wrong...

On a ________Adjective day in March, the LPL field trip began. Everybody met at the_________Place, except ______Any person on the field trip, who was running late. Apparently s (he) forgot their ______Noun______, causing them to not show up until ______Time___. When the ________Type of vehicle was packed up, we finally left. When driving on the I-10 towards _________Place, suddenly the tire pressure light came on. The vehicle pulled over and alerted the rest on the **CB**. Unfortunately everybody's elses **CB's** were turned off so nobody else heard and continued on their way. While pulled over, __________Person on the field trip #1 checked the tires and noticed there was a __________Noun in the rear left tire. They tried to get it out of the tire, but unfortunately it was __________Adjective, which gave __________Person on the field trip #1 __________Medical issue or disease in their __________Body part.

__________Different person on field trip decided to put__________Noun on it while the others in the car patched up the tire. Finally, the vehicle was back on its way but decided to stop at__________Place to check on __________Person on the field trip#1's __________Same medical issue. After a heavy dose of __________Noun – Plural, __________Person on the field trip #1 feels well enough to continue with the trip. The other vehicles finally realize they are missing a vehicle and call the others. Everybody decides to meet up at __________Place to get food. However, the __________food gives __________Any person on the field trip food poisoning and within _______number hours of being on the road, s(he) is __________Verb - Present ends in ING all over the place. Still not even close to the Mojave, everybody decides to stop early. Those feeling up to it decide to go hiking. While hiking, __________Person on field trip #2 steps on a ____Text____Noun. The __________Same Noun, obviously disgruntled, goes in to __________Verb – Base Form __________Person on field trip #2's __________Body part. Fortunately, __________Person on field trip #2 moves _______Adverb and avoids yet another mishap. Whew! That was a close one. Meanwhile, __________Different person on field trip, part of the meat food group, decides the __________Same noun would make excellent dinner and catches the __________Same Noun using a __________weapon. Back at camp, everybody is setting up for dinner when__________Any person on the field trip realizes they forgot the cooler back at campus! Everybody else reluctantly gives them some of their dinners, so they end up eating a random dinner of __________Meat food, __________Asian food and __________Generic food.

To let off steam,__________Any person on the field trip busts out a bottle of __________Type/brand of alcohol and it gets passed around the fire. When no one is looking, __________Any person on the field trip takes a big swig and proceeds to get drunk and start singing __________Song. Everybody, exhausted, goes to bed. In the middle of the night, a pack of __________animal plural surround the camp and scare__________Any person on the field trip, who screams and wakes everybody up. Nobody can get back to sleep, and it is decided to get an early go at the day. After everybody packs up, one of the suburbans won't start. No one brought jumper cables. __________Any person on the field trip takes a vehicle off-roading to find cell phone reception and calls AAA. AAA refuses to drive on ATV trails, however, and says they can't help us. So, everybody packs into the remaining vehicles and they drive back to Tucson, leaving the UA motor pool to deal with it. Everybody goes home and sleeps forever, skipping the rest of the semester's classes. The end.

Arizona Trivia

K Miller

No spaces included in solutions.

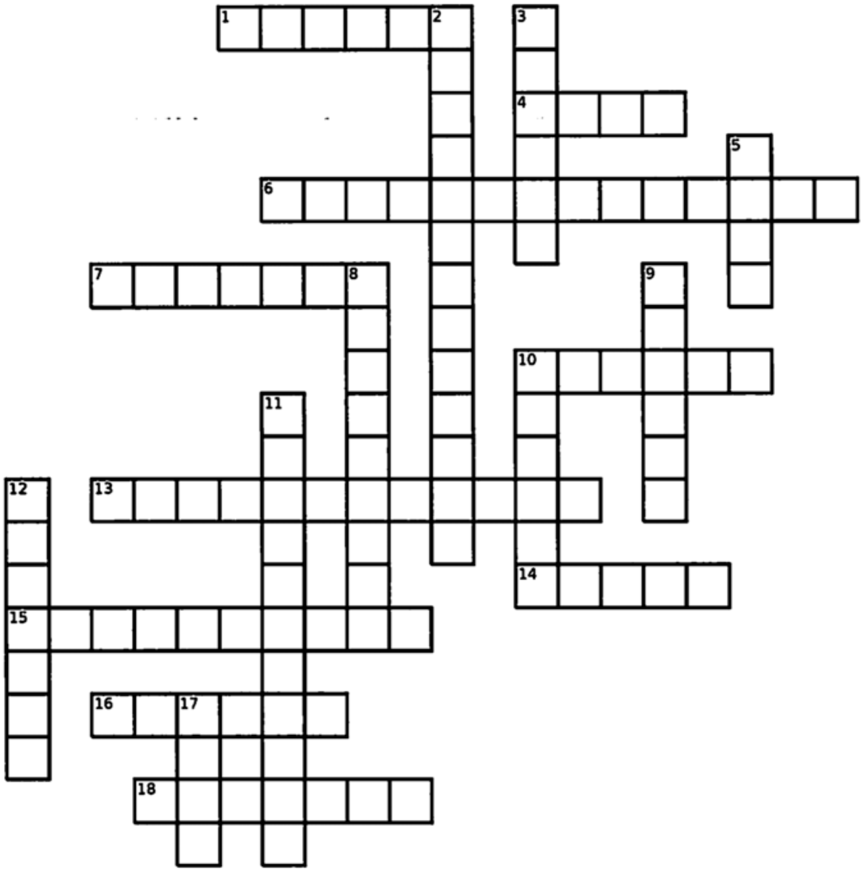

Across

1 In terms of fractions, about one [ ] of the state is federal land designated for Native Americans Reservations.
4 Actor [ ] Stone is from Scottsdale.
6 Where is the 1831 London Bridge? (3 Words)
7 The largest employer in Arizona as of 2010 was [ ].
10 There are 91 [ ] in Arizona.
13 [ ] [ ] can live up to 200 years (2 Words)
14 Arizona is the [ ] largest state
15 Arizona has the largest population of all the [ ] states.
16 "Arizona" probably either comes from the O'odham "ali sonak", which means small [ ]. (The word is a time, a verb, and something you might find outside.)
18 The official state neckwear is the [ ]. (2 Words)

Down

2 The highest elevation in Arizona is [ ] [ ] at 12.643 ft. (2 Words)
3 Arizona became a state in the year nineteen [ ].
5 How many different national flags have flown over Arizona land?
8 [ ] is the state gemstone.
9 The [ ] of a saguaro is closely related to its age.
10 Arizona is popular for Major League Baseball spring training because it has the [ ] League.
11 The Arizona state slogan is [ ] State. (2 Words)
12 In 2009, the five largest ancestry groups in Arizona were Mexican, German, Irish, English, and [ ].
17 The amount of copper on the Capitol's [ ] is equal to 4,800,000 pennies.

Can you find 22 words related to this field trip to the Mojave Desert?

T	H	B	B	H	E	A	U	K	J	X	C	Y	M	E
V	U	E	E	Y	R	A	D	A	R	L	S	G	A	N
O	E	F	P	D	K	I	R	Q	I	K	C	O	E	O
R	G	W	F	R	S	U	V	M	C	J	S	L	R	C
V	R	H	X	O	E	L	A	O	O	E	Y	O	C	R
K	I	V	L	L	C	T	R	P	N	J	M	E	E	E
B	P	C	Z	O	E	H	R	U	L	G	A	G	C	D
A	I	D	E	G	W	S	D	U	W	A	Y	V	I	N
G	N	S	P	Y	C	D	H	F	Q	J	Y	E	E	I
E	G	U	A	I	N	P	F	Y	I	S	A	A	B	C
O	I	E	A	A	L	A	V	A	T	U	B	E	V	Y
L	Q	R	S	F	E	X	A	R	O	L	F	R	H	O
O	M	D	L	E	I	F	C	I	N	A	C	L	O	V
G	A	E	R	U	T	L	U	C	I	R	G	A	X	R
Y	P	H	U	M	A	N	H	I	S	T	O	R	Y	D

Scale bar